EVALUATION OF A DEEP PLAN OFFICE SPACE

DAYLIT WITH AN OPTICAL LIGHT PIPE AND A SPECULAR LIGHT SHELF

A Thesis

by

KAPIL UPADHYAYA

Submitted to the Office of Graduate Studies of
Texas A&M University
in partial fulfillment of the requirements for the degree of

MASTER OF SCIENCE

August 2008

Major Subject: Architecture

EVALUATION OF A DEEP PLAN OFFICE SPACE

DAYLIT WITH AN OPTICAL LIGHT PIPE AND A SPECULAR LIGHT SHELF

A Thesis

by

KAPIL UPADHYAYA

Submitted to the Office of Graduate Studies of
Texas A&M University
in partial fulfillment of the requirements for the degree of

MASTER OF SCIENCE

Approved by:

Chair of Committee,	Liliana O. Beltran
Committee Members,	F. Michael Speed
	Jorge A. Vanegas
Head of Department,	Mark Clayton

August 2008

Major Subject: Architecture

ABSTRACT

Evaluation of a Deep Plan Office Space

Daylit with an Optical Light Pipe and a Specular Light Shelf. (August 2008)

Kapil Upadhyaya, B.Arch. Hons., Indian Institute of Technology, Kharagpur

Chair of Advisory Committee: Dr. Liliana O. Beltran

This research developed the Optical Light Pipe (OLP) as a feasible solution to solve the problem of insufficient daylighting in deep plan office spaces for predominantly sunny climates. It further combined the OLP with a Specular Light Shelf (SLS) to achieve uniform daylighting.

This research was performed with an experimental setup of two 1:4 scale models of deep plan office spaces, modified from an earlier research on optical light pipe at College Station, TX. Blinds and shading devices were installed on the south façade to provide daylight to the front zone of a 20 feet by 30 feet office module. The back zone was daylit by the OLP hidden in the plenum. The existing OLP design was optimized through computer aided ray-tracing. The SLS design was based on an earlier prototype designed at Lawrence Berkeley National Labs (LBNL).

Results were based on observations made on clear and cloudy sky days between February 3rd and March 17th. The OLP achieved more than 300 lux of average workplane illuminance for 7.4 hours, when global horizontal illuminance was greater than 40,000 lux. It also achieved 200 lux of illuminance higher than an earlier prototype

(Martins-Mogo, 2005) on workplane between 1000hrs and 1630hrs. It exhibited a glare free daylight distribution with luminance ratios well within prescribed limits on most of the vertical surfaces, with a relatively uniform illuminance distribution on back taskplane. OLP was better than windows with blinds and shading at providing diffuse daylight in backzone on a cloudy day, when global horizontal illuminance was greater than 20,000 lux.

The OLP used in combination with SLS achieved more than 500 lux of average workplane illuminance for 6 hours, when global horizontal illuminance was greater than 40,000 lux. SLS also produced more uniform illuminance levels on the workplane at all times and on the leftwall at most times. However, it produced non-uniform luminance distribution on walls and ceiling and luminance ratios higher than allowable limits on the sidewall for some morning hours, and hence needed further refinement in design.

DEDICATION

To my friend and inspiration - Mota.

ACKNOWLEDGEMENTS

I express deep gratitude towards Dr.Liliana O.Beltran to have provided me the opportunity, inspiration and guidance to work on this project. My sincere thanks to Dr. Jorge Vanegas for his suggestions, Dr. Michael Speed and Dr. Webster West for their valuable time.

I would also thank Danny Bass who allowed me tremendous flexibility while working in the woodshop. Many thanks to the following people with whose help the project could reach a successful completion:

Andrew Sabel for a generous donation of Miro Silver; Jordan Katz for donation of DFPM film; Barbara J. Calt for granting a full license of Trace-Pro; Mark Roberts at Harbortronics and Fawaz Mamaari at Soft Energy for their quick replies to my questions; Energy Systems Lab, TAMU for giving me access to the shadow band.

Thank you Brian Malarkey for your kind understanding. And thanks to my friends for the odd hour help that they provided during the project.

NOMENCLATURE

OLP	Optical Light Pipe
SLS	Specular Light Shelf
5DEG	OLP prototype with side walls rotated in by 5°.
10DEG	OLP prototype with side walls rotated in by 10°.
6F6B	OLP prototype with 6 feet front transport section and 6 feet back transport-section.
6F4B	OLP prototype with 6 feet front transport section and 4 feet back transport-section.
6F2B	OLP prototype with 6 feet front transport section and 2 feet back transport-section.
6F2B5C	OLP prototype with 6 feet front transport section and 2 feet back transport-section and side walls of back transport section rotated by 5 °.
6F2B510C	OLP prototype with 6 feet front transport section and 2 feet back transport-section and side walls of back transport section rotated by 10°.
6F2B515C	OLP prototype with 6 feet front transport section and 2 feet back transport-section and side walls of back transport section rotated by 15°.
WWAR	Window to wall-area ratio
ICG	Illuminance contrast gradient
CV	Coefficient of variation
LR	Luminance ratio
IESNA	Illuminating Engineering Society of North America

TABLE OF CONTENTS

Page

Page

LIST OF TABLES

LIST OF FIGURES

I. INTRODUCTION

1.1 PROBLEM OF DAYLIGHTING IN DEEP PLAN SPACES

Energy efficiency in buildings was never more aggressively pursued than today. Many US cities are upgrading local building codes following the general acceptance of global warming and the impact of buildings on a city's carbon footprint. Appendix-G of ASHRAE Standard 90.1-2004 has been set as a baseline by USGBC for obtaining Energy and Atmosphere credits for LEED certification. Amongst many such measures, daylighting still remains an underutilized resource in buildings. The United Nations Energy Program estimates that daylighting is the single energy saving strategy applicable to six out of eleven global climate zones (UNEP, 2007). Fig.1.1 depicts the average lighting energy consumption for US offices to be above 20%.

Over the years, the design of commercial office complexes has evolved to give rise to multi-storied floor plates which are hundred feet or more in bay depth, resulting in building cores with limited access to daylight. With most of the offices in use during daytime, it appears wasteful to use electric lighting most of the time. It has been proved that daylight harvesting with lighting controls bring down the energy consumption of side lit buildings (Heschong et al, 2005) and that of toplit buildings (Pande et al, 2006). More importantly, daylight is considered necessary for workers' productivity and health (Boyce et al, 2003) and there are numerous studies supporting this.

This thesis follows the style and format of Solar Energy.

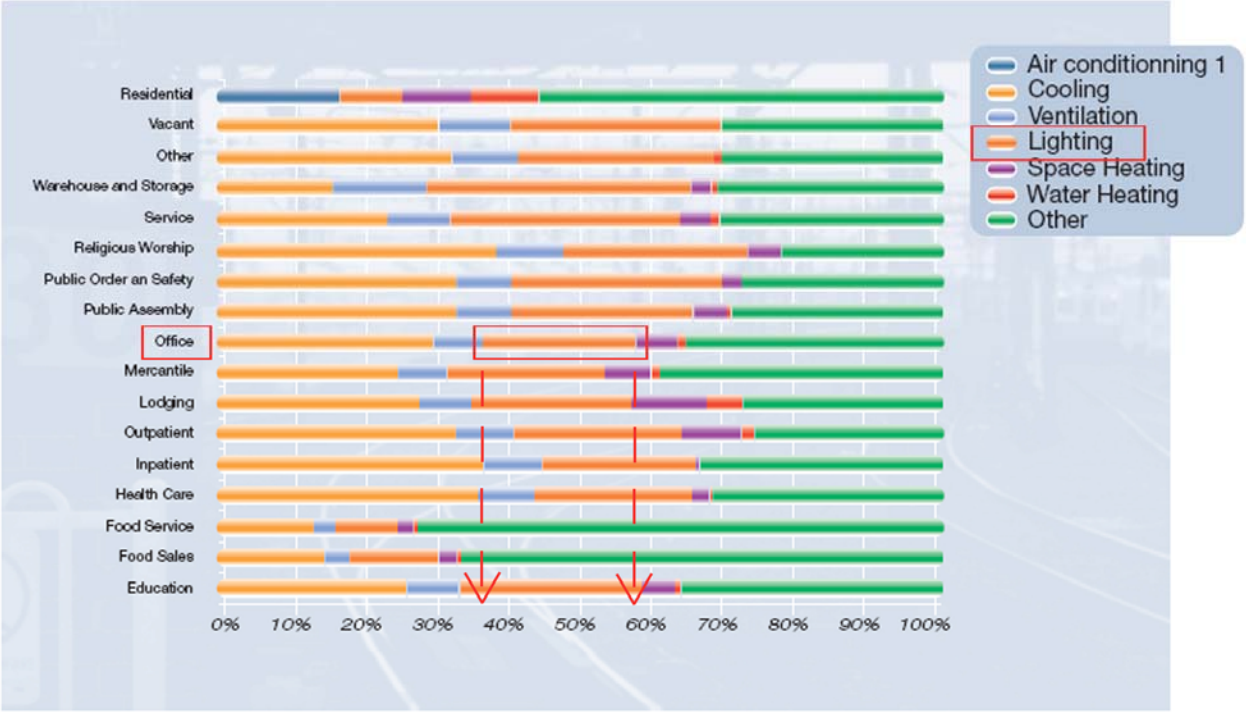

Fig. 1.1. Electricity use by building type in US. Source: US EIA, 1999 plotted in Buildings and Climate Change, 2007.

The most common form of daylighting occurs through windows. The amount of daylight in this case, however, depreciates exponentially as shown in Fig. 1.2a. and hence the popular rule of thumb for sidelighting as shown in Fig. 1.2b.

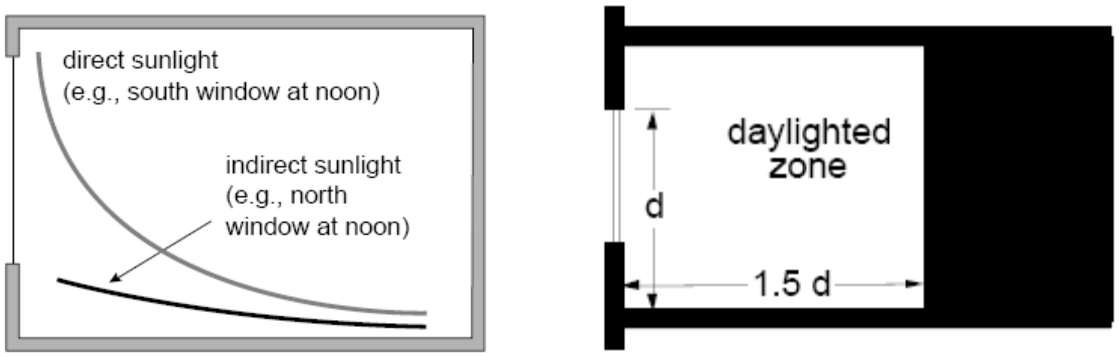

(a) (b)

Fig. 1.2. Characteristics of side lit spaces. (a) Reducing daylight levels with distance, (b) daylight penetration for standard windows. *Source: Tips for daylighting with window, LBNL (1997) Derek, (2004).*

But this leaves most of the core areas inaccessible to daylight. A fifteen feet deep daylit zone is typical for offices; the zone depth can be increased to twenty feet in an open office with low height partitions, ceiling higher than nine feet and correspondingly high windows (O'Connor, Lee, Rubinstein, Selkowitz, 1997). One example is the Heifer International Headquarters in Little Rock, Arkansas where the bay depth is 62feet and the average floor to ceiling height is more than 15feet. Fig. 1.3a shows the north facing part of the office building. Another solution that occurs in some daylit buildings is an increased perimeter area as in the office building at 88 Wood Street in London, UK, as shown in Fig. 1.3b.

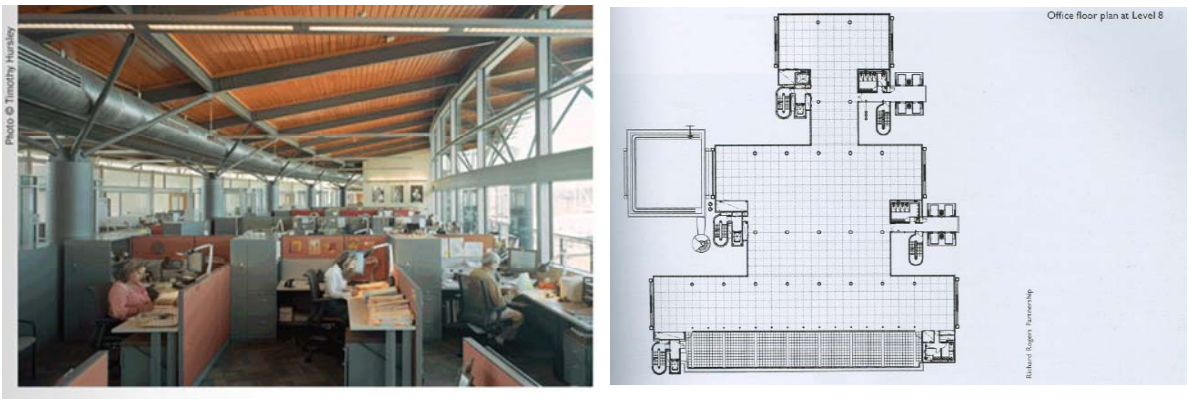

(a) (b)

Fig. 1.3. Case studies. (a) Heifer International Headquarters, Little Rock, Arkansas. *Source: High Performance Buildings (Winter 2008), ASHRAE,* (b) 8th floor plan of 88 Wood Street, London. *Source: Daylighting: natural light in architecture by Derek, (2004).*

These solutions, however, involve increased fenestration costs which may not appear economical for commercial building developers who face high costs per square foot; and hence only a few examples of such kind. Another factor that contributes to smaller daylit zones is shading. Office buildings, due to high and continuous occupancy fall, under the category of internal-load dominated buildings and need to avoid heat gains using strategies like shading or low-e glazing. Fig. 1.4 shows the daylight distribution without and with different types of shading. A more uniform daylight distribution near the window, however, does not solve the problem of core daylighting.

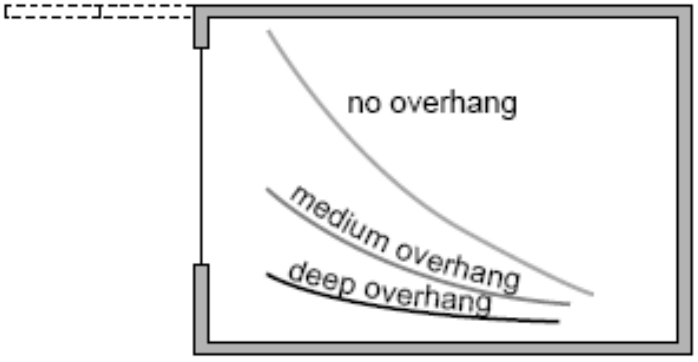

Fig. 1.4. Comparison of three types of shading, *Source: Tips for daylighting with window, LBNL (1997).*

1.2 BACKGROUND RESEARCH

Vertical light pipes were derived as extensions of skylights (Oakley et al., 2000) and could solve the problem of insufficient daylight in deep plan spaces. But they are mostly applicable for top floors of buildings only. Reflective shaft combined with heliostats (Aizenberg, 1997) is one solution but uses precious floor area and was designed for three floors only. Fiber optics based systems are another solution but come at a high price. The horizontal optical light pipe (Beltran et al., 1994, Beltran et al., 1997, Martins-Mogo, 2005) is a simple solution which is applicable for all floors of a multi-storied building.

The earliest study on horizontal light pipes was done by Beltran et al. (1994) which was lined inside with a reflective film and installed in a space as deep as 30 feet from the south window. The light pipe consisted of reflectors which projected out of the south façade as shown in Fig.1.5. The reflectors directed sunrays to a diffuser flush with the ceiling and onto the workplane. Integration of Directional Coefficient Method was used to combine observed photometric data from 1:12 scale models into computer routines to simulate various sky conditions and calculate workplane illuminances. The light pipe achieved over 200 lux of workplane illuminance annually at 27.5 feet annually between 10am-2pm for surface-solar azimuth<30˚.

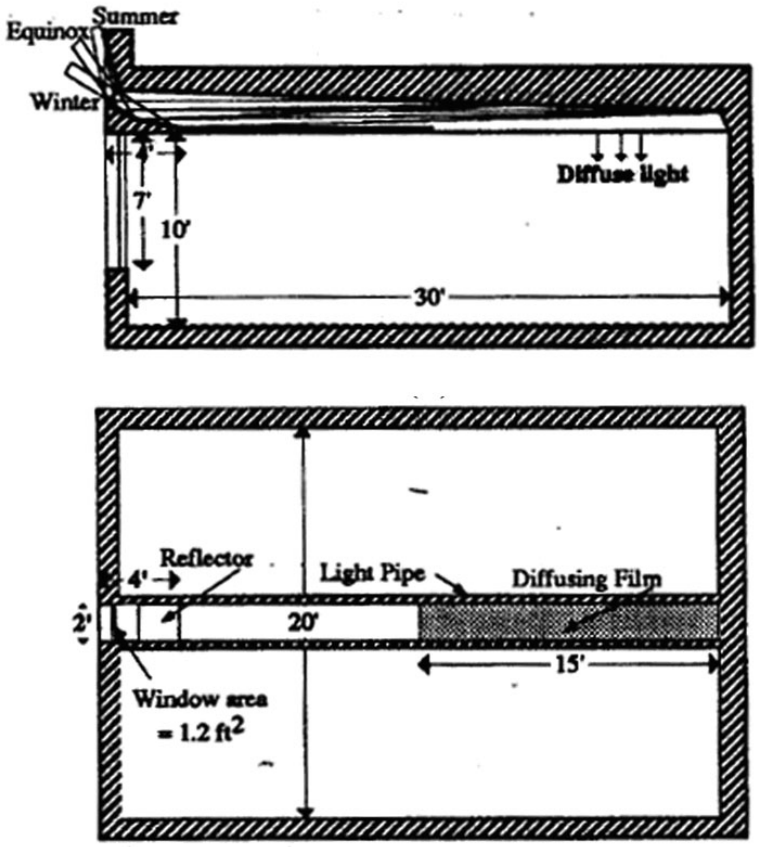

Fig. 1.5. The earliest prototype of optical light pipe. (a). Section, (b) plan. *Source: Beltran et al .(1994).*

Another study by Beltran et al. (1997) analyzed four alternatives of horizontal light pipes using 1:20 scale models, IDC method and DOE-2 simulations for a 20 feet wide and 30 feet deep open office with south fenestration. The light pipes had inlet aperture area varying from 0.2% to 2.6% of floor area. The reflective film used was 95% reflective. In Fig. 1.6 light pipe (a) had a trapezoidal elevation (height decreases from front to back), light pipes (b) and (c) have a rectangular elevation (constant height) and a trapezoidal plan, and light pipe (d) had a trapezoidal section (varying height), trapezoidal plan and the tail end wider by 1 feet.

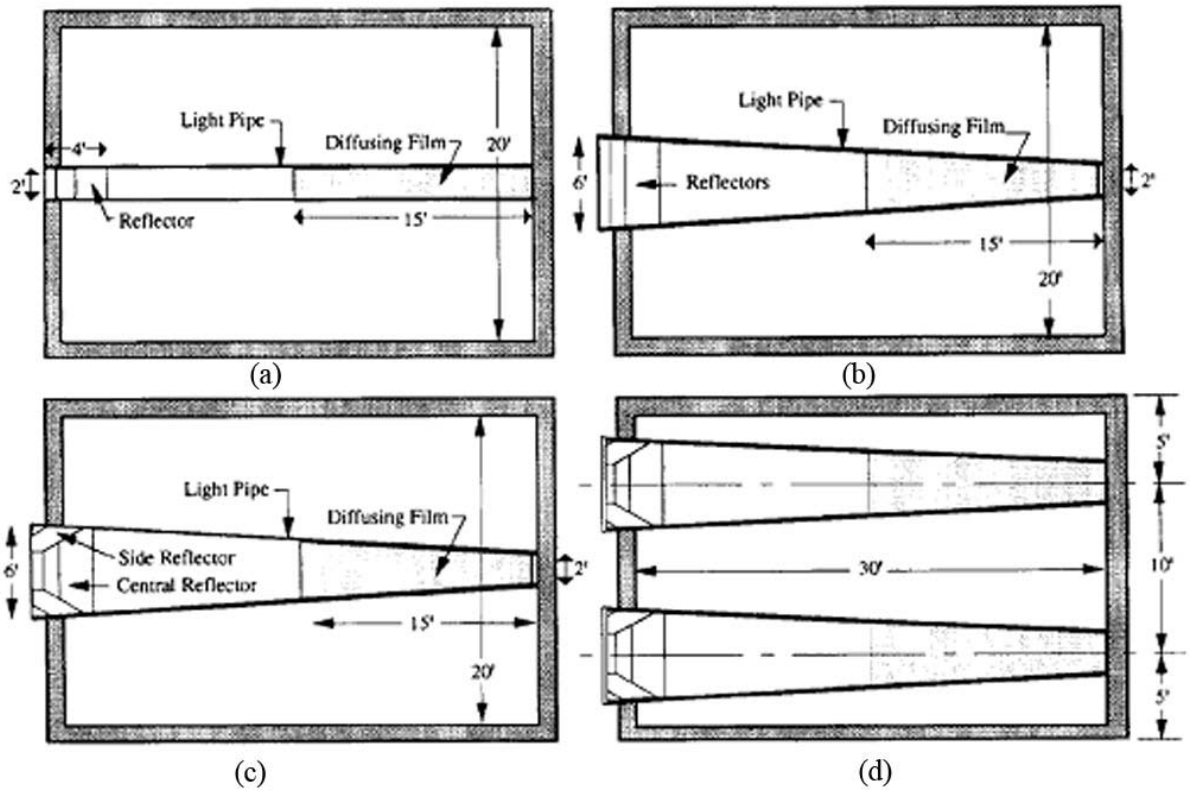

Fig. 1.6. Plans showing the four configurations of light pipes. (a) Basecase light pipe, (b) rectangular section light pipe with central reflectors, (c) rectangular section light pipe with side reflectors, (d) two trapezoidal section light pipes with side reflectors. *Source: Beltran, Lee, Selkowitz (1997).*

The trapezoidal section light pipe with side reflectors performed best with over 200 lux taskplane illuminance at a distance of 27.5 feet from the window between 9am and 3pm with maximum values over 500 lux. It was suggested to place these at center line distances of 15-20ft.

A follow-up on the Beltran et al. (1997) light pipes was done by Martins-Mogo (2005) who constructed two large scale models (scale 1:4) of an office space 20 feet wide and 30 feet deep, one of them with an OLP and compared it to a reference model which did not have the OLP.

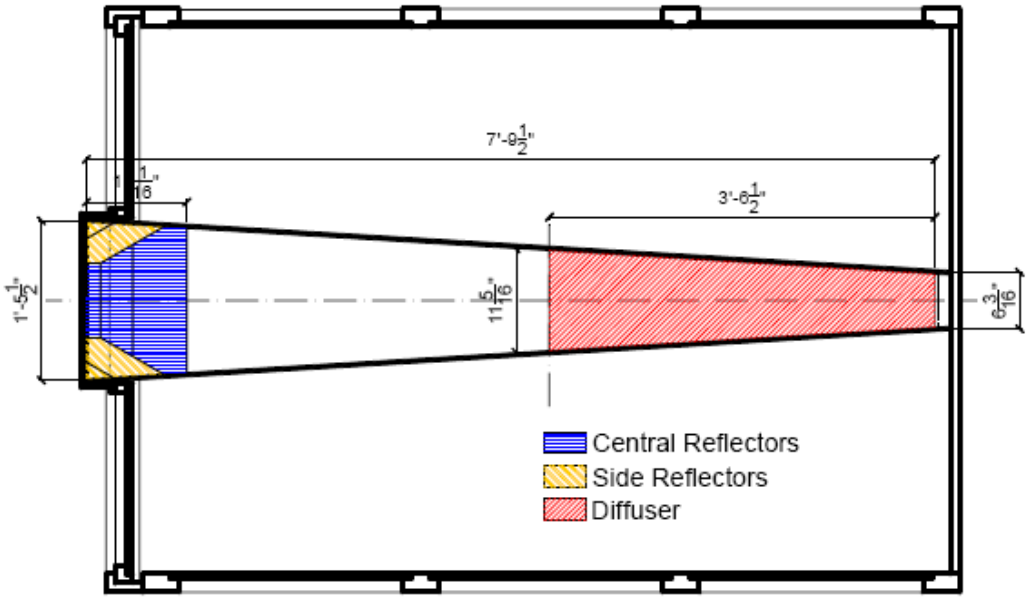

(a)

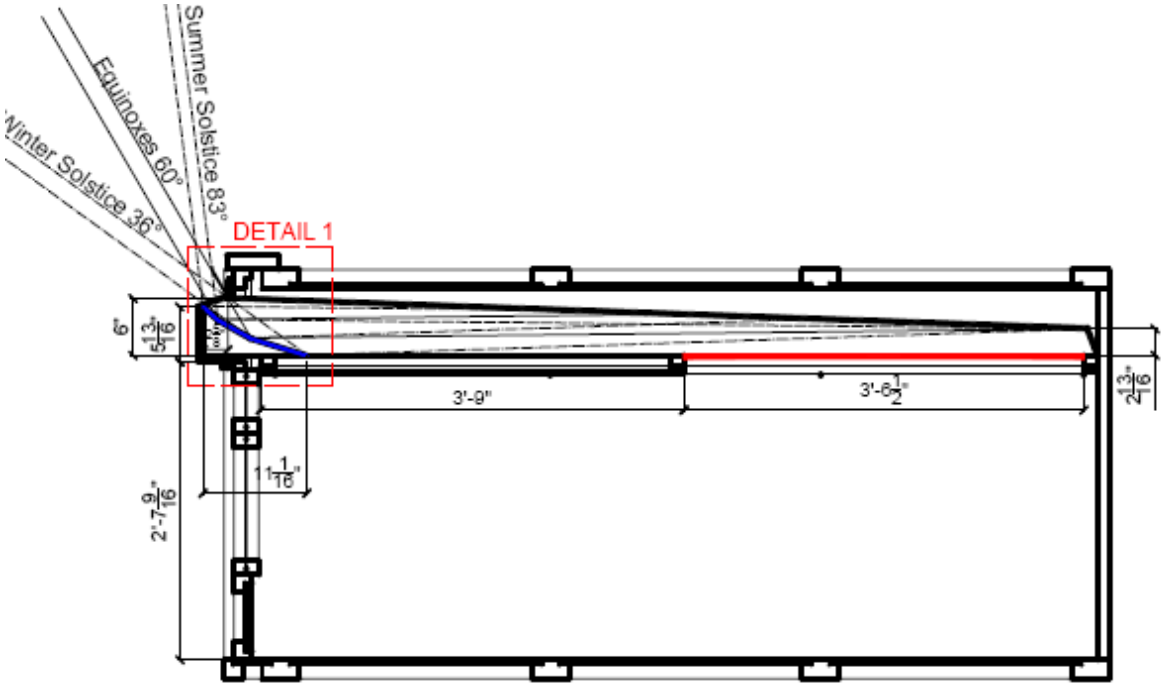

(b)

Fig. 1.7. Optical Light Pipe. (a) Plan (b) Section. *Source: Martins-Mogo, (2005).*

The basic design of the Optical Light Pipe followed the LBNL prototype with a trapezoidal plan and trapezoidal cross section as shown in Fig.1.7. The reflective film used on the interior of light pipe had reflectance>95%. Two diffusers were tested: one with transmittance of 34% and the other with that of 70%. The results showed workplane illuminances at the back greater than 300 lux for close to six hours using the diffuser with 70% transmittance; the maximum illuminance values were over 1000 lux.

1.3 PROBLEM STATEMENT

In all the experiments above, there was a distinct difference between illuminance values in front and back zones leading to non-uniformity; the back zone was perceived darker due to lower illuminance values on the walls and ceiling (Martins-Mogo, 2005). Also observed was an inefficiency to direct oblique angle sunrays before 900 hours and after 1500 hours. Conclusions from the latest experiment (Martins-Mogo, 2005) suggested the use of partitions to avoid any possible direct glare, and shading devices for windows to reduce window to workplane luminance ratio. The need of using building materials that could be used to reproduce a full scale OLP prototype was identified. Also identified was the need to study effect of blinds and shading devices on the south façade in combination with OLP, to represent real office-like conditions.

1.4. HYPOTHESIS

The main hypotheses of the present research is that it is possible to achieve 300 lux of illuminance for more than 6 hours in the back zone of a deep plan office space using an OLP on a clear sky day.

The second hypotheses is that it is possible to achieve more uniform daylight levels by combining a static light shelf (SLS) with OLP.

The third hypotheses is that it is possible to achieve a visually comfortable office space using OLP and a combination of OLP and SLS when the south façade is installed with blinds and exterior shading devices.

1.5. OBJECTIVES

The objective of the present research is to advance the existing research on optical light pipes by proving the above mentioned hypotheses. The specific objectives are as follows:

- Determining if OLP design could be optimized for maximum efficiency using computer based raytracing methods.

- Assessment of materials for construction of OLP and construction of a prototype to be used for long periods of observation and further research.

- Determining if specular light shelf (SLS) could enhance uniformity of daylight conditions when combined with OLP.

- Assessment of any possible glare with use of OLP and the combination of OLP and SLS.

1.6. SCOPE OF RESEARCH

The research addresses office spaces side lit on the south façade. A 20’X30’X13’ module is considered as a typical office bay facing south, with a plenum of 3’. Fig. 1.8. gives the dimensions of the module used. The two models were kept on the roof with minimum external shadow casting objects on the south and therefore do not represent a location like a typical downtown. Though contemporary office spaces have a variety of open, semi-open and enclosed work areas, full height walls enclose the above mentioned module in the present research. A partition of 15” height (5 feet in real scale) was used to represent a partition in the real scale, though partitions of 4’ and 5’2” are more common. The partition height could not be increased due to the fixed height of the opening through which the partition was to be introduced and removed.

The designs of the OLP and SLS were done for the latitude of 30˚ 36’N, and would need substantial modification for use in other latitudes. Raytracing was limited to direct solar component only, though both the optical light pipe and the light shelf were known to reflect diffuse solar component from the sky as well.

Observations were made for a set of days which were within a month of each other. Due to time constraint, comparisons were made for clear and cloudy sky conditions only. For the life-cycle benefit and full scale integration of the optical light pipe with electrical lights, it would be necessary to make an annual observation.

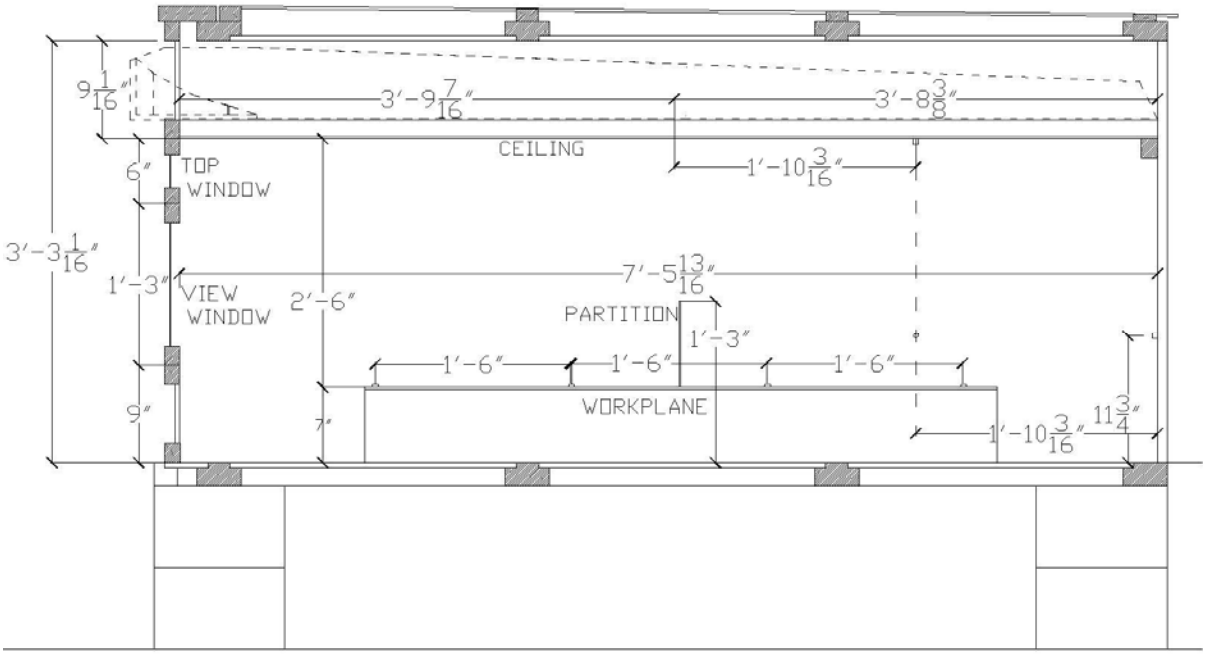

Fig. 1.8. Section of Test Model showing location of OLP and sensors.

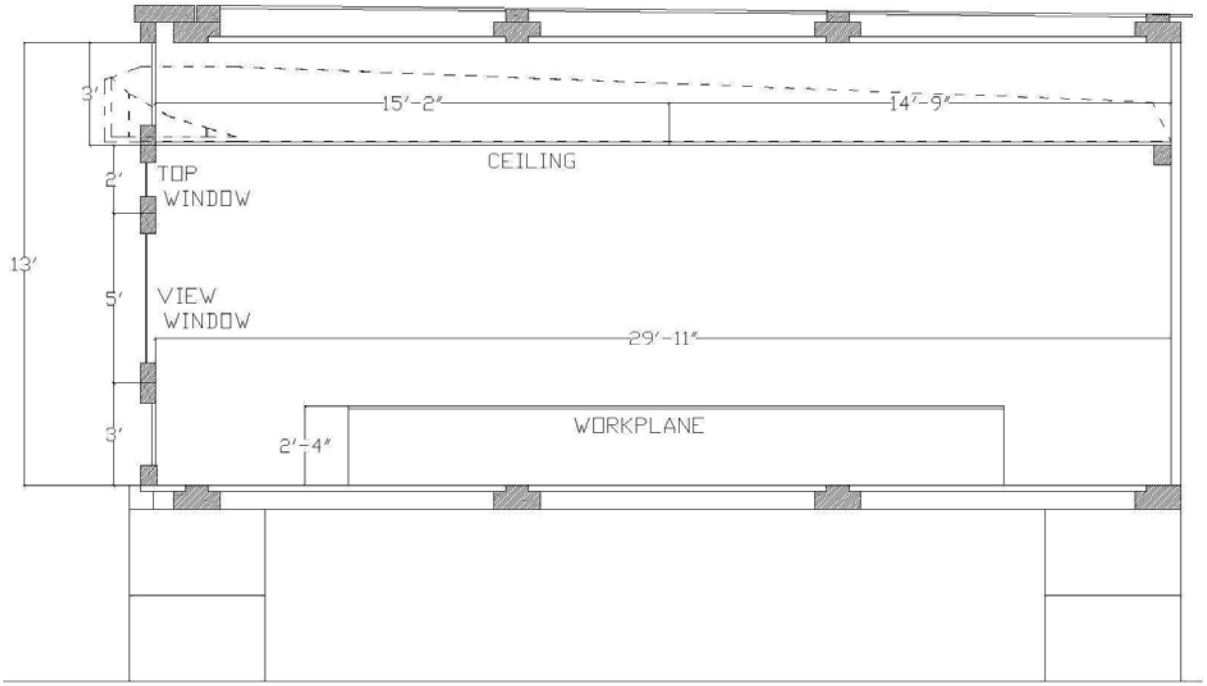

Fig. 1.9. Section of the real space represented by the models.

1.7. METHODOLOGY OF RESEARCH

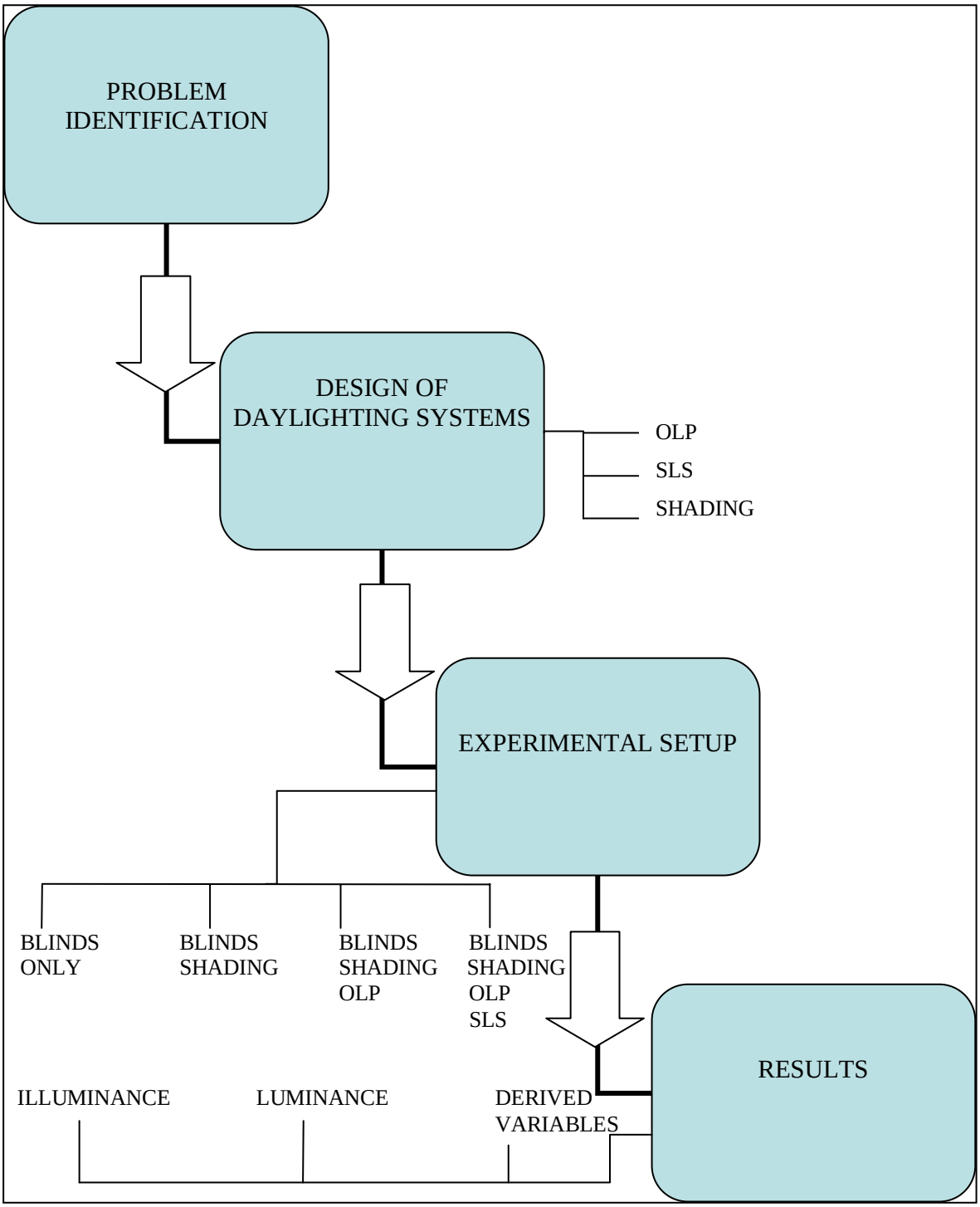

Fig. 1.10. Methodology of research.

1.8. LIMITATIONS OF RESEARCH

- One of the limitations of this research was the assumption of an unobstructed southern sky which may not be a typical situation for commercial buildings.
- Evaluations in the research were based on short periods of time, namely 8 clear days in February and March of 2008, which lie between winter and equinox sun angles.
- A number of obstacles closer to Reference Model (existing building, railing) blocked the sky component and hence the amount of daylight in Reference Model (refer to appendix k for details).
- Miro-Silver sheets were hand-cut using a metal cutter and alignment with the machine cut plywood was not perfect, leaving unwanted gaps at edges and joints. This may have reduced overall lighting efficiency of the OLP.
- One other limitation was the low reflectance value of partition (25%) used in the project as compared to the prescribed minimum reflectance value for partitions (40%) set by Illuminating Engineering Society of North America (IESNA).
- One of the limitations of clear glass used in the research was the cohesion of water droplets after rain which tend to stay on the glass surface of the collector for a longer period of time as opposed to the vertical face of windows.
- Lastly, while the daylighting conditions of the actual space were represented accurately in the scale model, the exact constructability issues do remain unsolved until the model is built in full scale.

II. DESIGN OF DAYLIGHTING SYSTEMS

2.1. OPTIMIZATION OF OLP DESIGN

The design of OLP consisted of optimizing the overall geometry using raytracing and identifying appropriate materials for construction which could be used for a full scale reproduction later on. The Martins-Mogo prototype was the starting point for optimizing the geometry. The nomenclature of OLP was retained and three distinct parts identified as: collector, transport section and diffuser.

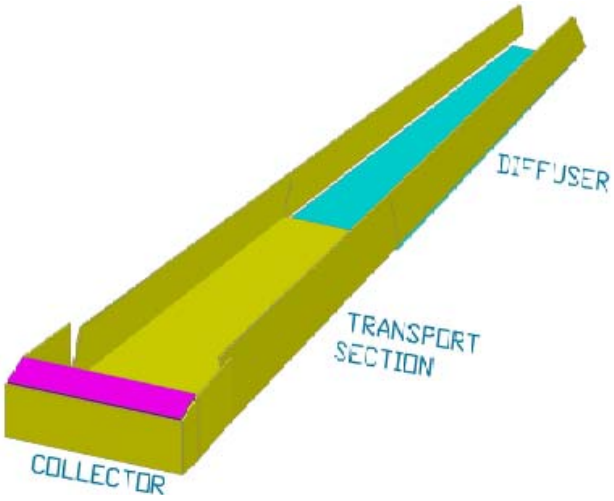

Fig.2.1. Three parts of OLP with the ceiling removed.

The collector would house primary-reflectors and side-reflectors to reflect direct sunrays through the transport section and right above the diffuser. The geometry of principal reflectors was derived using manual raytracing to direct all rays entering the collector towards the ceiling of diffuser for solstices and equinox.

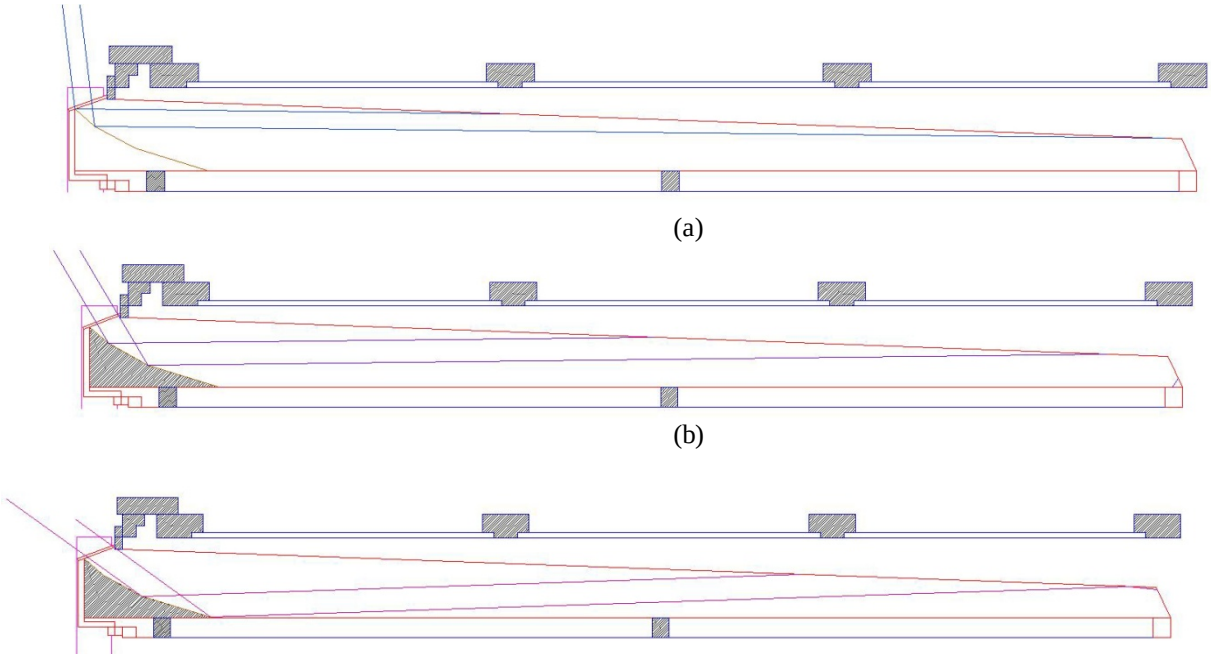

Fig.2.2. Raytracing to define angles of primary reflectors. (a) Raytracing for June 21, (b) March 21, (c) December 21.

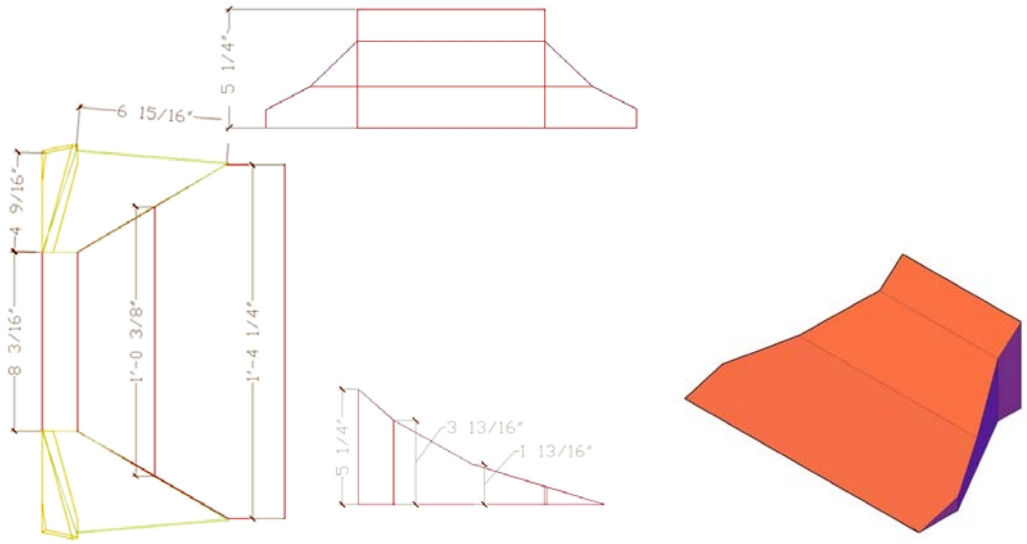

Fig.2.3. Drawings and model of principal reflectors

As mentioned earlier, the Martins-Mogo prototype had useful daylight output for close to 6 hours. For the OLP to be useful for more number of hours, it needed to direct sunrays at low angles effectively. The first attempt to do so was by tilting the side walls of the Martins-Mogo prototype by 5° (5DEG) and then 10° (10DEG). Raytraces were performed for June 21, March 21 and December 21 with the position of diffuser and light source constant for each alternative and only the geometry of OLP changing. The three days were chosen because solstices represent two extreme conditions of sunpath and equinox represents the middle condition of sunpath. The output on diffuser for other days would lie in between these values. 5DEG and 10DEG had a better output between 9am and 3pm for March 21 and December 21 as shown in Fig. 2.5.

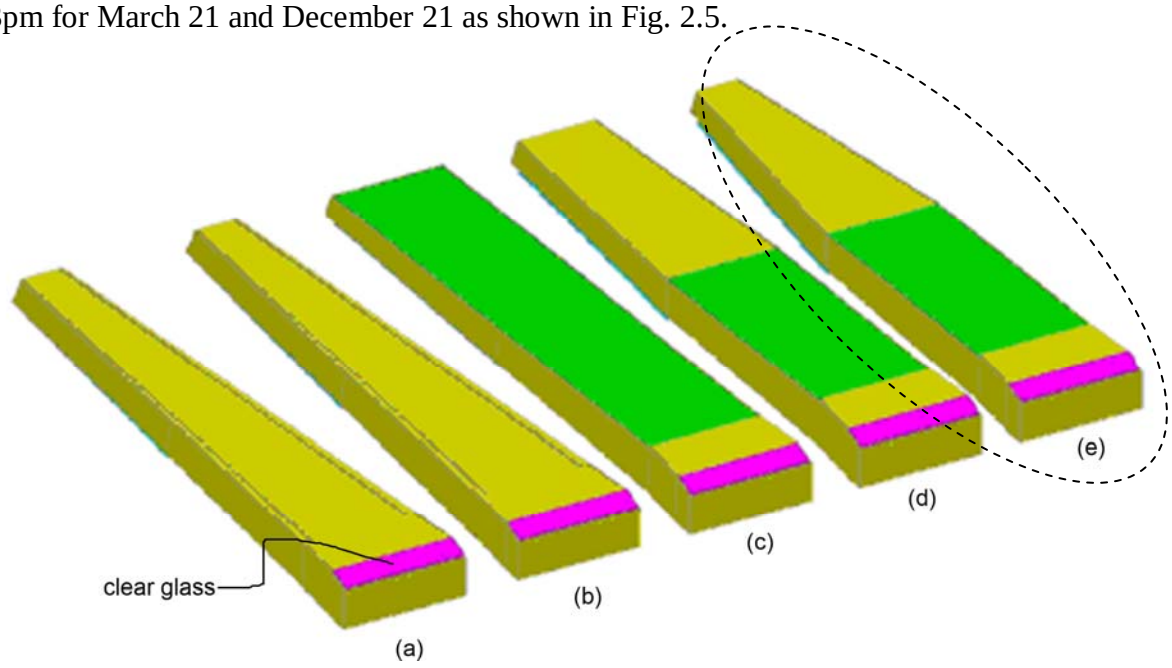

Fig. 2.4. Different prototypes tested with raytracing. (a) Martins-Mogo protytype, (b) 5DEG, (c) 6F6B, (d) 6F4B, (e) 6F2B5C.

With different raytraces it was observed that most of the sunrays at low angles underwent multiple reflections laterally and lost their intensity before reaching the diffuser

(refer to Appendix A: Ray-tracing with Trace-Pro). A prototype with a constant width of 6feet (6F6B) was then tested to observe if increasing the width reduces lateral reflections. 6F6B performed even better than 5DEG and 10DEG on all the three days.

With the objective of reducing the overall volume of OLP, the width of the back-half of transport section was reduced to 4 feet (6F4B) and then to 2 feet (6F2B) while keeping the width of front-half at 6'. Fig. 2.4. shows the geometry of some of these variations. The output from 6F2B was less than 6F6B and 6F4B for December 21. Rotation of the sidewalls of the back-half of transport section by 5° (6F2B5C) increased this output to match that of 6F6B. Further rotation to 10° (6F2B10C) and 15° (6F2B15C) did not change the output significantly. Hence, 6F2B5C was chosen as the final design because of maximum output for sunrays at low sun angles, and a reduced overall volume.

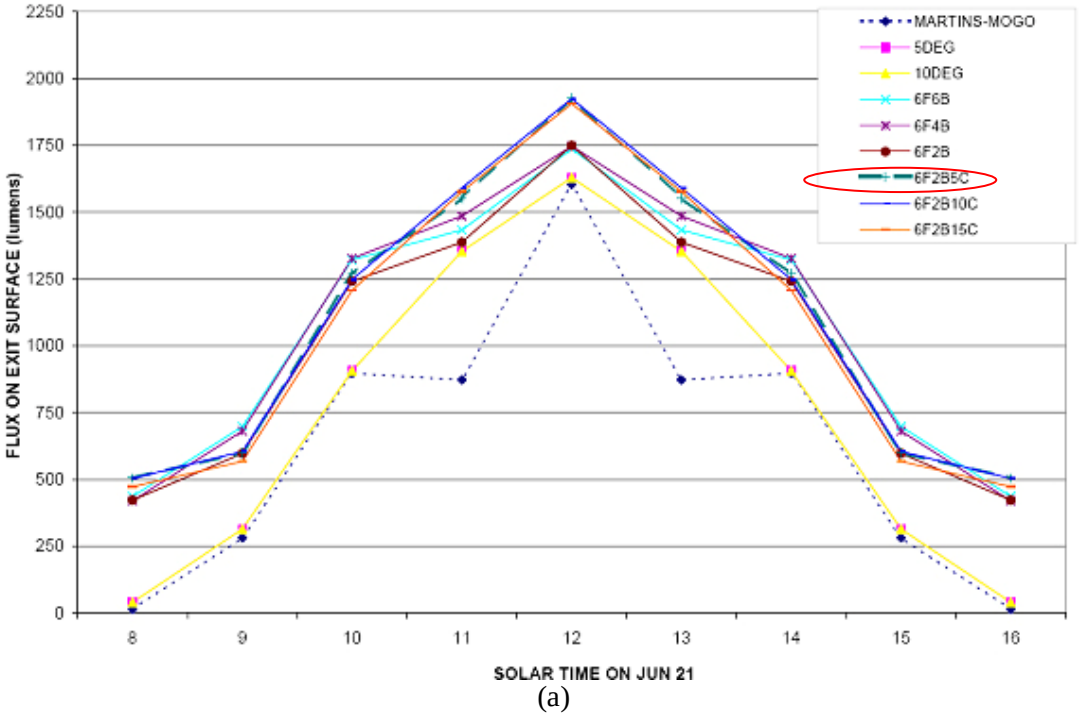

(a)

Fig.2.5. Output flux on diffuser for the three test days at different times. (a) June 21, (b) March 21, (c) December 21.

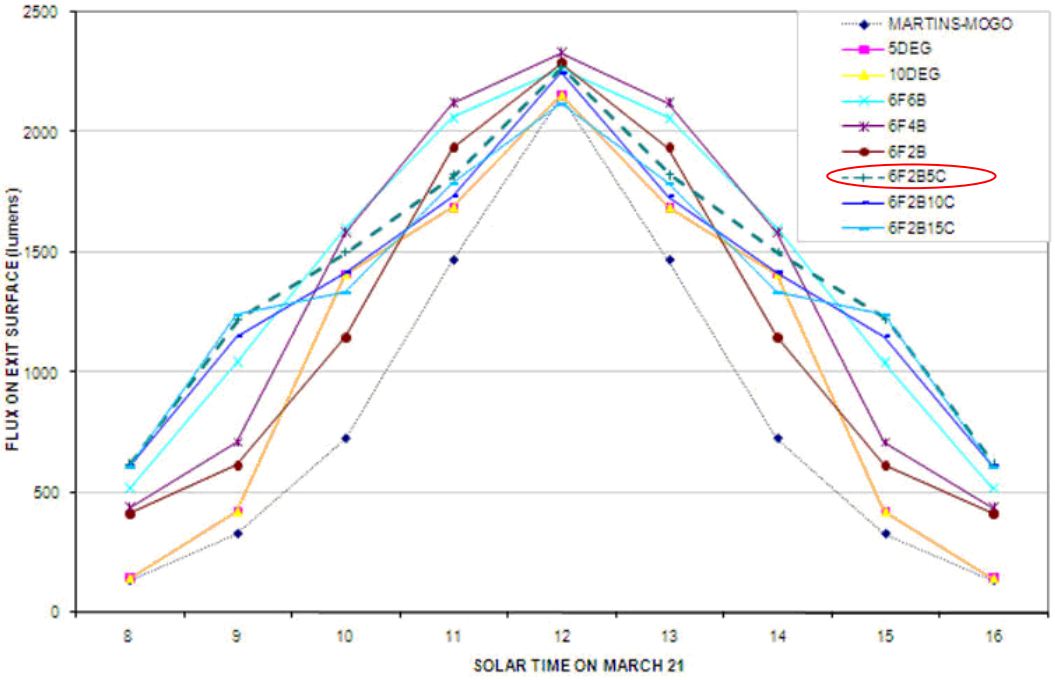

(b)

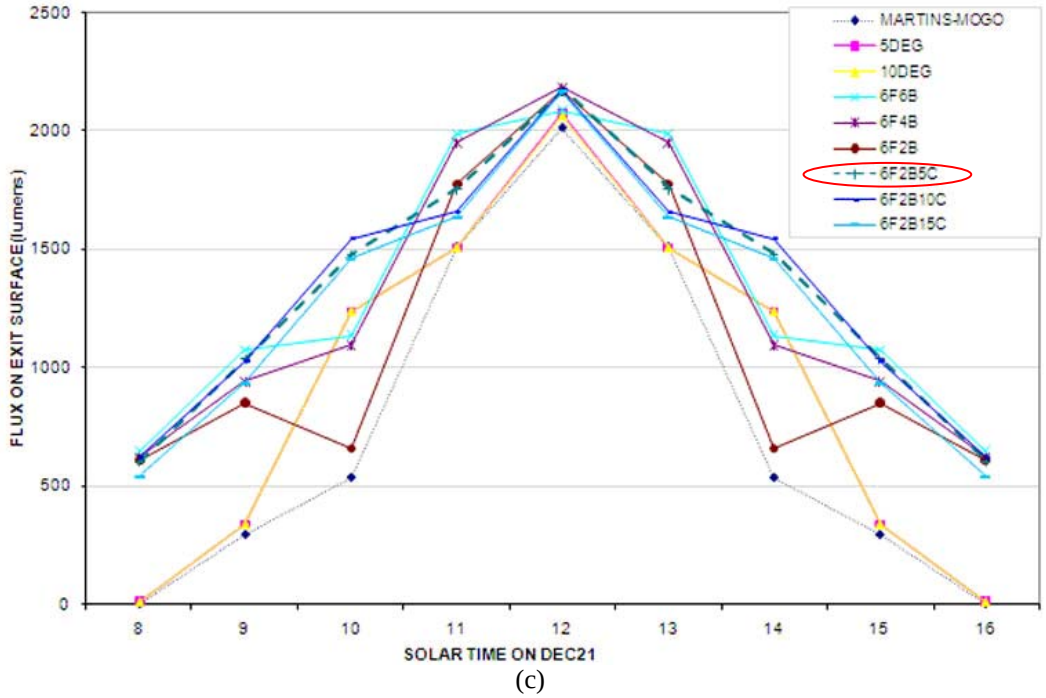

(c)

Fig.2.5. Continued.

Table 2.1. gives a summary of all the prototypes.

Table 2.1. Summary of various OLP prototypes tested with Trace-Pro.

	MARTINS-MOGO PROTOTYPE	5DEG	10DEG	6F6B	6F4B	6F2B	6F2B5C	6F2B10C	**6F2B15C**
DECRIPTION	REFERENCE	SIDEWALLS OF FRONT & BACK TRANSPORT SECTIONS ROTATED IN BY 5°	SIDEWALLS OF FRONT & BACK TRANSPORT SECTIONS ROTATED IN BY 10°	BOTH FRONT AND BACK TRANSPORT SECTIONS WIDENED TO 6FEET	BACK TRANSPORT SECTION REDUECD TO 4FEET	BACK TRANSPORT SECTION REDUECD TO 2FEET	SIDEWALLS OF BACK TRANSPORT SECTION ROTATED IN BY 5°	SIDEWALLS OF BACK TRANSPORT SECTION ROTATED IN BY 10°	SIDEWALLS OF BACK TRANSPORT SECTION ROTATED IN BY 15°
PERFORMANCE	REFERENCE	BETTER THAN REFERENCE ON MARCH21 AND DEC 21 BETWEEN 900 HRS. & 1500HRS.	BETTER THAN REFERENCE. ON MARCH21 AND DEC 21 BETWEEN 900 HRS. & 1500HRS	BETTER THAN REFERENCE, 5DEG, AND 10DEG ROUND THE YEAR	BETTER THAN REFERENCE. DECREASED OUTPUT AS COMPARED TO 6F6B BEFORE 1100HRS. & AFTER 1300HRS.	BETTER THAN REFERENCE. DECREASED OUTPUT AS COMPARED TO 6F6B BEFORE 1100HRS. & AFTER 1300HRS.	BETTER THAN REFERENCE. OUTPUT COMPARABLE TO 6F6B BEFORE 1000HRS. AND AFTER 1400HRS.	BETTER THAN REFERENCE. OUTPUT SIGHTLY LESS THAN 6F2B5C FOR SOME HOURS	BETTER THAN REFERENCE. OUTPUT SIGHTLY LESS THAN 6F2B5C FOR SOME HOURS
AREA OF REFLECTIVE SHEET FOR A FULL SCALE PROTOTYPE (sf)	18.4	18.3	18.3	22.0	21.2	20.4	20.3	20.3	20.3

Lastly, the sidereflectors were optimized to direct sunrays for low sunangles. The sunpath was proportionately divided into three areas corresponding to principal reflector, side-reflector-1 and side-reflector-2. Physical models of various options of sidereflectors were also constructed (for the comparison of different sidereflectors, refer to Appendix A: Ray-tracing with Trace-Pro).

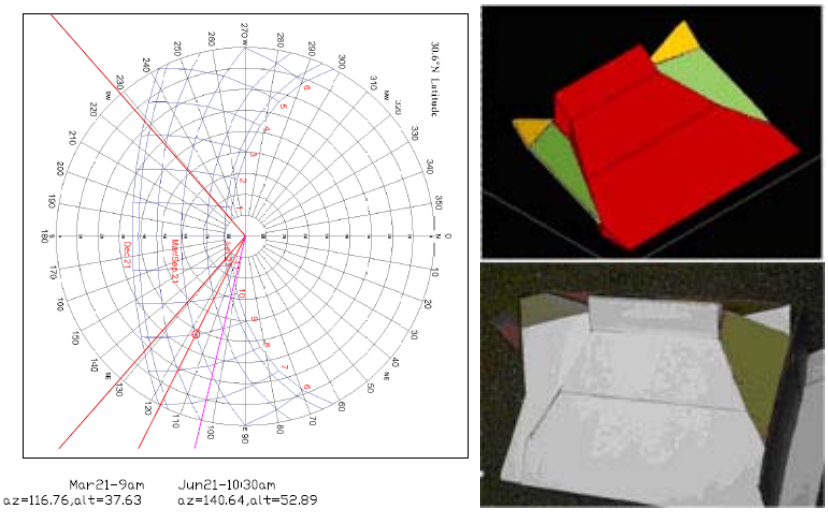

(a) (b)

Fig.2.6. Design of sidereflectors. (a). Division of sunpath into three parts corresponding to the three reflectors, (b) small scale models compared for constructability with computer models.

The transport section and the reflectors were constructed of MiroSilver, a reflective aluminum film with reflectance varying from 93% to 99% (refer to Appendix H for characteristics of MiroSilver). The diffuser was constructed of DFPM from Optigrafix with a transmission of 87% and haze of 88% (for selection test of diffuser refer to Appendix E: Selection of Diffuser for OLP). Table 2.2 compares areas of reflective film and diffuser used for OLP in the present research and Martins-Mogo prototype.

Table 2.2. Comparison of areas between new OLP and Martins-Mogo prototype. (a) Reflective film, (b) diffuser.

	BASE (sf)	SIDEWALLS (sf)	CEILING (sf)	BACKWALL (sf)	FRONTWALL (sf)	REFLECTORS (sf)	
OLP film, present research (93% - 99% reflective)							
BACK TRANSPORT SECTION	0.06	2.68	3.39	0.14			6.27
FRONT TRANSPORT SECTION	4.39	4.2	5.38		0.68	1.47	13.97
						total	20.24
OLP film, Martins-Mogo prototype (95% reflective)							
BACK TRANSPORT SECTION	0.06	2.7	2.61	0.14			5.51
FRONT TRANSPORT SECTION	3.79	4.26	4.84		0.68	1.47	12.89
						total	18.4
						%difference	**9.1%**

(a)

	DIFFUSER (sf)
OLP diffuser, used in present research (T_v=87%)	3.39
OLP diffuser used in Martins-Mogo prototype (T_v=70%)	2.68
%difference	26%

(b)

Area of reflective sheet that would be needed in a full scale prototype would be 324 sq.ft. while that of the diffuser would be 54 sq.ft. Fig.2.7 shows dimensions of the proposed OLP in two parts: front transport section and back transport section. Dimensions shown are for a full scale prototype.

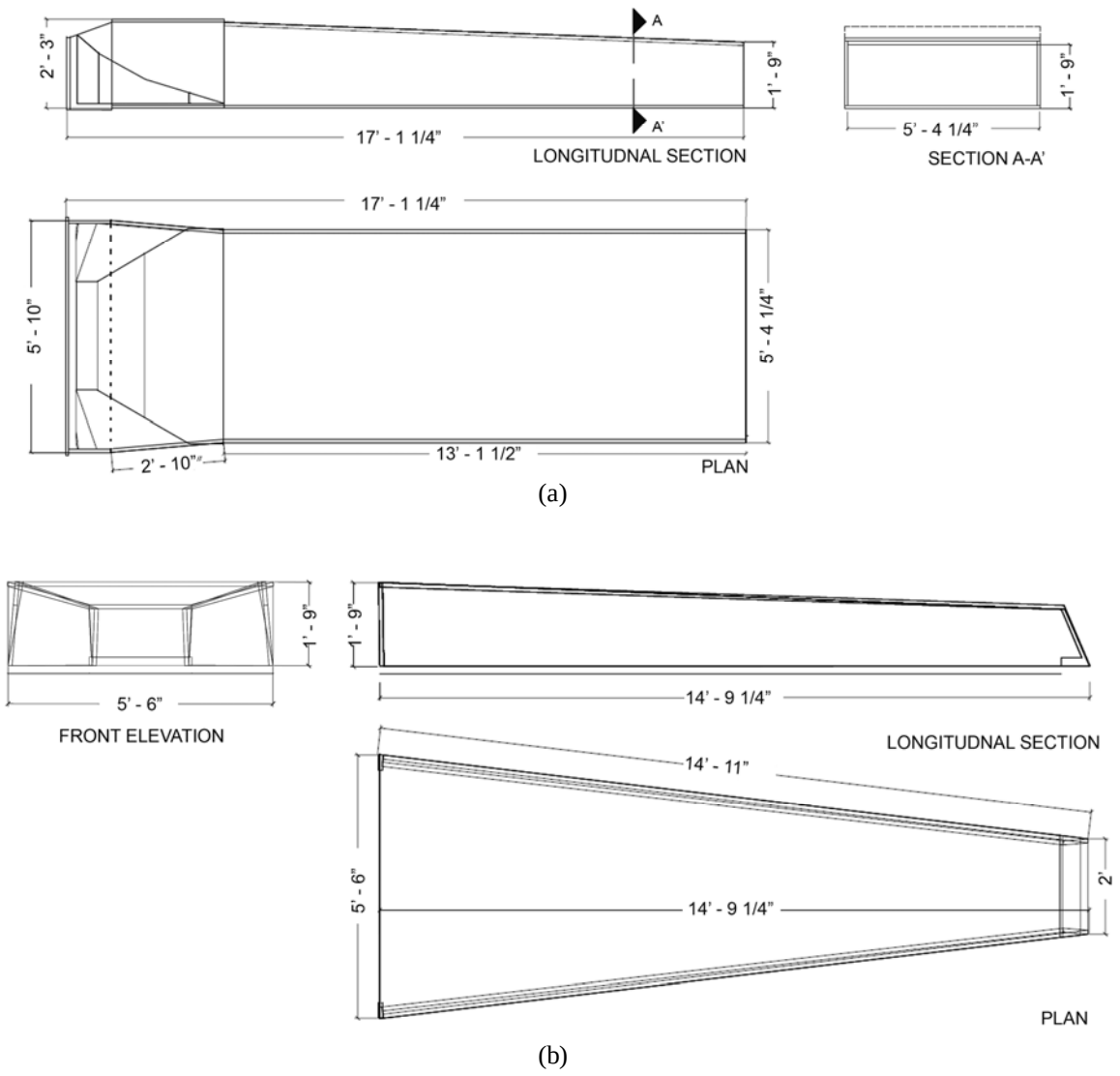

Fig.2.7. Dimensions of OLP in full scale. (a). Plan and sections of front transport section, (b) plans, section and elevation of back transport-section and diffuser.

Fig. 2.8 shows step-by-step construction of the front transport section. Fig. 2.9 shows the same for the back transport section and Fig. 2.10 shows the OLP with the two sections joined together.

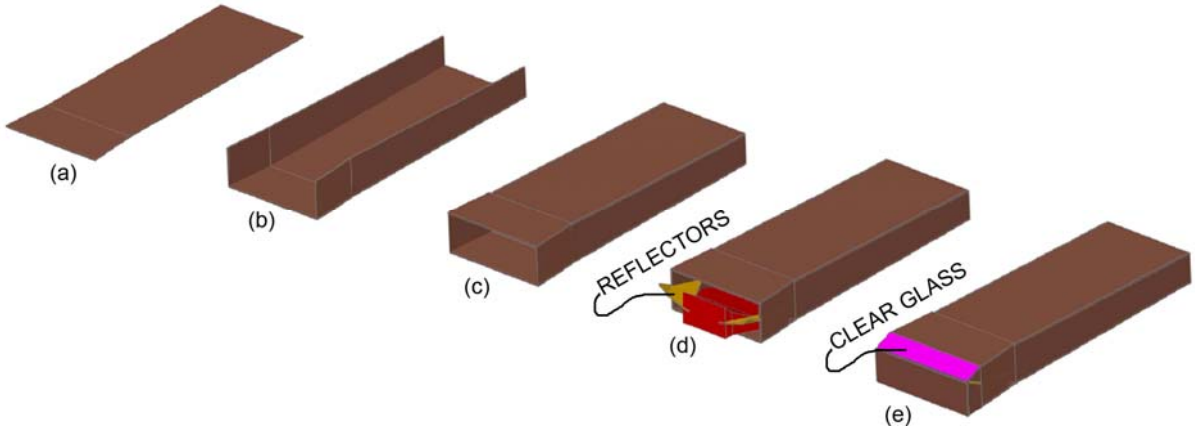

Fig.2.8. Step-by-step construction of front transport section of OLP from (a) to (e).

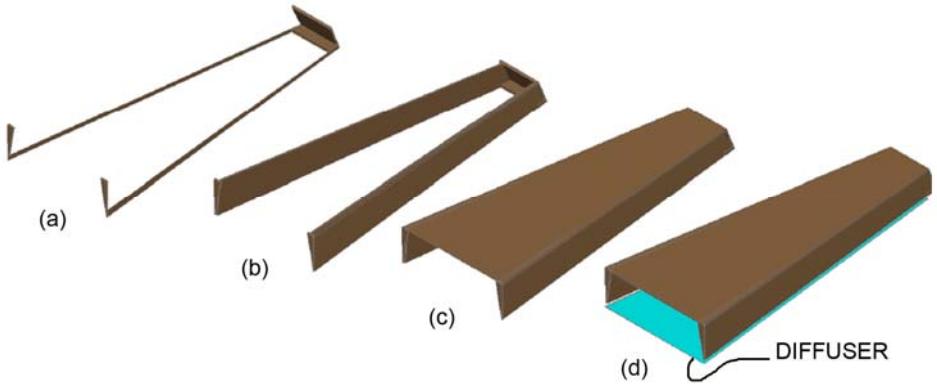

(b)

Fig.2.9. Step-by-step construction of back transport section of OLP from (a) to (d).

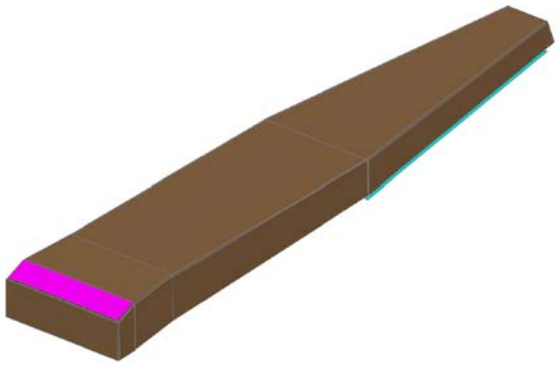

Fig.2.10. OLP with front and back transport sections joined.

2.2. ADAPTATION OF SLS DESIGN

The objective of using SLS in the present research was to increase daylight uniformity when combined with the OLP. The design of specular light shelf (SLS) follows from an earlier set of experiments on light shelves at LBNL (Beltran et al., 1994, Beltran et al., 1997). The single level light shelf, was the best strategy to redirect sunlight to ceilings and walls as well as for redirecting oblique sun angles (Beltran et al., 1997). It was effective between 10am to 2pm due to the rays hitting the wall at lower sun angles.

The reflectors of SLS in the present research were designed to reflect direct sunlight to the back-half of ceiling (refer to Appendix L for more raytrace drawings). The LBNL design, shown in 2.11a was adapted to the latitude 30˚ 36'N alongwith: (a) addition of two planes to block low sun angle at Dec 21, 8am (solar time), (b) extension of the third reflector to block Dec 21, 9am & 10am (solar times) rays. Fig 2.11b shows the dimensions of the SLS and Fig. 2.12. shows the effect of additions. The width of SLS used in the present research is 4' 4-$^{5}/_{8}$" in full scale (1' 1-$^{3}/_{16}$" in 1:4 scale) while the LBNL design (Beltran et al., 1994) was close to 5 feet wide. A compound reflective film from 3M acted as the optical surface. It was selected because of its ability to reflect and disperse the reflected rays within a 12° - 15° angle.

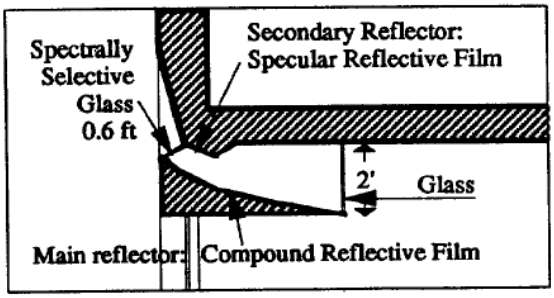

(a)

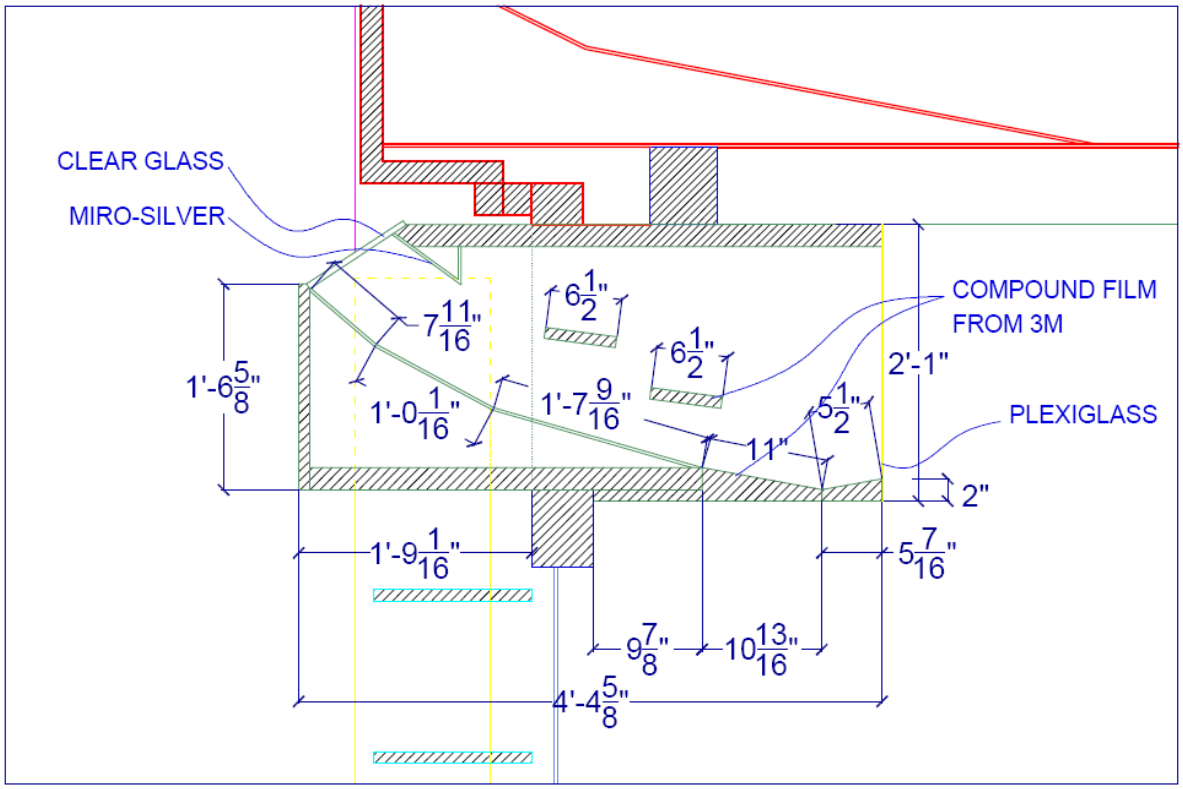

(b)

Fig. 2.11. Dimensions of specular light shelf (a) LBNL prototype, *source: Beltran et al .(1994),* (b) SLS used in present research.

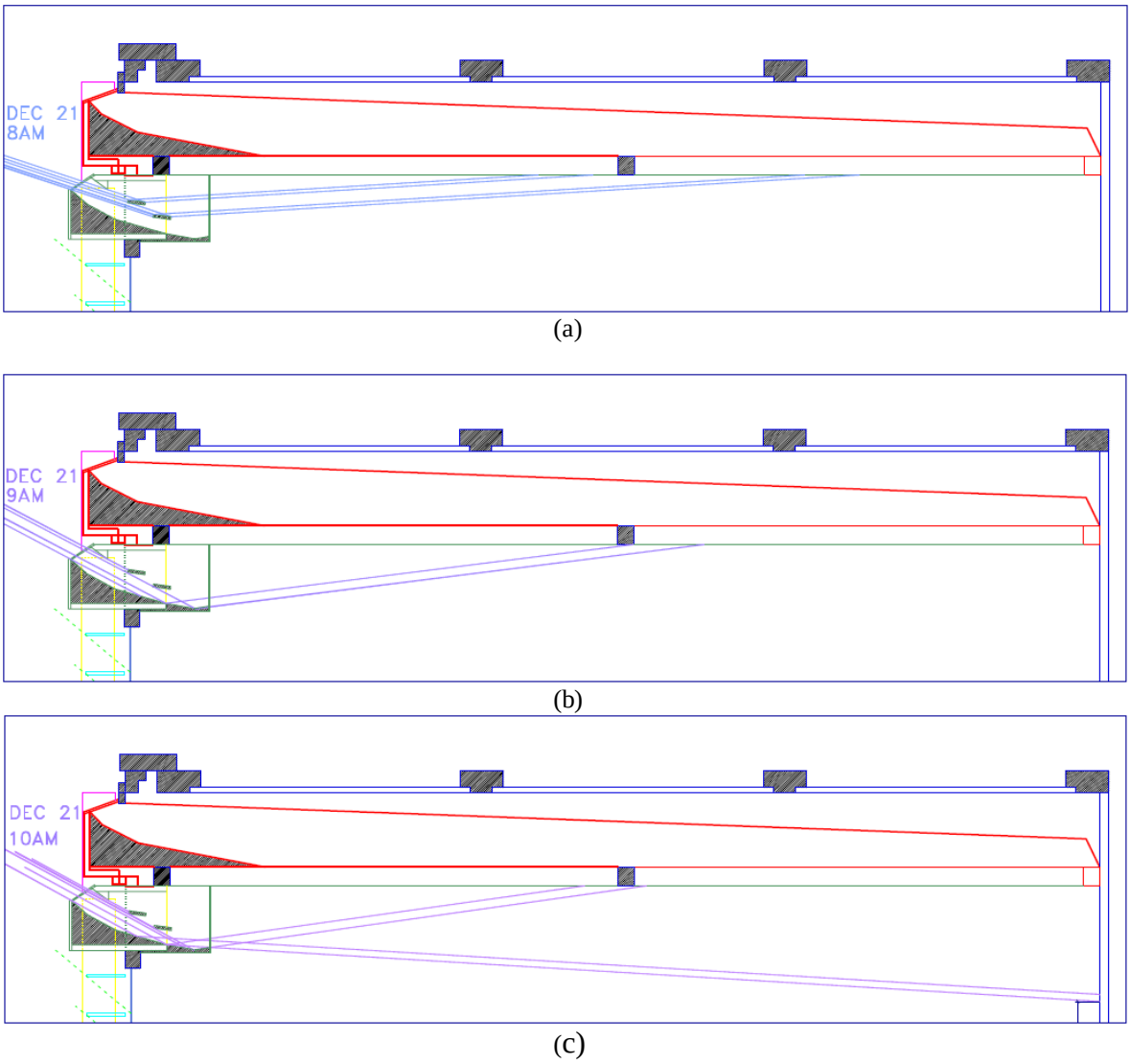

Fig. 2.12. Raytrace for Dec.21showing the effect of additions to the LBNL design. (a) 8am solar time, (b) 9am solar time, (c) 10am solar time.

The SLS was broken into two identical modules (shown in Fig.3.4) to avoid deflection of plywood used for its construction and also to allow easier handling than one bulky module. One of the modules is shown in Fig.2.13. A glass of transmittance 87%, which represents single clear glazing, was used to cover the front aperture. Plexiglas, which

had visual transmittance> 90% was used to cover the back to allow maximum transparency to outgoing sunrays. A reflective obstacle topped with Miro-Silver was placed next to the aperture to cut off very low sun altitudes. A 2" high obstacle was the last addition to arrest the Dec 21, 10am rays from going down any further than 6 feet as shown in Fig. 2.12c.

(a) (b)

Fig. 2.13. Specular light shelf. (a) Front view, (b) back view without Plexiglass.

Table 2.3 compares the area of clear glass aperture used in OLP, SLS and Martins-Mogo prototype. The window to wall area ratio in OLP case was kept the same as in the Martins-Mogo prototype, while it got reduced in SLS case due to the SLS occupying the top portion of window (refer Fig.3.4).

Table 2.3. Comparison of clear glass area for OLP, SLS and Martins-Mogo prototype.

	OLP only (sf)	SLS only (sf)	SLS & OLP (sf)	MARTINS-MOGO prototype (sf)
CLEAR GLASS APERTURE (in full scale)	5.5	14.7	20.2	5.5
% OF FLOOR AREA	0.91	2.43	3.6	0.91
Window to wall area ratio	33.4	26.4	26.4	33.4

2.3. DESIGN OF SHADING DEVICE

Exterior shading device was provided for year round shading with the objective of minimizing heat gains while maintaining views to outside. An outside view is preferred for all work areas (Heschong et al., 2003); hence a shading strategy which would provide an outside view was preferred. Also, because multiple shading devices have a better daylight distribution as compared to a single large one (Derek, 2004), a balance was reached between the two criteria. Shading needs were plotted on sunpath diagram and then superimposed on a shading mask protractor to derive angles for shading devices as shown in Fig.2.14 (refer Appendix G for details). Four horizontal overhangs had a 40° profile angle and the frame on which they were mounted acted as a vertical shading device for 20.5° azimuth. As can be seen in Fig.2.14a, the shading devices allow sun in from October 21 to March 21.

Subsequently, blinds were installed to cover sun angles for these times. It was deduced from literature study that users may close blinds to avoid direct sun on VDT screens or to reduce heat gain (Inkarojrit, 2005, Boyce et al, 2003). Blinds are opened for visual contact and daylight, and are more likely to be opened at the beginning of the day and closed later on (Inkarojrit, 2005). For lack of an automated motorized system, semi-open blinds were chosen to represent the situation. 1” aluminum blinds were installed and kept at 45º to prevent direct sun penetration round the year. The angle was derived from the lowest profile angle of the sun at Dec 21, 8am (solar time) as shown in Fig. 2.14d.

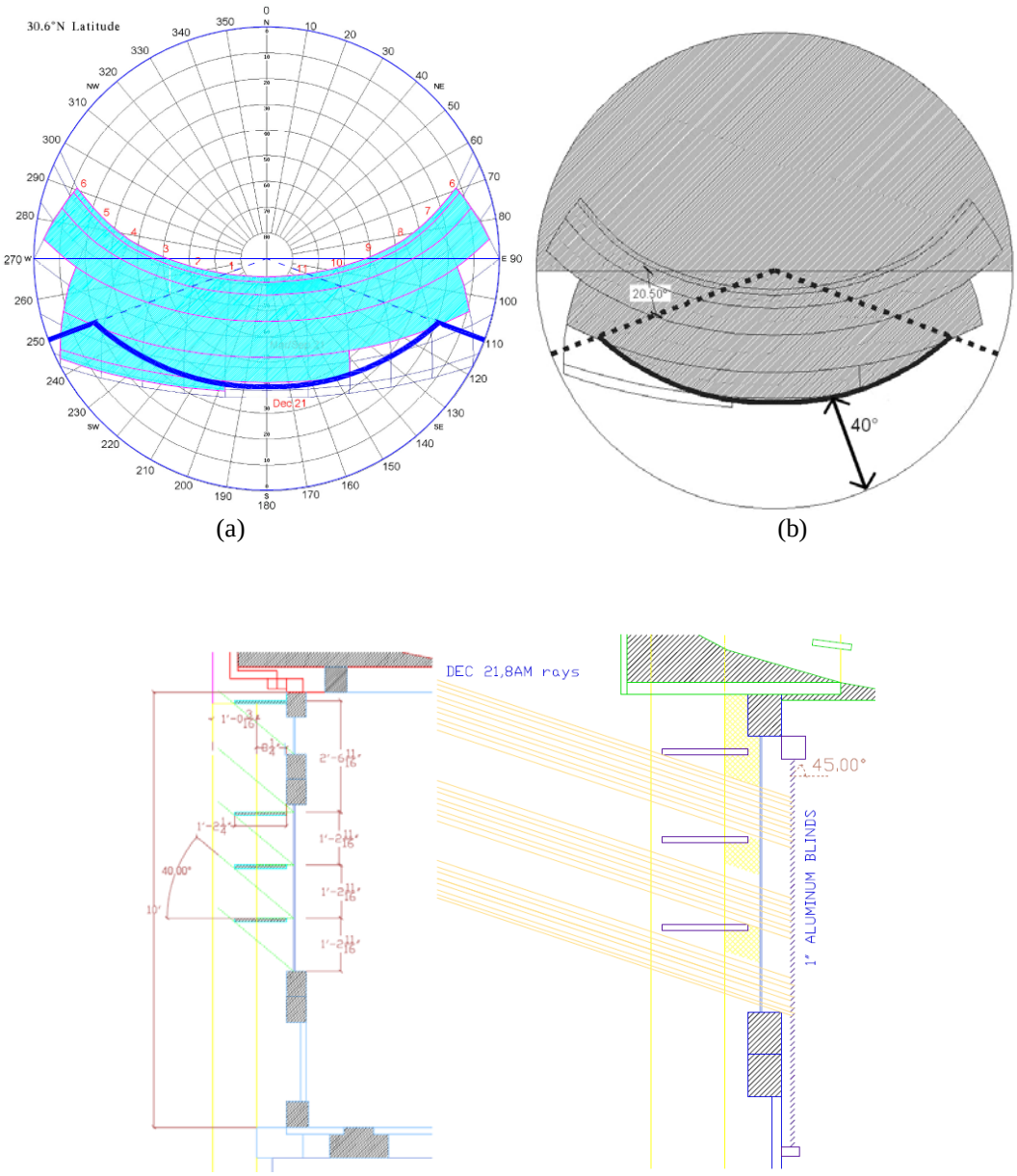

(a) (b)

(c) (d)

Fig.2.14. Shading Devices & blinds. (a) Shading needs plotted on sunpath, (b) profile angle from shading mask used to derive the extent of overhang, (c) profile angle shown in section for a full-scale prototype, (d) blinds kept at 45° to block 8am sunrays on Dec 21.

III. EXPERIMENT METHODOLOGY

3.1. EXPERIMENTAL SETUP

The two 1:4 scale models that were used for this experiment were constructed during an earlier research by Martins-Mogo (2005). One would be referred to as Reference Model with fixed daylighting design with blinds and shading devices. The other would be Test Model, which would have the OLP and SLS installations. A measured drawing of the models was performed before any design process was started. To view or take illuminance measurements, the models had two openings on the north and one opening on the south, both of which were covered otherwise. The models were cleaned and painted from time to time before the final installation. A new ceiling was installed on each of them to support the new heavier OLP prototype. Table tops, representing furniture, were also installed between the three rows of sensors inside each model, and a removable partition was designed to be brought in and out from the side opening of Test Model. Following are the average surface reflectances of interior surfaces measured by an LS-100 Konica Minolta luminance meter: floor - 0.21, walls – 0.43, ceiling – 0.81, furniture – 0.35, partition – 0.25. All surfaces, except the partition, are within IESNA standards which recommend 0.2 to 0.4 for floors, 0.5 to 0.7 for walls, 0.8 or more for ceilings, 0.25 to 0.45 for furniture and 0.4 to 0.7 for partitions. The partition of 0.25 reflectance was preferred over the next available value of 0.5 to reduce any significant effect of reflection in the back zone. The transmittance of clear glass existing on the windows was 0.87, measured by Konica Minolta illuminance meter (some discrepancies could occur due to scratches and stains existing on the glass). The same glass type was used to cover the OLP and SLS.

Blinds and shading devices were installed on both models as shown in Fig.3.1. and Fig.3.2. Test Model with OLP is shown in Fig.3.3. The addition of SLS required removal of the top shading device as shown in Fig.3.4. Window to wall-area ratios are also mentioned.

Fig. 3.1. Models with blinds installed. The opening for OLP in Test Model is covered (WWAR=33.4).

(c) (d)

Fig.3.2. Models with shading device installed. The opening for OLP in Test Model is covered (WWAR=33.4).

Fig.3.3. OLP installed on test model, presently covered (WWAR=33.4).

Fig.3.4. Two SLS prototypes installed on test model below OLP (WWAR=26.4).

A solar site analysis was conducted to analyze shadow effects of existing onsite obstacles on both the models. It was found that Reference Model was shaded up to 900 hours for almost half the year (refer to Appendix K). Test Model was shaded up to 830 hours from December 10 to January 10. Since most offices work between 8am to 6pm, it

was decided to compare Reference Model with the Test only after 900 hours. Evaluations were made for the following conditions:

1. Blinds only (without and with partition)

This was the first reference condition representing office spaces with only blinds as the daylight controlling component. Both Reference Model and Test Model were similar in this condition.

2. Blinds and shading device (without and with partition)

This represented another reference case, better than the 'blinds only' case because of presence of shading devices. This could be compared to a typical contemporary office space. Both Reference Model and Test Model were similar in this condition.

Reference Model was kept fixed after this.

3. OLP, blinds and shading device (without and with partition)

This represented the first test case in which Test Model was installed with OLP. It was compared to Reference Model, which had blinds and shading device, and also compared to Test Model in the previous two conditions.

4. OLP, SLS, blinds and shading device (without and with partition)

This represented the second test case in which SLS was also added to Test Model besides the already installed OLP. It was compared to Reference Model, which had blinds and shading device, and also compared to Test Model in the previous three conditions.

The partition was placed in the center of Test Model as shown in Fig.1.8. In this case, however, because Reference Model did not have a partition, no comparison was made between Test Model and Reference Model.

3.2. MEASUREMENT OF ILLUMINANCE

Illuminance is luminous flux per unit area (IESNA, 2000). It has been one of the most popular daylight metrics owing to its ease of measurement, in scale models as well as in real buildings. It is measured using photometric sensors, which are essentially photodiodes; they generate a current in the range of milli-amperes proportional to the amount of light that falls on them. The workplane illuminance is a standard measurement for office spaces and Table 3.1 gives the values prescribed by IESNA.

Table 3.1. Illuminance levels prescribed for common visual tasks. *Source: IESNA Lighting Handbook, 2000.*

Performance of visual tasks of high contrast and large size	300 lux (30 fc)
Performance of visual tasks of high contrast and small size, or visual tasks of low contrast and large size	500 lux (50 fc)
Performance of visual tasks of low contrast and small size	1000 lux (100 fc)

There were 32 photometric sensors used in the experiment. Twelve were installed on the workplane in each of the models. Fig.3.5 shows the layout of sensors in reference model and Fig.3.6 shows that in Test Model (refer to Fig.1.8 for the section). The sensors were named according their position in Reference Model (R) or Test Model (T), followed by the row (A,B,C), followed by position (1,2,3,4). For example, KRB3 represents a sensor in reference model, in B row at third position from the front. Four additional sensors were added to Test Model: one on the ceiling, two on side walls and one on the back wall. KTVL on left wall, KTVR on right wall and KTVB on back wall would measure illuminance on walls. These were installed at the average sitting height for office spaces, which is 47”.

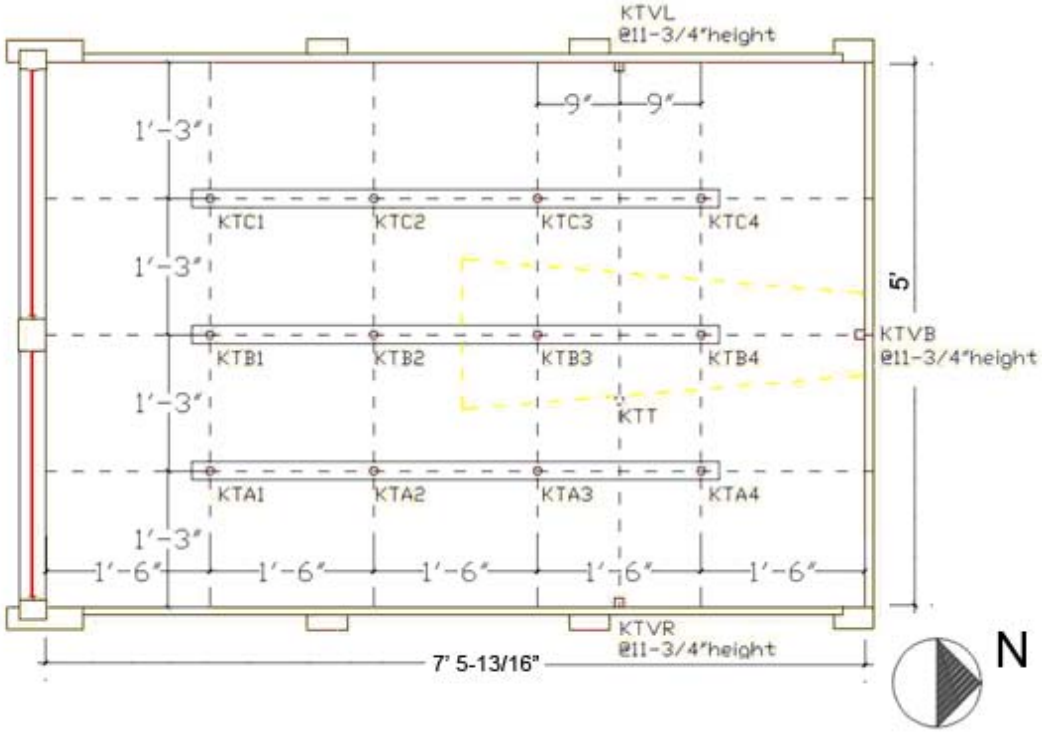

Fig.3.5. Layout of sensors in Reference Model in 1:4 scale.

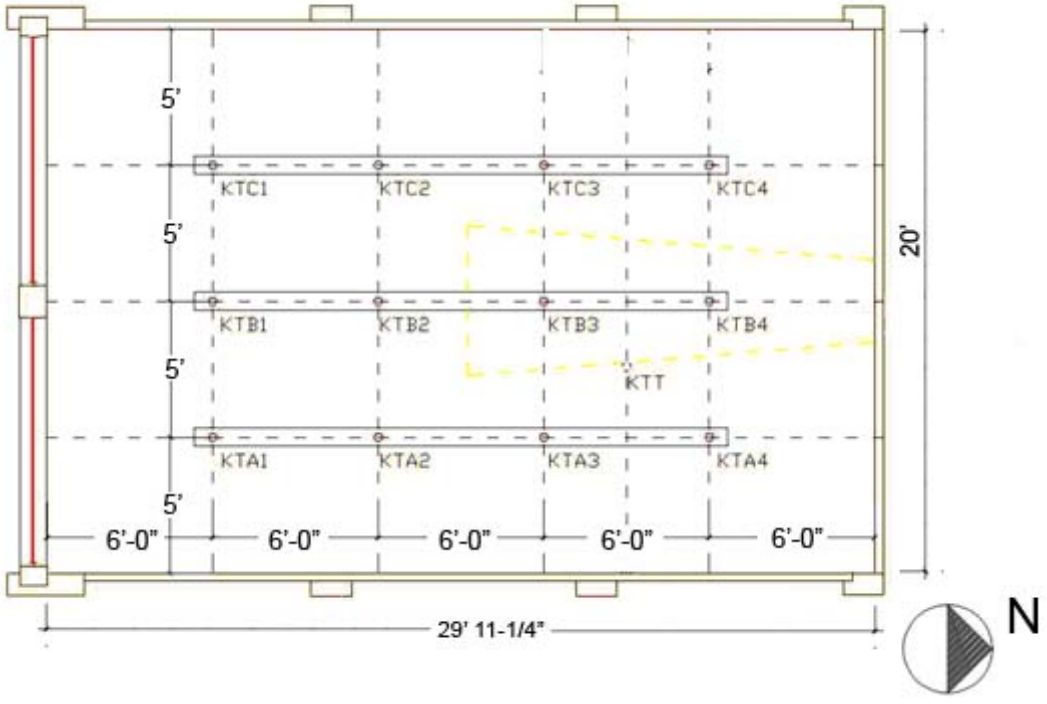

Fig.3.6. Layout of sensors in Test Model in full scale.

Two sensors shaded by a shadow band measure the exterior diffuse horizontal and exterior diffuse vertical illuminance as shown in Fig.3.7a. The declination of the shadow band needed adjustment every ten days because of the changing sunpath. Two others measure the exterior horizontal direct illuminance and vertical (south) exterior direct illuminance as shown in Fig.3.7b. The sensors were tested for effect of temperature and humidity before being sent for calibration. (Refer to Appendix C for information on calibration and performance of sensors).

All sensors were connected to a CR23X Campbell Scientific datalogger to record data every minute (for instructions used for the datalogger refer to Appendix J).

(a) (b)

Fig. 3.7. External illuminance sensors. (a) Diffuse horizontal and diffuse vertical, (b) global horizontal and global vertical.

3.3. MEASUREMENT OF LUMINANCE

Luminance, which is commonly understood as brightness, is measured using a luminance meter. It is defined as luminous intensity of any surface in a given direction per unit area of projected area of the surface viewed from that direction (IESNA, 2000). However, because daylighting changes rapidly, the luminance meter measurements may not be helpful to analyze a space due to the time it takes to measure each point. The use of CCD cameras to generate luminances for a space (Dubois, 2001; Velds, 2001; Martins-Mogo, 2005; Inkarojrit, 2005) is getting popular due to recent developments in digital cameras. A combination of photographs taken with multiple exposure values can provide a much higher range of luminances for a space, than that provided by a single exposure (Ward, 2001) , and hence a better analysis of luminances, contrast ratios and glare problems is possible. Culp et al. (1999) had developed a method to plot luminance values from multiple-exposure images using Photoshop, Rascal and Microsoft XL. Photosphere, a Mac based application, combines multiple-exposure images more easily and generates high dynamic range images and false color luminance maps (Martins-Mogo, 2005). Photolux, a Window based application, can be used to generate luminance maps while also performing basic statistical analysis of surfaces (Howlett, 2007).

However, accurate results can only be expected with this method if lighting conditions remain stable (Inanici et al., 2004) over the period of time when photographs with different exposures are taken; errors like vigenetting effects increase as aperture size is increased. A number of methods exist to calibrate CCD cameras for taking HDR images with different luminance ranges (Inanici et al., 2004; Inkarojrit, 2005). Photolux provides a

range of luminances that can be measured for an exposure value for a particular camera, and hence is handier.

For taking time lapse images, Nikon Coolpix with a fish eye lens was installed on one of the side openings of Test Model. To get the entire range of luminances, generally starting from 1cd/m^2 to 20,000 cd/m^2 for the present research, it was necessary to get 9 images. So hourly samples of 9 images were taken manually with different exposures (for details of exposure values used refer to Appendix D).

Fig. 3.8. Arrangement of camera with fish-eye lens. (a). Inside Test Model, (b) outside Test Model.

3.4. DERIVED VARIABLES

Illuminance Contrast Gradient (ICG) is defined as the ratio of average front task illuminance and average back task illuminance. There is no standard for it but as used in the Martins-Mogo (2005) research, it would give an idea about the uniformity of illuminance between the two task planes.

Luminance ratio, between two surfaces gives an idea about the relative brightness of surfaces and is used to determine direct glare sources; luminance ratios recommended by IESNA are 3:1 or 1:3 between visual task (paper or screen) and adjacent surfaces, and 10:1

or 1:10 between the visual task and the non-adjacent surfaces (IESNA Lighting Handbook, 2000).

Coefficient of variation (CV) of luminance represents the normalized dispersion of a distribution.

Unified glare rating or UGR, as defined by CIE (2002), is used to determine glare possibility in a particular lighting configuration. Originally defined for electrical luminaries (CIE, 1995) and then modified for small, large and complex sources (CIE, 2002), the metric was used for the first time for daylit spaces by Howlett et al. (2006). The following formula defines UGR as measured by Photolux (UGR_m):

$$UGR_m = 8\log_{10}\left[\left(\frac{0.25}{L_b}\right)\sum\left(\frac{L_s^2\omega}{p^2}\right)\right]$$

where, L_s = luminance of the source (window, OLP, SLS).

p = Guth position index.

L_b = background luminance, i.e., average luminance of the field of view excluding glare sources.

In the present research, UGR values are taken from Photolux and then compared against each other to determine the glare potential of each daylighting system. The source luminance threshold was taken as the average room luminance, plus twice the standard deviation (Howlett et al., 2006). The suggested maximum limits are shown in Table 3.2 below. IESNA suggests a maximum limit of 20 for office spaces (IESNA, 2000). The advantage of UGR as a daylight metrics lies in its ability to summarize the glare potential and hence the overall daylighting design of a space.

Table 3.2. Maximum allowed UGR for different spaces. *Source: http://www.learn.londonmet.ac.uk*

Working area	**Maximum allowed UGR**
Drawing rooms	16
Offices	*19*
Industrial work, fine	22
Industrial work, medium	25
Industrial work, coarse	28

IV. RESULTS

4.1. EVALUATION OF DAYLIGHT QUANTITY

The observations are made with the office module considered to be divided into a front zone and a back zone. While all sensors were used in calculating average values wherever necessary, only the central row of sensors (KTB1-KTB4) was plotted when comparing Reference Model with Test Model. The data sample was classified into following categories for evaluation of daylight quantity:

- Comparison of Test Model with Reference Model.
- Comparison of Test Model in different daylighting designs without the partition.
- Comparison of Test Model in different daylighting designs with the partition.
- Comparison with output of Martins-Mogo prototype.

4.1.1. Comparison of test model with reference model

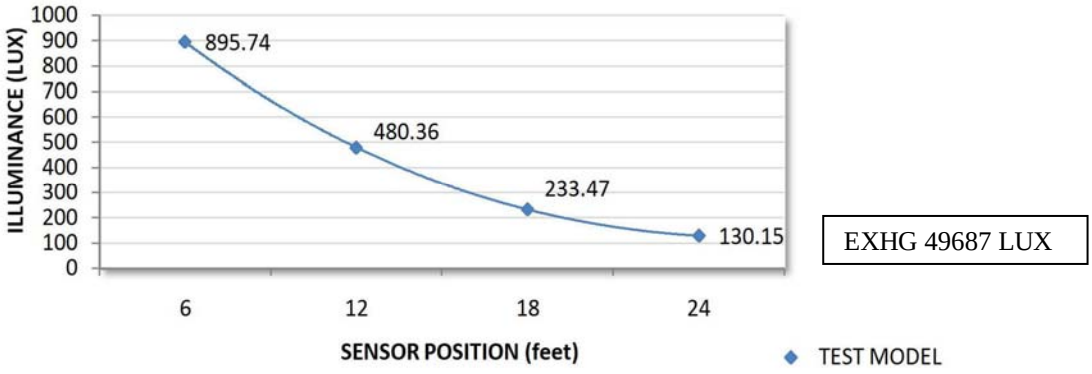

(a)

Fig. 4.1. Plot of Test Model only. (a) Workplane distribution at 900 hrs on Feb 6th with both models having blinds and shading device, (b) workplane distribution at 900 hrs on Feb 7th with both models having blinds and shading device, test model having OLP, (c) workplane distribution at 900 hrs on March 5th with both models having blinds and shading device, test model having OLP and SLS.

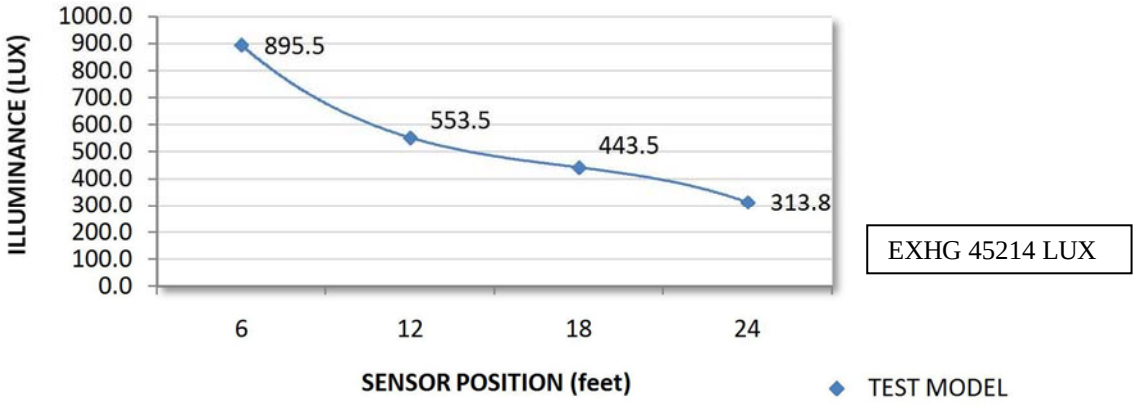

(b)

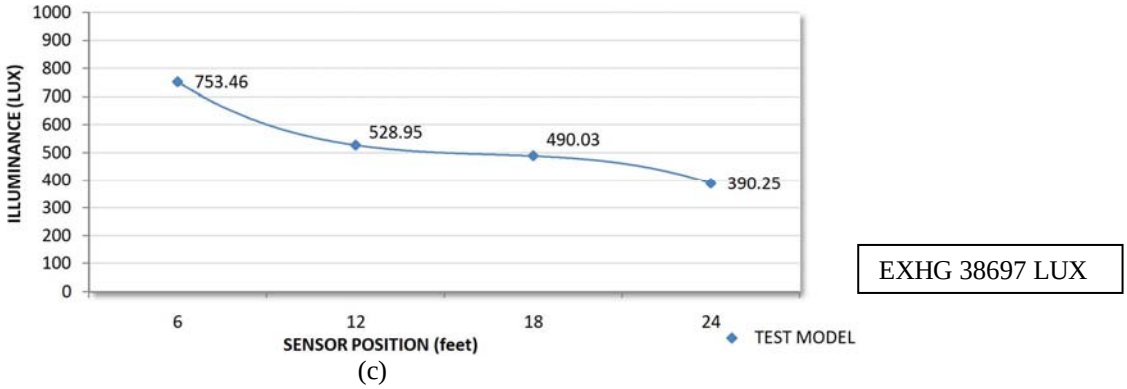

(c)

Fig. 4.1. Continued.

Fig. 4.1. compares Reference Model with Test Model at 900 hours. A value of above 300 lux was observed for sensor KTB4 (24 feet) in Test Model in the OLP case and the SLS case; KTB3 (18feet) was above 400 lux. All sensors except the first one had a higher illuminance value with introduction of OLP; a lower external illuminance value could be attributed to this.

Fig. 4.2. compares Reference Model with Test Model at 1300 hours.

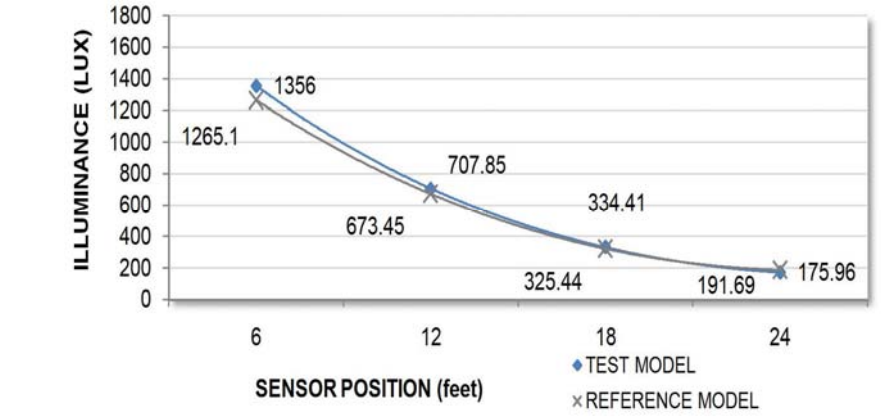

EXHG 94568 LUX

(a)

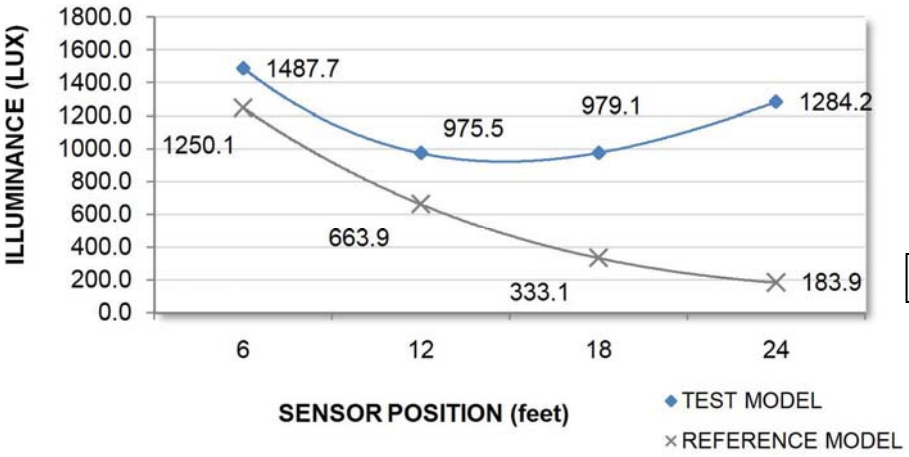

EXHG 92464 LUX

(b)

Fig.4.2.Comparison of Reference Model with Test Model. (a) Workplane distribution at 1300 hrs on Feb 6th with both models having blinds and shading device, (b) workplane distribution at 1300 hrs on Feb 7th with both models having blinds and shading device, test model having OLP, (c) workplane distribution at 1300 hrs on March 5th with both models having blinds and shading device, test model having OLP and SLS.

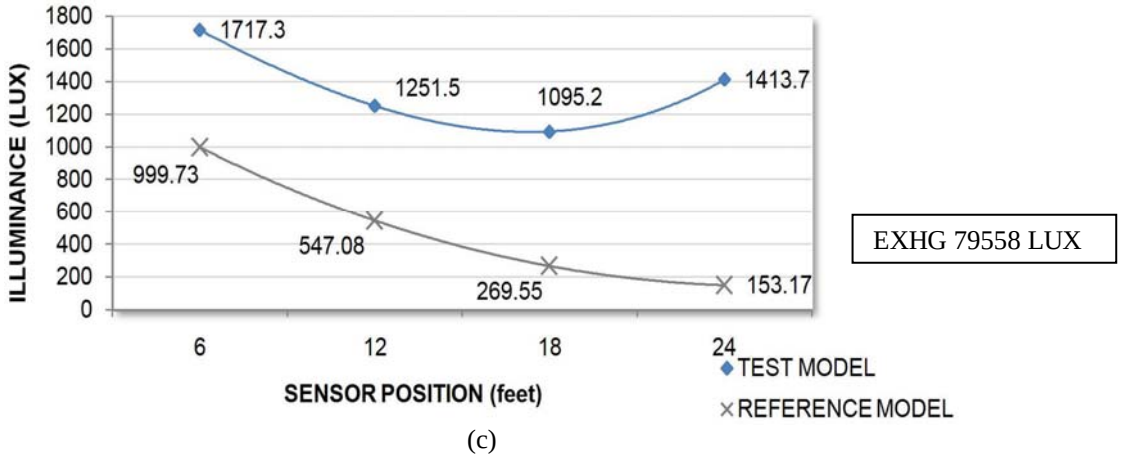

(c)

Fig.4.2. Continued.

It could be deduced that the introduction of OLP increased illuminance at 24 feet by approximately 1101 lux; light also diffuses to the sensor at 6 feet (KTB1) and increased the value by about 200 lux. A much flatter curve could be appreciated in Test Model as compared to Reference Model.

Further addition of SLS increased illuminance at 24 feet by approximately 1260 lux. There is much more light introduced at KTB1 in this case (700 lux approximately).

Fig. 4.3. compares Reference Model with Test Model at 1600 hours.

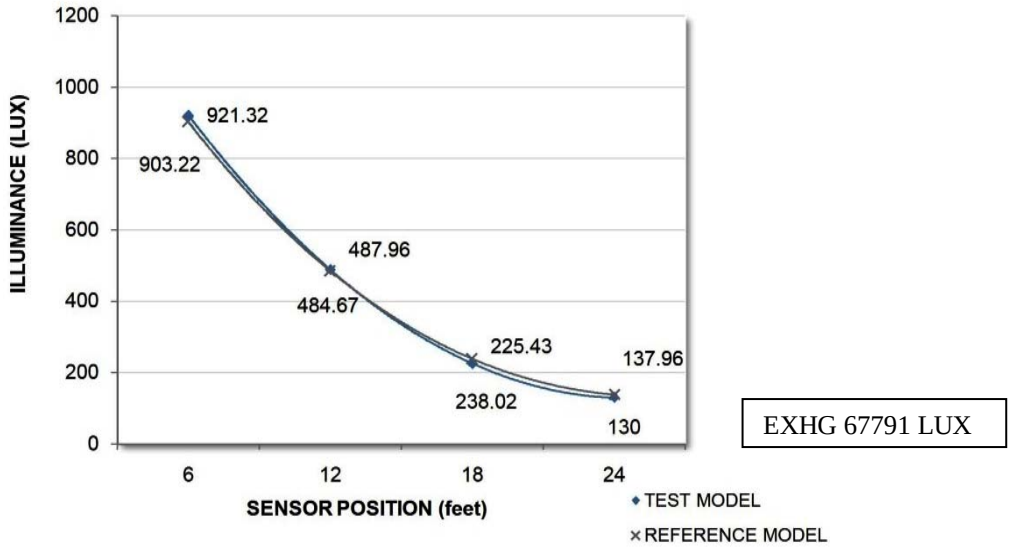

(a)

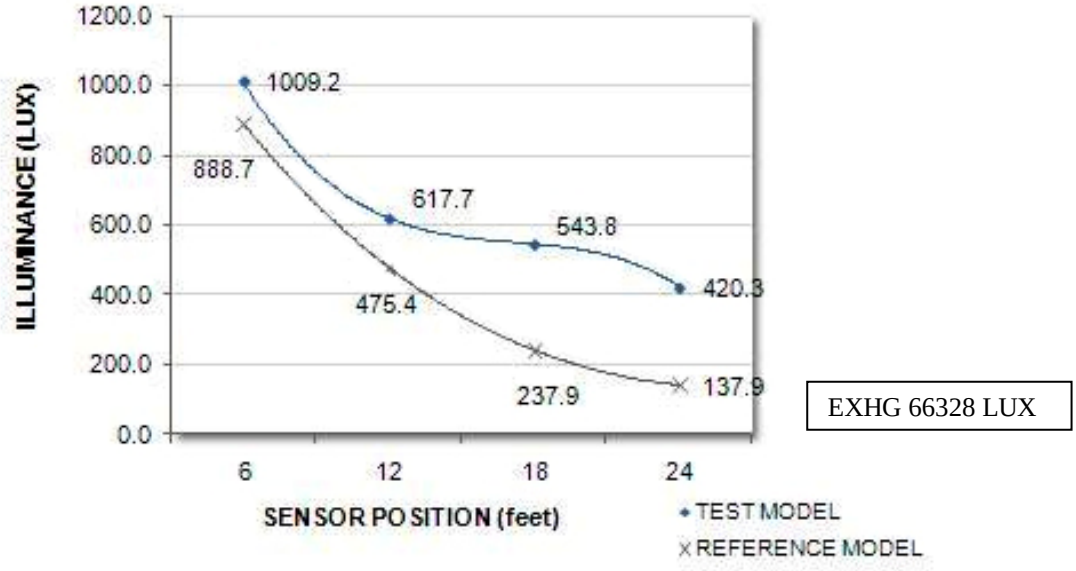

(b)

Fig. 4.3. Comparison of Reference Model with Test Model. (a) Workplane distribution at 1600 hrs on Feb 6th with both models having blinds and shading device, (b) workplane distribution at 1600 hrs on Feb 7th with both models having blinds and shading device, test model having OLP, (c)) workplane distribution at 1600 hrs on March 5th with both models having blinds and shading device, test model having OLP and SLS.

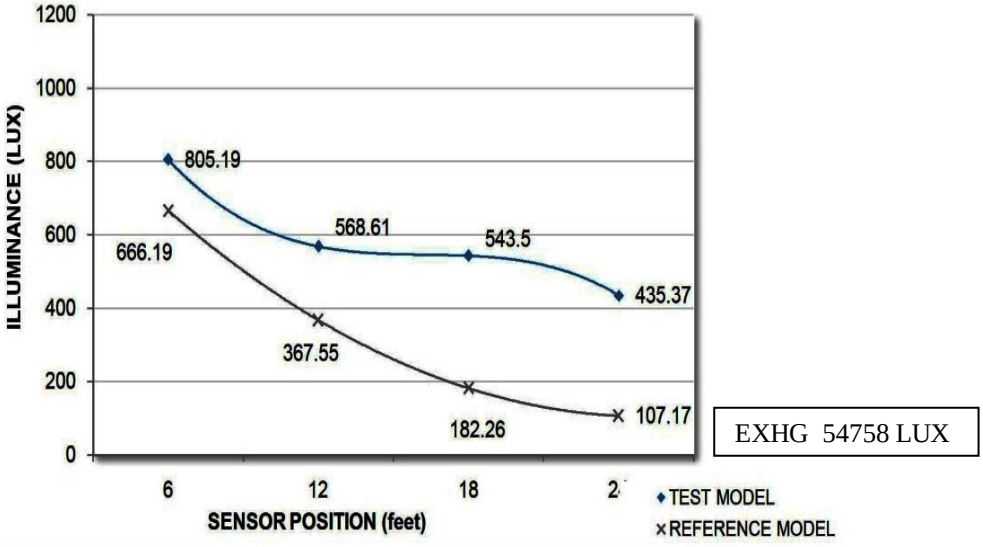

(c)

Fig. 4.3. Continued.

In this case, a value of above 400 lux was observed for sensor KTB4 (24') in Test Model in the OLP case and the SLS case; KTB3 (18feet) was above 500 lux.

Fig. 4.4. compares the wall and ceiling characteristics for Reference Model and Test Model on three different days, namely Feb 6th, Feb 7th and March 5th for three different daylighting conditions. Between 1000 hours to 1540 hours, backwall illuminance varied significantly in Test Model with OLP (Fig. 4.4b), changing from 475 lux at 1000 hours to 1140 lux at 1238 hours (solar noon). This may imply extension of the backzone of the module beyond 30 feet (and a possible reduction of illuminance on sensor KTB4 in a deeper module). The variation for the same period without OLP is between 200 lux to 260 lux (Fig. 4.4a).

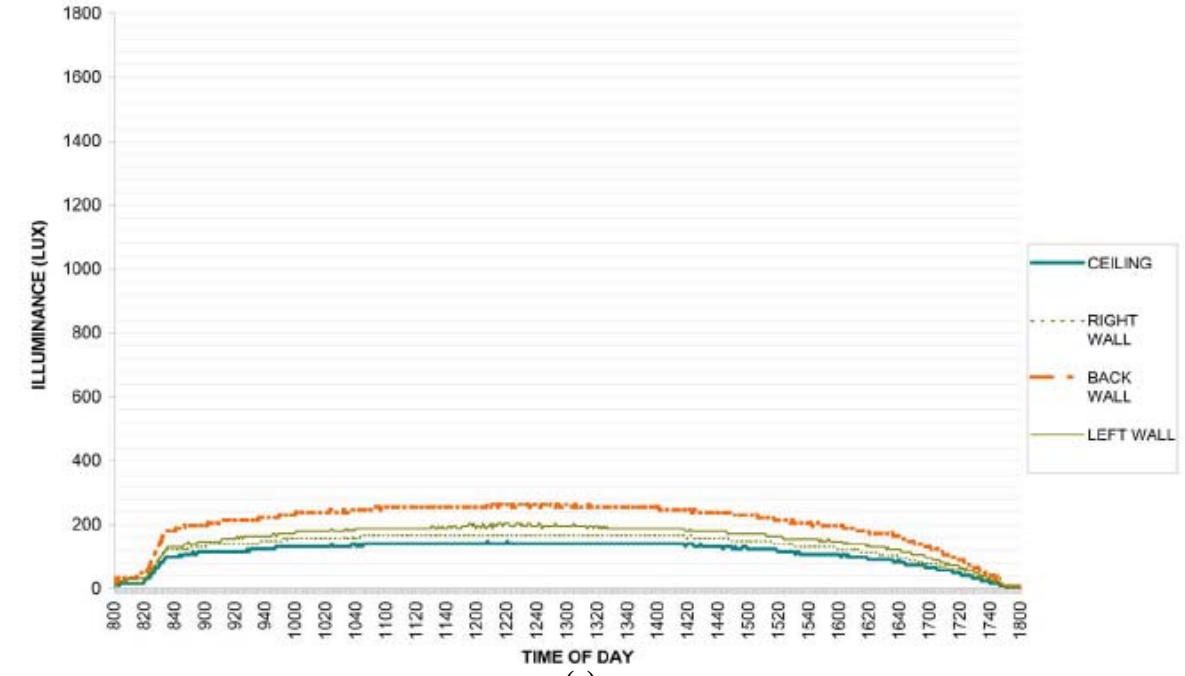

(a)

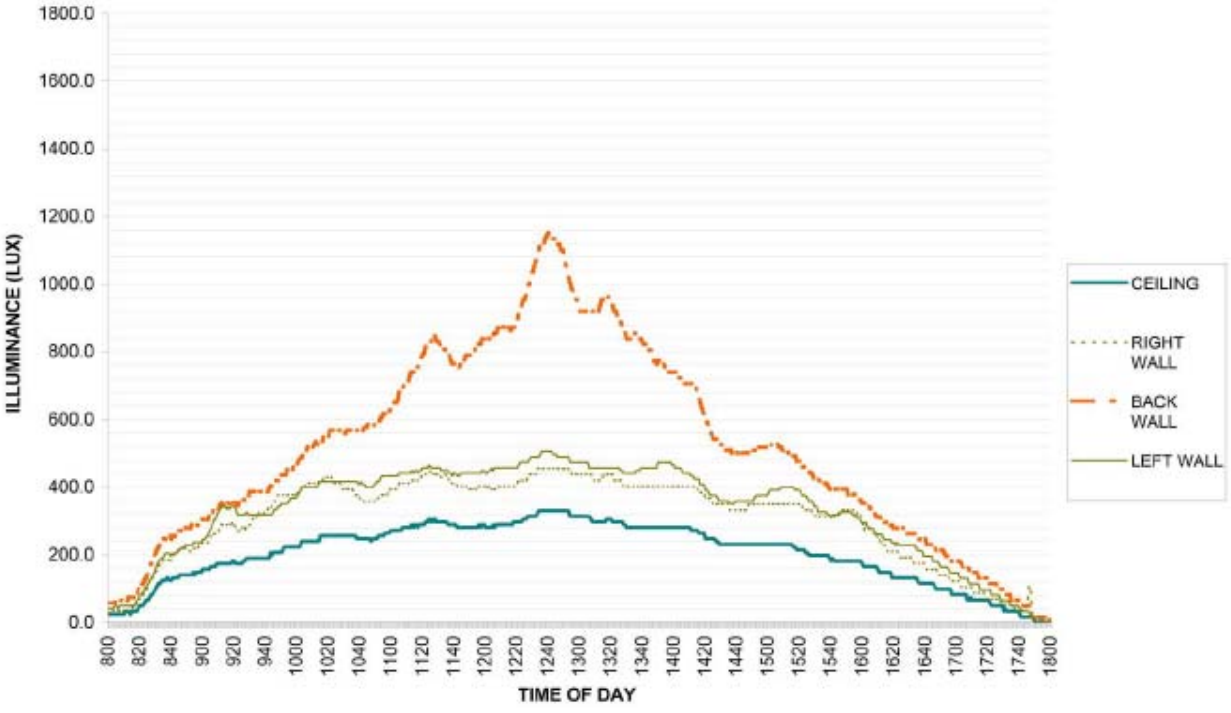

(b)

Fig. 4.4. Wall and ceiling characteristics. (a) Wall and ceiling distribution on Feb 6th with both models having blinds and shading device, (b) wall and ceiling distribution on Feb 7th with both models having blinds and shading device, test model having OLP, (c) wall and ceiling distribution on March 5th with both models having blinds and shading device, test model having OLP and SLS.

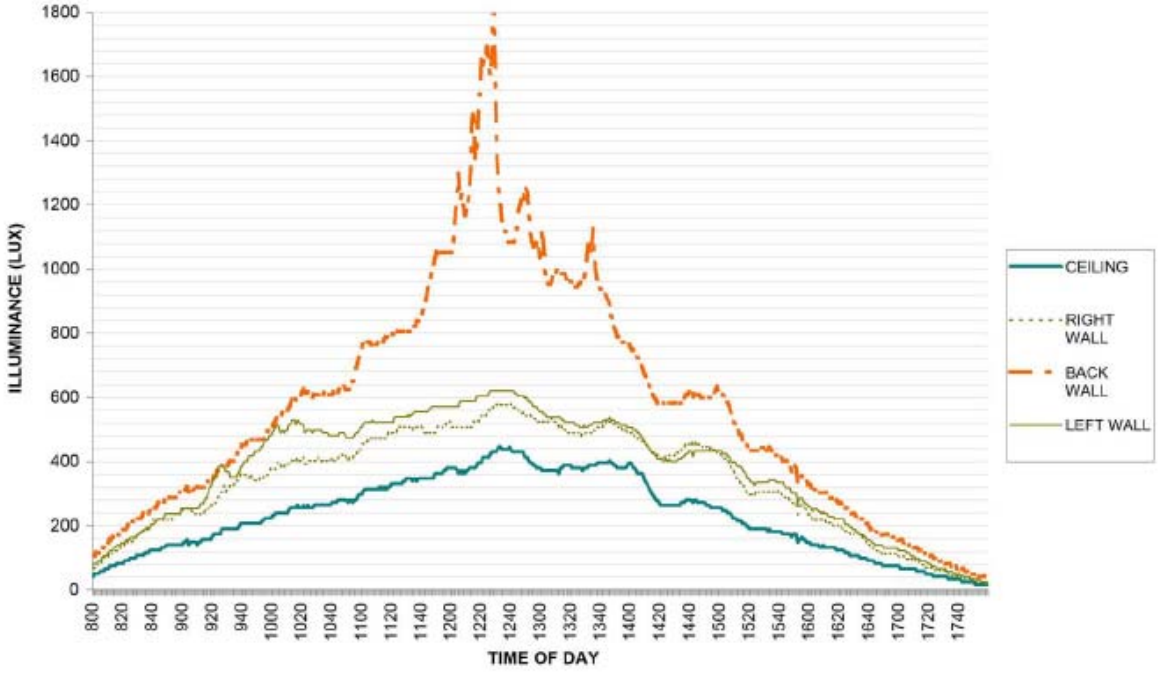

(c)

Fig. 4.4. Continued.

The backwall illuminance increases to 1800 lux at solar noon, with the introduction of SLS (Fig. 4.4c).

Between 900 hours and 1700 hours, ceiling illuminance varied from 148 lux to 330 lux to 100 lux in Test Model with OLP, while that without OLP varied from 115 lux to 140 lux to 66 lux; side wall illuminances varied from 230 lux to 497 lux to 130 lux in Test Model with OLP; without OLP the variation was from 145 lux to 240 lux to 100 lux. There was a difference in values between the two walls (45 lux maximum) which in ideal diffused light conditions should be 0 lux. Between the same time period, ceiling illuminance varied from 148 lux to 437 lux to 75 lux in Test Model with OLP and SLS; side wall illuminance varied from 253 lux to 619 lux to 130 lux in Test Model with OLP. The difference in values between the two walls (110 lux maximum) was higher.

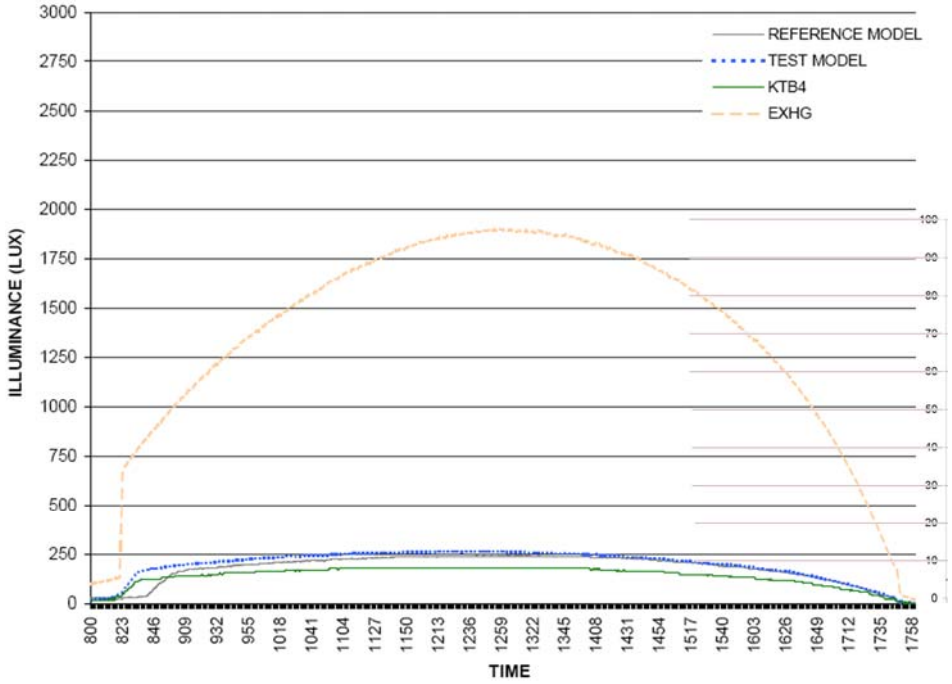

(a)

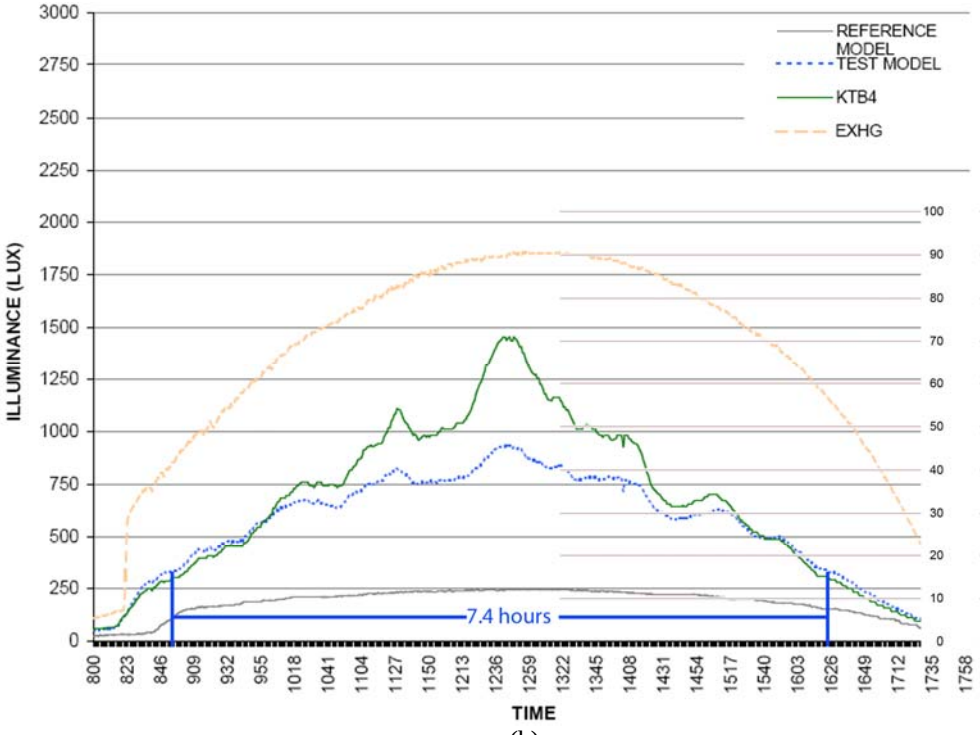

(b)

Fig.4.5. Average workplane distribution in back zone. (a) Feb 6th with both models having blinds and shading device, (b) Feb 7th with both models having blinds and shading device, test model having OLP, (c) March 5th with both models having blinds and shading device, test model having OLP and SLS.

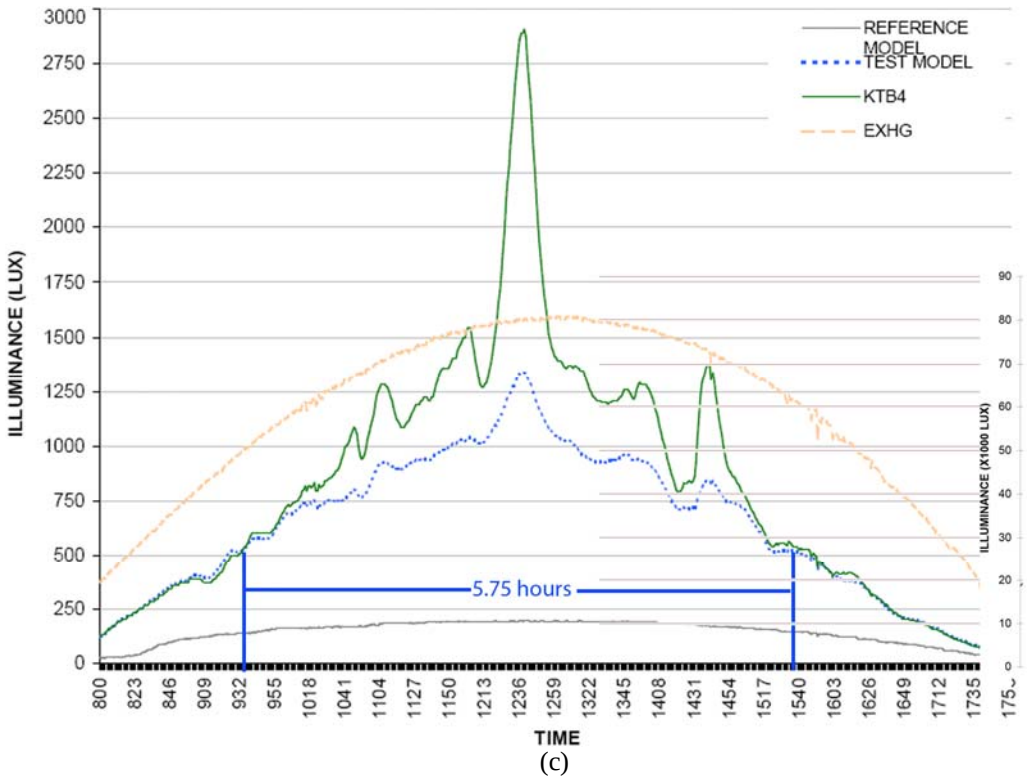

(c)

Fig.4.5. Continued

Fig. 4.5. compares the average workplane illuminance for Reference Model and Test Model on three different days, namely Feb 6th, Feb 7th and March 5th for three different daylighting conditions. Also shown are illuminances of KTB4 and exterior horizontal global (EXHG). The workplane in back zone of Reference Model received about 50 lux of daylight less than Test Model (Fig.4.5a), possibly due to solar and sky obstructions. Test Model with OLP (Fig.4.5b) received 300 lux or more daylight between 856 hours to 1621 hours (7.4 hours); it received over 500 lux between 945 hours and 1530 hrs (5.75 hours). Test Model with OLP and SLS (Fig.4.5c) also received 300 lux or more daylight between 845 hours to 1630 hours (7.75 hours); it received over 500 lux between 930 hours and 1530 hours (6 hours).

Fig.4.6. compares KTB4 and KRB4 sensors, and the average workplane illuminance for Reference Model and Test Model with OLP on a cloudy day. The windows on Test Model were covered so that the only light source on task plane was the OLP. The Reference Model was kept open with blinds and shading devices. It could be observed that when the external direct global value becomes higher than 10,000 lux, OLP contributed above 100 lux on an average. For EXHG values between 20,000 and 30,000, the OLP contributed above 200 lux on an average. KRB4 in Reference Model remained close to 50 lux on an average. This showed the potential of OLP to transport diffused daylight. It may be deduced from here that during cloudy days, if blinds are in open position, illuminance on front taskplane could reach the IESNA recommended levels of 300 lux.

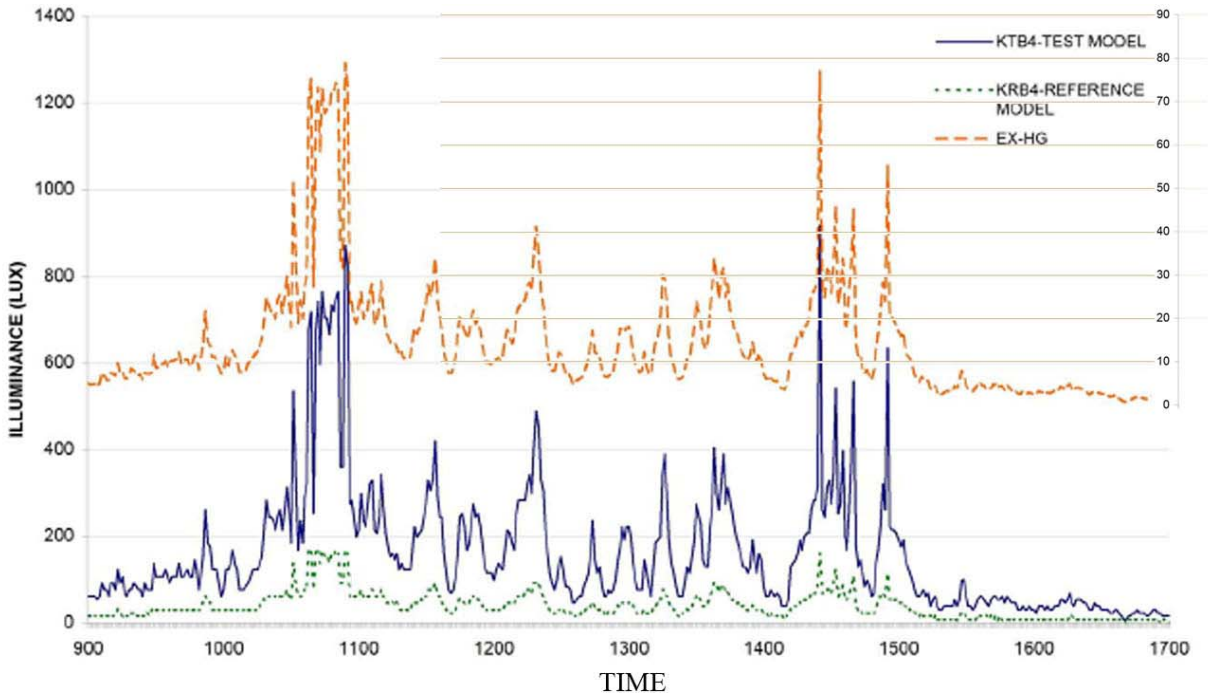

Fig.4.6. Comparison of Reference and Test model on March 2nd, 2008, a cloudy day, with windows covered in Test Model.

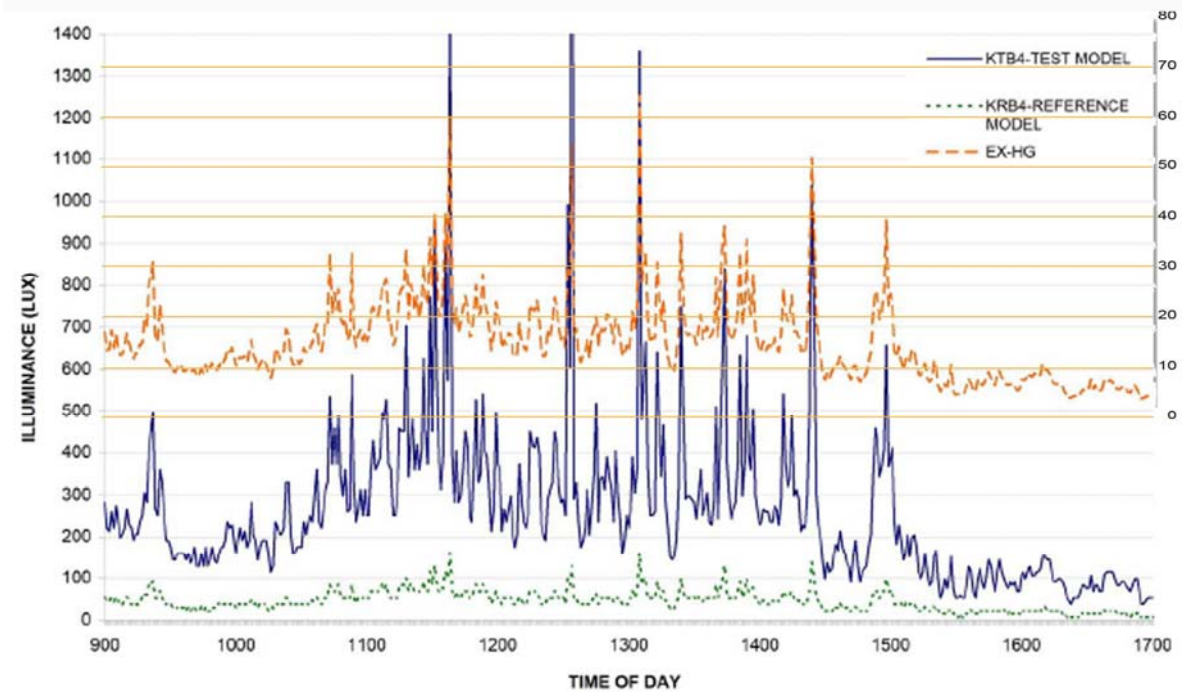

Fig.4.7. Comparison of Reference and Test model on March 17th, 2008, a cloudy day, with windows covered in Test Model.

Fig.4.7. compares KTB4 and KRB4 sensors, and the average workplane illuminance for Reference Model and Test Model with OLP and SLS on a cloudy day. The windows on both models were left uncovered in this case. It could be observed that when the external direct global value becomes higher than 10,000 lux, OLP and SLS contributed above 150 lux on an average. For EXHG values between 20,000 and 30,000, the OLP and SLS contributed between 275 lux to 450 lux more than the Reference Model with average above 300 lux between 1045hours and 1430hours.

4.1.2. Comparison of four daylighting systems without the partition in test model

Fig. 4.8. shows fish eye views of the four dayligihting conditions at 900hrs on different days without partition. Fig.4.9 to Fig. 4.13 compare the four daylighting systems without partition at different times of the day.

(a)

(b)

(c)

(d)

Fig. 4.8. Fish eye view of four different daylighting systems at 9 am. (a) Blinds only on Feb 13th, (b) blinds and shading devices on Feb. 6th, (c) blinds, shading devices and OLP on Feb 7th, (d) blinds, shading devices, OLP and SLS on March 5th.

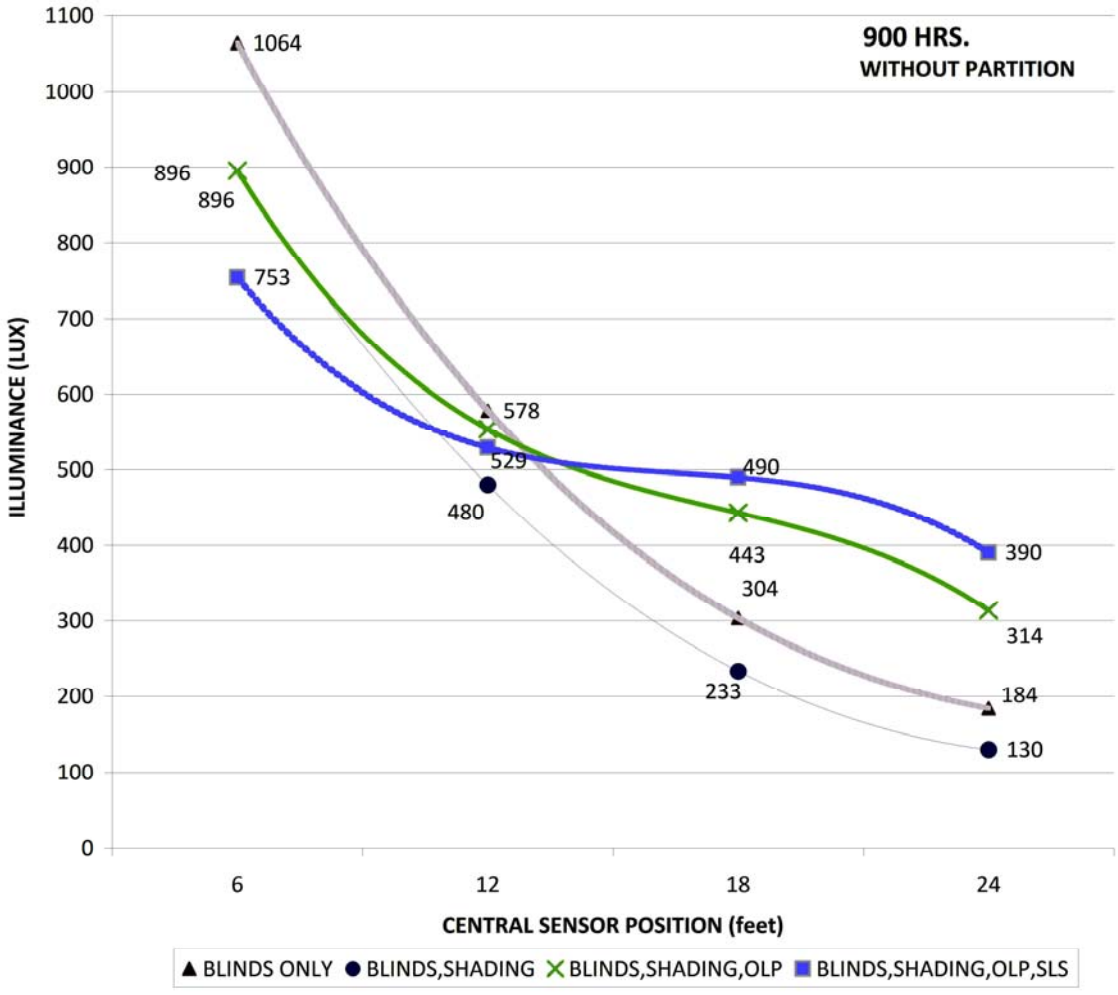

Feb 13th EXHG 45142 lux	Feb 6th EXHG 49687 lux	Feb 7th EXHG 45214 lux	Mar 5th EXHG 43196 lux

Fig. 4.9. Comparison of four daylighting designs at 900 hrs in Test Model on different days without partition.

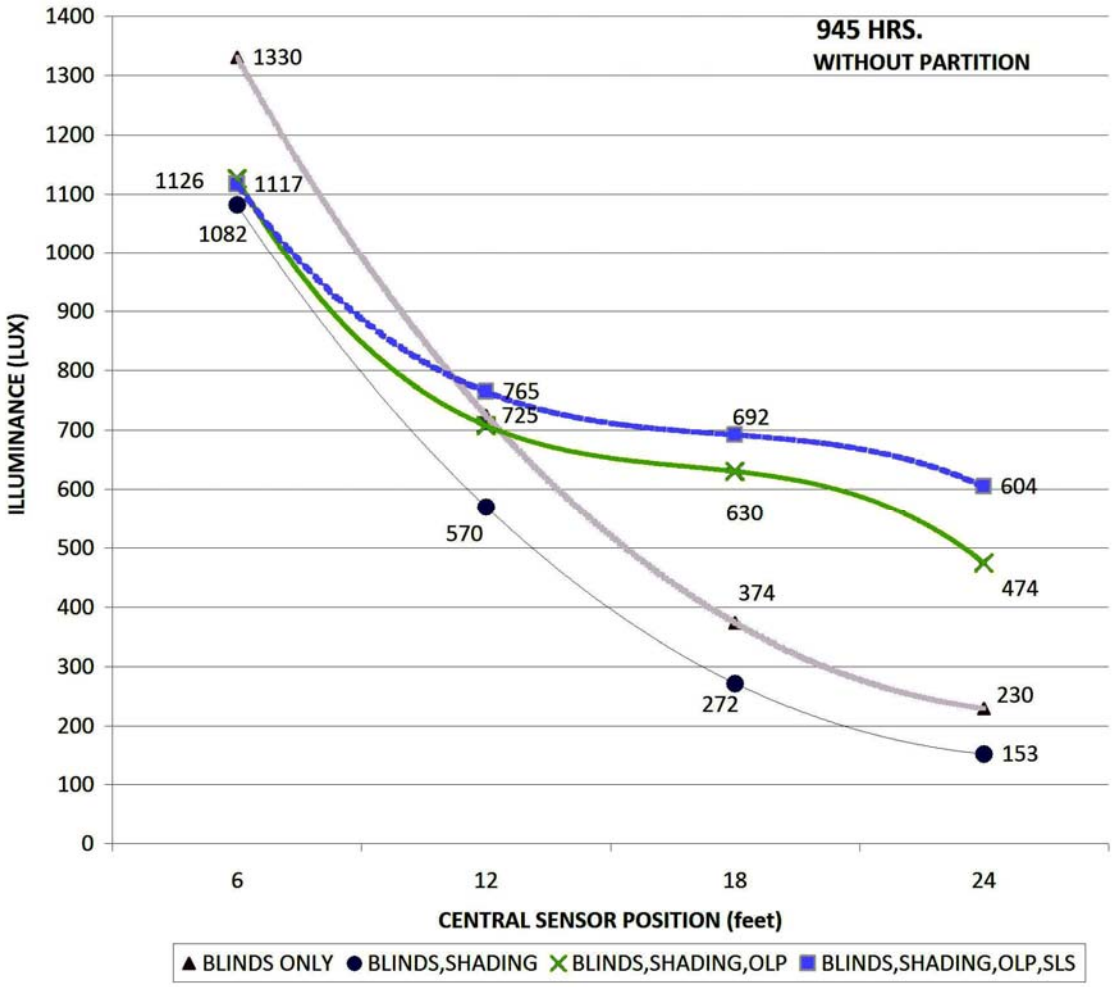

Feb 13th EXHG 60153 lux	Feb 6th EXHG 64641 lux	Feb 7th EXHG 60457 lux	Mar 5th EXHG 52048 lux

Fig.4.10. Comparison of four daylighting systems at 945 hrs in Test Model on different days without partition.

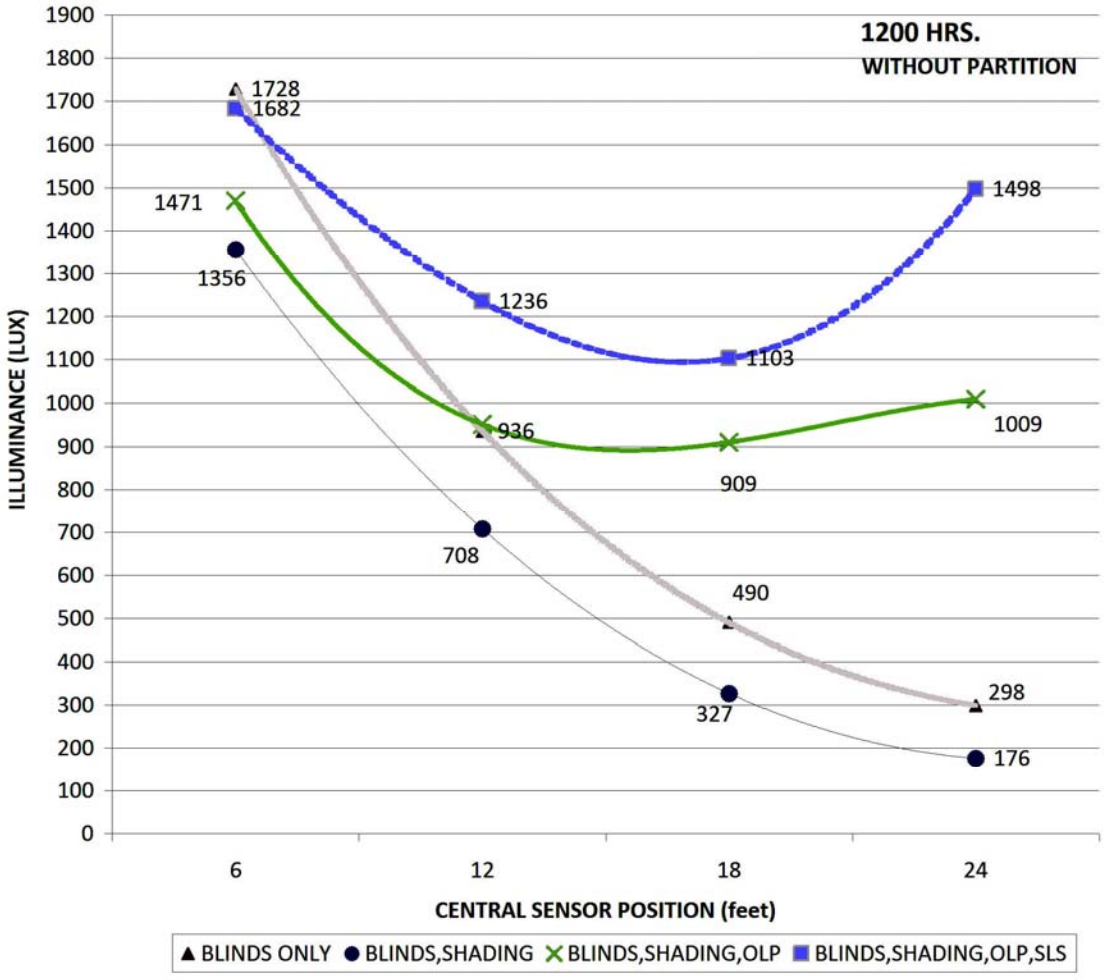

Feb 13th EXHG 87259 lux	Feb 6th EXHG 91555 lux	Feb 7th EXHG 88784 lux	Mar 5th EXHG 75828 lux

Fig.4.11. Comparison of four daylighting systems at 1200 hrs in Test Model on different days without partition.

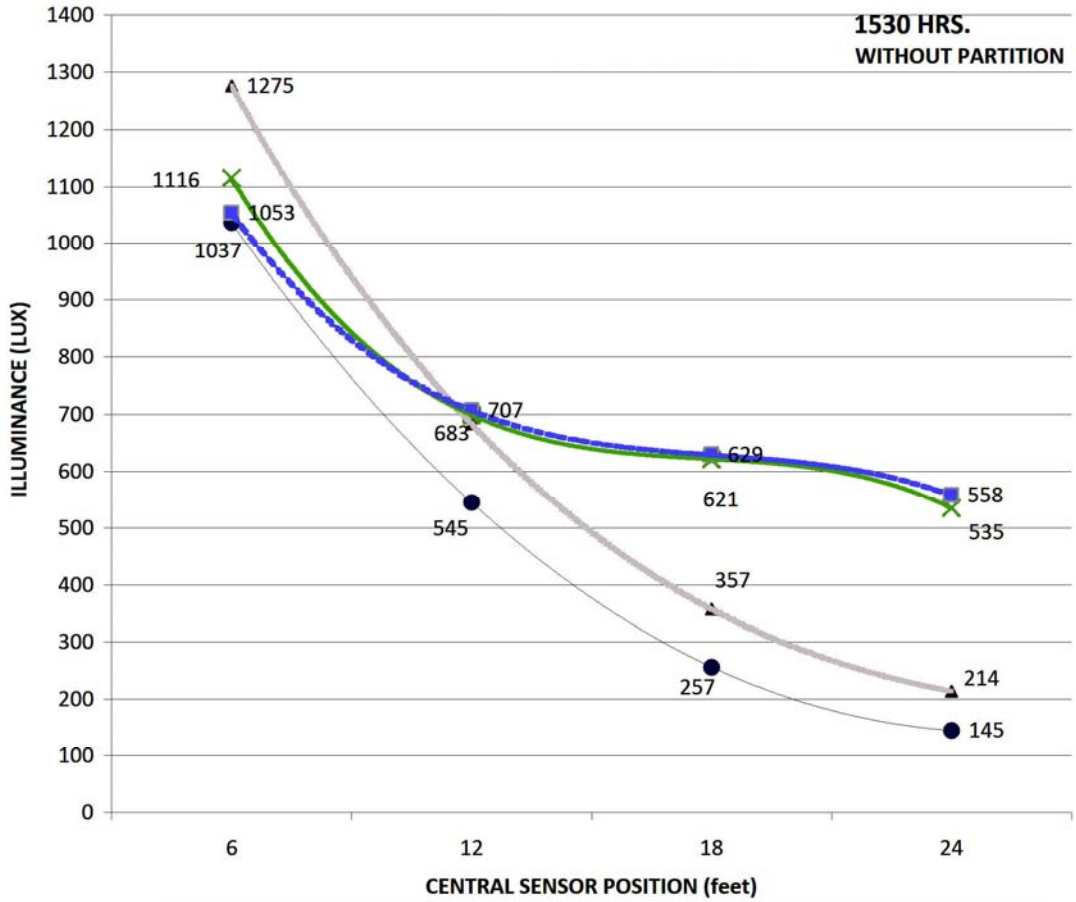

Feb 13th EXHG 72635 lux	Feb 6th EXHG 76733 lux	Feb 7th EXHG 74199 lux	Feb 5th EXHG 62207 lux

Fig.4.12. Comparison of four daylighting systems at 1530hrs in Test Model on different days without partition.

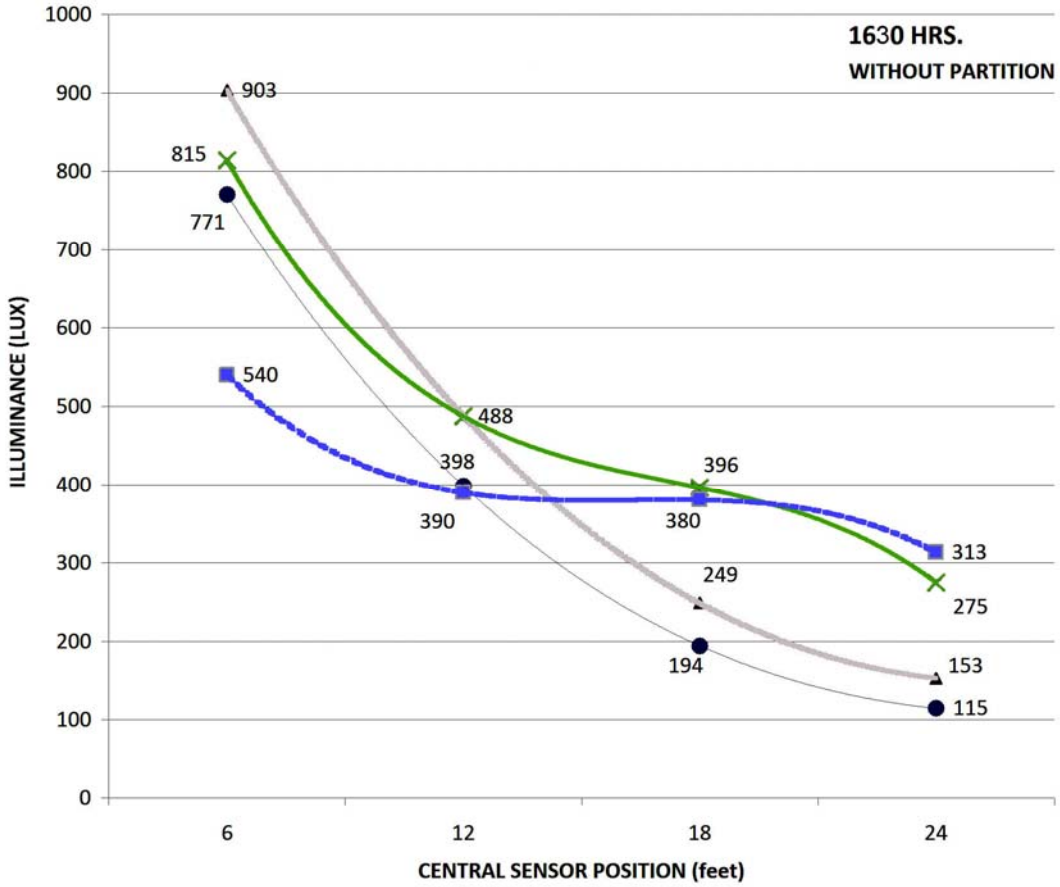

Feb 13th EXHG 54109 lux	Feb 6th EXHG 56704 lux	Feb 7th EXHG 55245 lux	March 5th EXHG 45103 lux

Fig.4.13. Comparison of four day lighting systems at 1630hrs in Test Model on different days without partition.

With blinds only, KTB4 (24 feet) does not reach more than 298 lux at any time. As expected, with blinds and shading device this value decreased further to 176 lux. KTB1 (6feet) value was also lower on all occasions where shading was present.

With blinds, shading device and OLP, KTB4 varied from 275 lux to 1009 lux between 900hrs and 1630hours; it did not drop below 300 lux between 900 hours and 1615 hours (not shown), which is the threshold illuminance for ambient lighting in office spaces (IESNA, 2000).

With the introduction of SLS, KTB4 varied between 313 lux to 1498 lux from 900hrs to 1630 hrs; it did not drop below 500 lux between 930hrs (not shown here) and 1530hrs, which is the threshold illuminance for task lighting in office spaces (IESNA,2000). Between 1100 hours and 1400 hours, the SLS contributed significantly more daylight at the backzone (approximately 300 lux more) in confirmation with results obtained at LBNL (Beltran et al., 1997). Also, during this period KTB4 (24 feet), received more daylight than KTB2 (12 feet). However, the flatness of curve (rate of change with distance) and hence the uniformity was less than that due to OLP alone.

4.1.3. Comparison of four daylighting systems in test model with partition

Fig. 4.14. shows fish eye views of the four dayligihting conditions at 900hrs on different days with partition. Fig.4.15 to Fig.4.19 compare the four daylighting systems with partition at different times of the day.

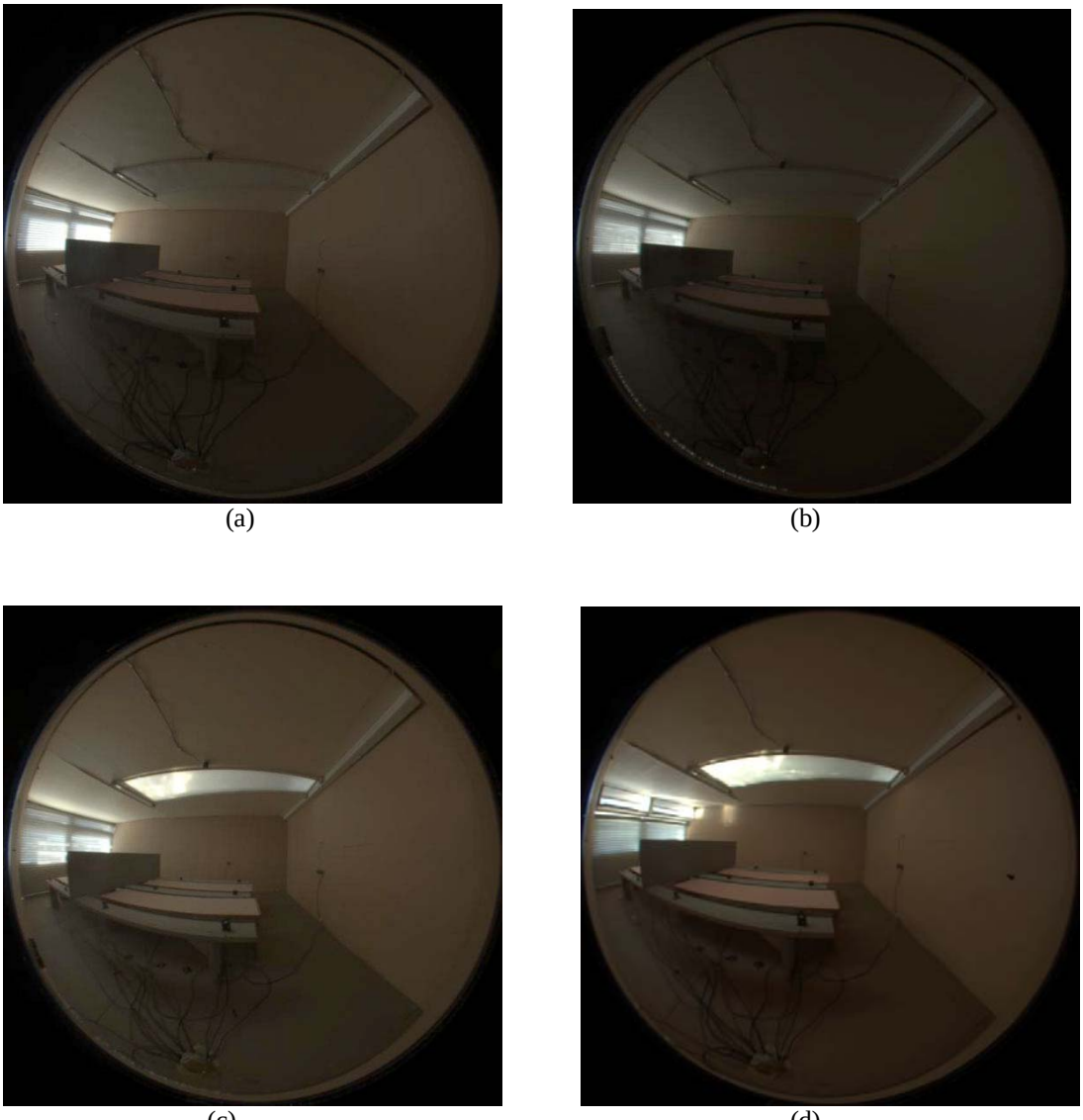

(a) (b)

(c) (d)

Fig. 4.14 Fish eye view of four daylighting systems with partition at 9 am. (a) Blinds only on Feb 17th, (b) blinds and shading devices on Feb 9th, (c) blinds, shading devices and OLP on Feb 8th, (d) blinds, shading devices, OLP and SLS on March 4th.

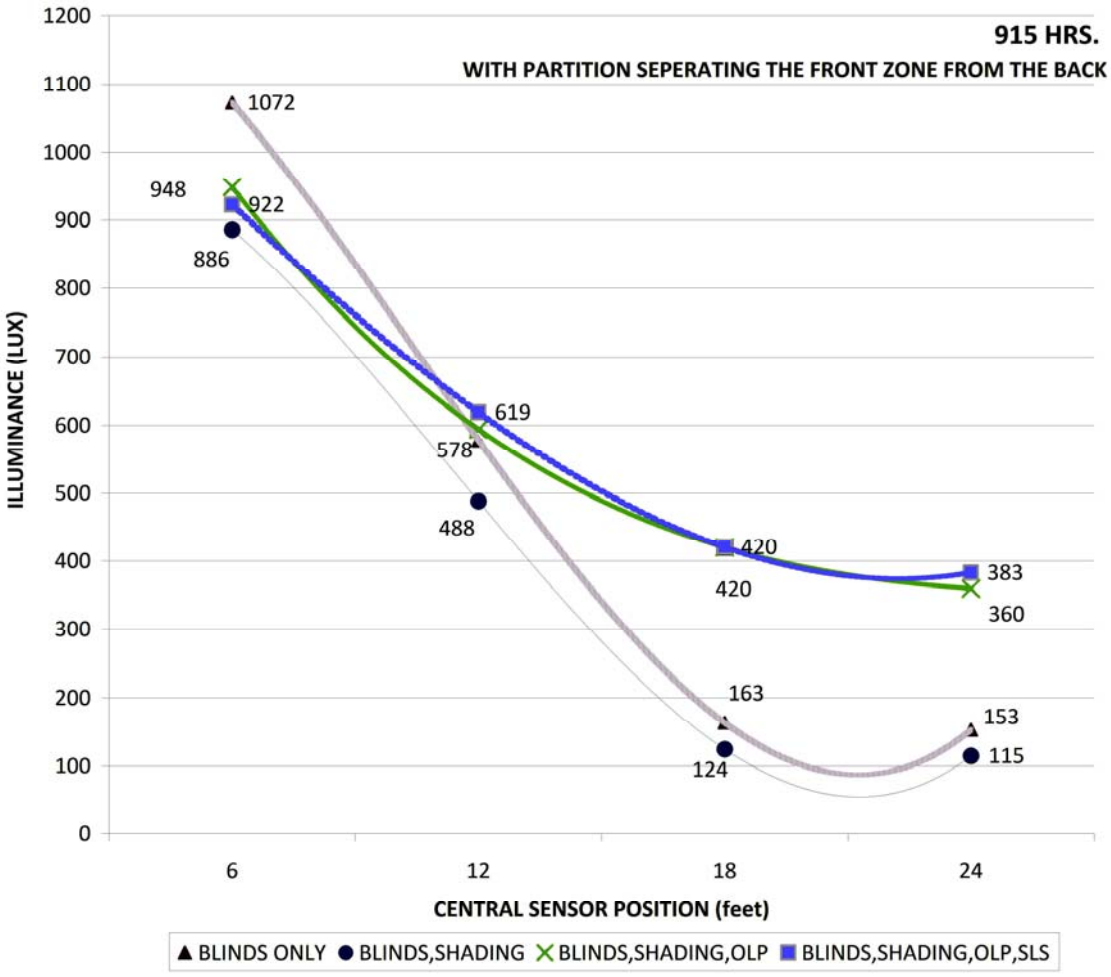

Feb 17th EXHG 50023 lux	Feb 9th EXHG 46659 lux	Feb 8th EXHG 48806 lux	Mar 4th EXHG 44331 lux

Fig. 4.15. Comparison of four daylighting systems at 915 hrs in Test Model on different days with the partition separating the front zone from the back.

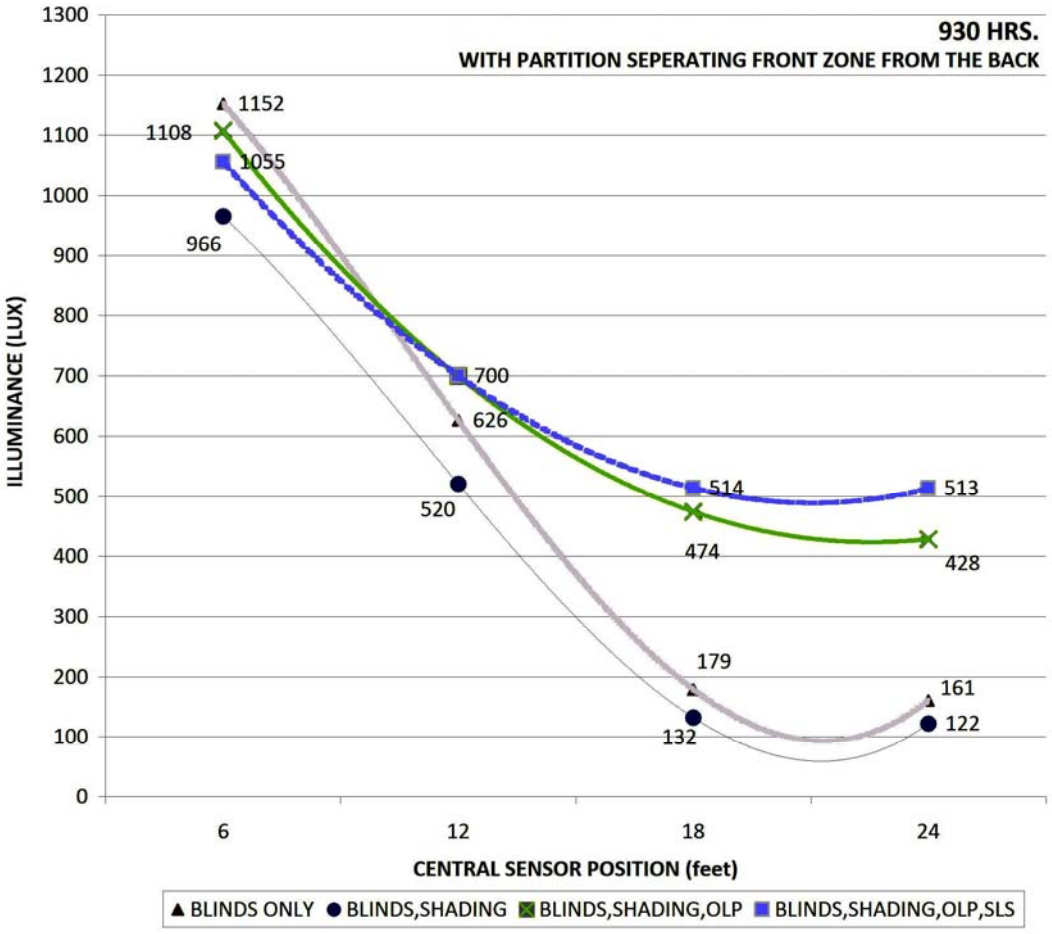

Feb 17th EXHG 54818 lux	Feb 9th EXHG 51334 lux	Feb 8th EXHG 59234 lux	Mar 4th EXHG 48604 lux

Fig. 4.16. Comparison of four daylighting systems at 930 hrs in Test Model on different days with the partition separating the front zone from the back.

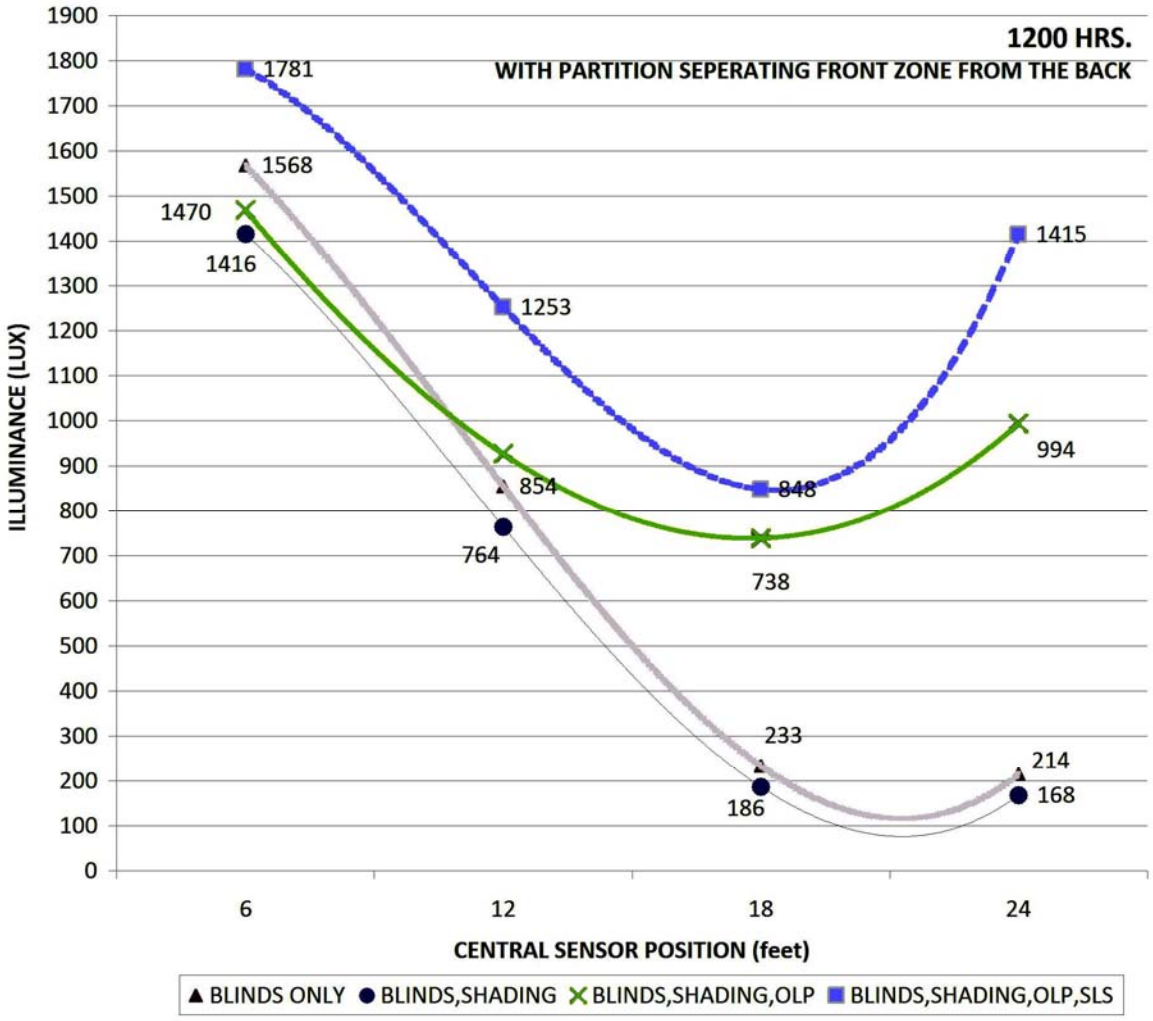

Feb 17th EXHG 85050 lux	Feb 9th EXHG 87369 lux	Feb 8th EXHG 89867 lux	Mar 4th EXHG 77354 lux

Fig. 4.17 Comparison of four daylighting systems at 1200 hrs in Test Model on different days with the partition separating the front zone from the back.

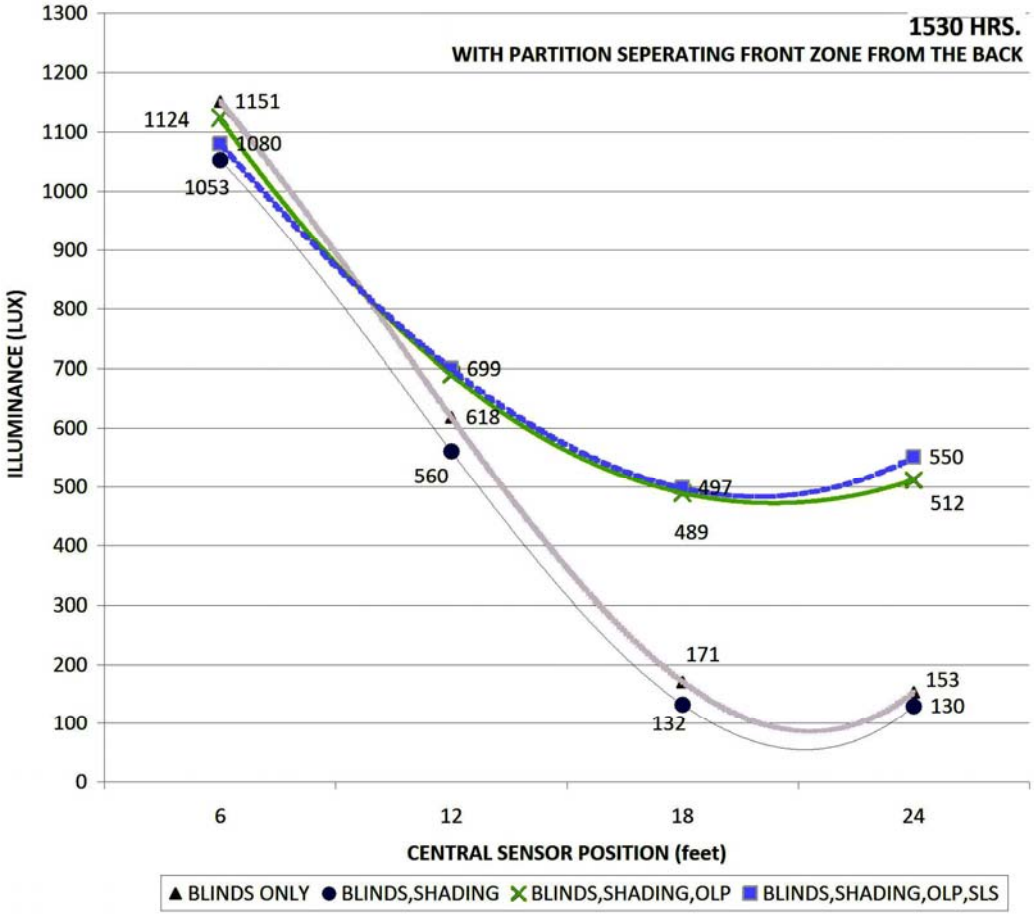

Feb 17th EXHG 70973 lux	Feb 9th EXHG 72713 lux	Feb 8th EXHG 74302 lux	Mar 4th EXHG 64172 lux

Fig.4.18. Comparison of four daylighting designs at 1530 hrs in Test Model on different days with the partition separating the front zone from the back.

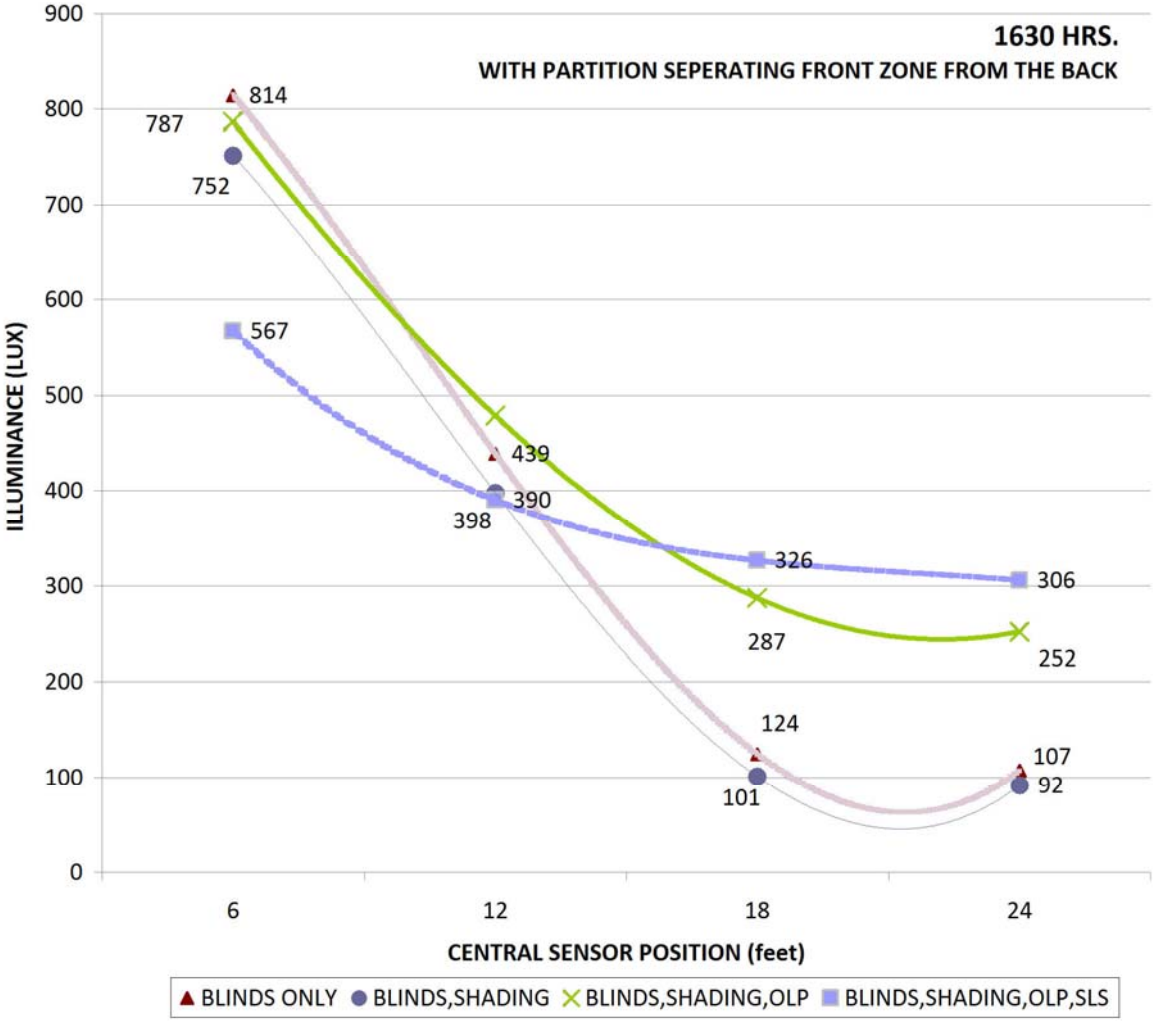

Feb 17th EXHG 52960 lux	Feb 9th EXHG 51715 lux	Feb 8th EXHG 52605 lux	Mar 4th EXHG 47880 lux

Fig. 4.19. Comparison of four day lighting designs at 1630 hrs on different days with the partition separating the front zone from the back.

Introducing the partition reduced overall illuminance values on the back workplane, for the blinds only and blinds and shading devices cases. With blinds only, KTB4 (24 feet) does not reach more than 214 lux at any time. With blinds and shading device this value was 175 lux.

With blinds, shading device and OLP, KTB4 varied from 138 lux to 1253 lux between 900 hours and 1630 hours; it did not drop below 300 lux between 915 hours and 1600 hours (not shown here), which is the threshold illuminance for ambient lighting in office spaces (IESNA,2000). Thus the effective number of hours was reduced from 7.25 to 6.75.

With the introduction of SLS, KTB4 varied between 306 lux to 1415 from 900 hours to 1630 hours; it did not drop below 500 lux between 930 hours and 1530 hours, which is the threshold illuminance for task lighting in office spaces (IESNA, 2000). Thus the effective number of hours remained 6.0 with introduction of partition.

Between 1100hrs and 1400hrs, the SLS contributed significantly more daylight at the backzone (approximately 300 lux more), again similar to results obtained at LBNL (Beltran et al., 1997). The flatness of curve (rate of change with distance) and hence the uniformity reduced with the introduction of partition. The SLS curve was flatter without partition between 1500hrs and 1630hrs and between 900hrs and 930hours.

4.1.4. Comparison with earlier prototypes

Figure 4.20 give a comparison between outputs of an earlier prototype of OLP installed at the same site (Martins-Mogo, 2005).

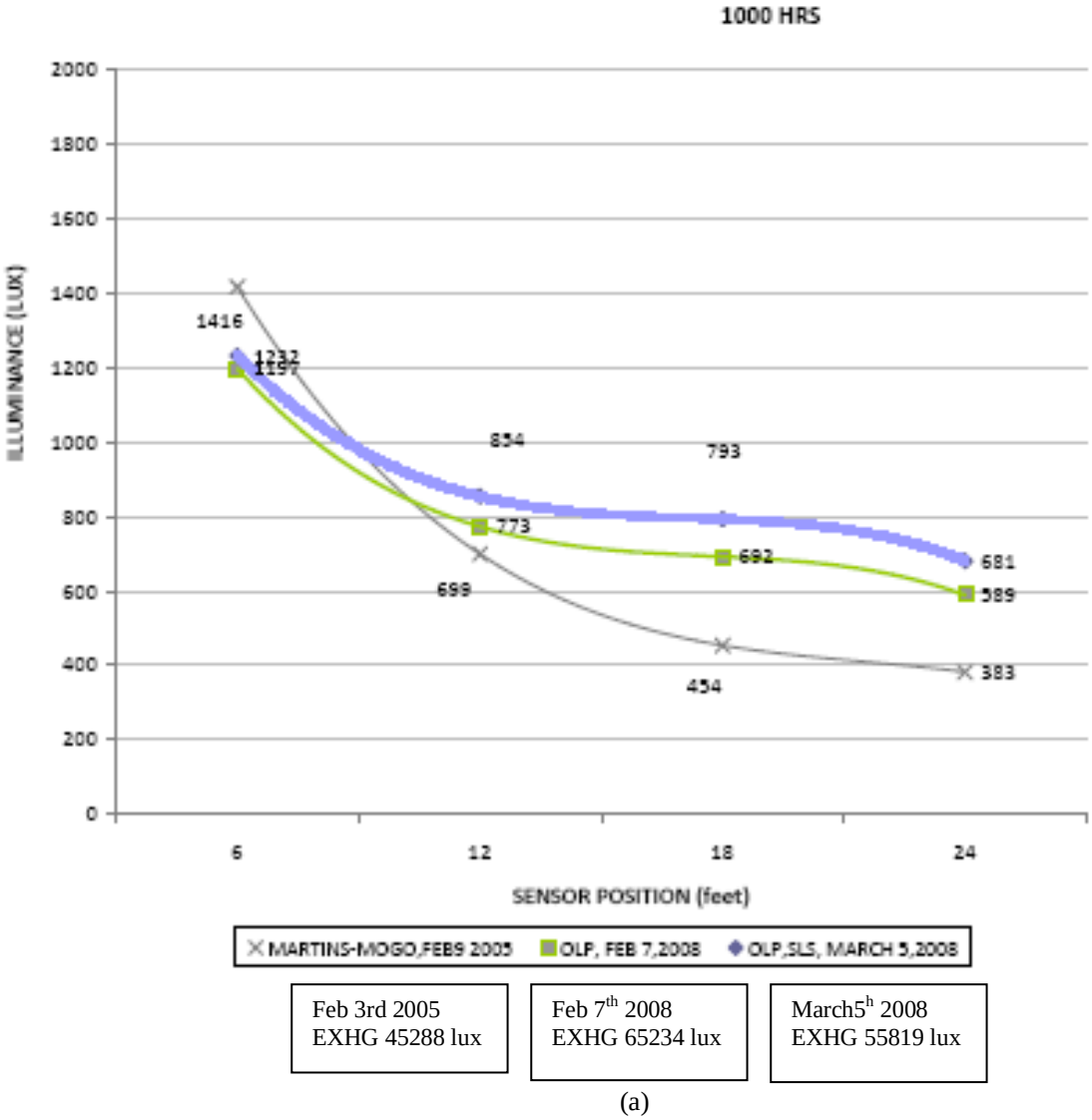

(a)

Fig. 4.20. Comparison of Martins-Mogo prototype with OLP in present research, and also with a combination of OLP and SLS. (a) 1000 hrs, (b) 1200 hrs, (c) 1530 hours.

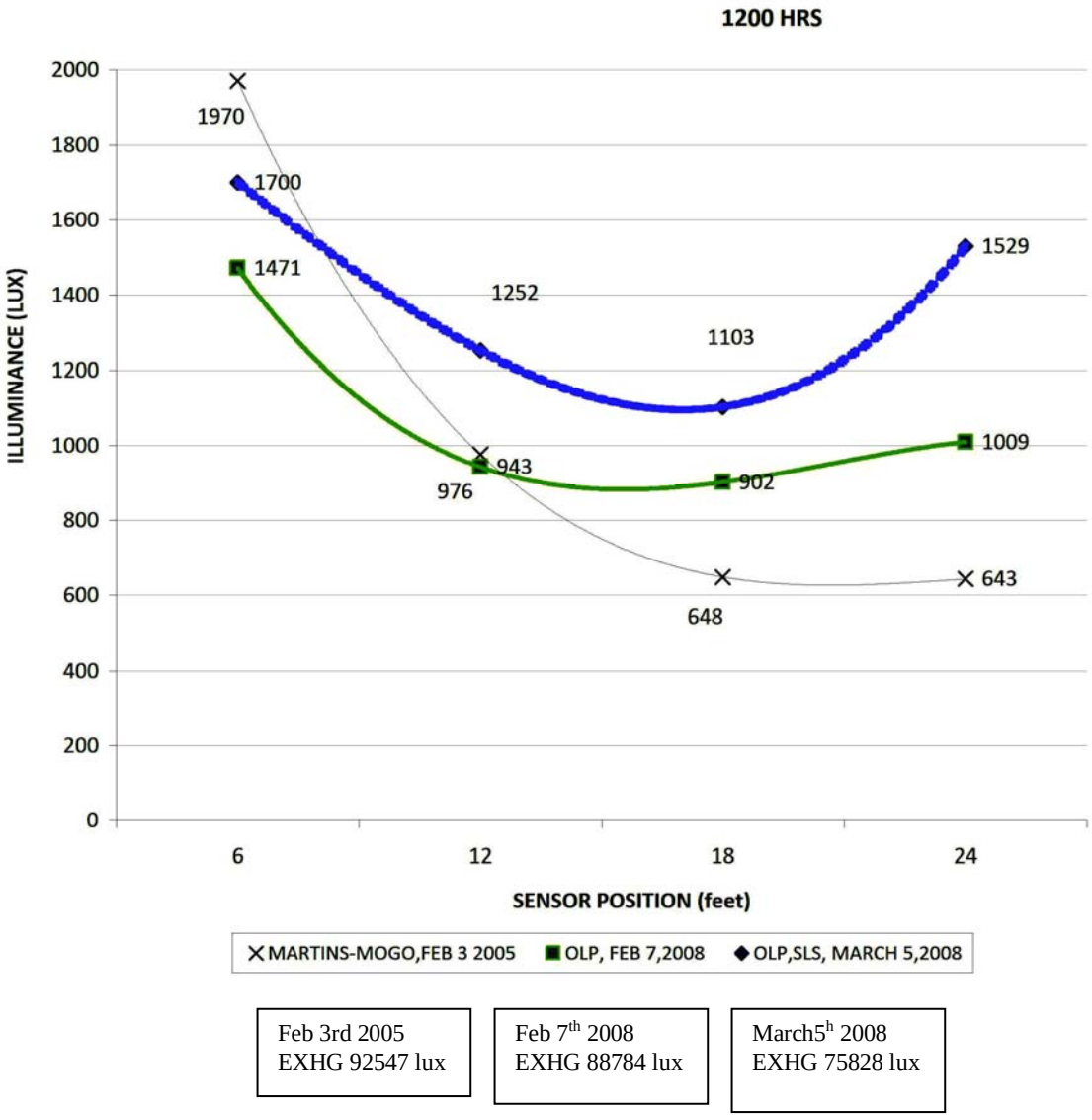

(b)

Fig. 4.20. Continued

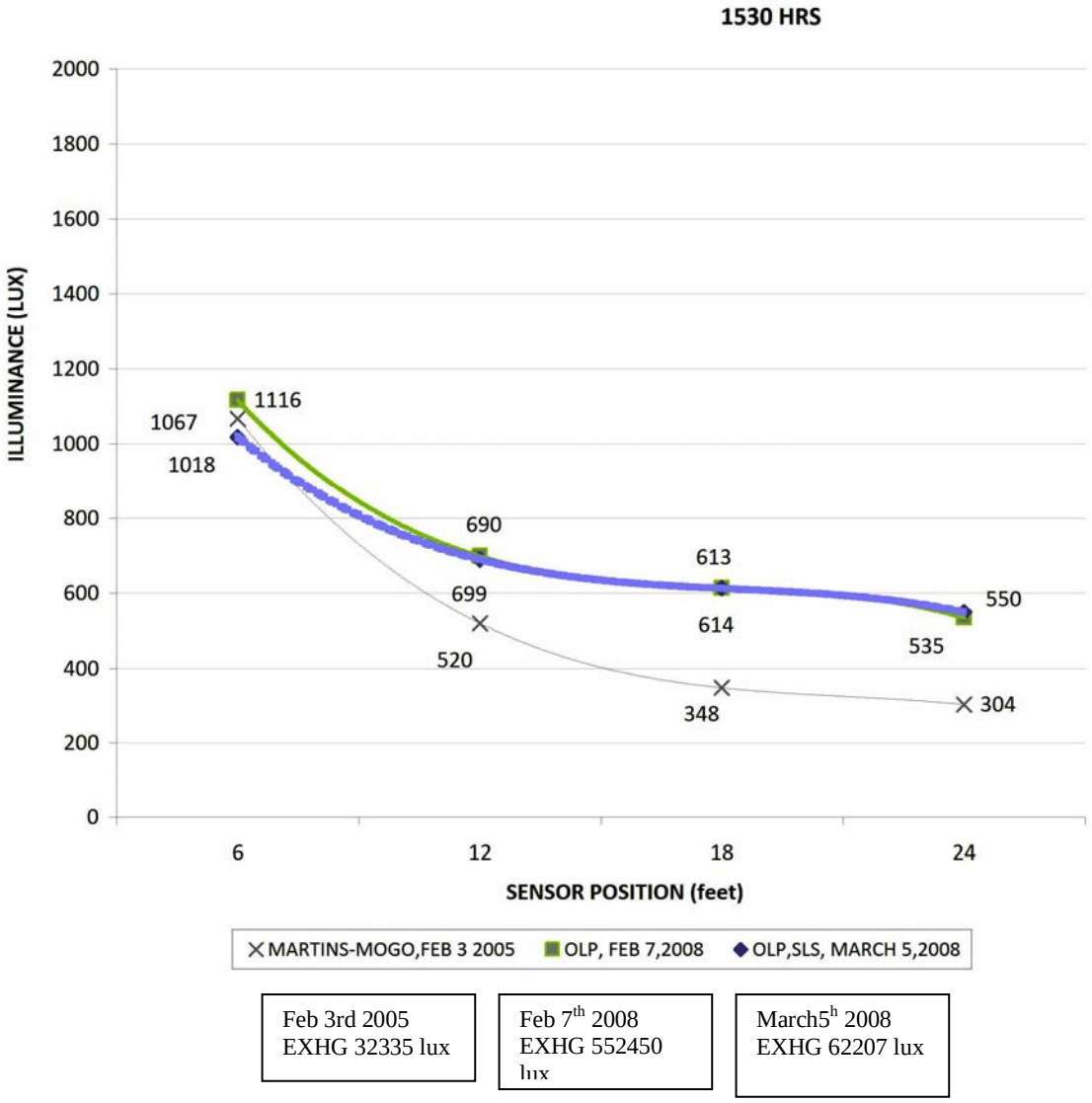

(c)

Fig. 4.20. Continued

The plots show an increase of 207 lux of output at 1000hrs by OLP alone, and 298 lux with addition of SLS; the corresponding increments at 1200 hours were 519 lux and 885 lux; and at 1600 hours were 230 lux and 245 lux. The present OLP also exhibited an increased flatness of curve over the three times.

Table 4.1 below compares OLP results with a similar prototype used by Beltran et al., 1997 for the month of February at 27.5 feet (sensor KTB4). The data shown was generated for a typical day in February using DOE2 simulation using a single light pipe with side reflectors (Beltran et al., 1997). The design of light pipe was done for the latitude of Los Angeles and hence would differ in geometry and output; it was included here for general output comparison only.

Table 4.1. Comparison of OLP with Beltran et al., 1997 prototype.

	Location: Los Angeles, CA Date: Average Feb day	Location: College Station, TX Date: Feb 7th, 2008	Difference
Solar time	Output of Prototype used by Beltran et al., 1997 (lux)	Output of OLP used in present research (lux)	
900 hours	311	452	141
1000 hours	542	742	200
1100 hours	693	849	156
1200 hours	921	1445	524
1300 hours	693	1024	331
1400 hours	542	642	100
1500 hours	311	489	178

4.2. EVALUATION OF DAYLIGHT UNIFORMITY

Data is evaluated under the following two categories to determine daylight uniformity:

- Illuminance contrast gradient, as stated earlier, is the ratio of average front task illuminance and average back task illuminance.
- Coefficient of variation of luminance were used to compare variation of luminance on surfaces over time.

4.2.1. Illuminance contrast gradient (ICG)

Fig 4.21 shows the ICG for blinds, shading and OLP without and with partition. An ICG of 1 would indicate equal average illuminance in front and back taskplanes. In both cases, ICG is closer to 1 in Test Model as compared to Reference Model. However, introducing the partition increased ICG in Test Model throughout the day; the minimum value increased from 1.2 to 1.4 and the maximum increased from 2.6 to 3.3. Also, there is an appreciable increase of intermittent variations. This indicated increase in non-uniformity due to the introduction of partition. Fig 4.21 shows the ICG with addition of SLS without and with partition. Here again, in both cases, ICG is closer to 1 in Test Model as compared to Reference Model. However, ICG remained close to 1.5 most of the time throughout the day in Fig. 4.22a, as opposed to its counterpart in Fig.4.21a. This is an indication of uniformity brought about by introducing SLS. Minimum ICG decreased from 1.1 to 1; the maximum value increased from 1.8 to 2.5. Again there is an appreciable increase of intermittent variations as seen in Fig.4.22b. This corroborated that non-uniformity increased due to the introduction of partition.

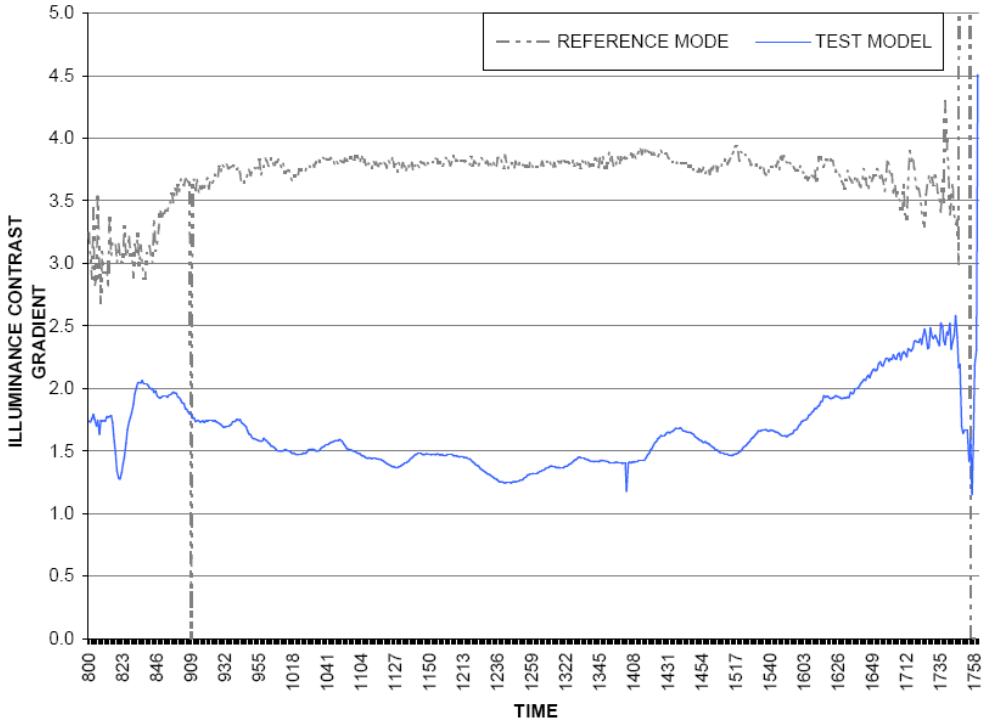

(a)

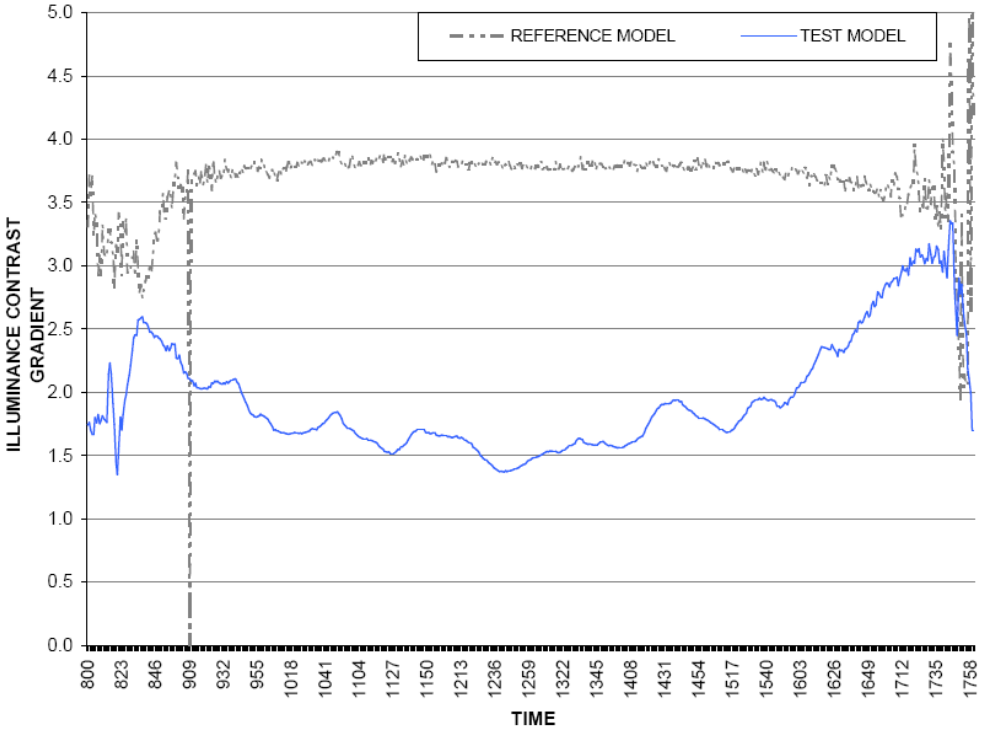

(b)

Fig. 4.21. Illuminance contrast gradient. (a) For Feb 7th with blinds, shading and OLP without partition, (b) for Feb 8th with blinds, shading and OLP with partition.

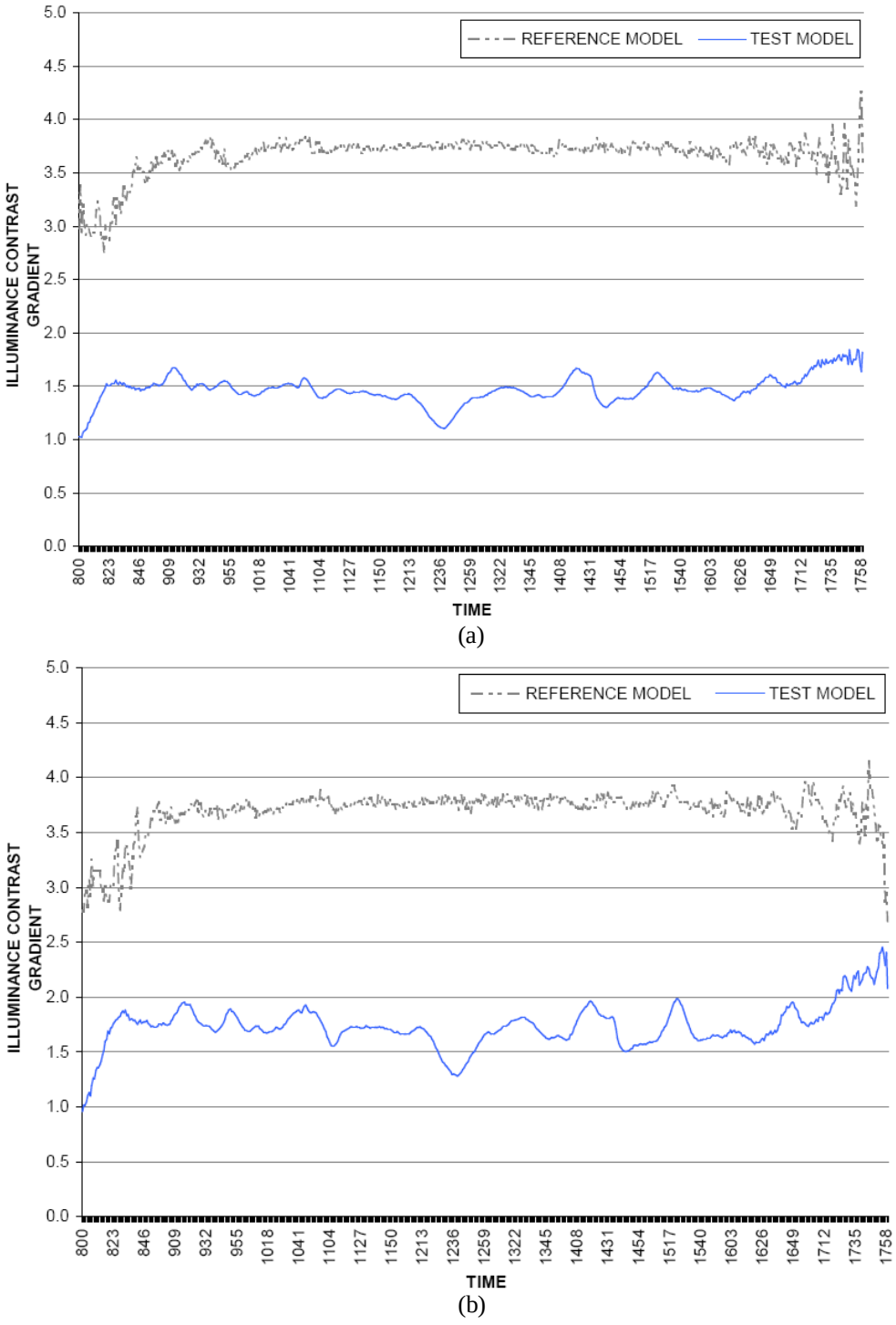

Fig. 4.22. Illuminance contrast gradient. (a) For March 5th with blinds, shading, OLP and SLS without partition, (b) for March 4th with blinds, shading, OLP and SLS with partition.

4.2.2. Coefficient of variation (CV) of luminance

Relevant surfaces were manually selected in luminance maps of Test Model namely: left wall, back wall, ceiling, back-taskplane and front-taskplane. The front-taskplane was not analyzed whenever the partition was kept because it blocked the view of the camera. Fig. 4.23 shows a sample set of luminance maps.

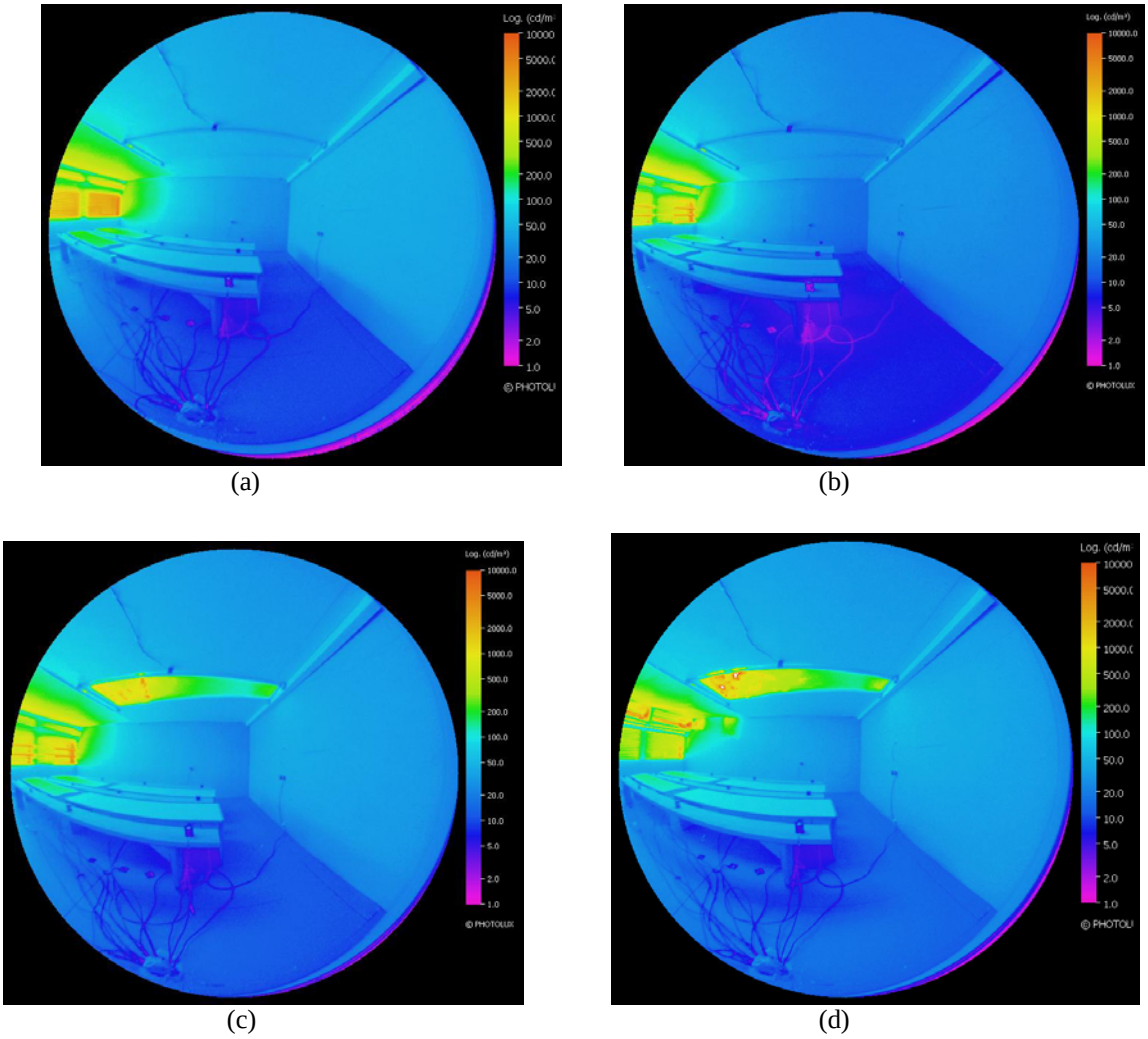

Fig. 4.23. Luminance maps at 9 am for four daylighting systems in Test Model. (a) Blinds only on Feb 13th, (b) blinds and shading devices on Feb. 6th, (c) blinds, shading devices and OLP on Feb 7th, (d) blinds, shading devices, OLP and SLS on March 5th.

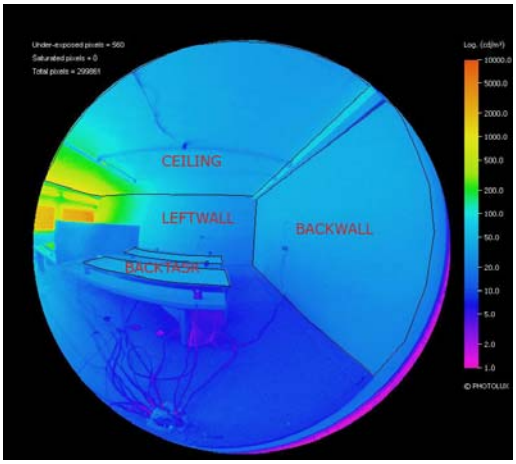

Fig. 4.24. Sample luminance map with definition of planes of interest.

Fig. 4.24 shows a sample of luminance map showing definitions of planes of interest. The front taskplane would not be visible in the presence of partition. Fig. 4.25 shows CV on back taskplane.

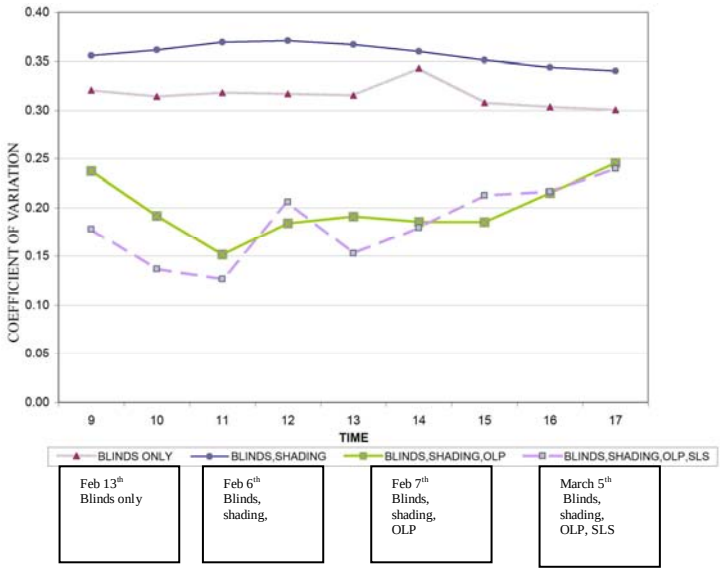

(a)

Fig. 4.25. Coefficient of variation of luminance on back taskplane. (a) Without partition, (b) with partition

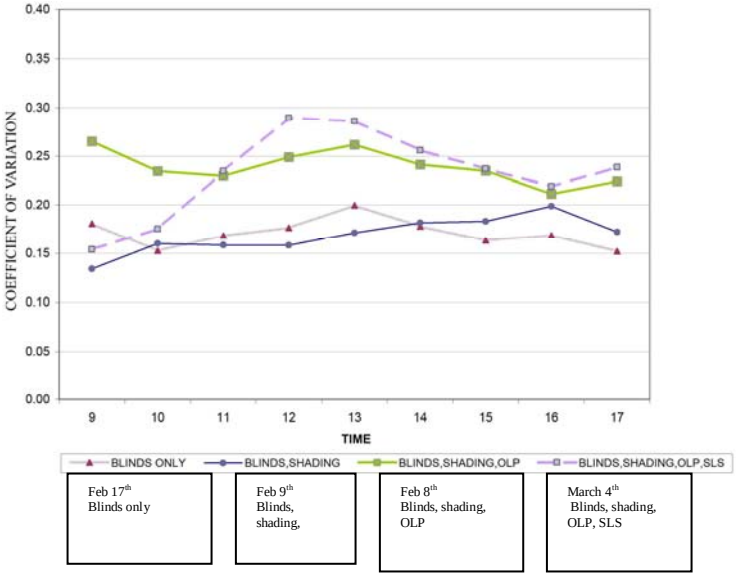

(b)

Fig. 4.25. Continued.

CV dropped for blinds only and blinds and shading case with the introduction of partition, as expected due to the window being blocked by the partition. SLS produced lower coefficient of variation on the back taskplane as compared to OLP on most times without partition, and was close to OLP case with partition.

CV increased however in OLP and SLS cases following the trend from ICG in the earlier section, reaffirming that variation of daylighting in the backzone increased with partition. Some interesting observations were made for the front taskplane shown in Fig. 4.26 below. The SLS case achieved the lowest CV for all hours. This was indicative of a more uniform daylighting level on the front taskplane, specially as compared to blinds only case which showed the highest variation for most of the times. The SLS case achieved the lowest CV for all hours. This was indicative of a more uniform daylighting level on the

front taskplane, specially as compared to blinds only case which showed the highest variation for most of the times.

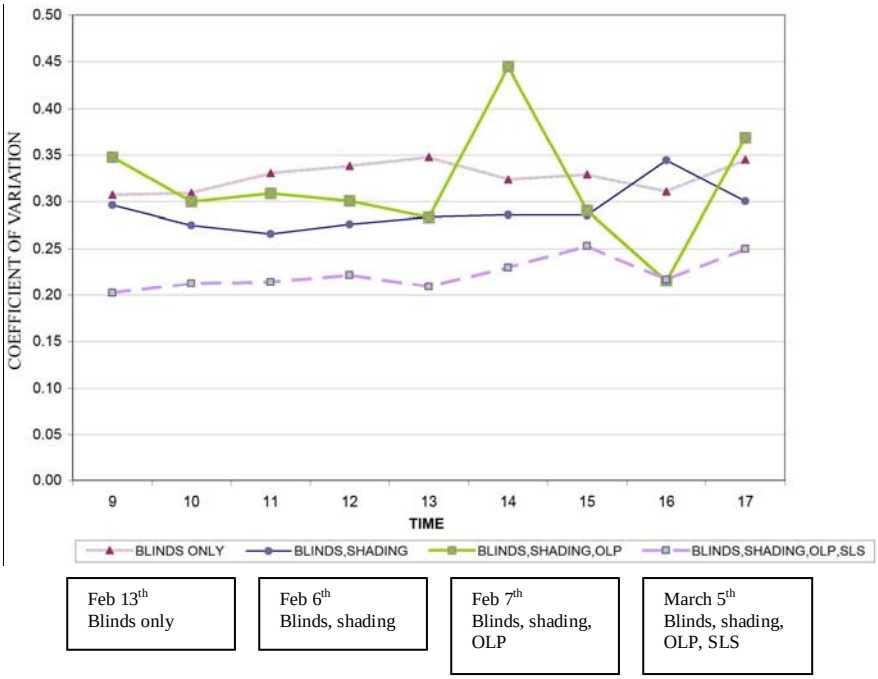

Fig. 4.26. Coefficient of variation of luminance on front taskplane without partition.

In the OLP case, the variation on front task increased at 1400 hours possibly due to reflection from the tail-end of the back-transport section. CV was lower for the shading case as compared to blinds only, reaffirming that shading provided more uniform daylighting as compared to blinds only.

CV for left wall was least and most uniform in the SLS case after 1200 hrs, followed by OLP case as shown in Fig.4.27. The SLS case had CV higher than all cases till 1100 hrs showing the movement of the bright spot reflected off SLS; the presence of partition did not significantly change this trend. The OLP exhibited an almost constant CV in both cases with very little effect of the partition.

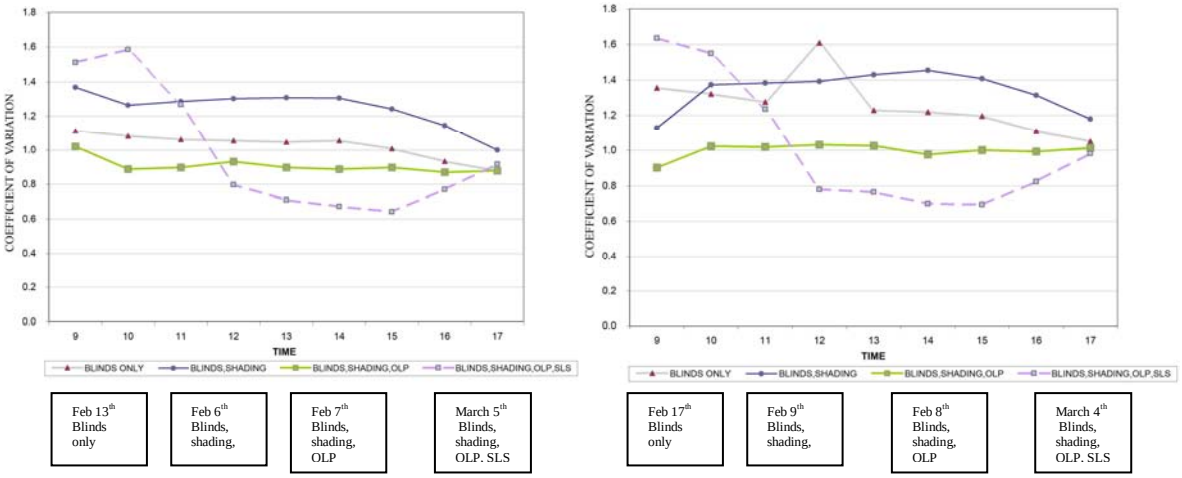

(a) (b)

Fig. 4.27. Coefficient of variation of luminance on left wall. (a) Without partition, (b) with partition.

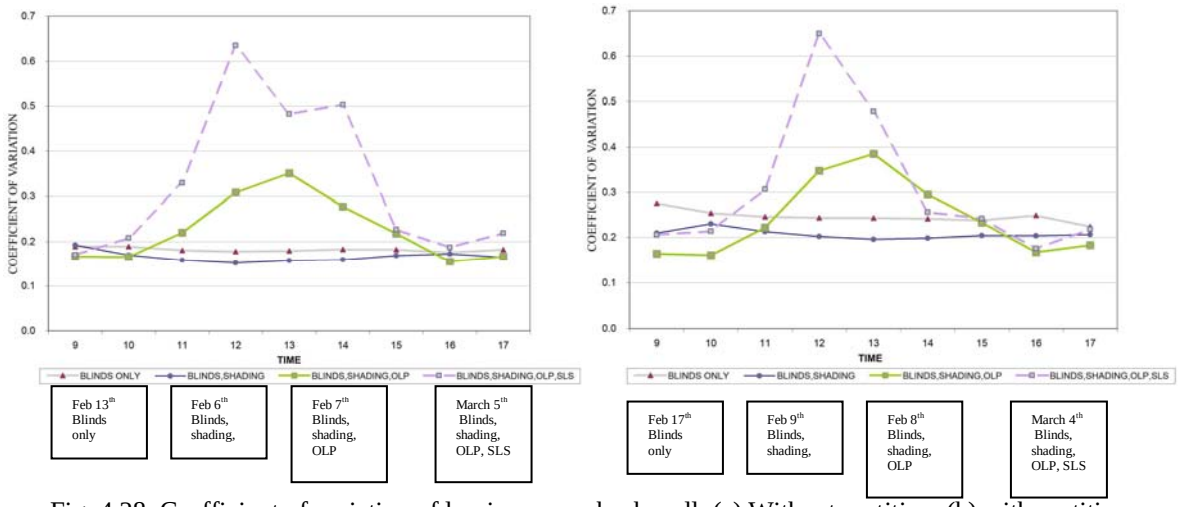

Fig. 4.28. Coefficient of variation of luminance on back wall. (a) Without partition, (b) with partition.

CV for back wall was not largely affected by the addition of partition except in the SLS case at 1400hrs as shown in Fig. 4.28. This points out the ability of the partition to block some of the rays from SLS that directly hit the backwall. A significantly higher variation due to SLS than OLP could be observed between 1130hrs and 1330hrs

corresponding to the presence of brighter spots on the backwall due to SLS (refer Fig.4.29 below).

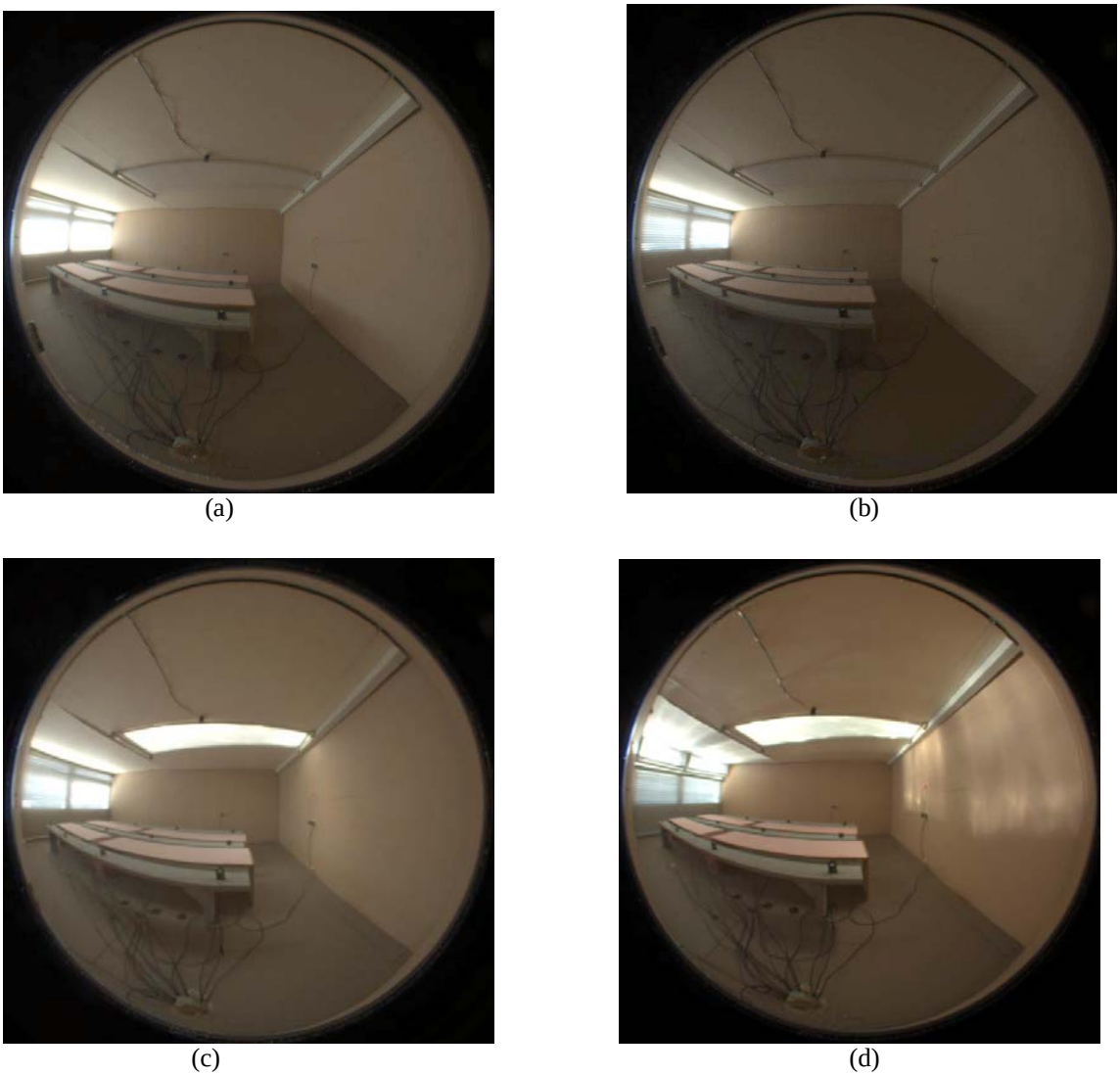

(a) (b)

(c) (d)

Fig. 4.29. Fish eye view of four daylighting systems at 1 pm in Test Model. (a) Blinds only on Feb 13th, (b) blinds and shading devices on Feb. 6th, (c) blinds, shading devices and OLP on Feb 7th, (d) blinds, shading devices, OLP and SLS on March 5th.

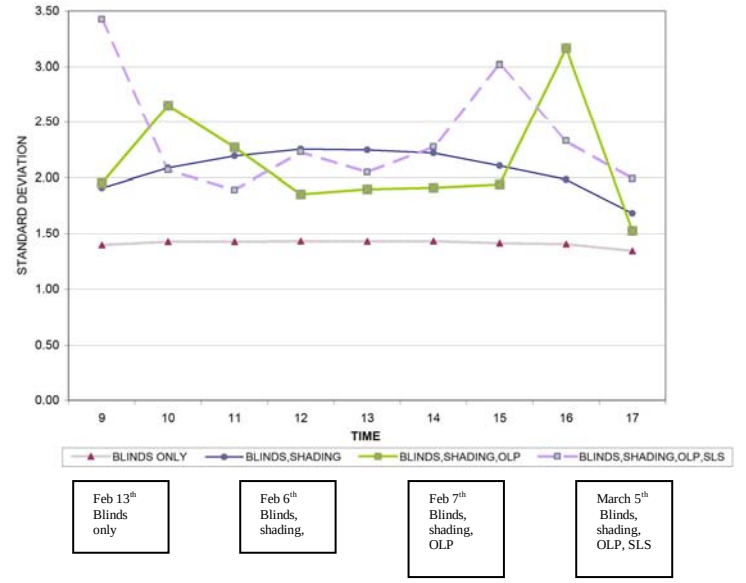

(a)

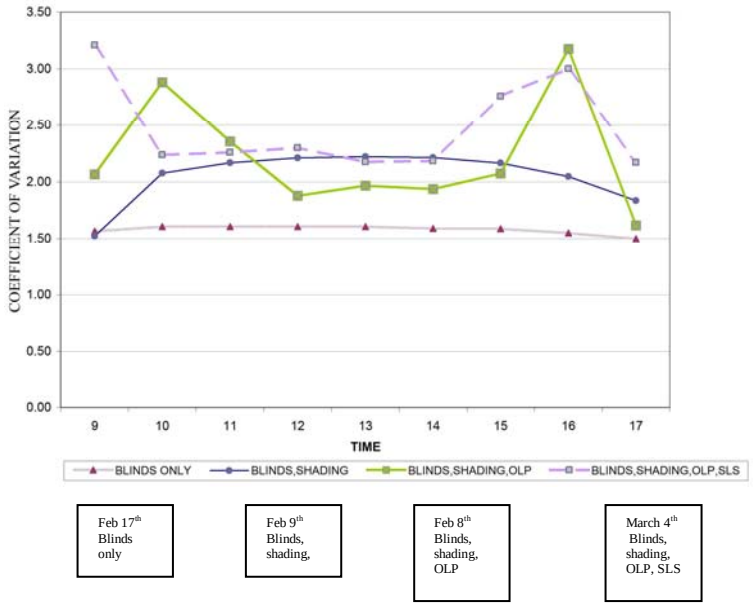

(b)

Fig. 4.30. Coefficient of variation of luminance on ceiling. (a) Without partition, (b) with partition.

CV for the ceiling did show differences with the addition of partition as shown in Fig. 4.30. They were attributed to differences in inter-reflections of light in the OLP on Feb 7th and Feb 8th, and March 5th and March 4th, more clearly visible in Fig. 4.29. A

significantly higher variation could be observed for OLP at 1000hrs and 1600hrs due to its ability to effectively transport the low angled sunrays to the diffuser. The SLS showed a higher variation than OLP on most cases.

4.3. GLARE ASSESMENT

Data is evaluated under the following two categories to assess glare:

- Unified glare rating as defined in section 3.1.
- Luminance ratios.

Standard VDT screens emits 100cd/m^2 (Luminance Test Patterns and Procedures). Luminance ratios were taken between walls and the VDT screen, as well as between walls and back taskplane. The minimum, maximum and average luminance of surfaces were considered.

4.3.1. Unified glare rating (UGR)

Fig. 4.31. shows the UGR values for the four daylighting designs without and with partition. The overall UGR values dropped with the introduction of partition. The glare potential due to OLP was highest at 1000hrs and 1600hrs, while that due to SLS was highest at 1500hours. With the introduction of partition, the glare potential of SLS was highest at 1200hrs and 1300hours. This was indicative of the partition able to block potential glare from SLS for low sun angles; but the partition, because it partly blocked the view of the bright window, caused UGR value to increase during noon hours.

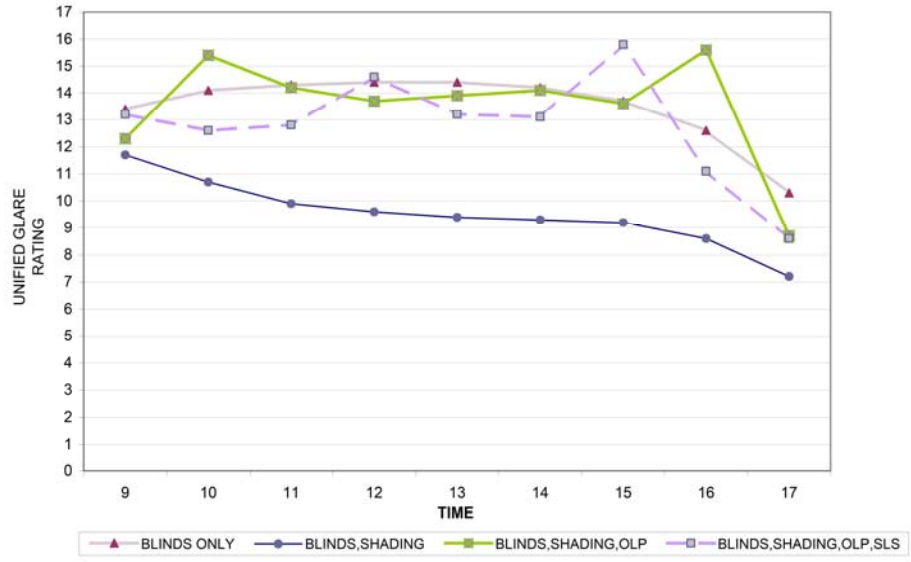

Feb 13th Blinds only	Feb 6th Blinds, shading	Feb 7th Blinds, shading, OLP	March 5th Blinds, shading, OLP, SLS

(a)

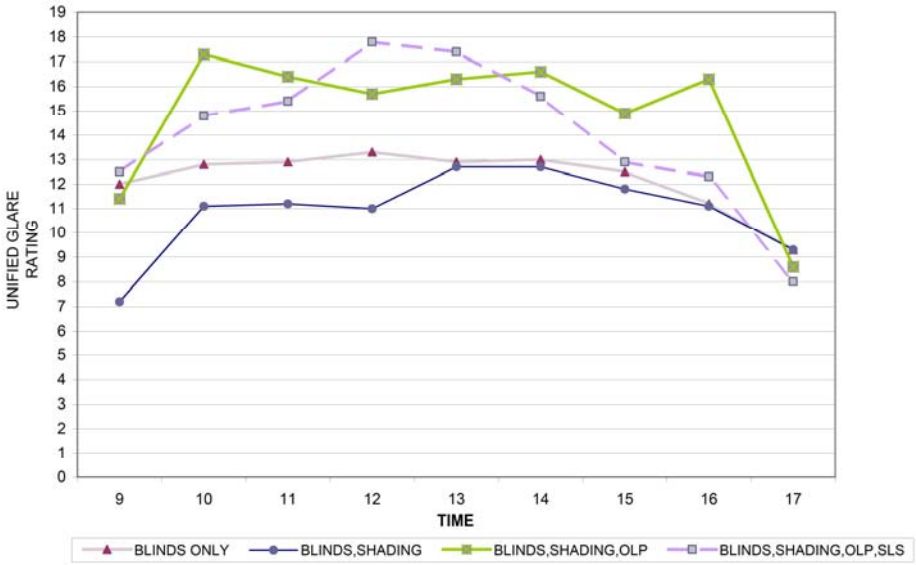

Feb 17th EXHG 52960 lux	Feb 9th EXHG 51715 lux	Feb 8th EXHG 52605 lux	Mar 4th EXHG 47880 lux

(b)

Fig. 4.31. UGR variation during the day for the four daylighting designs. (a) Without partition, (b) with partition.

With reference to Table 3.2, the UGR values were within the maximum allowable range for offices, namely 19. However, it would be worth to mention that the UGR as an index is lenient for large sources of glare (CIE, 1995). The section that follows, analyses the glare potential with the more established metric of luminance ratio.

4.3.2. Luminance ratios (LR)

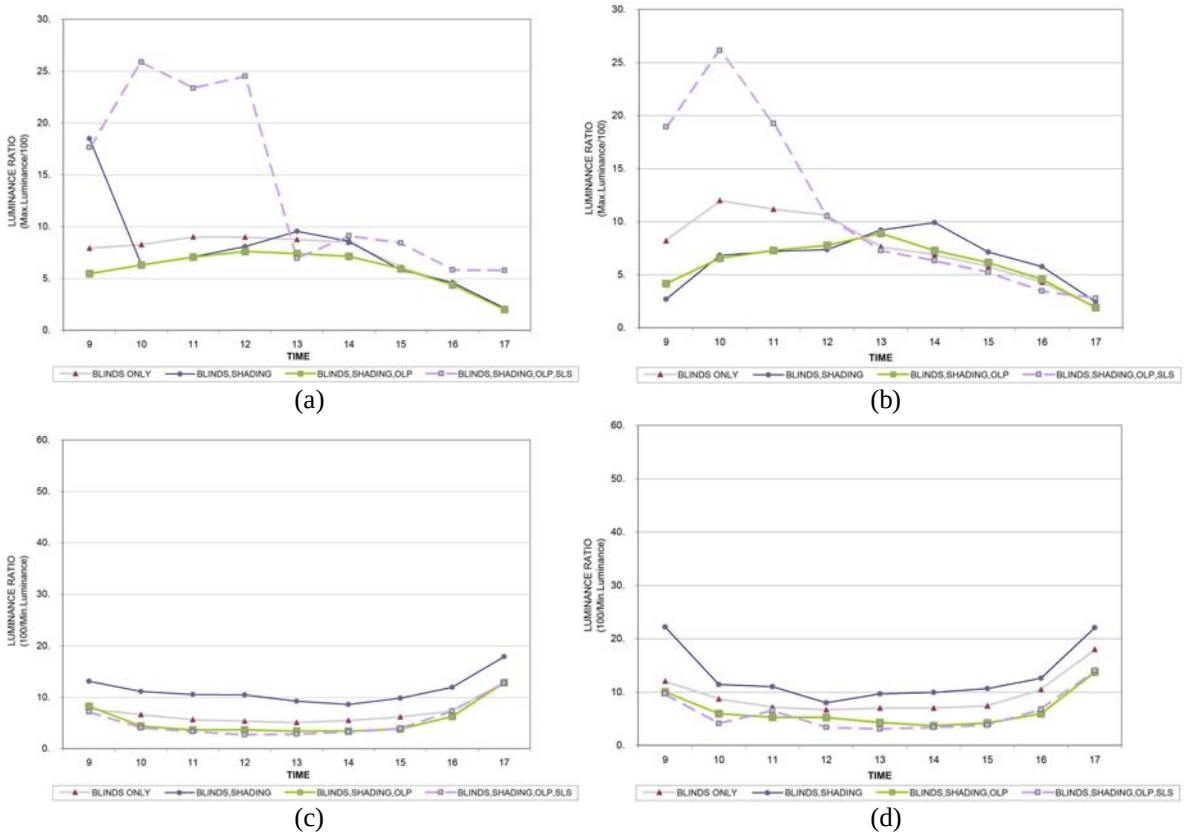

Fig. 4.32. Luminance ratios between VDT (100cd/m^2) with left wall. (a) Maximum luminance without partition, (b) maximum luminance with partition, (c) minimum luminance without partition, (d) minimum luminance with partition, (e) average luminance without partition, (f) average luminance with partition.

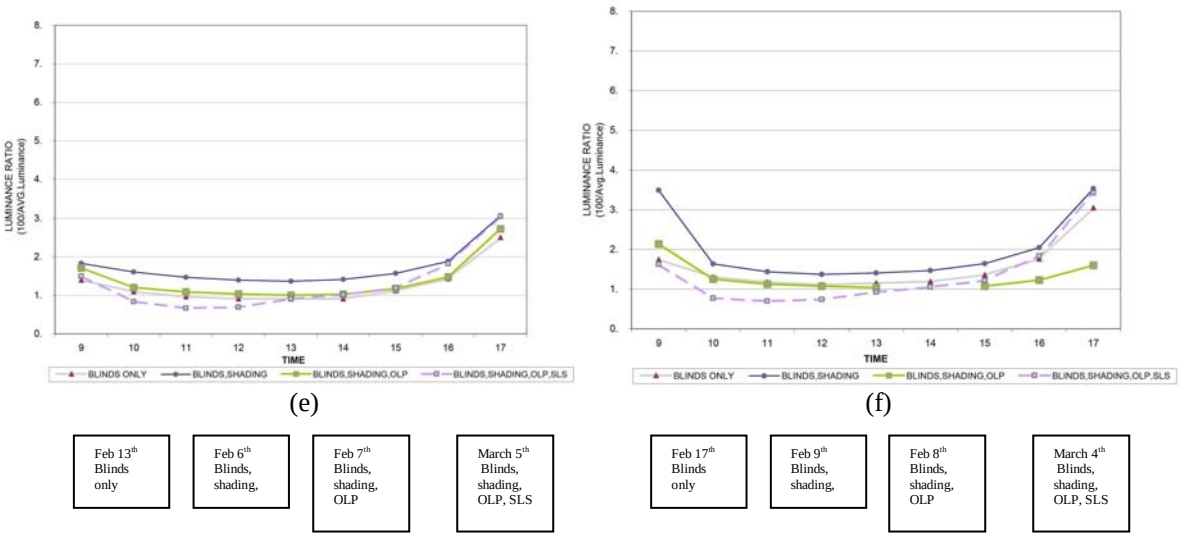

Fig. 4.32. Continued.

Fig. 4.32. indicates that LR between VDT and average luminance on left wall remained less than 3 for all cases, indicating no glare even if left wall were an adjacent work surface. However, the left wall might not be an ideal background in the blinds and shading device case before 1000 hours and after 1600 hours without partition, and almost round the day with partition, due to low luminance levels. With maximum luminances, the SLS case had LR values greater than 10 before 1300 hours without partition and before 1200 hours with partition, indicating glare possibility during those hours. The OLP case remained within prescribed LR limits.

Fig. 4.33 indicates that LR between VDT and maximum luminance of back wall remained less than 3 for OLP without and with partition. It increased to about 6 for the SLS case indicating that with SLS, the back wall could produce glare if it was an adjacent worksurface but would otherwise be glare free as a background object. Based on the

minimum luminances, the backwall would not be an ideal background in the blinds and shading device case for all hours; it would not be an ideal background in all other cases before 1000hrs and after 1600hrs especially with the partition present.

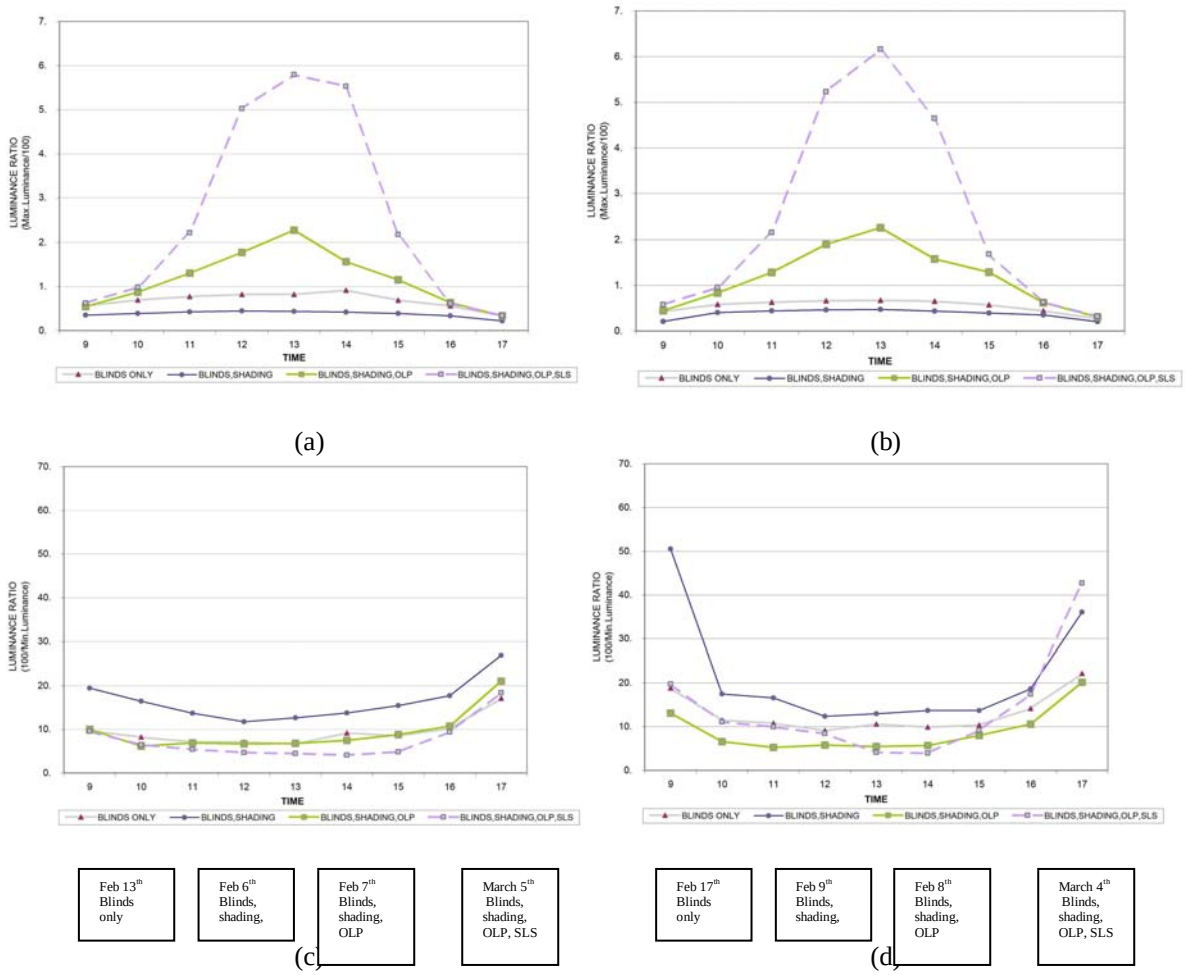

Fig. 4.33. Luminance ratios between VDT with back wall (a) Maximum luminance without partition, (b) maximum luminance with partition, (c) minimum luminance without partition, (d) minimum luminance with partition.

Fig. 4.34 compares LR values between the back taskplane and other surfaces. Average luminance values were taken for all surfaces. The plots indicated that LR values

fell well within the prescribed range of 0.1 to 10 for wall surfaces to serve as backgrounds, and 0.33 to 3 for them to serve as adjacent work surfaces.

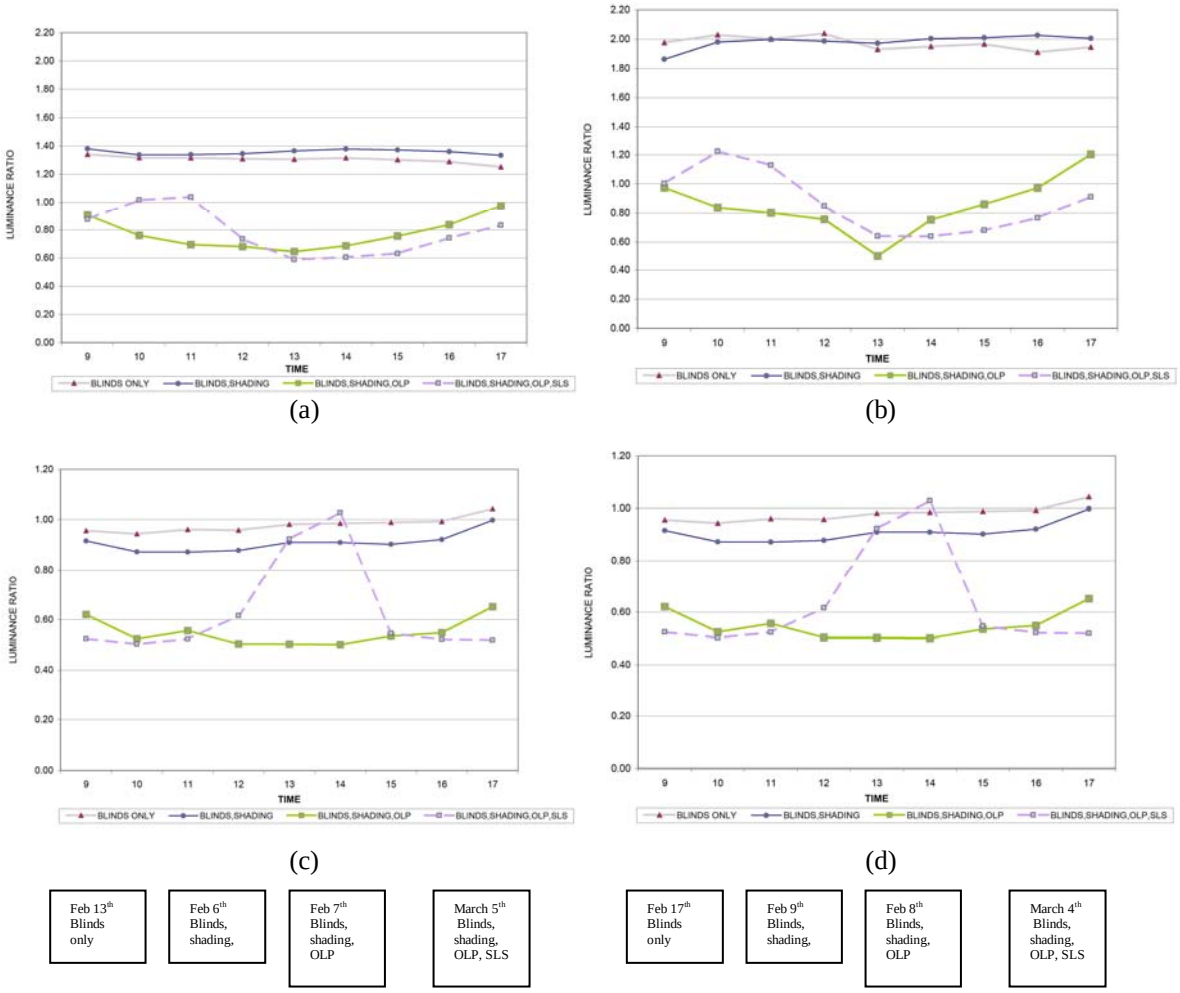

Fig. 4.34. Luminance ratios between back taskplane and walls (=average value on wall/average value on back taskplane). (a) Average luminance on left wall without partition, (b) average luminance on left wall with partition, (c) average luminance on back wall without partition, (d) average luminance on back wall with partition.

V. CONCLUSIONS

5.1. SUMMARY OF RESULTS

The results summarized include comparison of daylighting systems on clear days between February and March of 2008 as discussed in Section IV. Of the three hypotheses, two were proved conditionally. Other useful results are also summarized subsequently.

First hypothesis: It is possible to achieve 300 lux of illuminance for more than 6 hours in the back zone of a deep plan office space using an OLP on a clear sky day.

Proof: Use of OLP substantially increased average illuminance on back workplane, over 300 lux for 7.4 hours.

Second hypothesis: It is possible to achieve more uniform daylight levels by combining a static light shelf (SLS) with OLP.

Conditional proof: SLS produced more uniform ICG levels on the work plane as compared to OLP. It also produced lower coefficient of variation on the back taskplane (as compared to OLP on most times without partition) and on all times on the front taskplane. SLS exhibited least CV for left wall on most times.

Condition: SLS exhibited highest CV on left wall before 1100hrs, and the highest CV on ceiling and backwall on all times.

Third hypothesis: It is possible to achieve a visually comfortable office space using OLP and a combination of OLP and SLS when the south façade is installed with blinds and exterior shading devices.

Conditional proof: With OLP, luminance ratios were well within prescribed limits and hence work surfaces were visually comfortable.

Condition: From the UGR standpoint, there was higher potential for glare at 1000hrs and 1600hrs in the OLP case; in the SLS case there was higher potential for glare at 1200hrs and 1300hrs when a partition was used. Also, in the SLS case, bright spots on left wall could produce non-uniform luminance between 900hrs and 1300hours.

In conclusion, the OLP may eliminate the need for ambient electric lighting in regular office areas as per IESNA standards for more than 7 hours. It also brought uniform illuminance on the back taskplane as compared to blinds only or blinds with shading device options. The high illuminance on the back wall could be of advantage to extend the effective depth of the back zone to beyond 30'. The OLP achieved 200lux of illuminance more than the Martins-Mogo prototype on the workplane between 1000hrs and 1630hrs, the comparisons being made for similar clear-sky days in 2005 and 2008. The OLP also performed better than windows with blinds and shading at providing diffuse daylight in the backzone on a cloudy day; it provided about 100 lux more than the latter when exterior illuminance was above 10,000 lux .

The introduction of SLS increased illuminance on back workplane: over 500 lux for 6 hours. This may completely eliminate the need of task lighting in regular office areas as per IESNA standards. The problem of glare existed at the end walls, and for a large office space with multiple SLS prototypes, this could be rectified by architectural design. The backwall exhibited high luminance values indicating that the SLS design needed more refinement to minimize any fall-off onto surfaces other than the ceiling. The combination of SLS with OLP also achieved about 300lux for close to 4 hours in the backzone on a cloudy day in the absence of any contribution from the window.

In general, the presence of partition increased non-uniformity in ICG levels and CV levels on workplane. However, the partition helped in reducing glare potential from sidewall and window.

5.2. SIGNIFICANCE AND FUTURE WORK

The research has paved way for a full scale development of OLP as an efficient means of providing daylight to deep plan office spaces. Mirosilver and DFPM used in the experiment would succeed as building materials for the full scale OLP. The research also encourages application of OLP to other building types and as a retrofit for existing buildings which have an available south facade. The optical light pipe on south facades may combine well with anidolic systems on the north façade to provide ideally daylit cores in office buildings. However anidolic systems would need to be tested for glare during clear days for the latitude of 30˚36'N for their effectiveness. Further studies and simulation for SLS would be needed to arrive at a better design, which could redirect all sunlight to the ceiling. Also worth exploring are heat gains from its much larger opening as compared to OLP.

REFERENCES

ASHRAE Standard 90.1-2004, Appendix-G – Energy Standard for Buildings Except Low-rise Residential Buildings. I-P Edition. American Society of Heating, Refrigerating and Air-Conditioning Engineers, Inc, Atlanta, GA.

Aizenberg, J.B., 1997. Principal new hollow light guide system “Heliobus” for daylighting and artificial lighting of central zones of multi storey buildings. In: Proceedings of the 4th International Conference on Energy Efficient Lighting—Right Light 4, Copenhagen, Denmark, November 19-21, 1997, 239-243.

ANSI/IESNA, 2004. American National Standard Practice for Office Lighting, RP-1-04. Illuminating Engineering Society of North America, New York, NY.

Beltrán, L.O., Lee, E.S., Papamichael, K.M., Selkowitz, S.E., 1994. The design and evaluation of three advanced daylighting systems: light shelves, light pipes and skylights. In: Proceedings of the American Solar Energy Society Solar 1994 Conference, San Jose, CA., June 25-30, 1994.

Beltrán, L.O., Lee, E.S., Selkowitz, S.E., 1997. Advanced optical daylighting systems: light shelves and light pipes. Journal of the Illuminating Engineering Society 26 (2), 91–106.

Boyce, P., Hunter, C., Howlett, O., 2003. The Benefits of Daylight through Windows. Lighting Research Center, Rensselaer Polytechnic Institute, Troy, NY.

CIE (International Commission on Illumination) Collection on glare, 2002. Technical committee report, International Commission on Illumination, Vienna.

CIE (International Commission on Illumination) Collection on glare, 1995. Technical committee report, International Commission on Illumination, Vienna.

Culp, J., Schoen, D., 1999. Image analysis procedures and supplemental tools. CERES, Ball State University. Based on: Interior Illuminance, Daylight Controls and Occupant Response, Vital Signs Resource Package by Schiler M., Japee, S., USC. Available from http://www.bsu.edu/classes/culp/litestuff/040703bsumanual.pdf

Derek, 2004. Daylighting: Natural Light in Architecture. Elsevier, Amsterdam.

Dubois, M.C., 2001. Impact of Solar Shading Devices on Daylight Quality, Measurements in Experimental Office Rooms. Available from http://www.ebd.lth.se/fileadmin/energi_byggnadsdesign/images/Publikationer/Bok-3061.pdf

Hansen, G. V., Edmonds, I., Hyde, R., 2001. The use of light pipes for deep plan office buildings - a case study of Ken Yeang's bioclimatic skyscraper proposal for KLCC, Malaysia. In: Proceeding of the 35th Annual Conference of the Australian and New Zealand Architectural Science Association, Wellington, New Zealand, November 21-23, 2001.

Heschong, L., Mahone, D., 2003. Windows and Offices: a study of office worker performance and indoor environment. Research Report for California Energy Commission, San Francisco. Available from http://www.energy.ca.gov/reports/2003-11-17_500-03-082_A-09.PDF

Heschong Mahone Group, Inc., 2005. Sidelighting photocontrols field study. Submitted to Northwest Energy Alliance, Pacific Gas and Electric Company, and South

California Edison. Available from http://www.hmg.com/downloads/Photocontrols/Final%20Report%20Sidelit%20Photocontrols%20including%20Errata%20031406.pdf

Helmut, K., 2004. Dynamic Daylighting Architecture, Birkhauser, Basel, Switzerland, 165.

Howlett, O., Heschong, L., L.C., McHugh, J., 2006. Scoping study for daylight metrics from luminance maps. LEUKOS 3(3), 201 – 215.

Hu, J., 2003. The design and assessment of advanced daylighting systems integrated with typical interior layouts in multi-story office buildings, Ph.D. Dissertation, North Carolina State University, Raleigh.

IESNA (Illuminating Engineering Society of North America), Reas, M. (Ed.), 2000. Lighting Handbook: Reference and Application, 9th ed. IESNA. New York, NY.

Inanici, M., Galvin, J., 2004. Evaluation of high dynamic range photography as a luminance mapping technique. Escholarship repository of Lawrence Berkley National Laboratory. Available from http://repositories.cdlib.org/lbnl/LBNL-57545/

Kischkoweit-Lopin, M., 2002. An overview of daylighting systems. Solar Energy 73 (2), 77–82.

Martins-Mogo, B.G., 2005. An experimental setup to evaluate the daylighting performance of an advanced optical light pipe for deep-plan office buildings. M.S.Thesis, Texas A&M University, College Station, TX.

Oakley, G., Riffat, S.B., Shao, L., 2000. Daylight performance of light pipes. Solar Energy 69 (2), 89–98.

O'Connor, J., Lee, E., Rubinstein, F., Selkowitz, S., 1997. In: Tips for Daylighting with windows - The integrated approach, p. 1-1. Building Technologies Program, Energy and Environment Division of the Lawrence Berkeley National Laboratory. Available from http://eetd.lbl.gov/btp/pub/designguide/dlg.pdf

Pande A., Heschong L., McHugh J., Ander G., 2004. Effectiveness of photocontrols with skylighting, IESNA National Conference , Tampa, FL. Available from http://www.h-m-g.com/downloads/Papers/Photocontrol_effectiveness_Paper13wcover.pdf

Pande A., Heschong L., McHugh J., Ander G., 2006. Photocontrols and daylighting savings from skylights: Urban myths and realities from a field study, National Conference on Building Commissioning, San Francisco, CA. Available from http://www.peci.org/ncbc/proceedings/2006/07_Pande_NCBC2006.pdf

Rosemann, A., Mossman, M., Whitehead, L., 2006. A cost effective solution for core daylighting in office buildings. In: Proceeding of American Solar Energy Conference, Denver, CO, July 7-13, 2006.

Scartezzini, J.L., Courret, G., Francioli, D., Meyer, J-J., 1998. Design and assesment of an anidolic light-duct. Energy and Buildings 28, 79-99.

Scartezzini, J.L., Courret, G., 2002. Anidolic daylighting systems. Solar Energy 73 (2), 123–135.

Selkowitz, S., Lee, E. S., 1998. Advanced fenestration systems for improved daylight performance. In: Proceedings of International Daylighting Conference 1998, Ottawa, Canada, 341–348.

UNEP (United Nations Environment Programme), Buildings and Climate Change: Status, Challenges and Opportunities, 2007. United Nations Environment Programme, 13-16. Available from http://www.unep.fr/pc/sbc/documents/ Buildings_and_climate_ change.pdf

Ward, G., 2001. High dynamic range imaging. In: Proceedings of the 9th Color Imaging Conference, Scottsdale, AZ, 9–16.

APPENDIX A
RAYTRACING WITH TRACE-PRO

Manual raytracing was performed for the existing design of OLP for different times of the year.

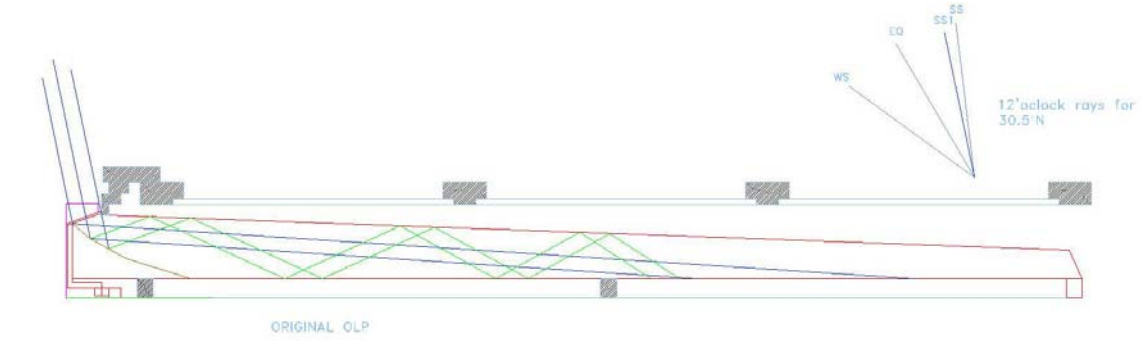

(a)

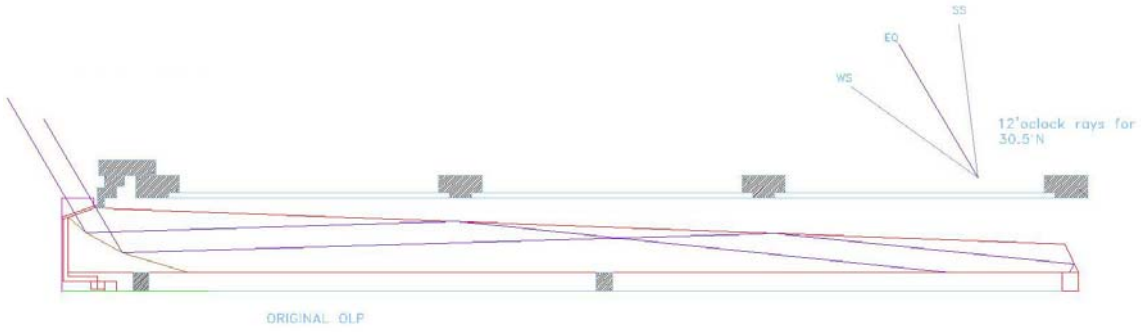

(b)

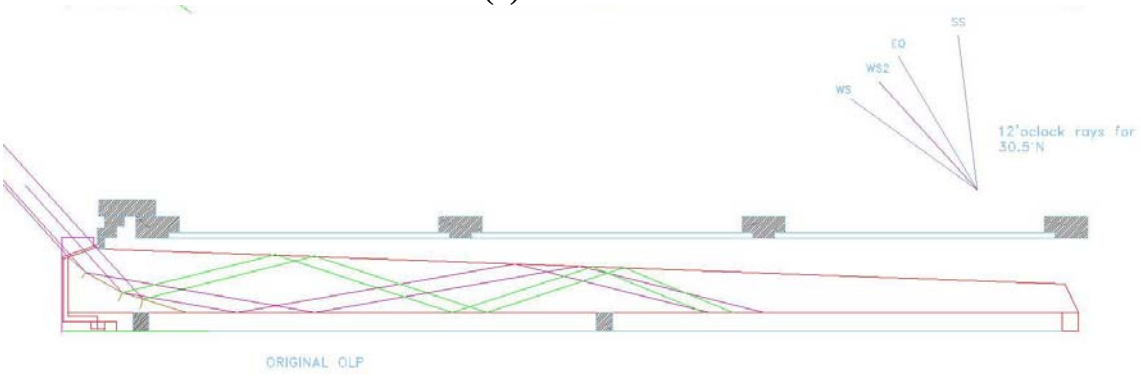

(c)

Fig. A-1 Samples of manual raytracing done for different times of the year on Martins-Mogo prototype. (a) Between summer solstice and equinox, (b) at equinox, (c) between equinox and winter solstice.

However, due to the changing angles of the sun at all times of the year, and hence the amount of flux incident on the collector, it was cumbersome and inaccurate to continue the process. A temporary student license of TracePro, a raytracing software which combines the Monte-Carlo algorithm with forward raytracing and is used extensively for optical designs, was granted by LambdaPro for the current research and raytracing was performed in the following manner:

Objective: To optimize the geometry of the OLP to get maximum amount of direct sunlight transferred to the diffuser.

Definition of source: Only direct sunrays going through the clear glass opening were of interest. So a plane was defined perpendicular to the sunrays and the size of the source was determined by projecting the clear glass on to that plane. All the rays in Tracepro were then emitted perpendicular by the source. (All modeling was done in Autocad2000 and then the file saved as '.sat' type, which was readily imported in TracePro.)

Fig. A-2. Solar rays represented by planar sources perpendicular to sun at different times of the day.

Definition of materials: The glass had a transmittance of 88%. All the reflective surfaces of the OLP had a reflectance of 99%. All other surfaces were considered absorptive with 0% reflectance. The diffuser was also considered 100% absorptive because the simulation was done to optimize the geometry of the OLP and not to determine the illuminance on the workplane. The diffuser was assigned as the importance target.

Images were visually compared with simulations of 100 rays. It provided a clear picture to the general reflection characteristics throughout the OLP. As the number of rays increased the graphic tends to get complicated and hence difficult to read. The final simulation to get the output on diffuser, however, was done with 10,000 rays. It was the most efficient limit considering the time taken by simulation and the number of simulations to be performed. The periods of raytracing were as follows:

June 21: solar times – 8am/4pm, 9am/3pm, 10am/2pm, 11am/1pm, 12pm.

March 21: solar times – 8am/4pm, 9am/3pm, 10am/2pm, 11am/1pm, 12pm.

Dec 21: solar times – 8am/4pm, 9am/3pm, 10am/2pm, 11am/1pm, 12pm..

The following variations of optical light pipe were ray-traced:

Martins-Mogo prototype, 5DEG (side walls rotated by 5˚), 10DEG (side walls rotated by 10˚), 6F6B (front 6', back 6'), 6F4B (front 6', back 4'), 6F2B (front 6', back 2'), 6F2B5C (front 6', back 2', sidewalls of back transport-section rotated by 5˚), 6F2B10C (front 6', back 2', sidewalls of back transport-section rotated by 10˚), 6F2B15C (front 6', back 2', sidewalls of back transport-section rotated by 15˚). A number of options were tested with sidereflectors also before arriving at the final configuration. (Raytracing images for June 21 only are included in the appendix).

Martins-Mogo prototype

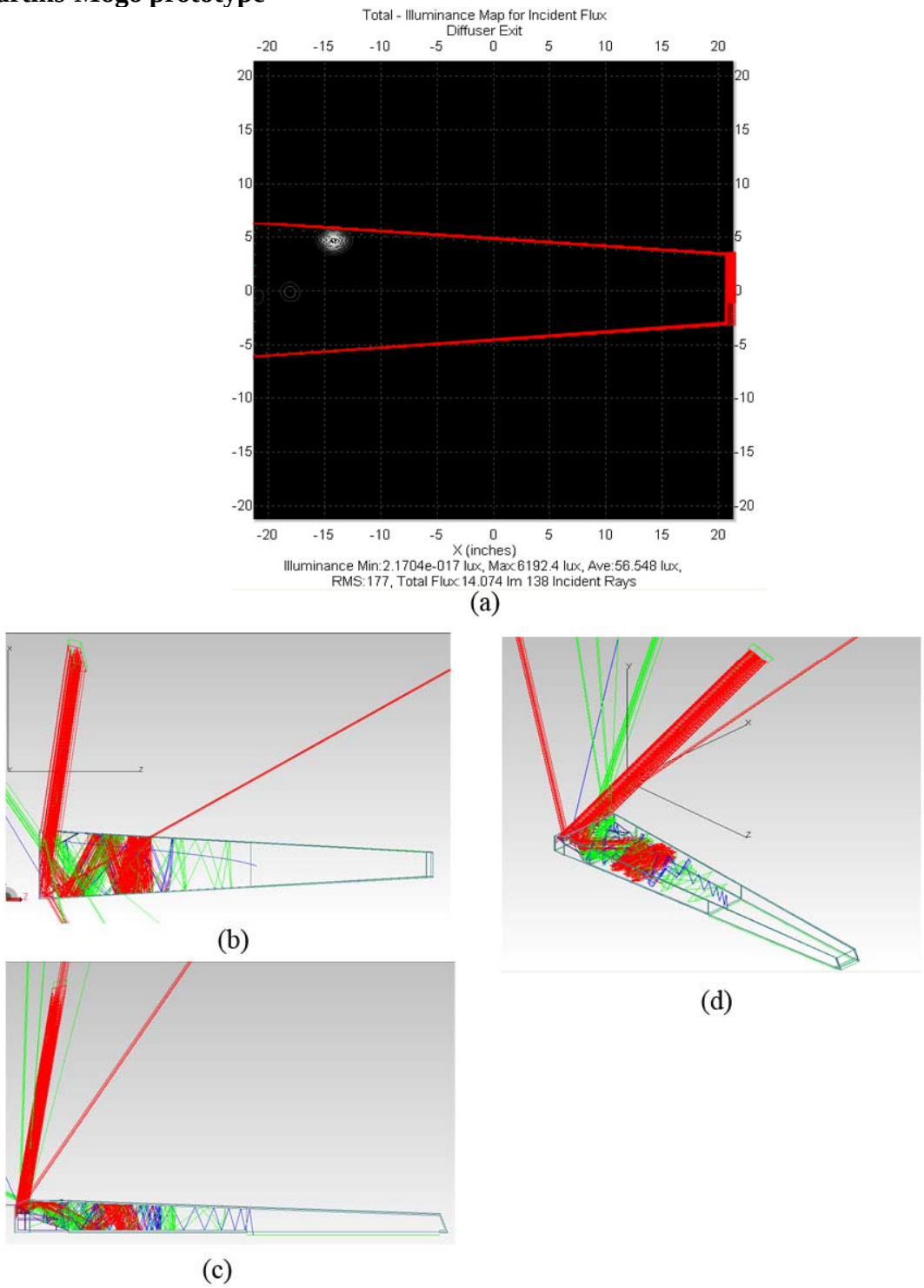

Fig. A.2. Tracepro simulation for June 21, 8am/4pm solar time. (a) Output of 10,000 rays on diffuser is 14.07 lumens (b) top view of 100 rays (c) side view of 100 rays (d) 3d view of 100 rays.

Martins-Mogo prototype

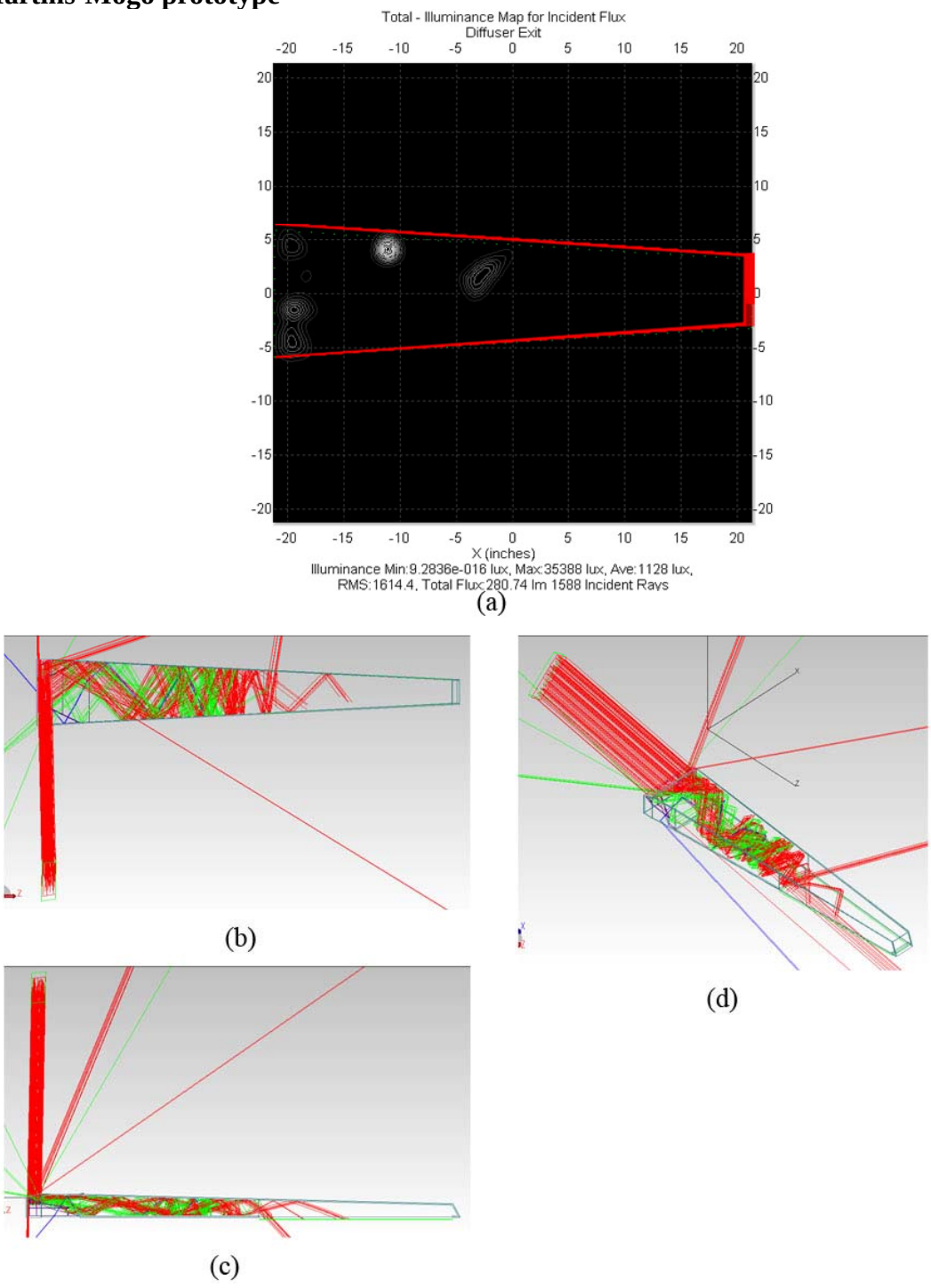

Fig. A.3. Tracepro simulation for June 21, 9am/3pm solar time. (a) Output of 10,000 rays on diffuser is 280.74 lumens (b) top view of 100 rays (c) side view of 100 rays (d) 3d view of 100 rays.

Martins-Mogo prototype

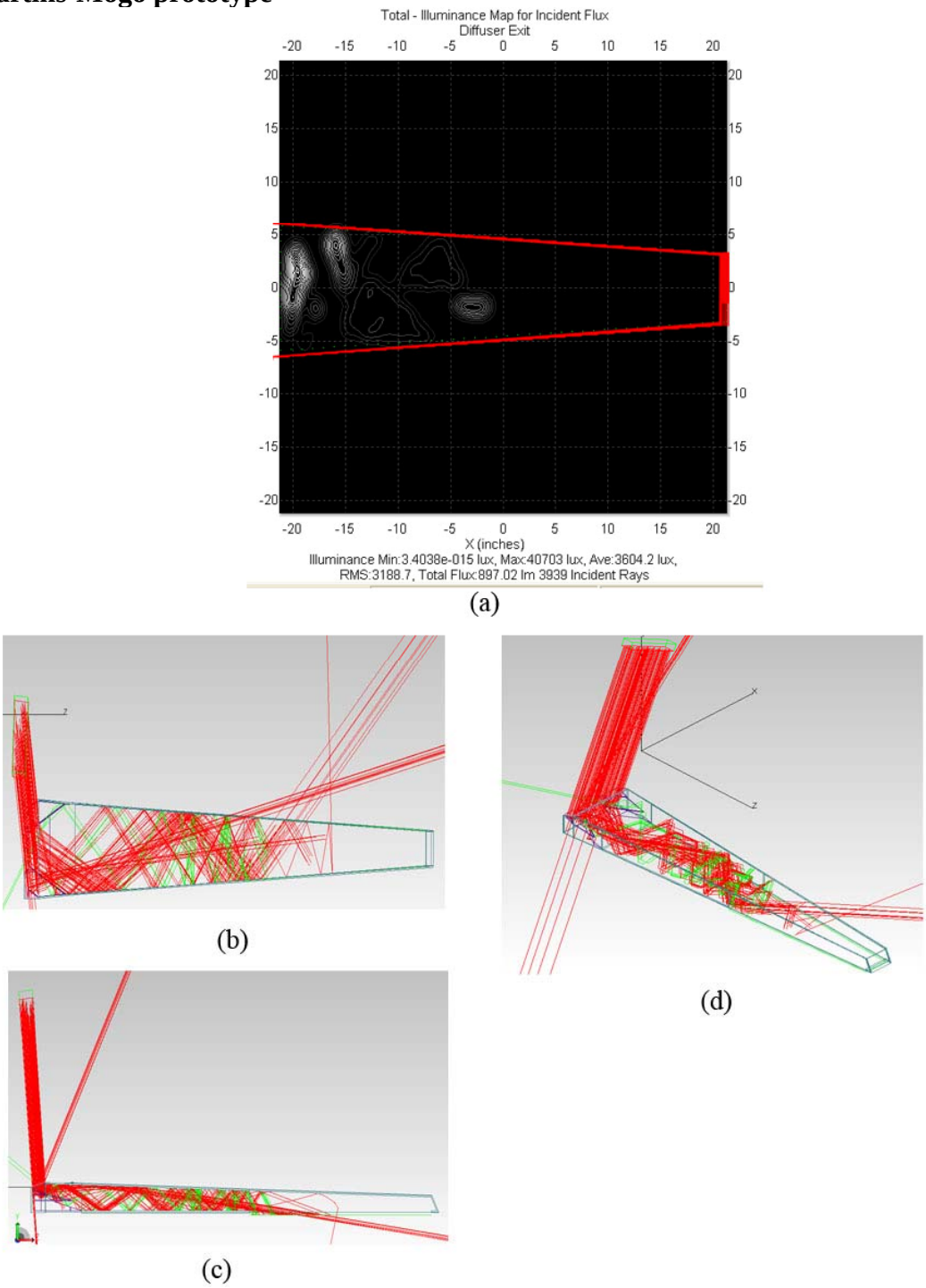

Fig. A.4. Tracepro simulation for June 21, 10am/2pm solar time. (a) Output of 10,000 rays on diffuser is 897.02 lumens (b) top view of 100 rays (c) side view of 100 rays (d) 3d view of 100 rays.

Martins-Mogo prototype

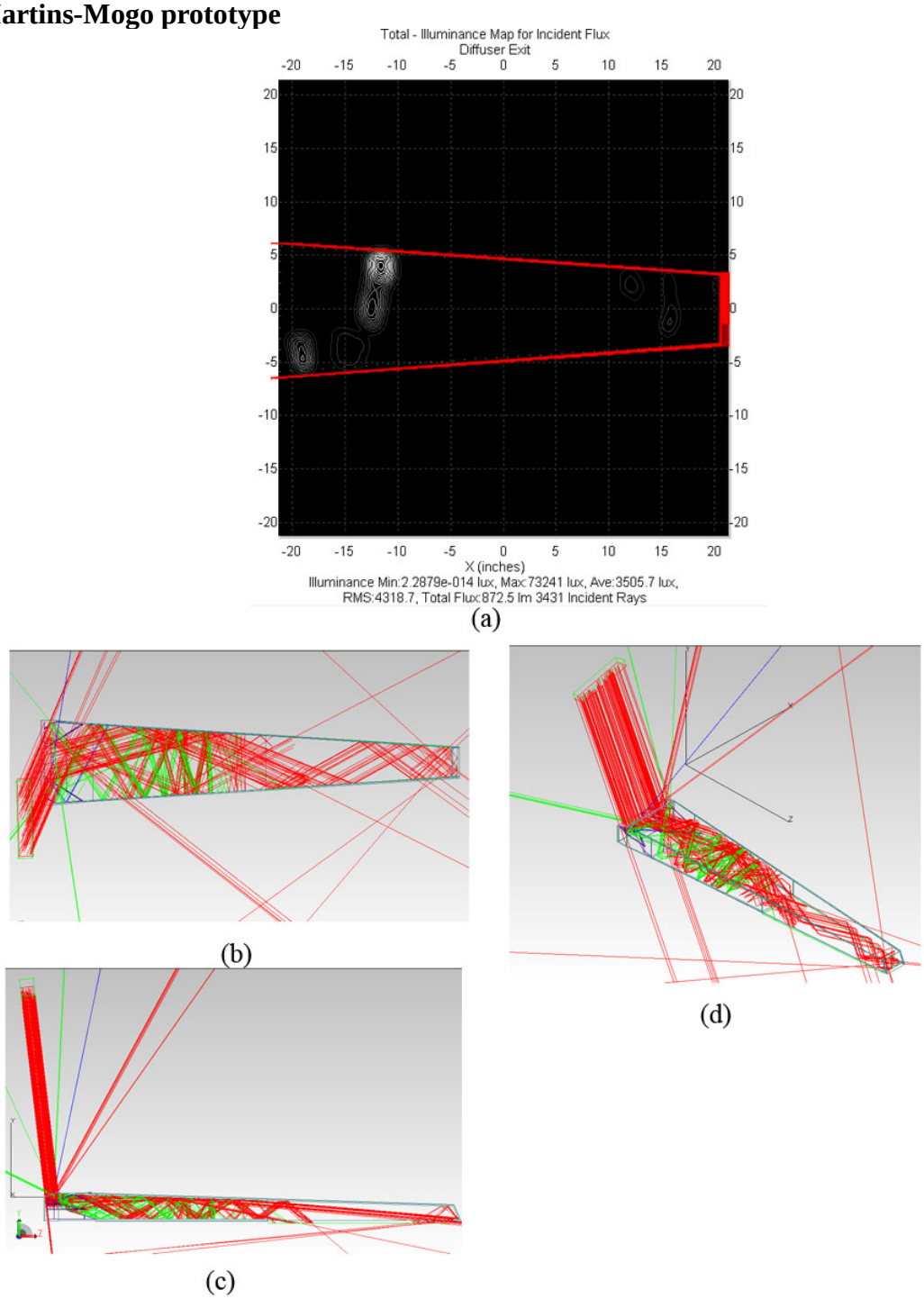

Fig. A.5. Tracepro simulation for June 21, 11am/1pm solar time. (a) Output of 10,000 rays on diffuser is 872.5 lumens (b) top view of 100 rays (c) side view of 100 rays (d) 3d view of 100 rays.

Martins-Mogo prototype

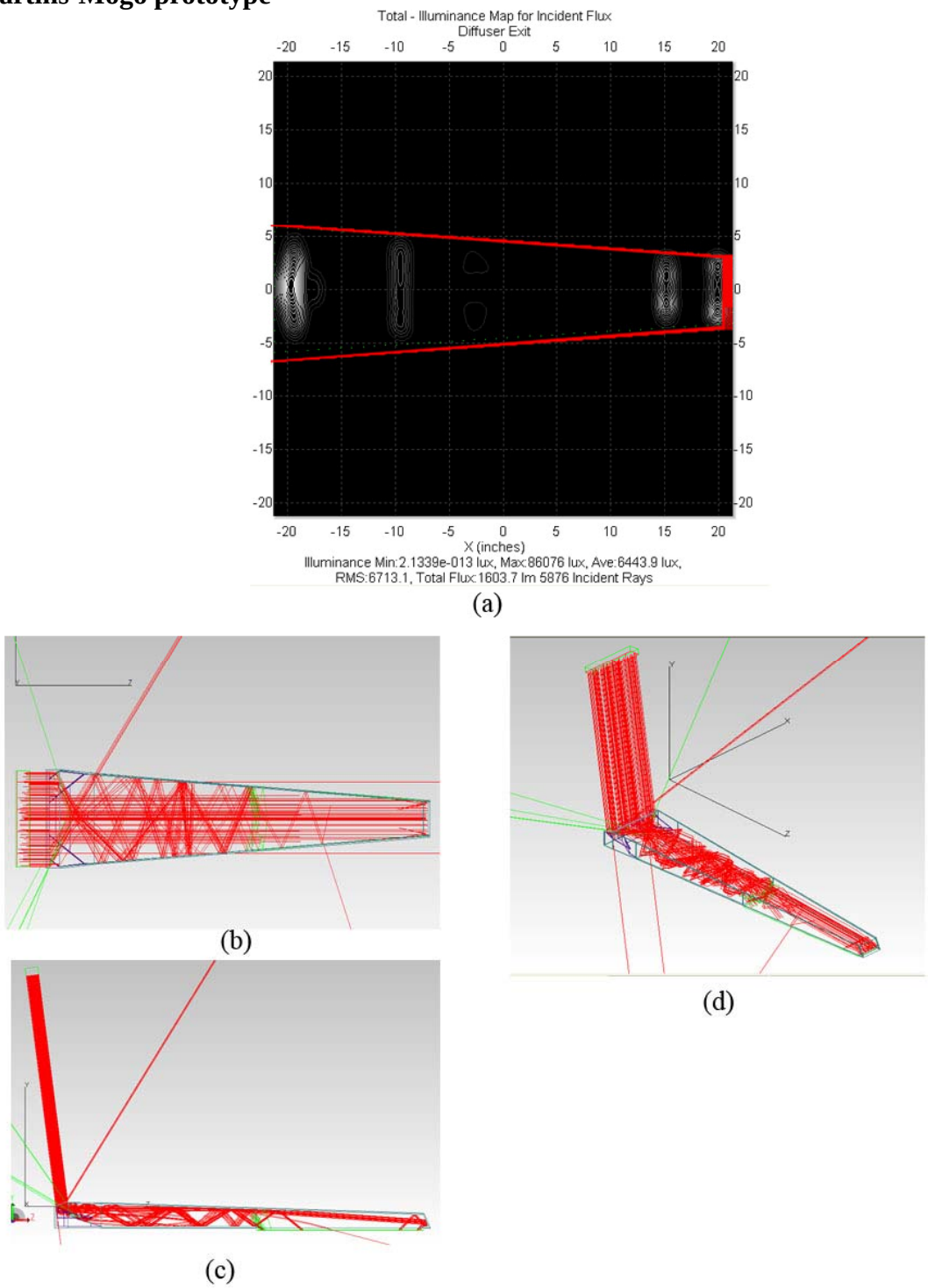

Fig. A.6. Tracepro simulation for June 21, 12 pm solar time. (a) Output of 10,000 rays on diffuser is 1603.7 lumens (b) top view of 100 rays (c) side view of 100 rays (d) 3d view of 100 rays.

5DEG (side walls tilted by 5°)

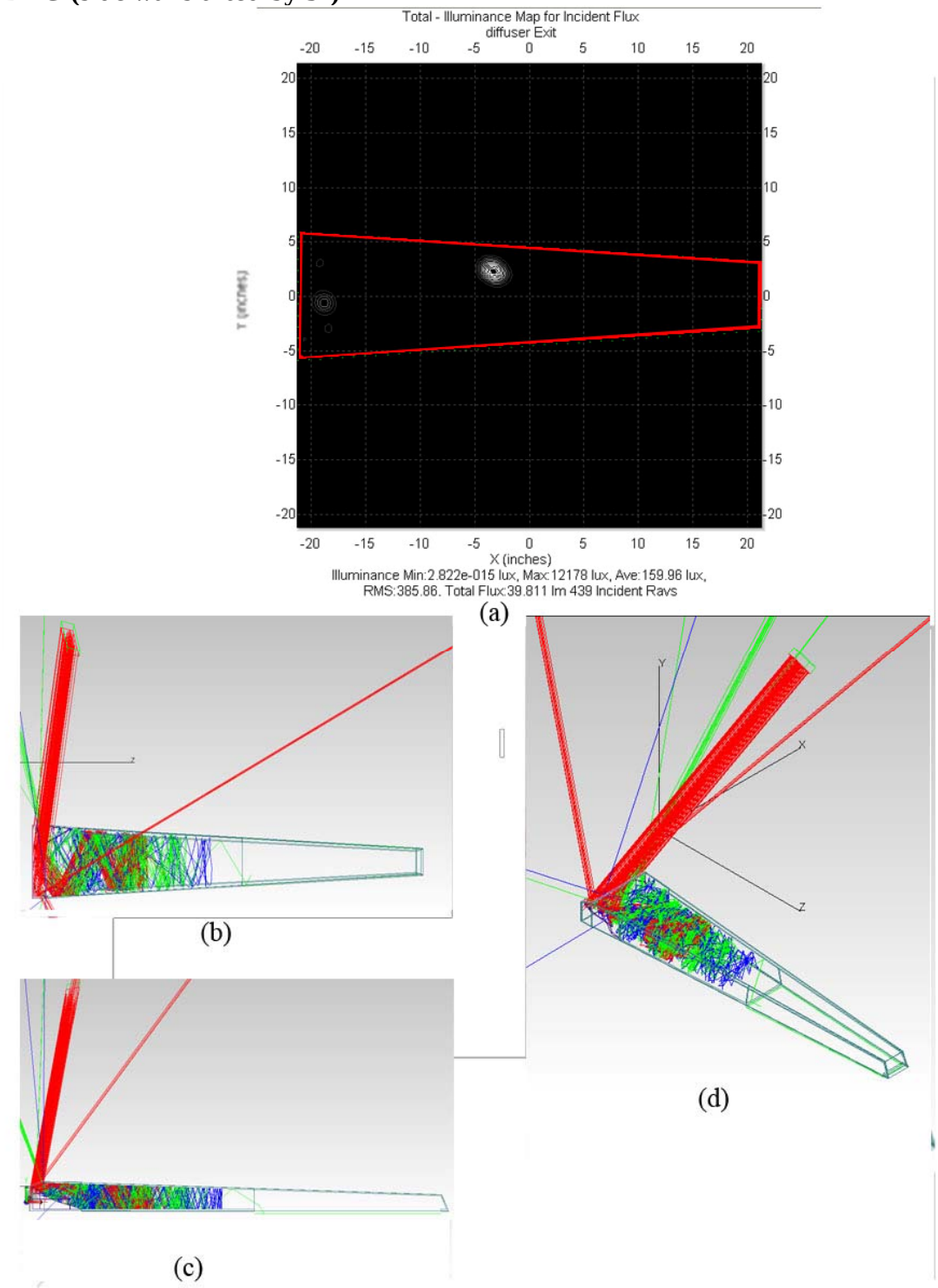

Fig. A.7. Tracepro simulation for June 21, 8am/4 pm solar time. (a) Output of 10,000 rays on diffuser is 39.811 lumens (b) top view of 100 rays (c) side view of 100 rays (d) 3d view of 100 rays

5 DEG (side walls tilted by 5°)

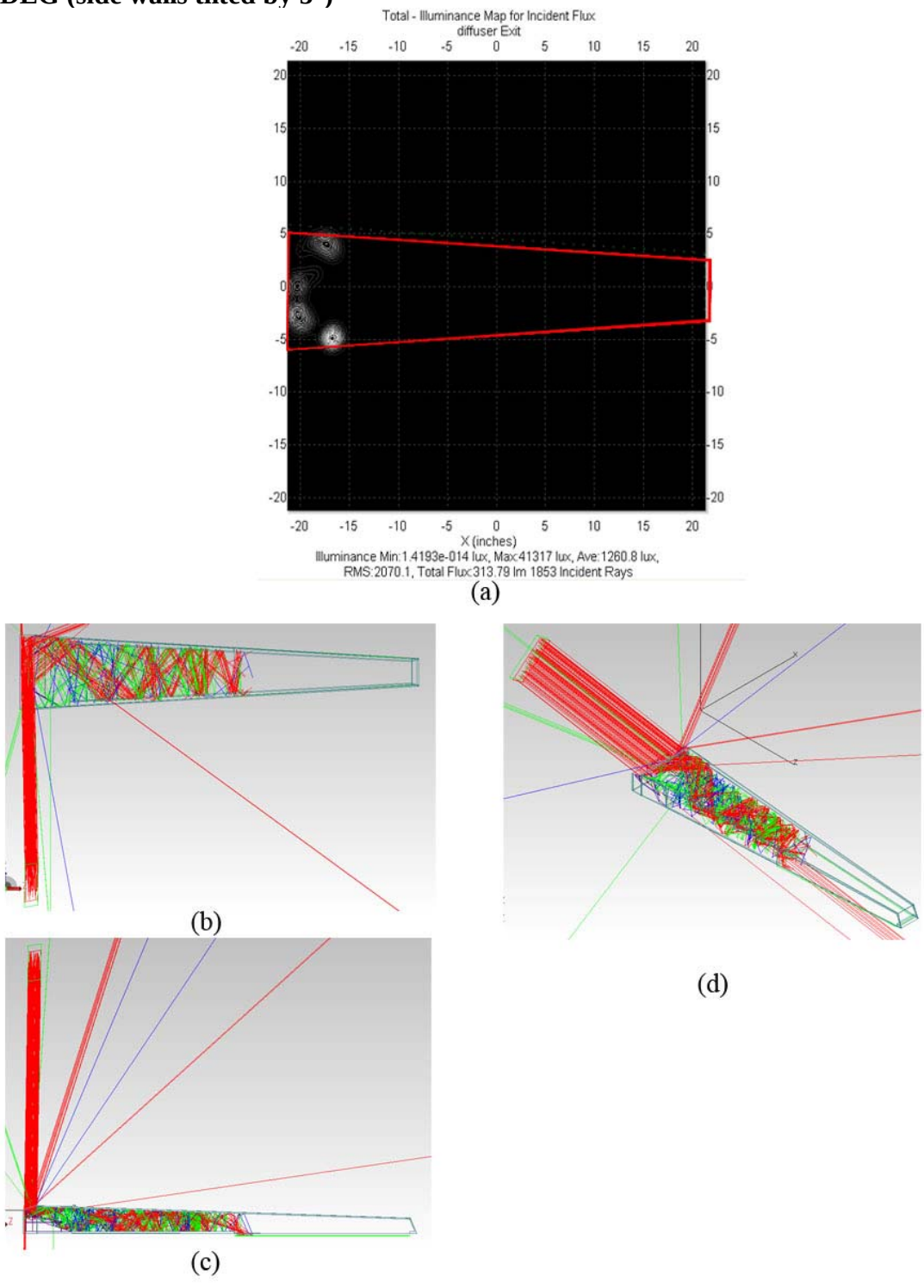

Fig. A.8. Tracepro simulation for June 21, 9am/3 pm solar time. (a) Output of 10,000 rays on diffuser is 313.79 lumens (b) top view of 100 rays (c) side view of 100 rays (d) 3d view of 100 rays

5 DEG (side walls tilted by 5°)

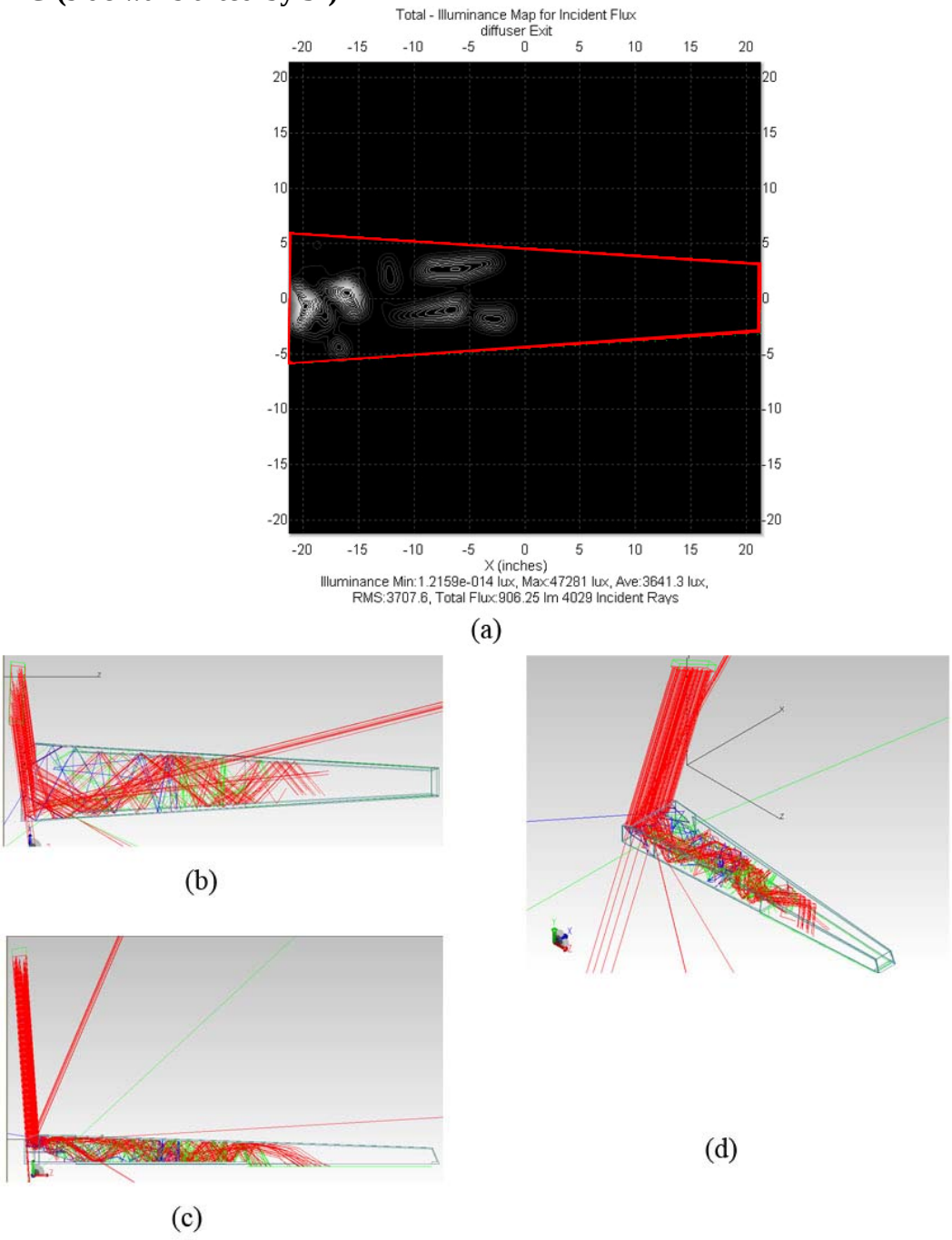

Fig. A.9. Tracepro simulation for June 21, 10 am/2 pm solar time. (a) Output of 10,000 rays on diffuser is 906.25 lumens (b) top view of 100 rays (c) side view of 100 rays (d) 3d view of 100 rays

5 DEG (side walls tilted by 5°)

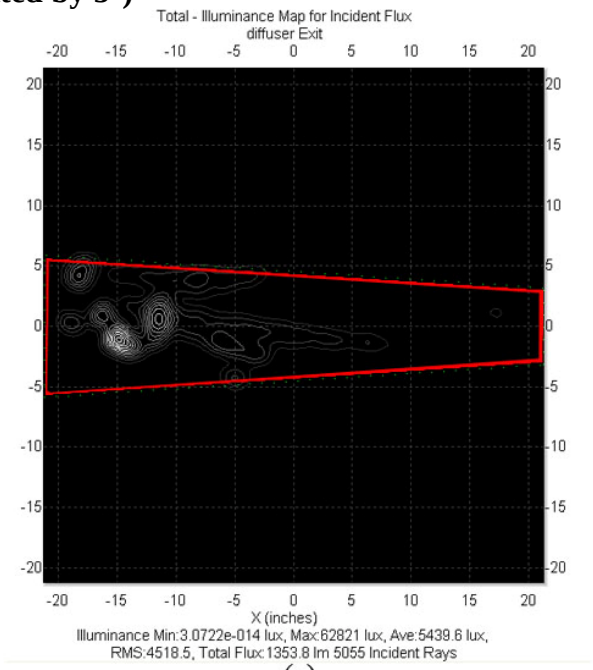

(a)

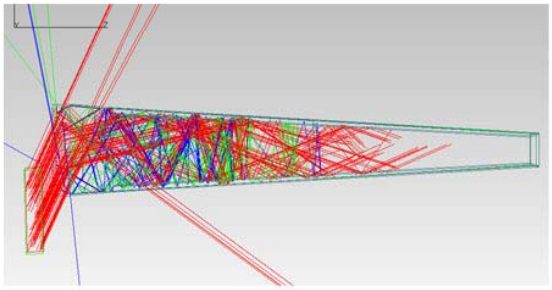

(b)

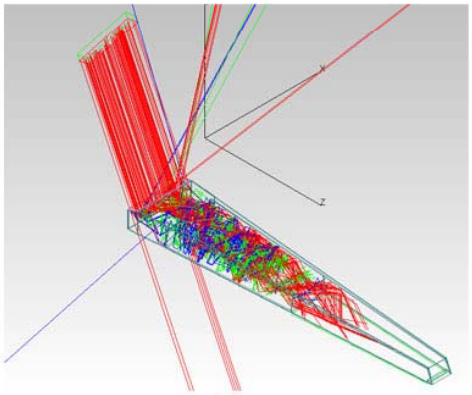

(d)

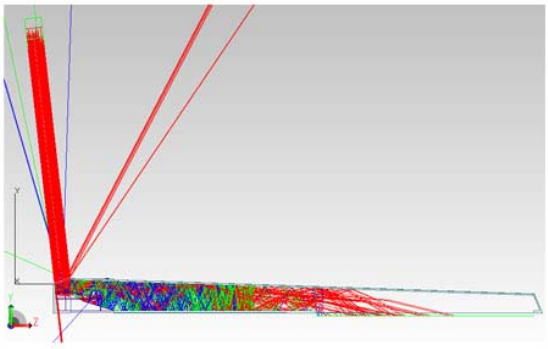

(c)

Fig. A.10. Tracepro simulation for June 21, 11 am/1 pm solar time. (a) Output of 10,000 rays on diffuser is 1353.8 lumens (b) top view of 100 rays (c) side view of 100 rays (d) 3d view of 100 rays

5 DEG (side walls tilted by 5°)

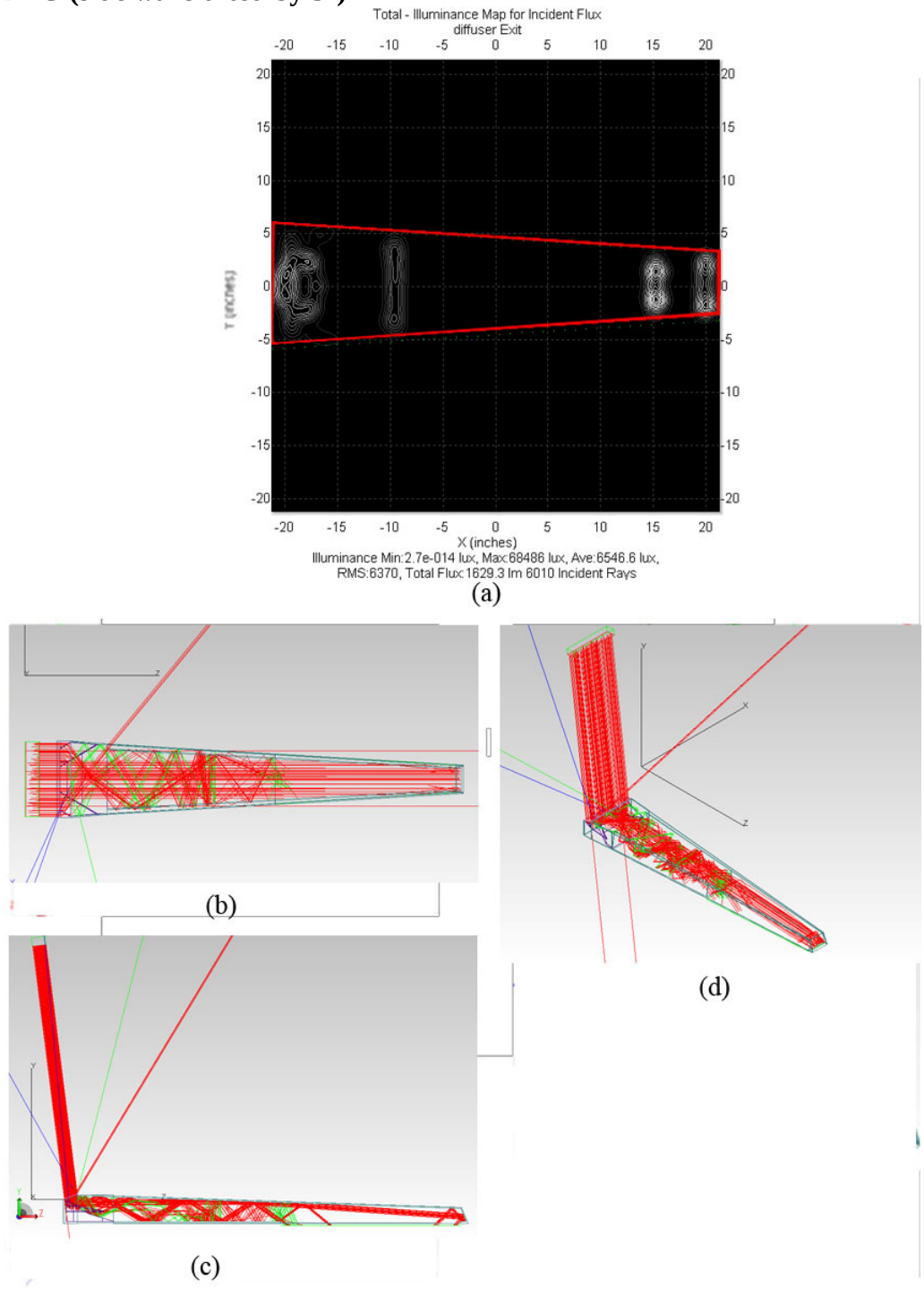

Fig. A.11. Tracepro simulation for June 21, 12 pm solar time. (a) Output of 10,000 rays on diffuser is 1629.3 lumens (b) top view of 100 rays (c) side view of 100 rays (d) 3d view of 100 rays

10 DEG (side walls tilted by 10°)

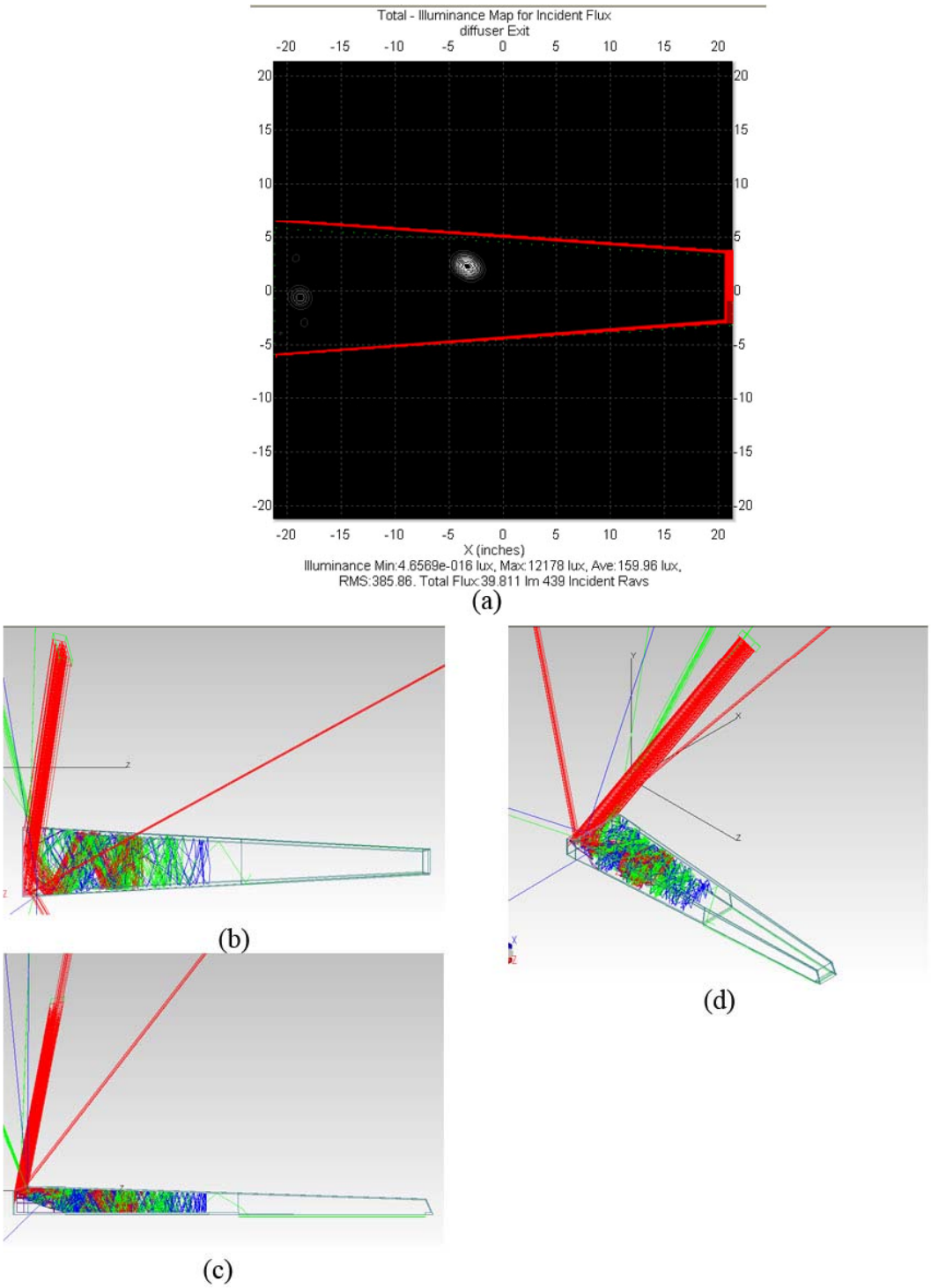

Fig. A.12. Tracepro simulation for June 21, 8 am/4 pm solar time. (a) Output of 10,000 rays on diffuser is 39.811 lumens (b) top view of 100 rays (c) side view of 100 rays (d) 3d view of 100 rays

10 DEG (side walls tilted by 10°)

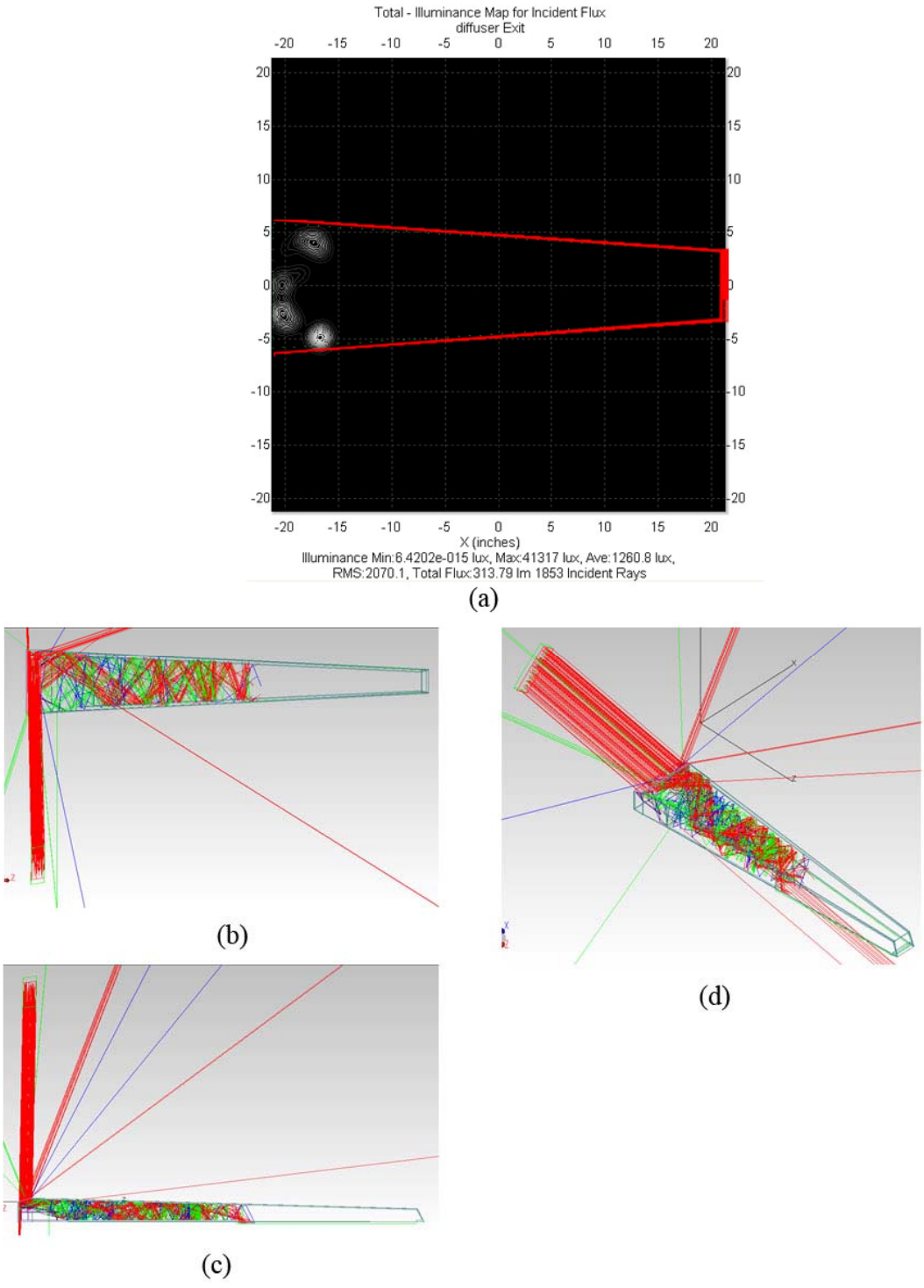

Fig. A.13. Tracepro simulation for June 21, 9 am/3 pm solar time. (a) Output of 10,000 rays on diffuser is 313.79 lumens (b) top view of 100 rays (c) side view of 100 rays (d) 3d view of 100 rays

10 DEG (side walls tilted by 10°)

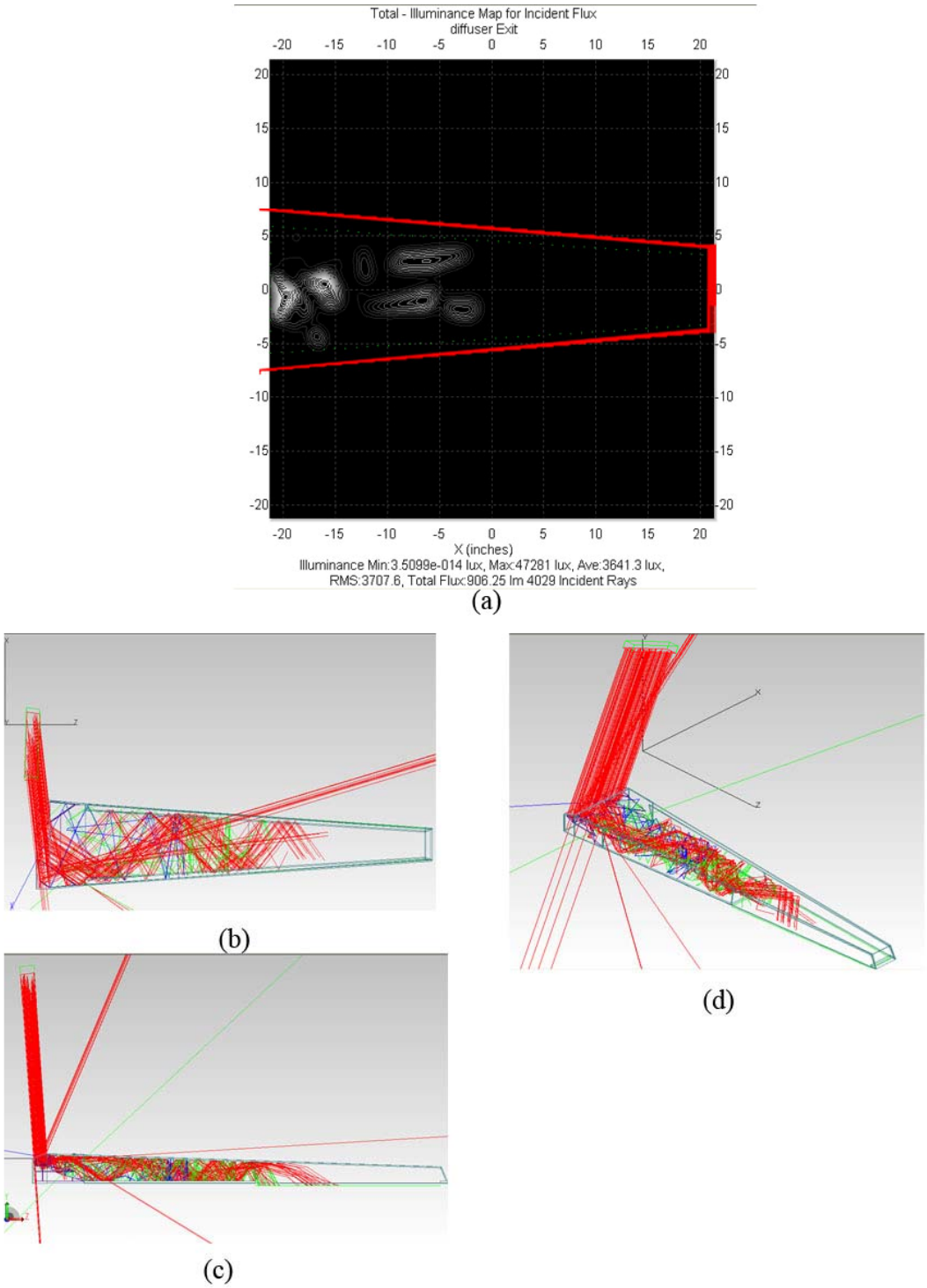

Fig. A.14. Tracepro simulation for June 21, 10 am/2 pm solar time. (a) Output of 10,000 rays on diffuser is 906.25 lumens (b) top view of 100 rays (c) side view of 100 rays (d) 3d view of 100 rays

10 DEG (side walls tilted by 10°)

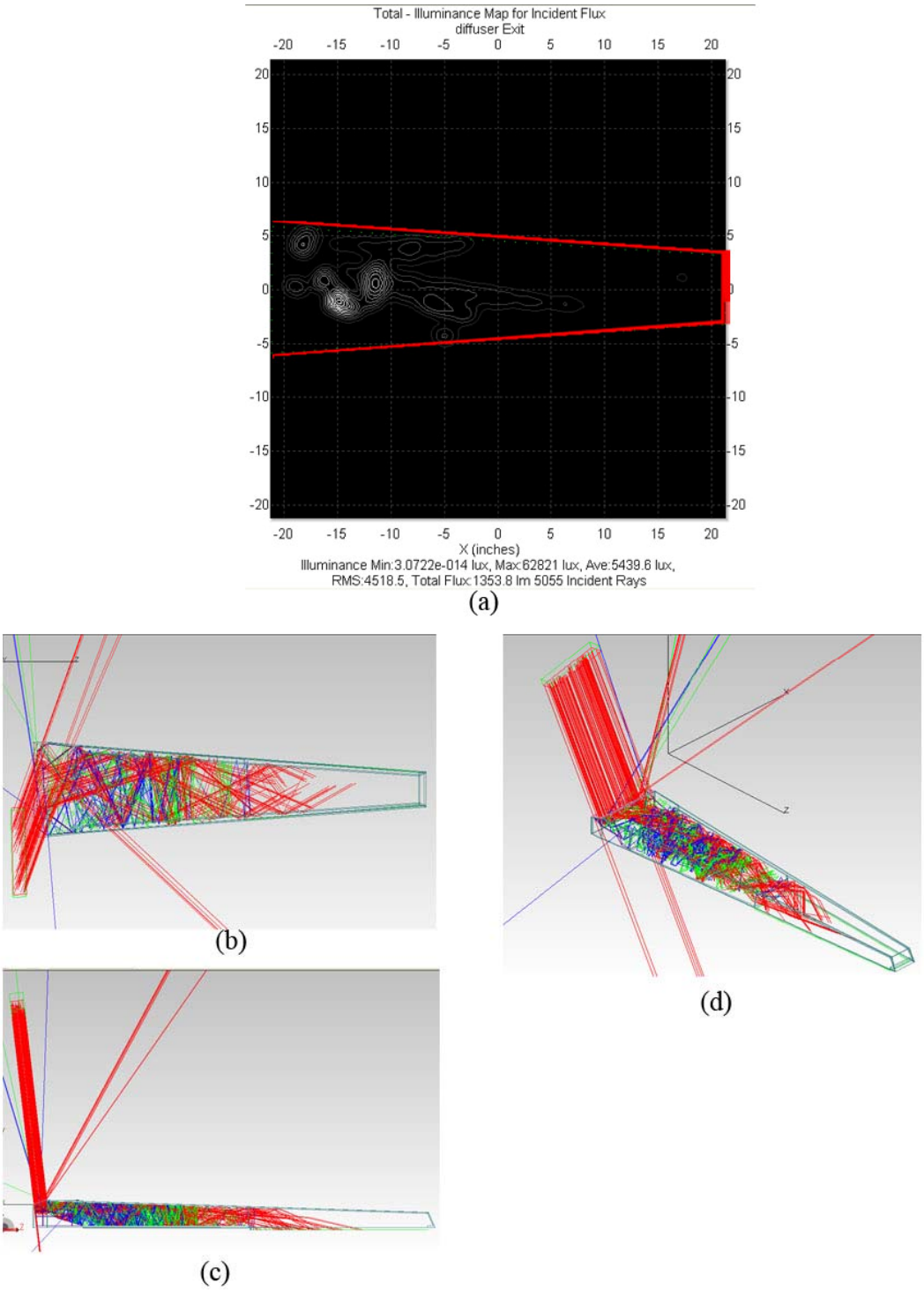

Fig. A.15. Tracepro simulation for June 21, 11 am/1 pm solar time. (a) Output of 10,000 rays on diffuser is 1353.8 lumens (b) top view of 100 rays (c) side view of 100 rays (d) 3d view of 100 rays

10 DEG (side walls tilted by 10°)

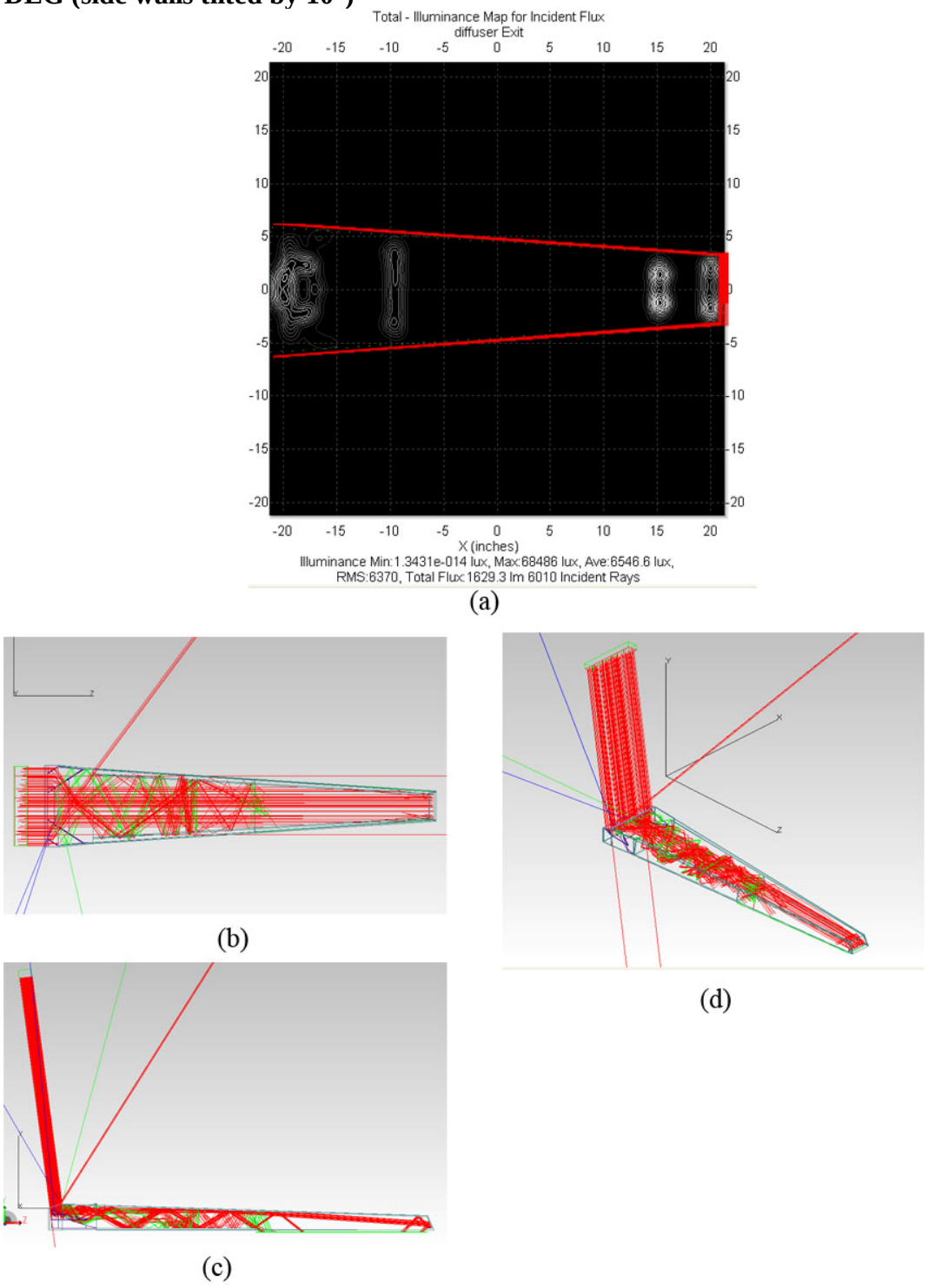

Fig. A.16. Tracepro simulation for June 21, 12 pm solar time. (a) Output of 10,000 rays on diffuser is 1629.3 lumens (b) top view of 100 rays (c) side view of 100 rays (d) 3d view of 100 rays

6F6B (front 6', back 6')

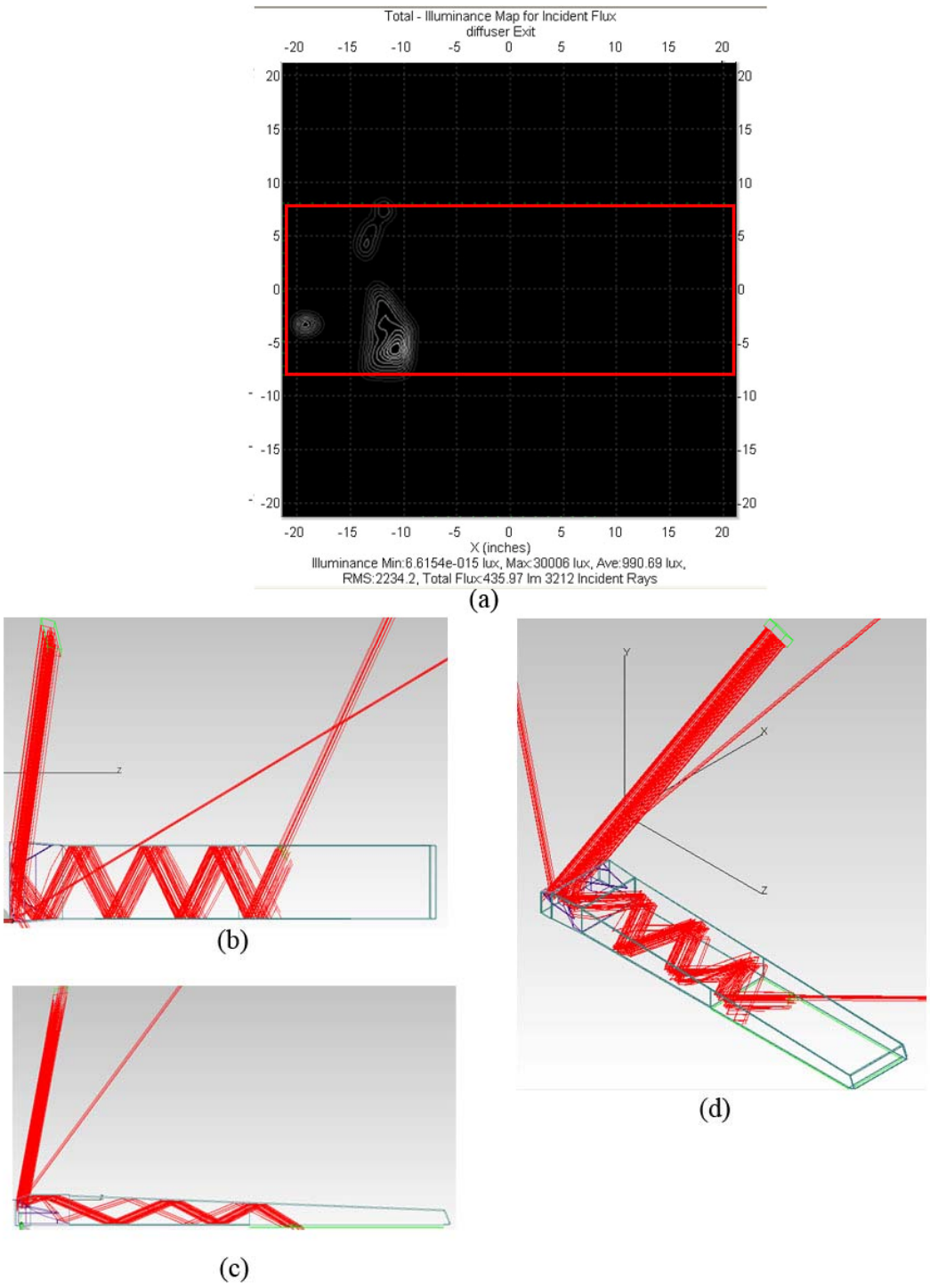

Fig. A.17. Tracepro simulation for June 21, 8am/4pm solar time. (a) Output of 10,000 rays on diffuser is 435.97 lumens (b) top view of 100 rays (c) side view of 100 rays (d) 3d view of 100 rays

6F6B (front 6', back 6')

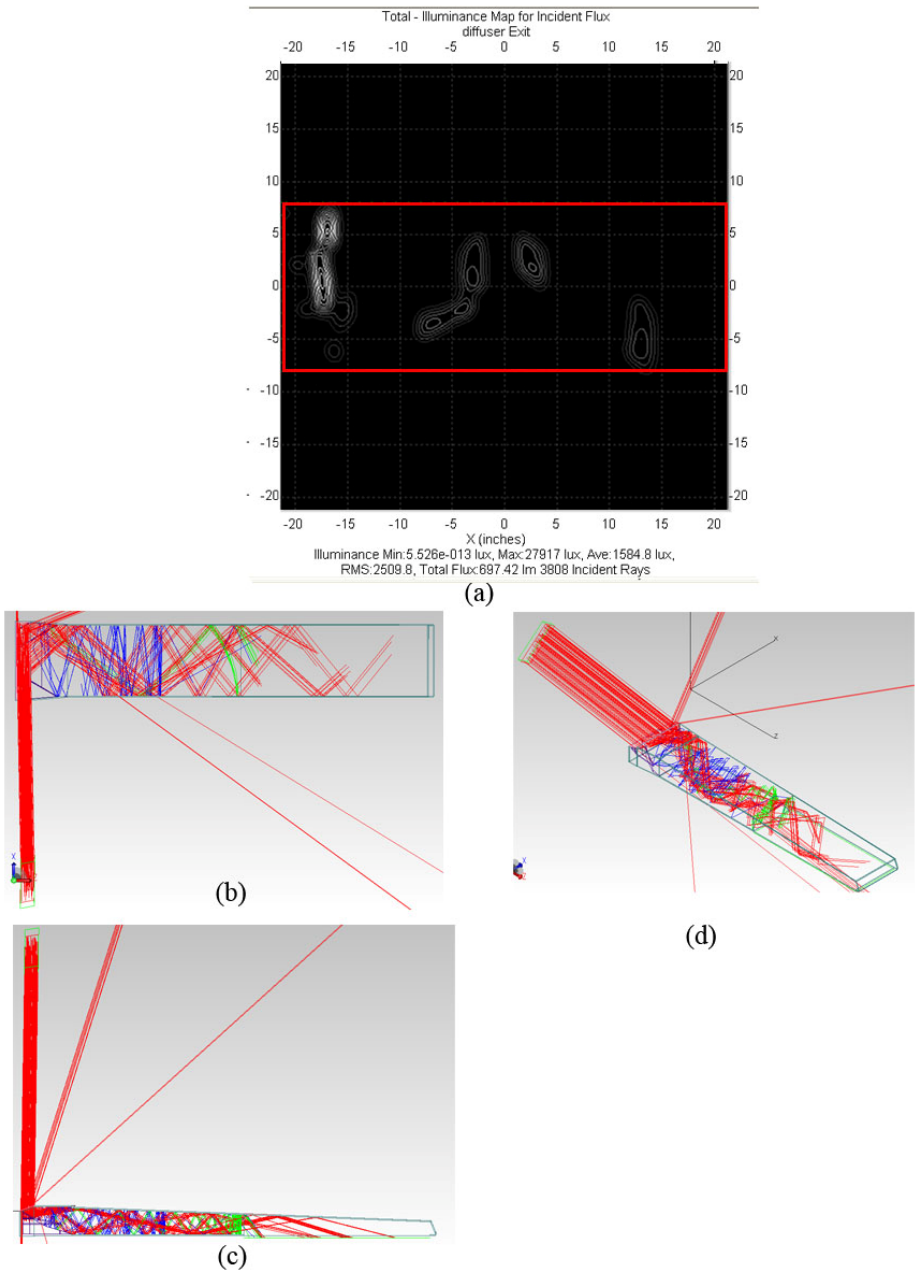

Fig. A.18. Tracepro simulation for June 21, 9am/3pm solar time. (a) Output of 10,000 rays on diffuser is 697.42 lumens (b) top view of 100 rays (c) side view of 100 rays (d) 3d view of 100 rays

6F6B (front 6', back 6')

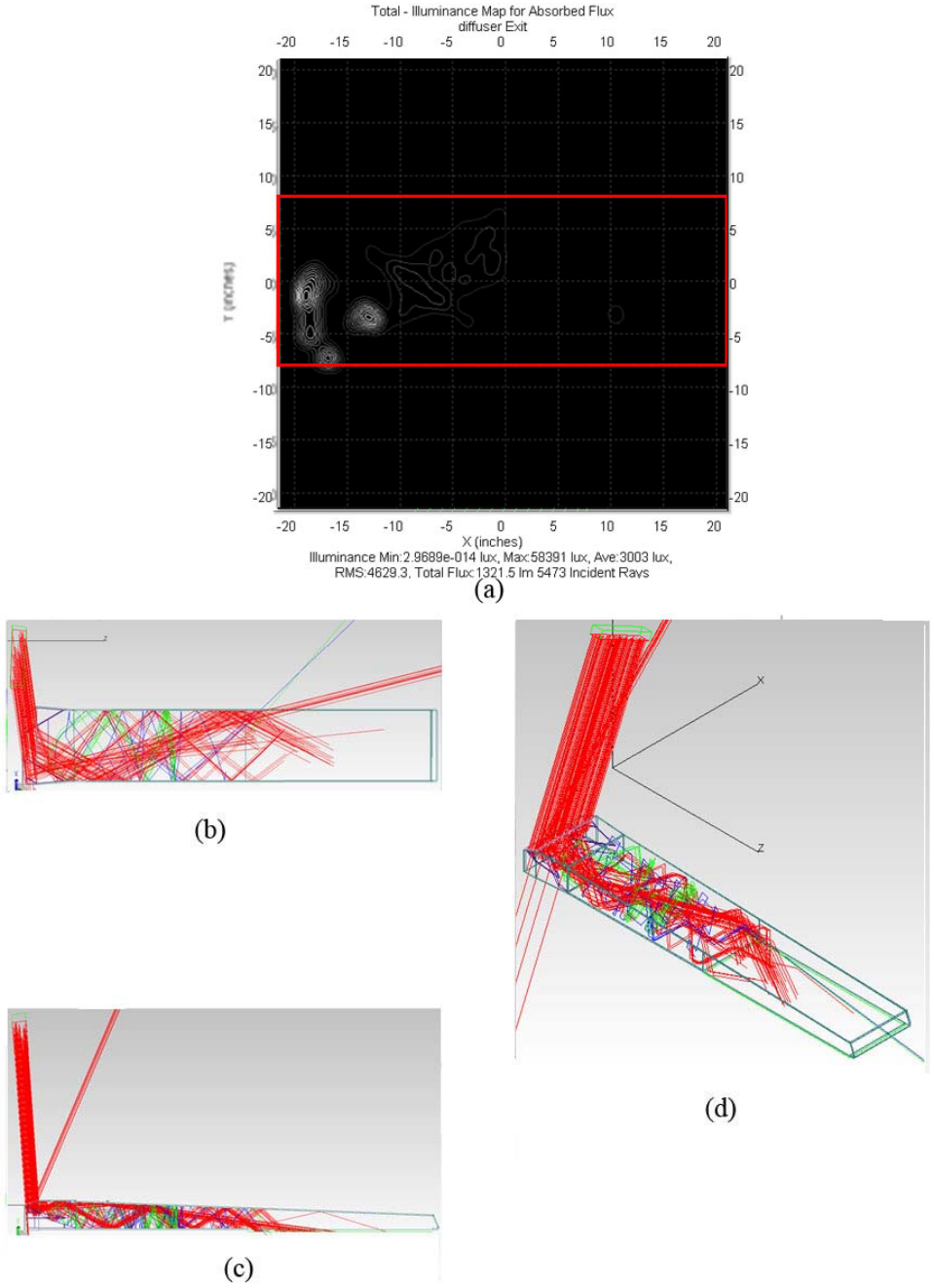

Fig. A.19. Tracepro simulation for June 21, 10am/2pm solar time. (a) Output of 10,000 rays on diffuser is 1321.5 lumens (b) top view of 100 rays (c) side view of 100 rays (d) 3d view of 100 rays

6F6B (front 6', back)

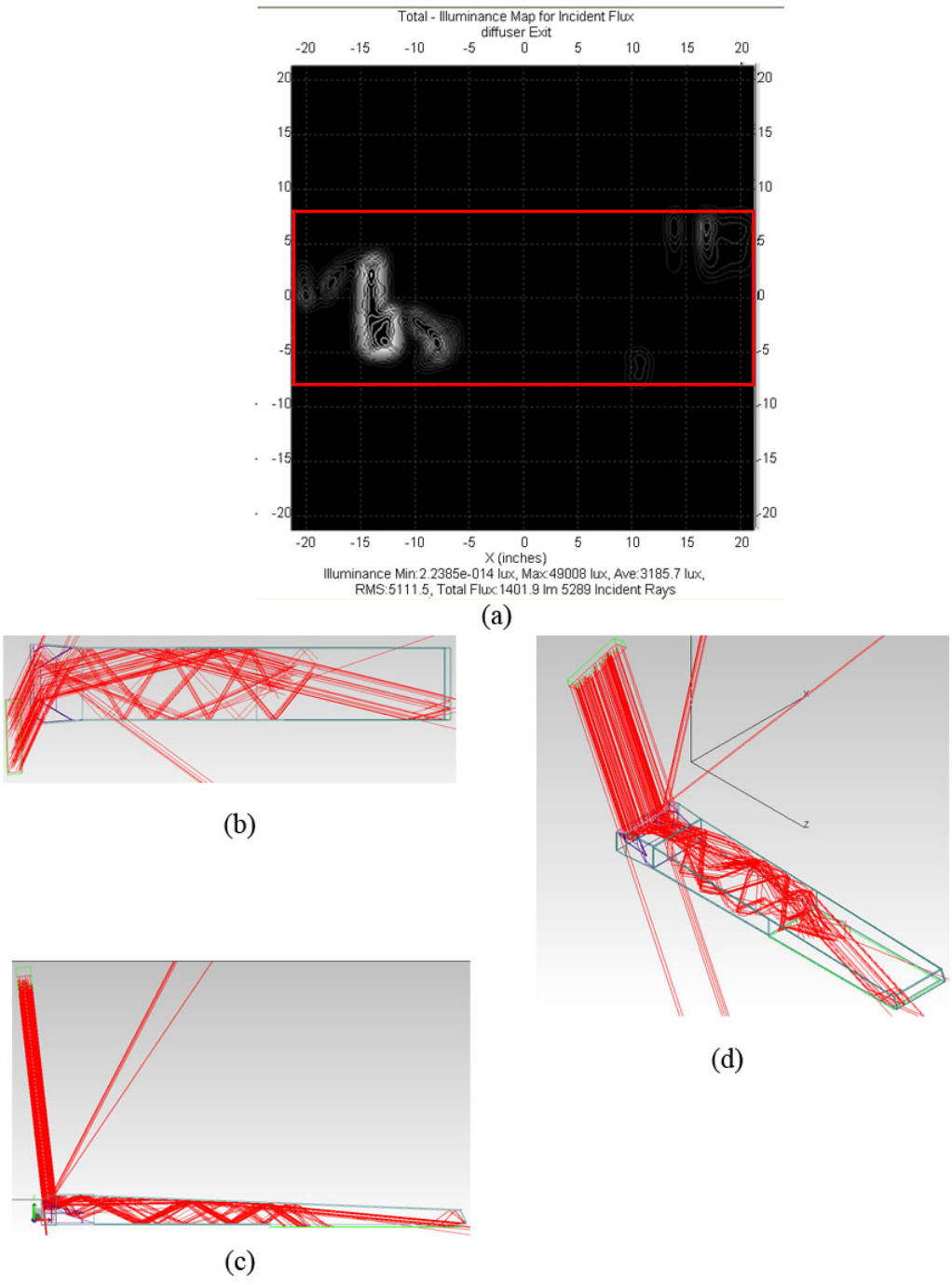

Fig. A.20. Tracepro simulation for June 21, 11am/1pm solar time. (a) Output of 10,000 rays on diffuser is 1321.5 lumens (b) top view of 100 rays (c) side view of 100 rays (d) 3d view of 100 rays

6F6B (front 6', back)

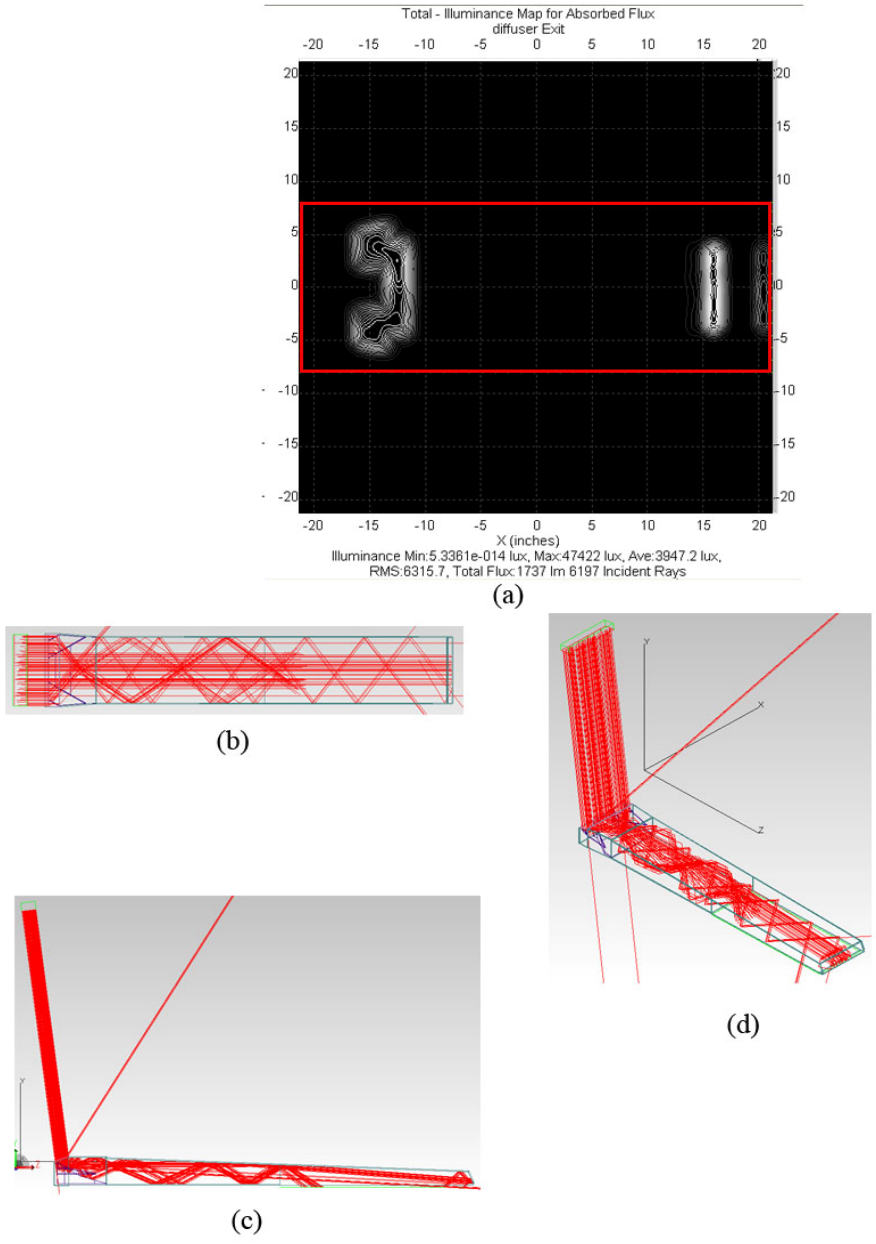

Fig. A.21. Tracepro simulation for June 21, 12pm solar time. (a) Output of 10,000 rays on diffuser is 1321.5 lumens (b) top view of 100 rays (c) side view of 100 rays (d) 3d view of 100 rays

6F4B (front 6', back 4')

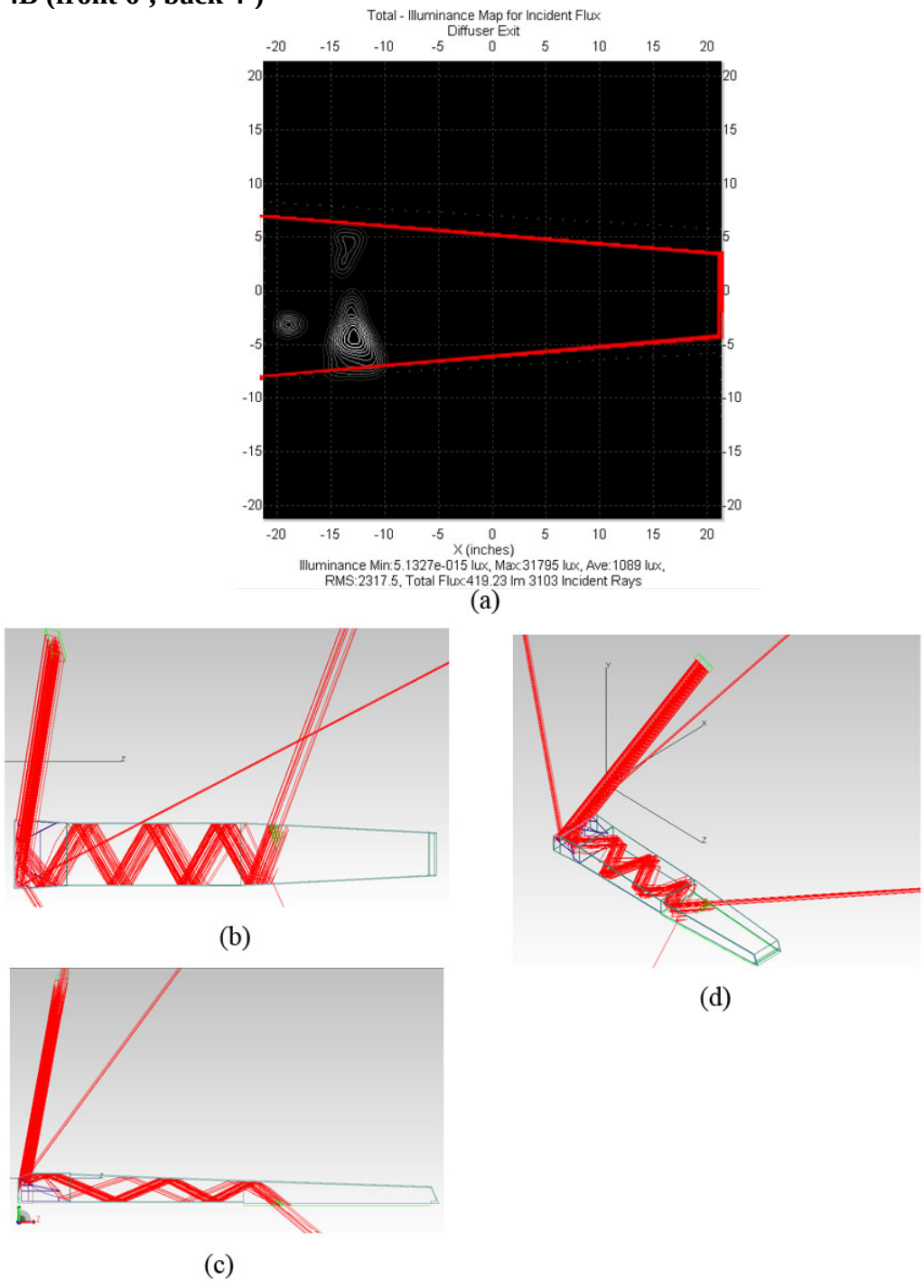

Fig. A.22. Tracepro simulation for June 21, 8am/4pm solar time. (a) Output of 10,000 rays on diffuser is 419.23 lumens (b) top view of 100 rays (c) side view of 100 rays (d) 3d view of 100 rays

6F4B (front 6', back 4')

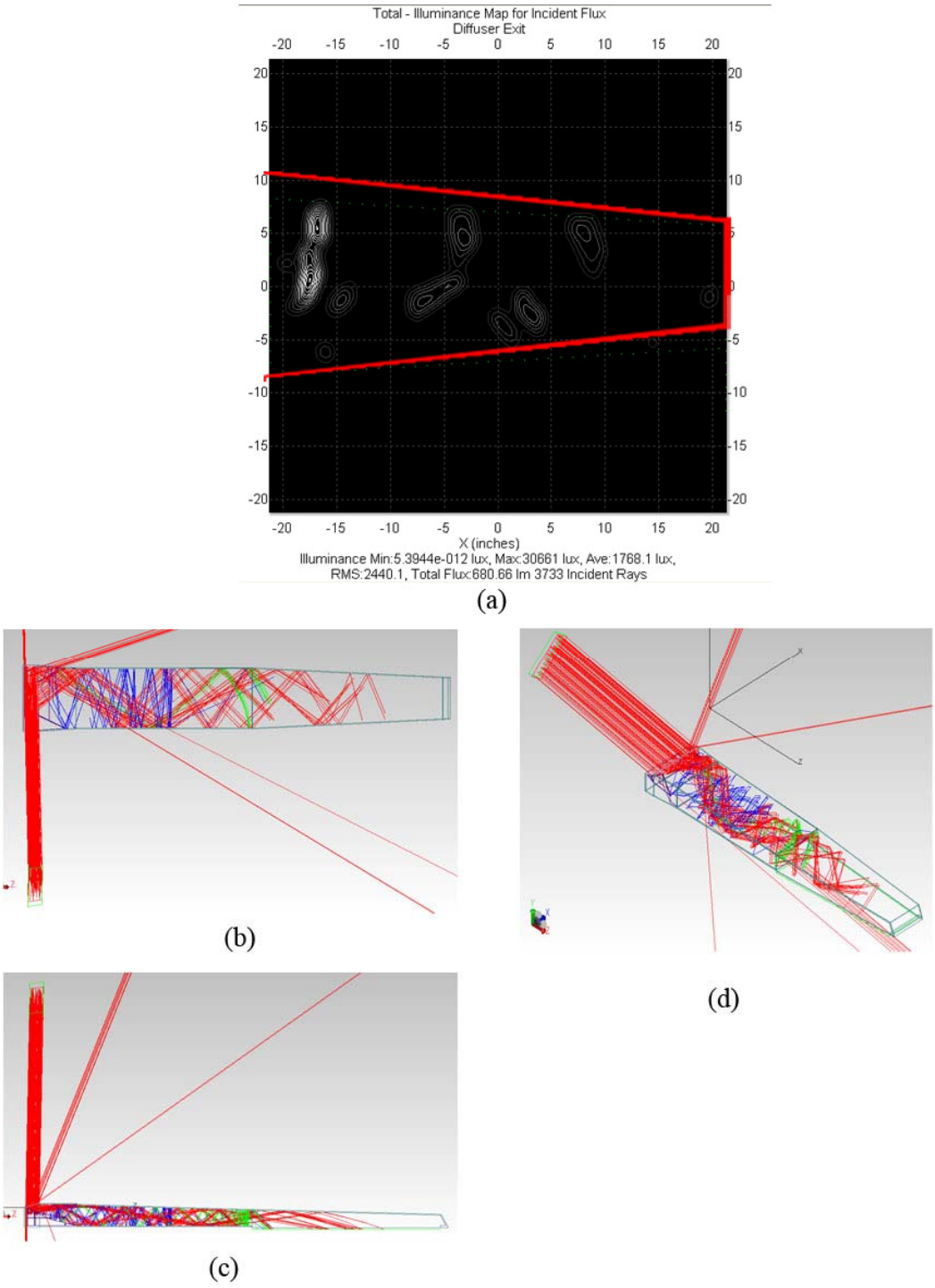

Fig. A.23. Tracepro simulation for June 21, 9am/3pm solar time. (a) Output of 10,000 rays on diffuser is 680.66 lumens (b) top view of 100 rays (c) side view of 100 rays (d) 3d view of 100 rays

6F4B (front 6', back 4')

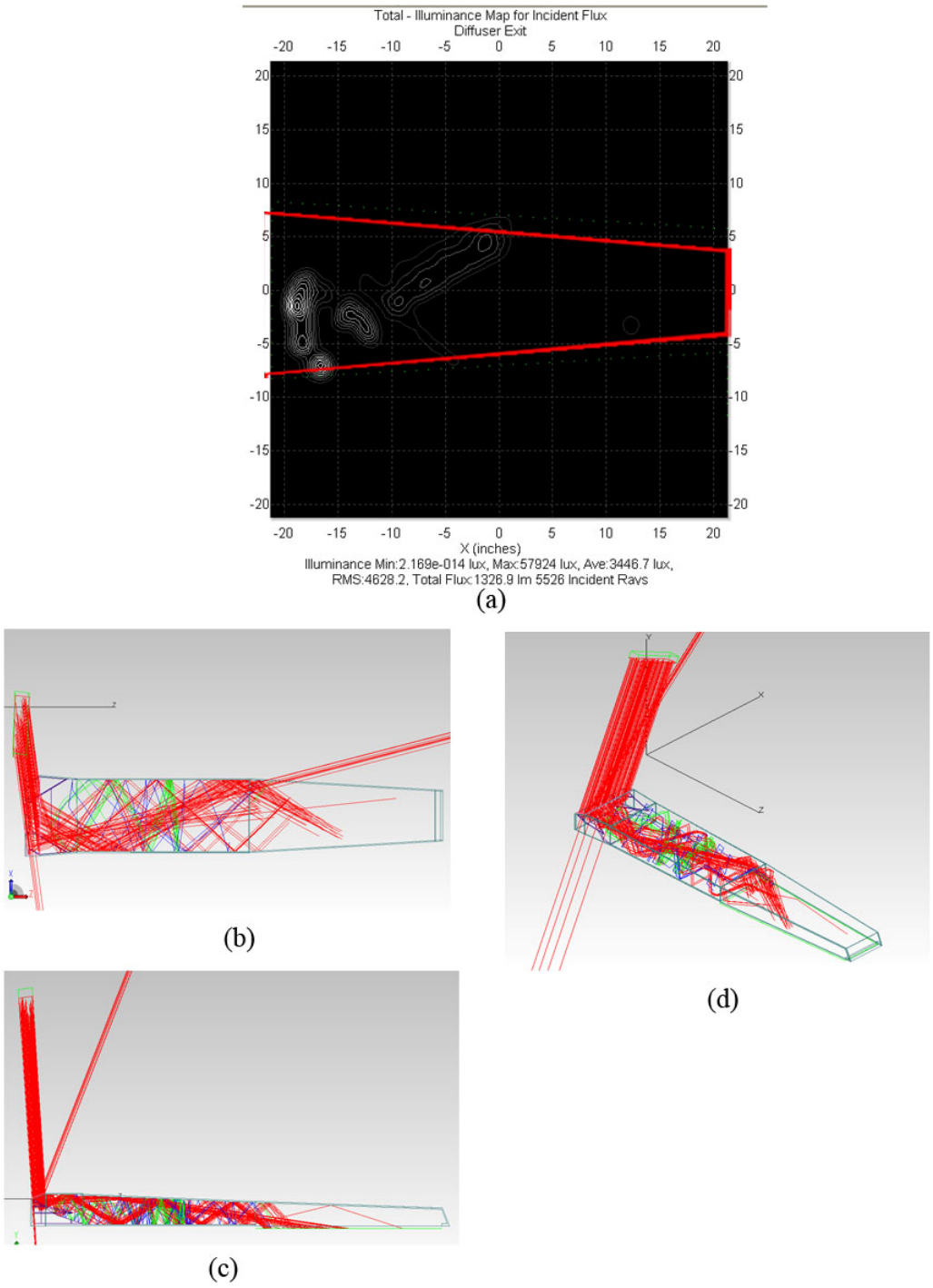

Fig. A.24. Tracepro simulation for June 21, 10am/2pm solar time. (a) Output of 10,000 rays on diffuser is 1326.9 lumens (b) top view of 100 rays (c) side view of 100 rays (d) 3d view of 100 rays

6F4B (front 6', back 4')

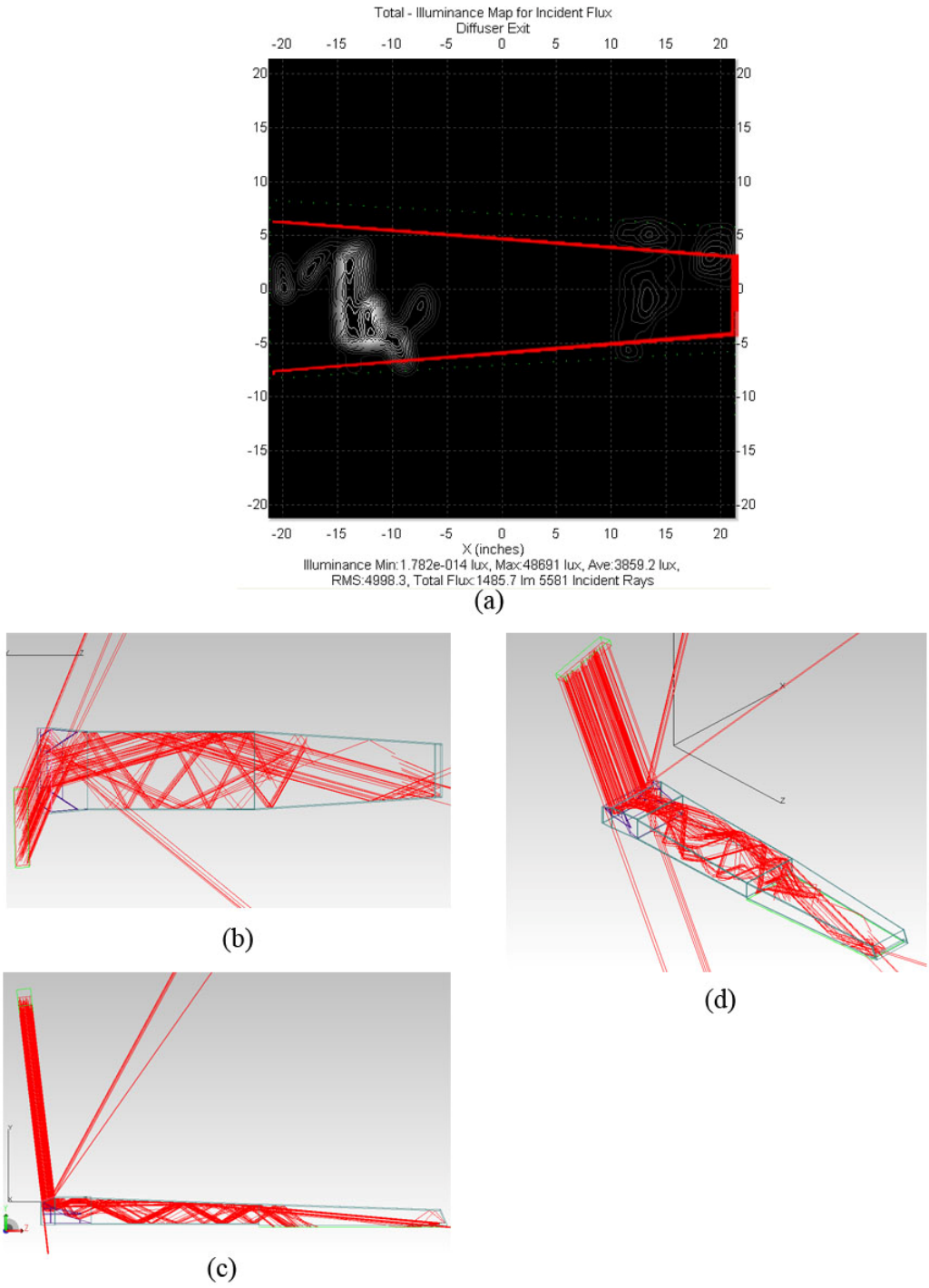

Fig. A.25. Tracepro simulation for June 21, 11am/1pm solar time. (a) Output of 10,000 rays on diffuser is 1485.7 lumens (b) top view of 100 rays (c) side view of 100 rays (d) 3d view of 100 rays

6F4B (front 6', back 4')

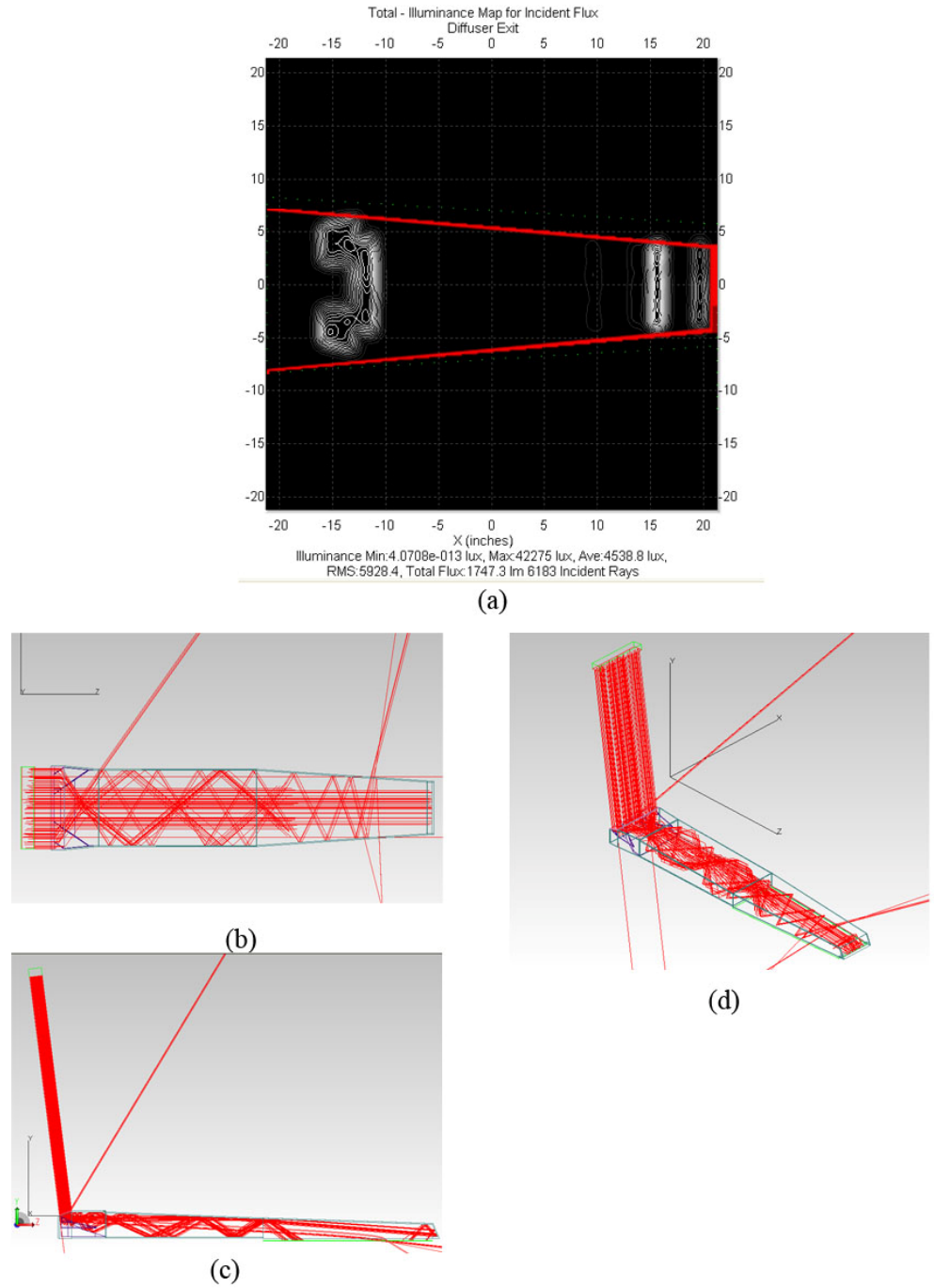

Fig. A.26. Tracepro simulation for June 21, 12pm solar time. (a) Output of 10,000 rays on diffuser is 1747.3 lumens (b) top view of 100 rays (c) side view of 100 rays (d) 3d view of 100 rays

6F2B (front 6', back 2')

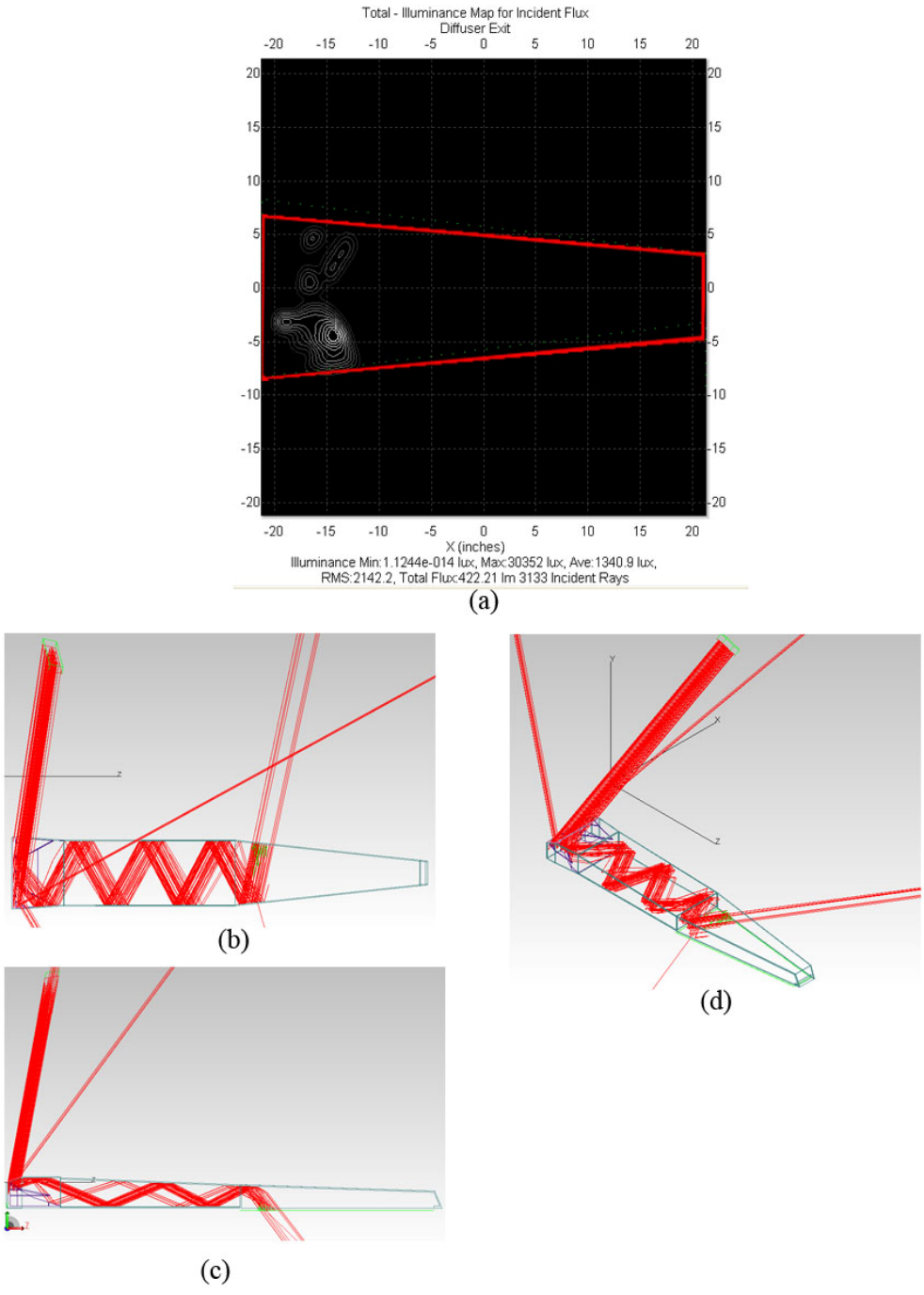

Fig. A.27. Tracepro simulation for June 21, 8am/4pm solar time. (a) Output of 10,000 rays on diffuser is 422.21 lumens (b) top view of 100 rays (c) side view of 100 rays (d) 3d view of 100 rays

6F2B (front 6', back 2')

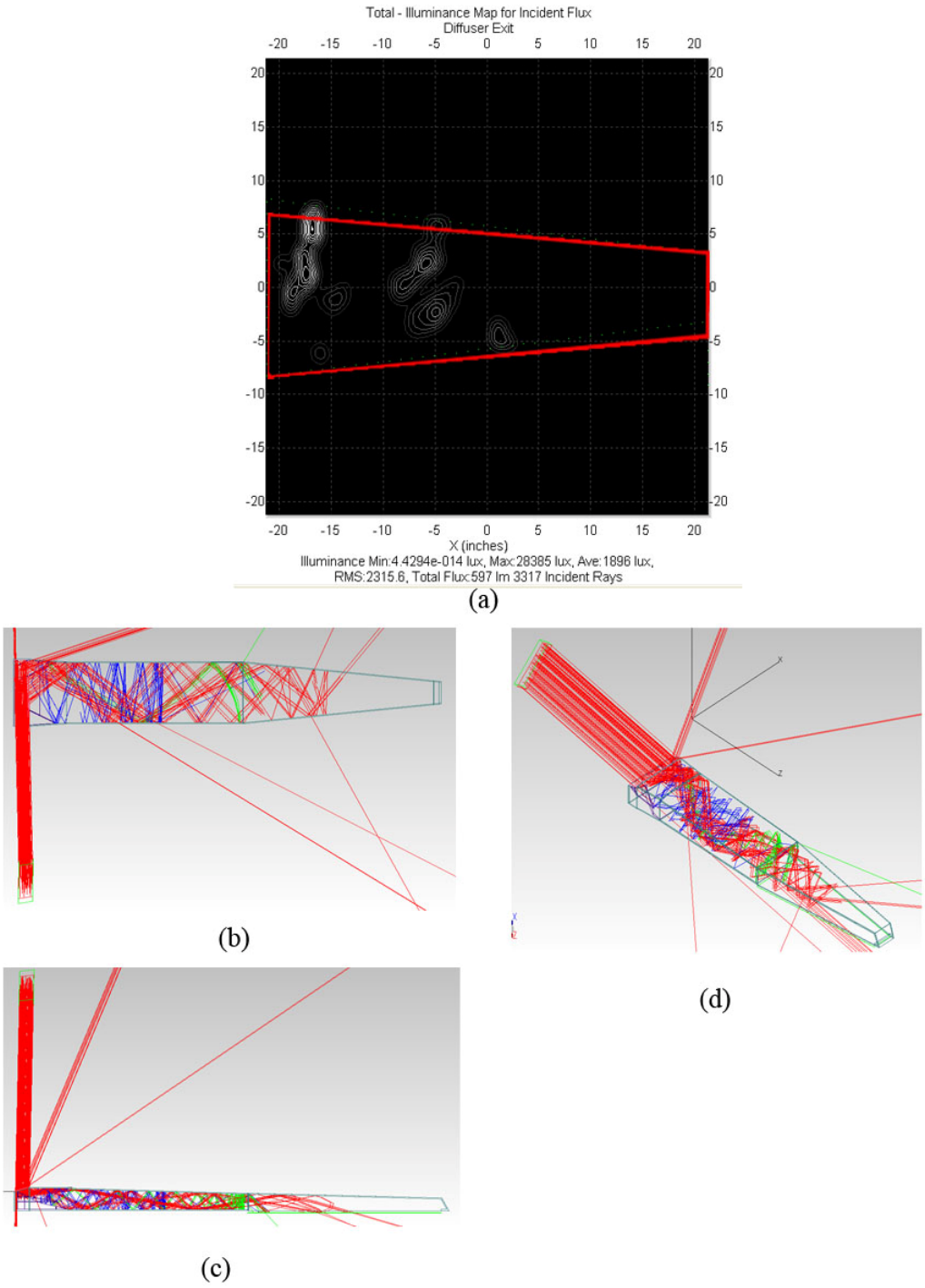

Fig. A.28. Tracepro simulation for June 21, 9am/3pm solar time. (a) Output of 10,000 rays on diffuser is 597 lumens (b) top view of 100 rays (c) side view of 100 rays (d) 3d view of 100 rays

6F2B (front 6', back 2')

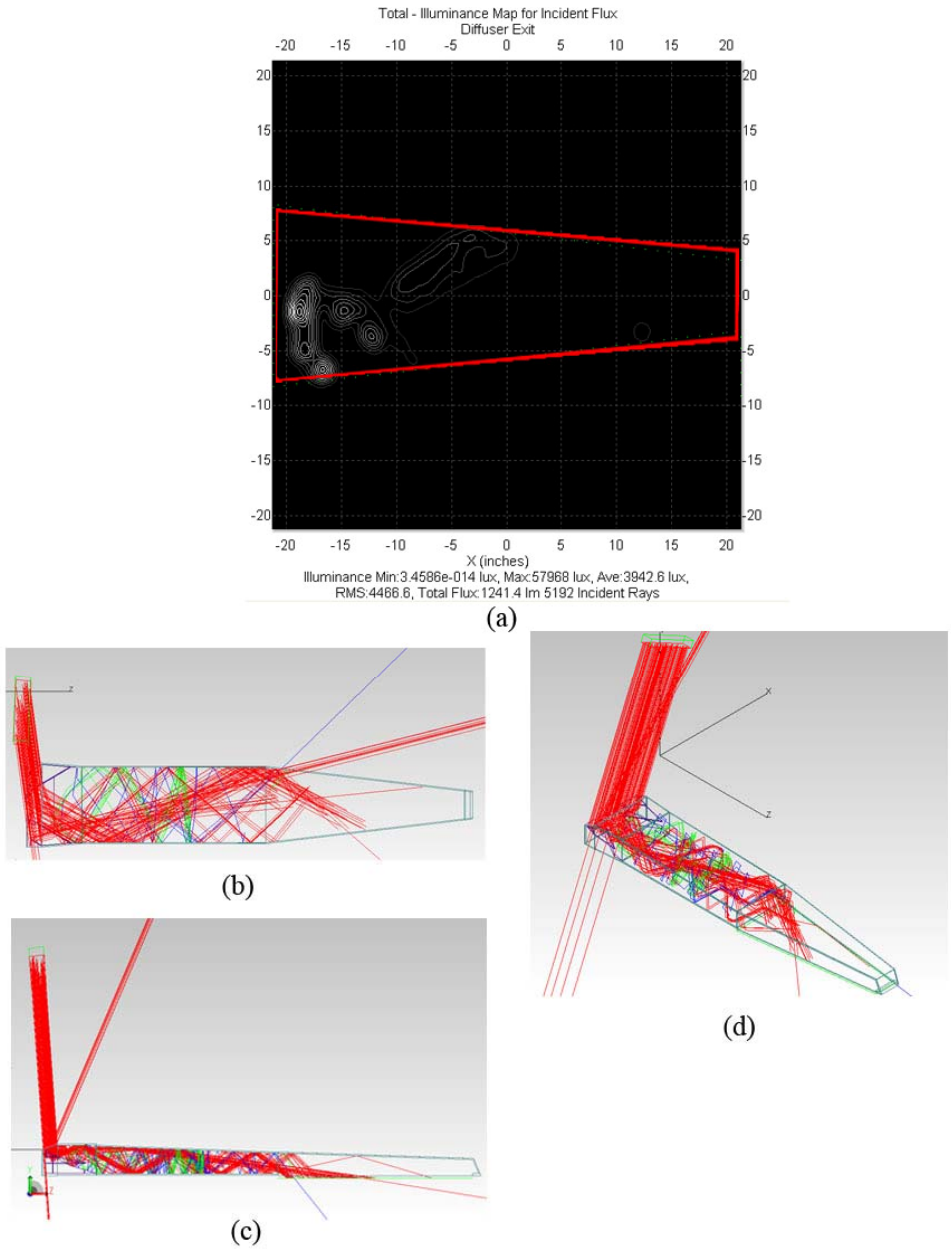

Fig. A.29. Tracepro simulation for June 21, 10am/2pm solar time. (a) Output of 10,000 rays on diffuser is 1241.4 lumens (b) top view of 100 rays (c) side view of 100 rays (d) 3d view of 100 rays

6F2B (front 6', back 2')

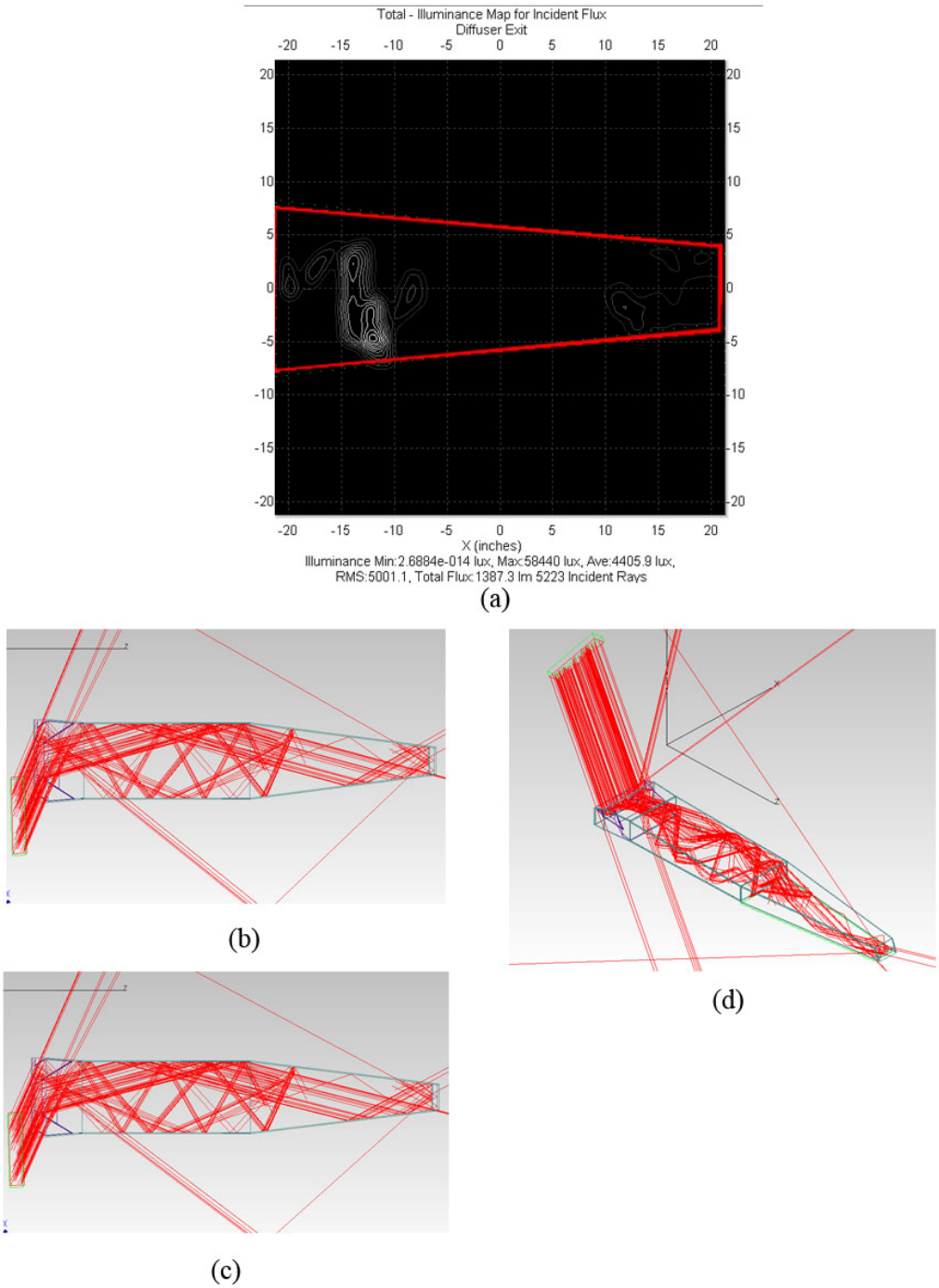

Fig. A.30. Tracepro simulation for June 21, 11am/1pm solar time. (a) Output of 10,000 rays on diffuser is 419.23 lumens (b) top view of 100 rays (c) side view of 100 rays (d) 3d view of 100 rays

6F2B (front 6', back 2')

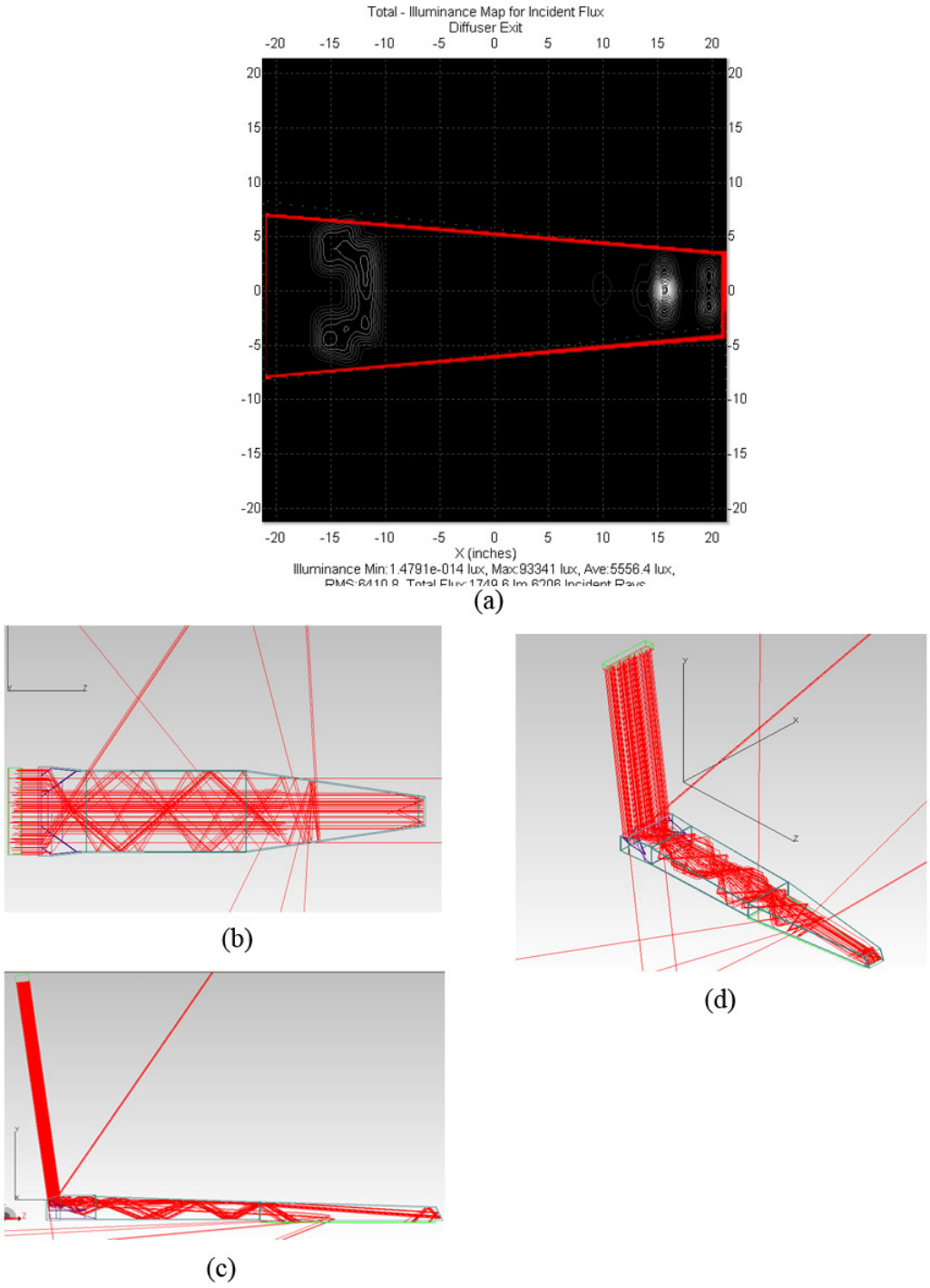

Fig. A.31. Tracepro simulation for June 21, 12 pm solar time. (a) Output of 10,000 rays on diffuser is 1749.8 lumens (b) top view of 100 rays (c) side view of 100 rays (d) 3d view of 100 rays

6F2B5C (front 6', back 2', side wall of back transport-section rotated by 5°)

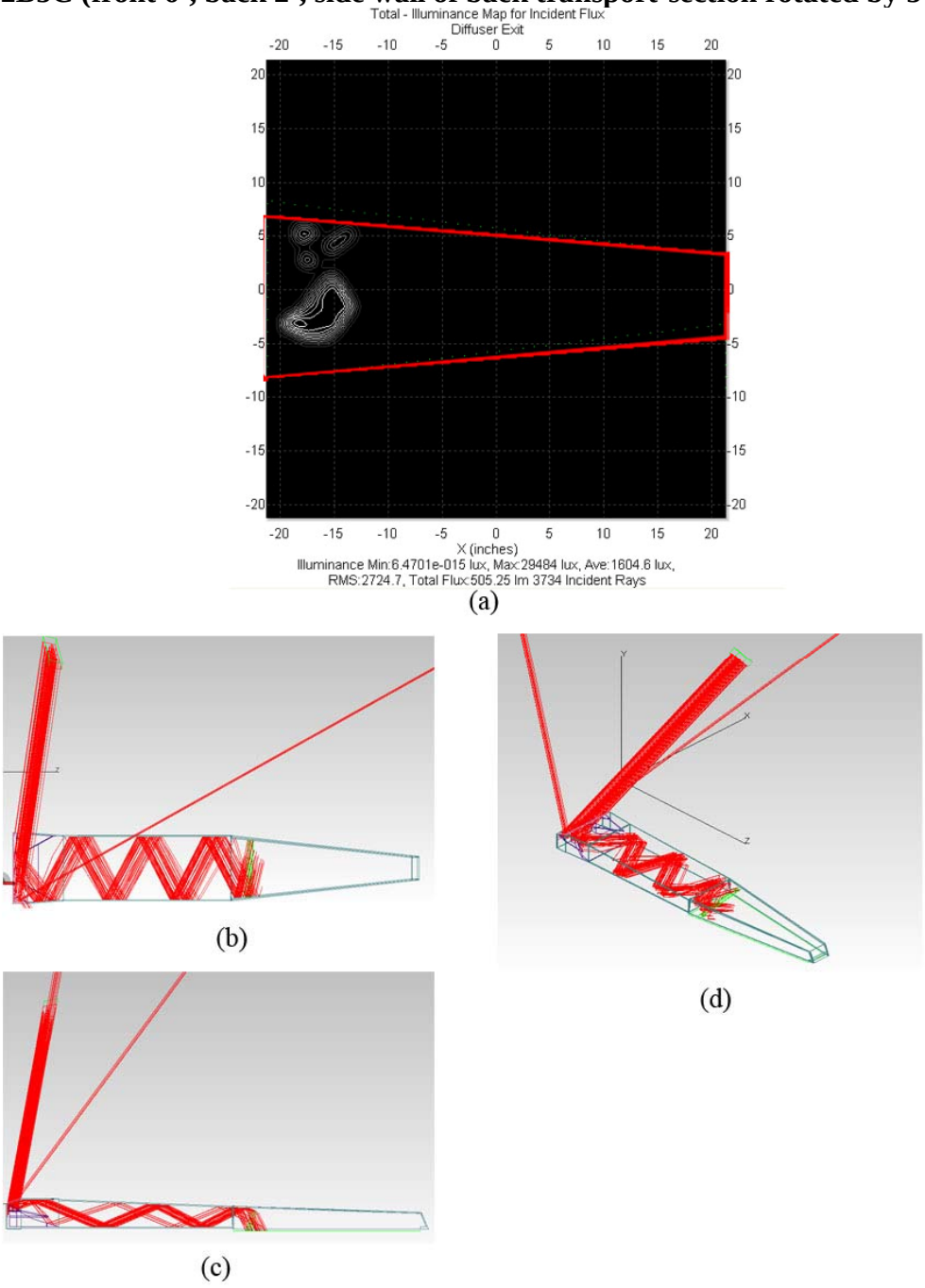

Fig. A.32. Tracepro simulation for June 21, 8am/4pm solar time. (a) Output of 10,000 rays on diffuser is 505.25 lumens (b) top view of 100 rays (c) side view of 100 rays (d) 3d view of 100 rays

6F2B5C (front 6', back 2', side wall of back transport-section rotated by 5°)

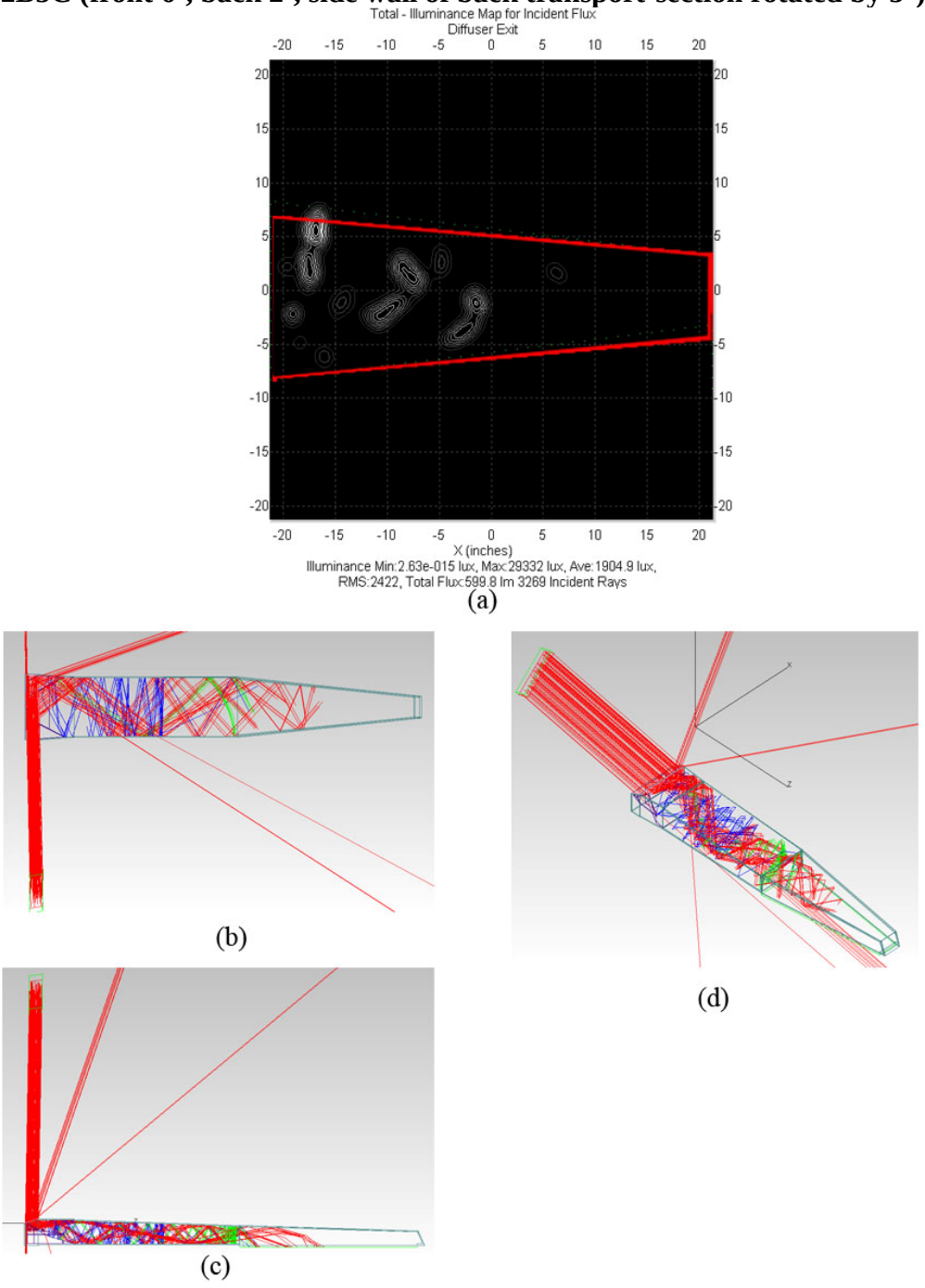

Fig. A.33. Tracepro simulation for June 21, 9am/3pm solar time. (a) Output of 10,000 rays on diffuser is 599.8 lumens (b) top view of 100 rays (c) side view of 100 rays (d) 3d view of 100 rays

6F2B5C (front 6', back 2', side wall of back transport-section rotated by 5°)

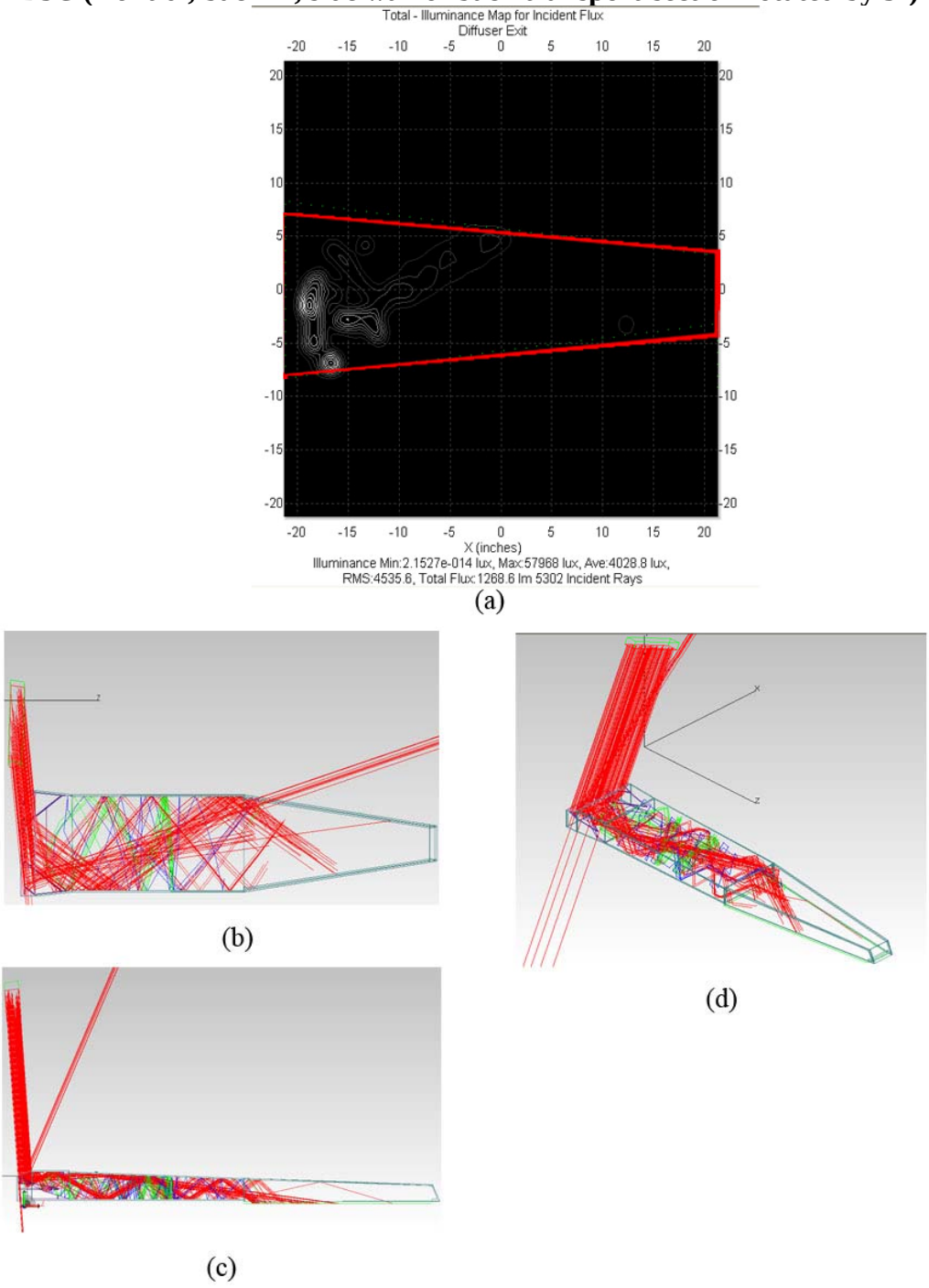

Fig. A.34. Tracepro simulation for June 21, 10am/2pm solar time. (a) Output of 10,000 rays on diffuser is 1268.6 lumens (b) top view of 100 rays (c) side view of 100 rays (d) 3d view of 100 rays

6F2B5C (front 6', back 2', side wall of back transport-section rotated by 5°)

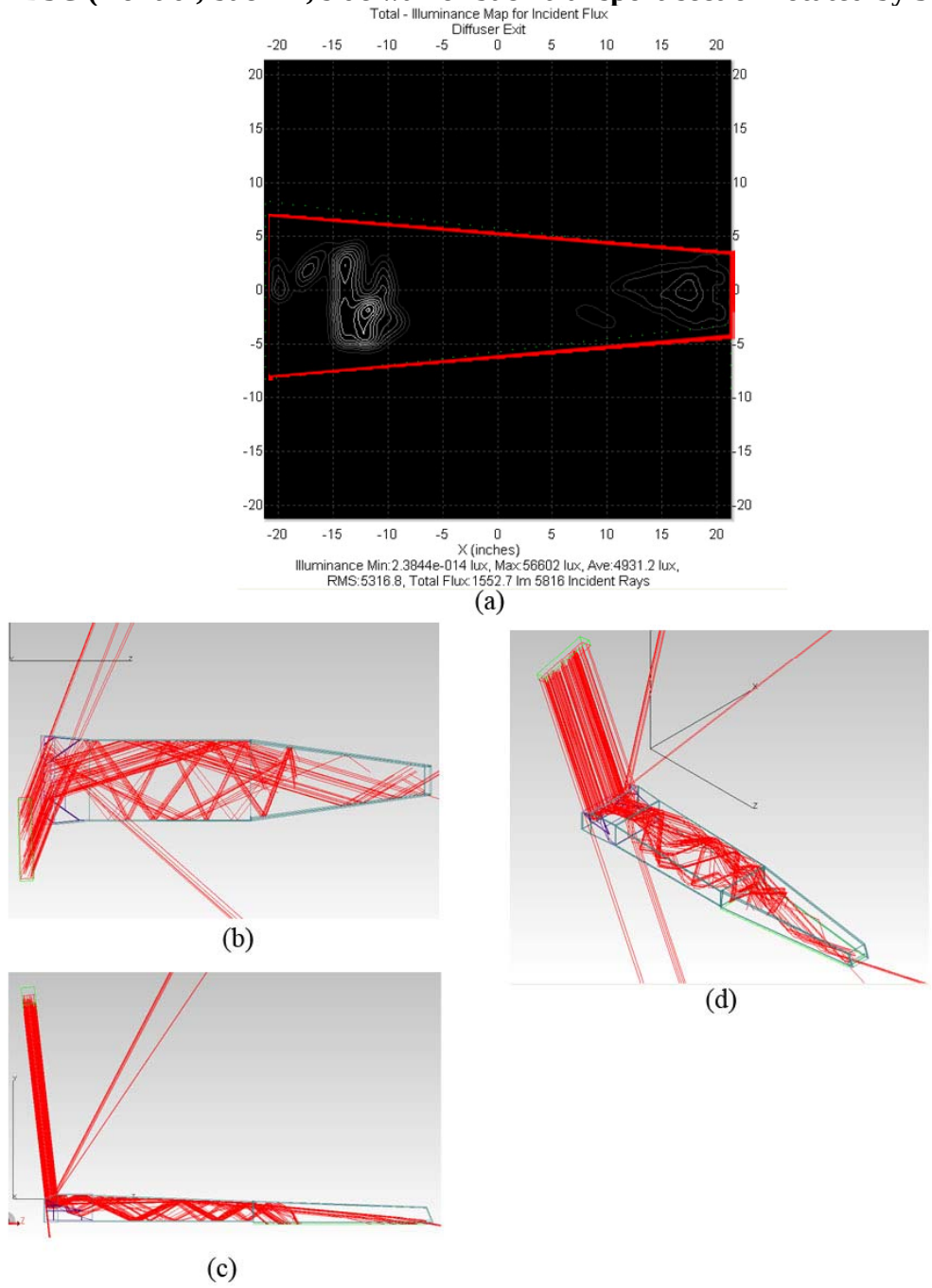

Fig. A.35. Tracepro simulation for June 21, 11am/1pm solar time. (a) Output of 10,000 rays on diffuser is 1552.7 lumens (b) top view of 100 rays (c) side view of 100 rays (d) 3d view of 100 rays

6F2B5C (front 6', back 2', side wall of back transport-section rotated by 5°)

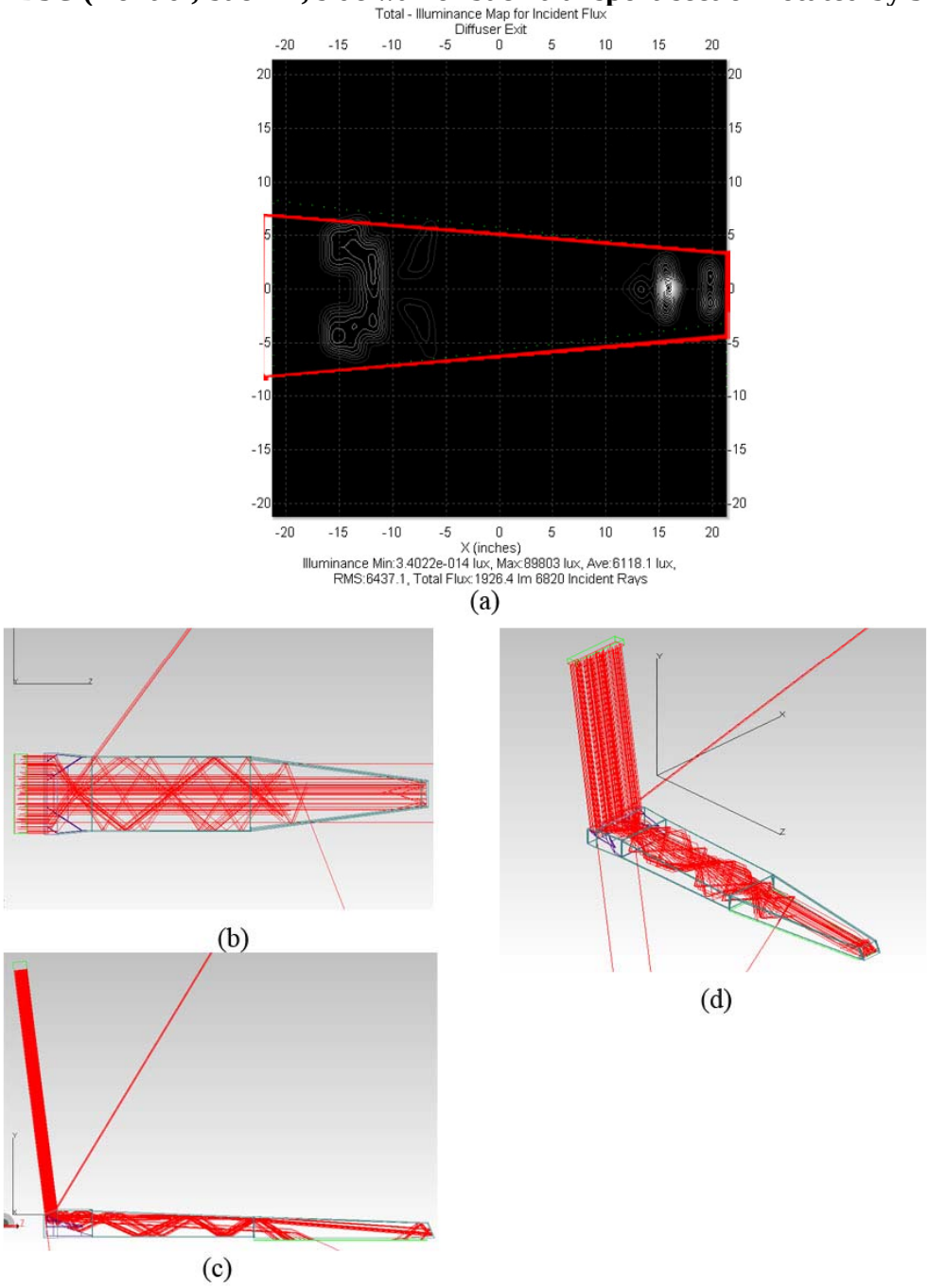

Fig. A.36. Tracepro simulation for June 21, 12pm solar time. (a) Output of 10,000 rays on diffuser is 6437.1 lumens (b) top view of 100 rays (c) side view of 100 rays (d) 3d view of 100 rays

21-Jun									
						NUMBER OF RAYS USED = 10,000			
						SURFACE SOURCE ILLUMINANCE = 100,000 LUX			
		O				A	B	C	D
SOLAR TIME	SOURCE FLUX (LUMEN)	BETINA'S OLP (OUTPUT FLUX, LUMEN)	TB4	RB4	ILLUMINANCE ON TASK PLANE DUE TO OLP	NEW OLP,BETINA'S SIDEREF (OUTPUT FLUX, LUMEN)	NEW OLP, AND SIDEREFLECTOR 6 with vertical walls of central reflector also reflective (OUTPUT FLUX, LUMEN)	Option 1 (angle changed, size reduced)	Option 2 (angle not changed, size reduced
8	1986.3	14.1	112.8	42.913	69.887	505.3	819.14	653.4	757.6
9	2691.3	280.7	208.17	60.058	148.112	599.8	936.57	872.8	860
10	3234.7	897	329.52	68.62	260.9	1268.6	1587.1	1535.5	1473.6
11	3575.5	872.5	442.12	68.601	373.519	1552.7	1669.9	1654.8	1545.6
12	3691.7	1603.7	572.06	68.588	503.472	1926.4	2026	1936.2	1880.3
13	3575.5	872.5	511.39	77.163	434.227	1552.7	1669.9	1654.8	1545.6
14	3234.7	897	372.65	77.151	295.499	1268.6	1587.1	1535.5	1473.6
15	2691.3	280.7	233.98	51.431	182.549	599.8	936.57	872.8	860
16	1986.3	14.1	112.64	42.855	69.785	505.3	819.14	653.4	757.6

Table A-1. Comparison of different reflector geometries of Final Design of OLP with Martins-Mogo prototype for June 21 (solar time).

21-Mar									
						NUMBER OF RAYS USED = 10,000			
						SURFACE SOURCE ILLUMINANCE = 100,000 LUX			
		O				A	B	C	D
SOLAR TIME	SOURCE FLUX (LUMEN)	BETINA'S OLP (OUTPUT FLUX, LUMEN)	TB4	RB4	ILLUMINANCE ON TASK PLANE FROM BETINA'S DATA	NEW OLP,BETINA'S SIDEREF (OUTPUT FLUX, LUMEN)	NEW OLP, AND SIDEREFLECTOR 6 with vertical walls of central reflector also reflective (OUTPUT FLUX, LUMEN)	Option 1 (angle changed, size reduced)	Option 2 (angle not changed, size reduced
8	1863	134.3	95.7	60.251	35.449	619.9	777.88	782.2	716.8
9	2631.4	328.5	191.4	94.656	96.744	1221.3	1422	1334	1304.2
10	3223.5	725.2	313.1	129.04	184.06	1502	1612.3	1562.5	1505.2
11	3594.1	1466.8	469.5	154.8	314.7	1823.2	1803.5	1775.6	1691.6
12	3721	2150.9	608.37	171.94	436.43	2268.9	2156.9	2250.8	2030.6
13	3594.1	1466.8	477.87	163.29	314.58	1823.2	1803.5	1775.6	1691.6
14	3223.5	725.2	330.12	137.49	192.63	1502	1612.3	1562.5	1505.2
15	2631.4	328.5	208.49	103.12	105.37	1221.3	1422	1334	1304.2
16	1863	134.3	121.7	60.19	61.51	619.9	777.88	782.2	716.8

Table A-2. Comparison of different reflector geometries of Final Design of OLP with Martins-Mogo prototype for March 21 (solar time).

22-Dec									
						NUMBER OF RAYS USED = 10,000			
						SURFACE SOURCE ILLUMINANCE = 100,000 LUX			
		O				A	B	C	D
SOLAR TIME	SOURCE FLUX (LUMEN)	BETINA'S OLP (OUTPUT FLUX, LUMEN)	TB4	RB4	ILLUMINANCE ON TASK PLANE FROM BETINA'S DATA	NEW OLP,BETINA'S SIDEREF (OUTPUT FLUX, LUMEN)	NEW OLP, AND SIDEREFLECTOR 6 with vertical walls of central reflector also reflective (OUTPUT FLUX, LUMEN)	Option 1 (angle changed, size reduced)	Option 2 (angle not changed, size reduced)
8	1424.8	3.9	43.493	25.813	17.68	593	685.59	693.7	692.9
9	2130.9	296	208.75	129.05	79.7	1037.2	1144.5	1141.6	1150.6
10	2673	536.2	234.79	111.82	122.97	1469.4	1546.5	1519	1532.5
11	3014.2	1509.9	130.45	43.01	87.44	1753.2	1637.8	1661.7	1630
12	3130	2011.8	69.536	34.391	35.145	2170.7	2090	2049.8	2048
13	3014.2	1509.9	173.82	68.775	105.045	1753.2	1637.8	1661.7	1630
14	2673	536.2	121.66	51.574	70.086	1469.4	1546.5	1519	1532.5
15	2130.9	296	182.47	103.14	79.33	1037.2	1144.5	1141.6	1150.6
16	1424.8	3.9	69.511	51.568	17.943	593	685.59	693.7	692.9

Table A-3. Comparison of different reflector geometries of Final Design of OLP with Martins-Mogo prototype for December 22 (solar time).

APPENDIX B

CONSTRUCTION PROCESS IMAGES

Vertical frames were made out of treated wood. Measured drawings of each of the existing models was done to accommodate custom changes to each of the shading devices. Brackets were then attached to the sides to catch the horizontal slats. Cracks were filled before applying a coat of primer.

Fig. B-1 Construction of shading devices.

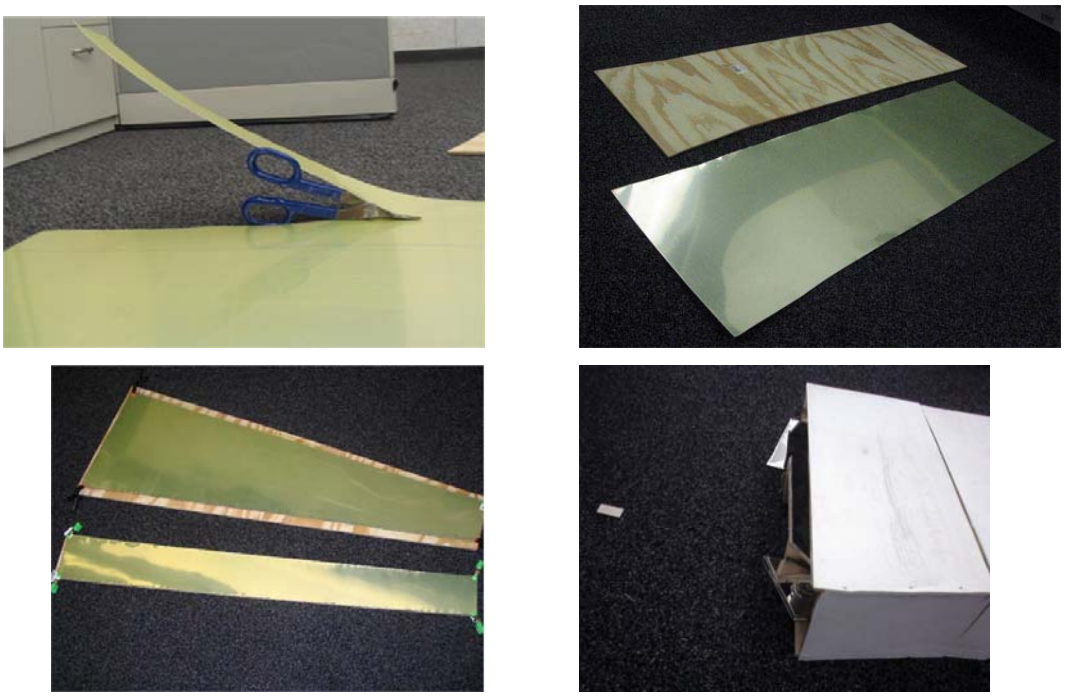

Fig. B-2. Miro-silver was manually cut using a metal cutter and then stuck to ¼” plywood using contact cement.

(a) (b)

Fig. B-3. Construction images. (a) Cover for OLP, (b) false ceiling with opening for diffuser,

(a) (b)

Fig. B-4. (a) Back half of transport section installed on the ceiling, (b) test model lying open. The diffuse can be seen at the back half of the ceiling.

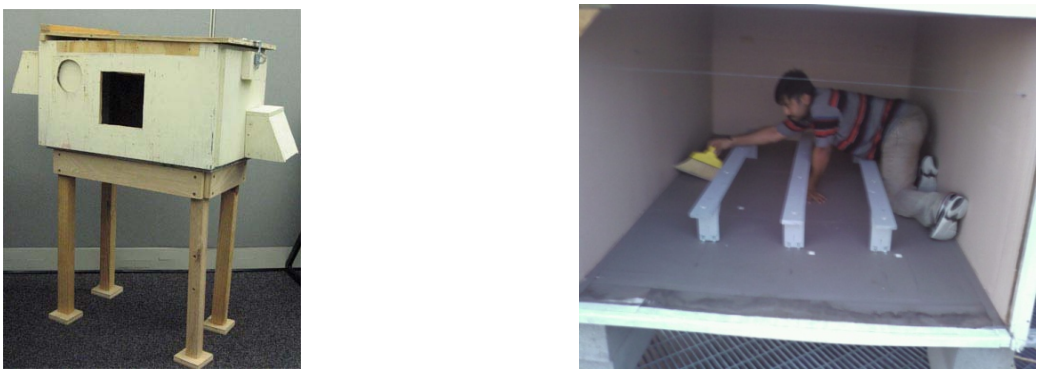

(a) (b)

Fig. B-5. Construction images. (a) envelope used to house the camera and digisnap, (b) clean up and ventilation of the model was done every six months.

APPENDIX C

COMPARISON OF PHOTOMETRIC SENSORS

BEFORE AND AFTER CALIBRATION

The Licor sensors are recommended for calibration every two years. 8 sensors to be used were more than four years old and the others were 3 years old. A test was performed on both the models to evaluate sensor performance in total darkness. Windows were covered with black opaque plastic sheets to prevent any light inside the model. While all other sensors showed a near 0 lux illuminance, it was observed that at least 15 sensors showed an illuminance of more than 5 lux with some negative values as well; the spikes occurred between 10am to 3pm. Temperature and humidity levels were also measured with Hobo external dataloggers and found to be in the range allowable for Licor sensors.

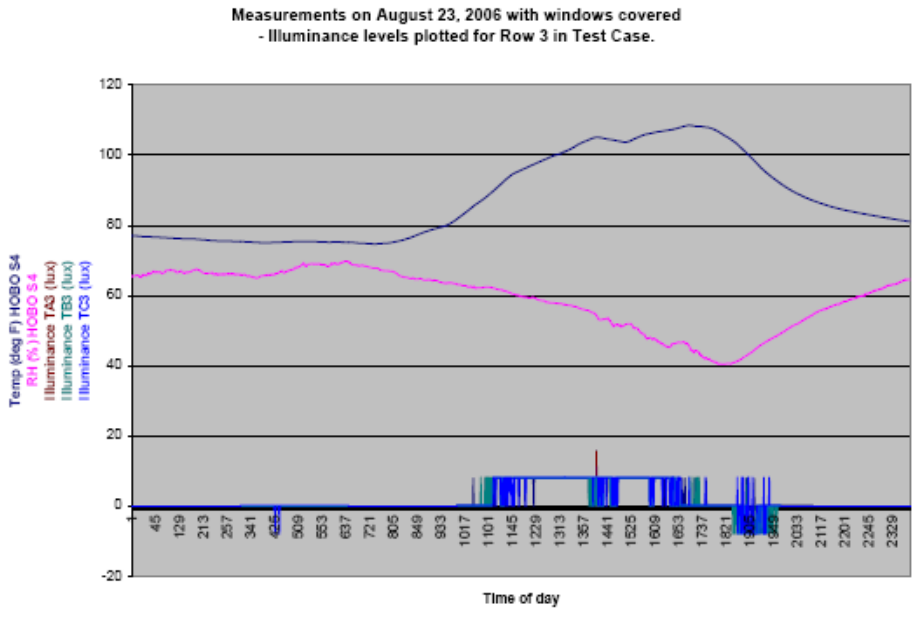

Fig. C-1 Measurements on Aug. 23, 2006 with windows covered- Illuminance levels plotted for Row 3 in test model.

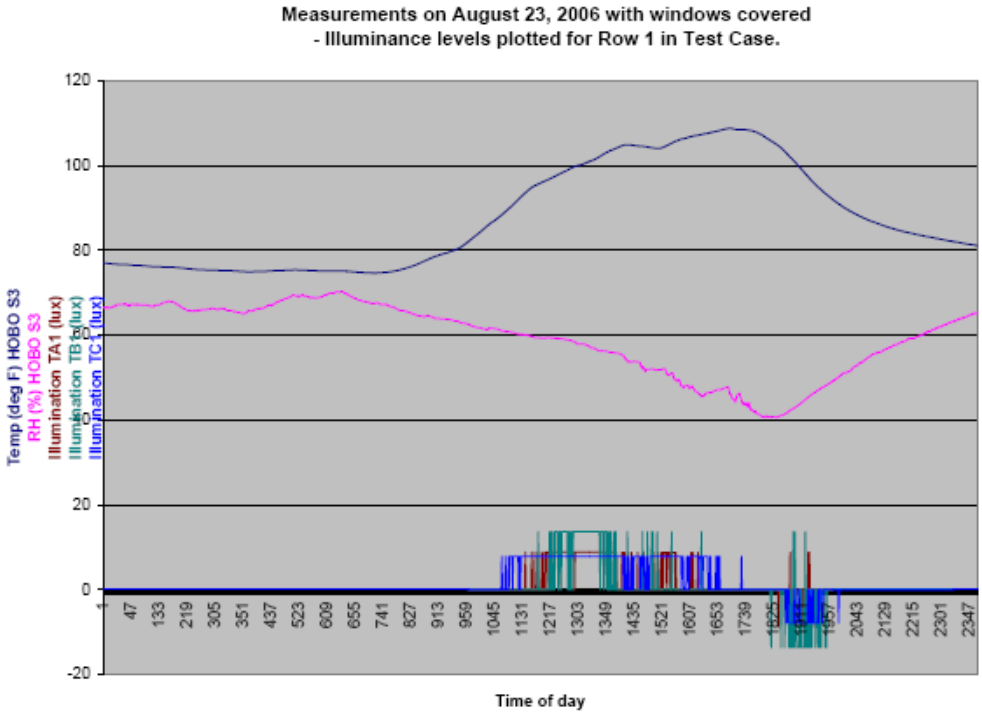

Fig. C-2 Measurements on Aug. 23, 2006 with windows covered- Illuminance levels plotted for Row 1 in test model.

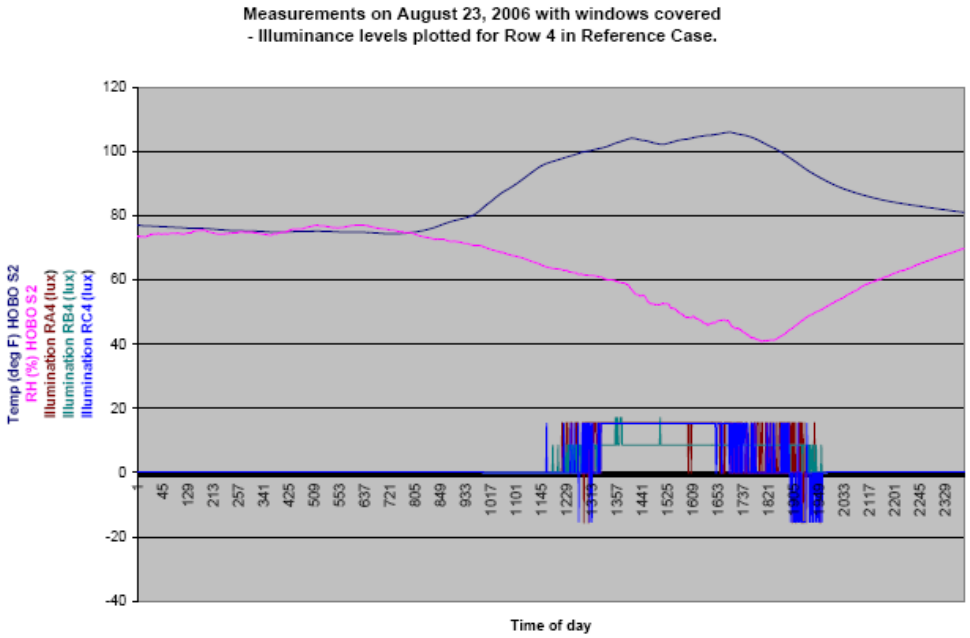

Fig. C-3 Measurements on Aug. 23, 2006 with windows covered- Illuminance leveles plotted for Row 4 in reference model.

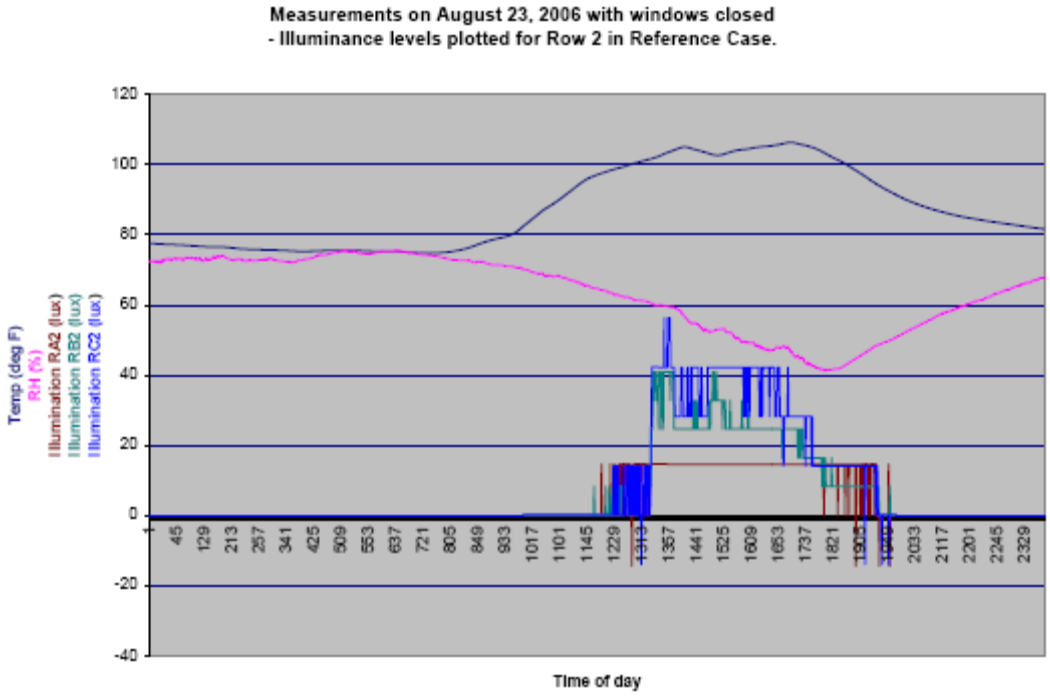

Fig. C-4 Measurements on Aug. 23, 2006 with windows covered- Illuminance leveles plotted for Row 2 in reference model.

The sensors were then compared to the Minolta T-10 light meter while kept in the model and outside, in artificial light and diffused daylight before it was decided that they needed calibration. The difference between similar sensors when kept inside the models was as high as 12% around noon and sometimes higher than 20% during afternoons. The highest difference with illuminance measured with Minolta T-10 was 13.2%. Calibration of the sensors was tried with different lighting conditions: 4’ under a 60 watt lamp, 3’ under a 500 watt lamp, 14’ under a 500 watt lamp, and diffuse daylight (evening and overclouded conditions). The overall lighting conditions were tried to be kept as homogenous as possible and the average illuminance of sensors was compared with each individual sensor.

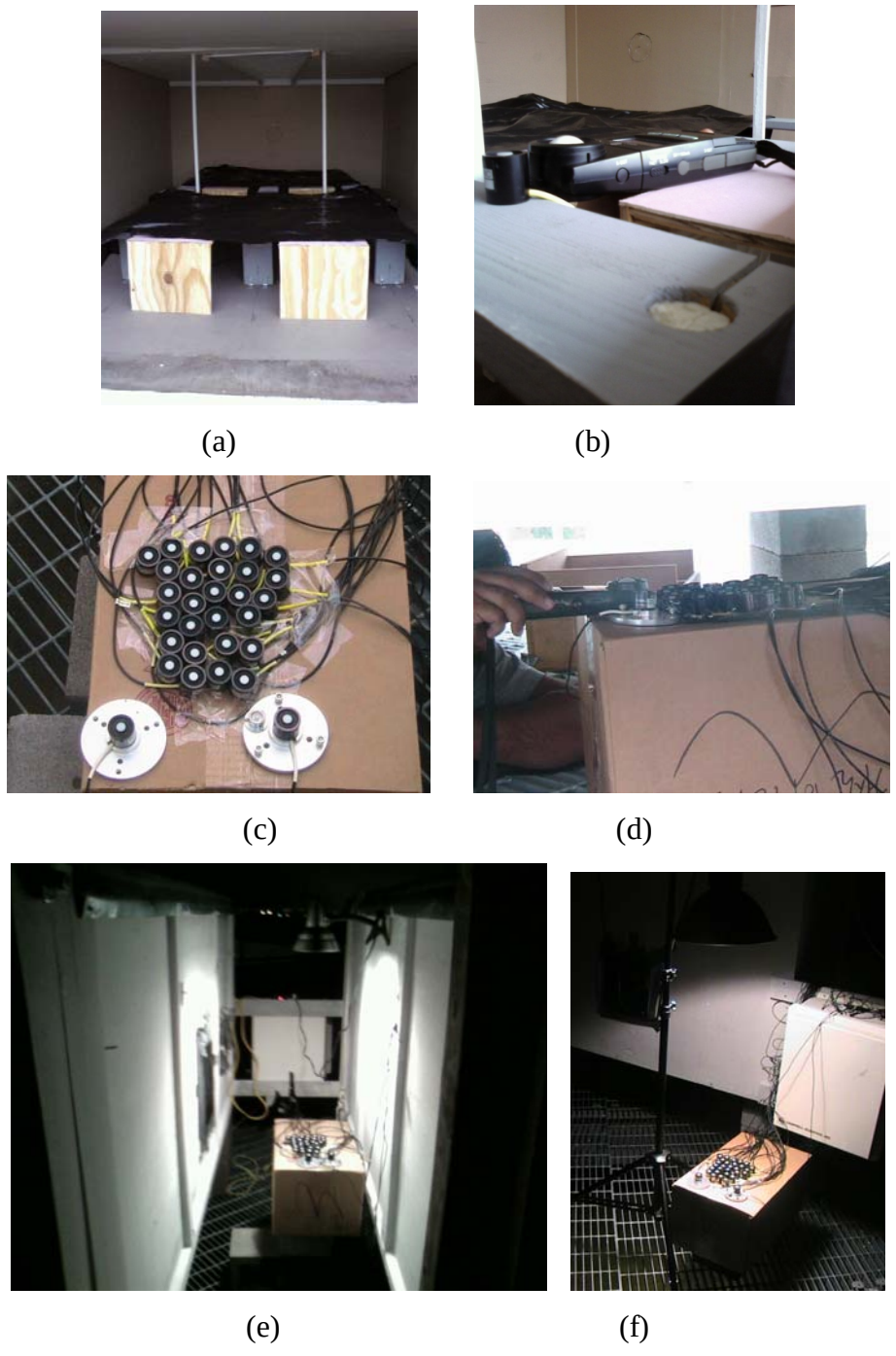

Fig. C-5. Comparison and calibration of sensors. (a) Sensors covered during day while comparing with Minolta T-10, (b) sensors covered during night while comparing with Minolta T-10, (c) sensor arrangement under overcast sky for calibration, (d) sensor arrangement under the models during evening, (e) sensors under a 60 watt lamp, (f) sensors under a 500 watt lamp.

Varying the multipliers subsequently did not produce appreciable results: when kept together, the difference with the average illuminance measure by Minolta T-10 was ±4.5% for diffuse daylight and ± 7.1% for electric light. The sensors were sent to Licor for recalibration, and a few of them had the cable-insulation patched, filter re-glued and cut-wires replaced. After they were back from Licor, the new multipliers were input into the datalogger instructions.

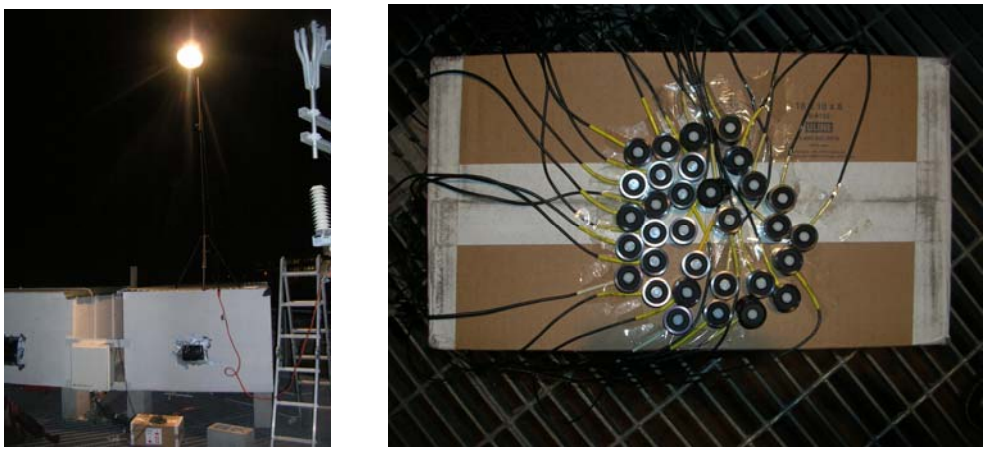

(a) (b)

Fig. C-6. Comparison of sensors with average illuminance (after calibration of sensors). (a) Sensors 14' under a 500 watt lamp kept, (b) arrangement of sensors under the 500 watt lamp.

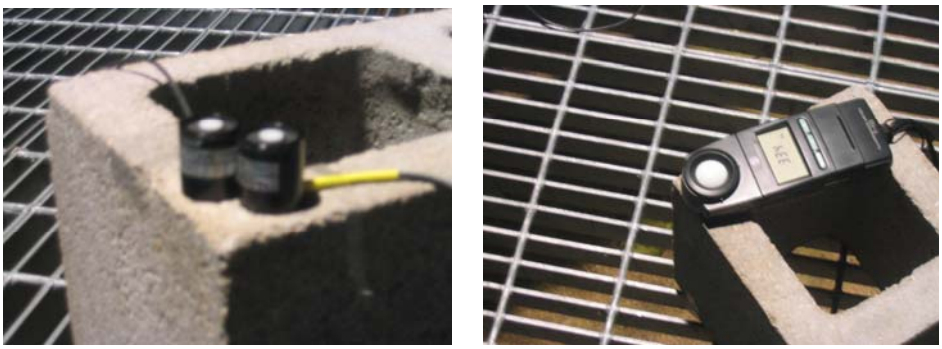

(a) (b)

Fig. C-7. Comparison of sensors with the reference sensor (after calibration of sensors). (a) arrangement of sensors when compared to the test sensor, (b) Minolta T-10 at the same location as the two sensors.

From earlier trials it was concluded that illuminance changed significantly on the area that the sensors were kept together. Subsequently, there was a need to keep the sensors closer together for comparison. Another test was devised where one of the newest sensor, PH-8492, was taken as the reference and all others compared to it one by one. This ensured that the difference in illuminance between the two was minimum, though the results would be based on the assumption that the new sensor would itself be perfect to act as a benchmark. The comparison yielded a difference of -1.75% to 2.87% with the reference sensor. The sensors were then installed back into the models.

APPENDIX D

EVALUATION OF PHOTOLUX

Photolux is an image analysis software developed by Soft Energy Consultants in France. It processes multiple images taken at different exposures and produces a luminance map which is essentially a shaded contour plot of luminance levels visible in a scene. One of the essential requirements of producing an accurate luminance map is to have minimum or practically zero variation in luminance while the images are taken. Fig.D-1 shows the camera settings for Nikon Coolpix 5400 that were used for the images.

White balance	daylight
Best shot selector	off
Image adjustment	normal
Saturation control	normal
Image quality	NORMAL
Image size	5M (2592x1944)
Sensitivity	100 ISO
Image sharpening	off
Lens	fisheye
Exposure options (AE lock)	off
Auto bracketing	off
Noise reduction	off

Fig. D-1 .Camera settings for Nikon Coolpix 5400 for Photolux.
(Source: Help folder, Photolux)

Auto bracketing, however, was not kept on so as to quickly take 5 images spaced out at 1EV intervals (7.9, 8.9, 9.9, 10.9, 11.0). Then 3 more images were taken at 5.0EV, 7.0EV and 14.0EV. Fig.D-2a shows these values along with the corresponding Aperture and Exposure times. Fig.D-2b shows the range of luminance values that are covered by an exposure value. For a fixed Aperture of 4.0 and changing Exposure Values of 5.0, 7.0, 7.9,

8.9, 9.9, 11.0, 12.0 and14.0, the following exposure times were selected respectively: 1/2, 1/8, 1/15, 1/30, 1/60, 1/125, 1/250, 1/1000.

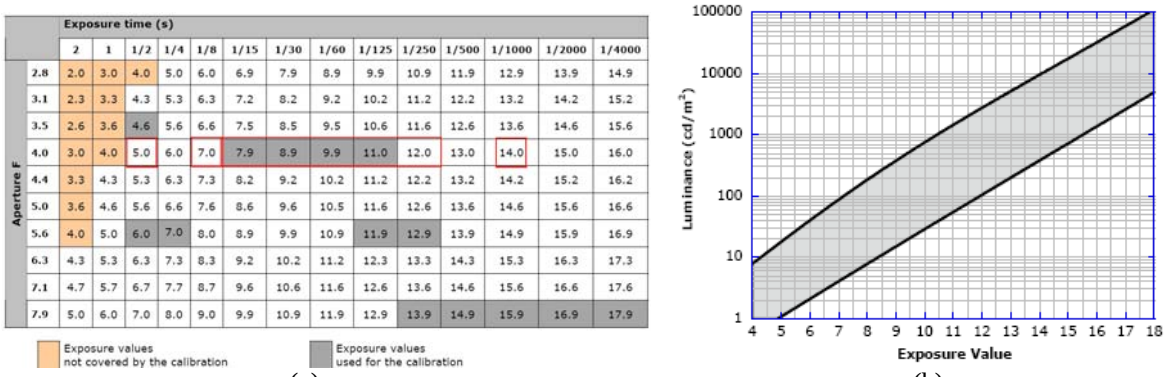

Aperture F	Exposure time (s)													
	2	1	1/2	1/4	1/8	1/15	1/30	1/60	1/125	1/250	1/500	1/1000	1/2000	1/4000
2.8	2.0	3.0	4.0	5.0	6.0	6.9	7.9	8.9	9.9	10.9	11.9	12.9	13.9	14.9
3.1	2.3	3.3	4.3	5.3	6.3	7.2	8.2	9.2	10.2	11.2	12.2	13.2	14.2	15.2
3.5	2.6	3.6	4.6	5.6	6.6	7.5	8.5	9.5	10.6	11.6	12.6	13.6	14.6	15.6
4.0	3.0	4.0	5.0	6.0	7.0	7.9	8.9	9.9	11.0	12.0	13.0	14.0	15.0	16.0
4.4	3.3	4.3	5.3	6.3	7.3	8.2	9.2	10.2	11.2	12.2	13.2	14.2	15.2	16.2
5.0	3.6	4.6	5.6	6.6	7.6	8.6	9.6	10.5	11.6	12.6	13.6	14.6	15.6	16.6
5.6	4.0	5.0	6.0	7.0	8.0	8.9	9.9	10.9	11.9	12.9	13.9	14.9	15.9	16.9
6.3	4.3	5.3	6.3	7.3	8.3	9.2	10.2	11.2	12.3	13.3	14.3	15.3	16.3	17.3
7.1	4.7	5.7	6.7	7.7	8.7	9.6	10.6	11.6	12.6	13.6	14.6	15.6	16.6	17.6
7.9	5.0	6.0	7.0	8.0	9.0	9.9	10.9	11.9	12.9	13.9	14.9	15.9	16.9	17.9

Exposure values not covered by the calibration

Exposure values used for the calibration

(a) (b)

Fig. D-2.Photolux settings. (a) Exposure values used with Photolux, (b) range of luminance values covered by an exposure value.

A number of observations were made while using Photolux and are enlisted here for future reference. While producing luminance maps, the processing time seemed to suddenly increase after a few minutes of usage and there were glitches while shifting from luminance map to JPGs if multiple sets of JPGs were open at the same time. The solution to this was to close one set of images before opening another.

A set of observations was made with different spaces to compare difference between UGR values under similar lighting conditions. Spaces were categorized under two lighting conditions: one predominantly daylit and the other predominantly electrically lit. UGR1 and UGR2 represent UGR values obtained from Photolux for two different view positions. Table D-1 lists the observations:

Electric lighting-night			Daylight				
UGR1	UGR2	SPACE	UGR1	UGR2	SPACE		
11.8	10.8	3rd floor	28.9	31.5	home	EXHG 1	EXHG 2
4	3.7	4th floor	26	26.1	langford-3floorlab	94906lux	94146lux
14.3	14.8	Azimuth	13.4	17.3	model	7000lux	11736lux

Table D-1 . UGR values calculated by Photolux for the same space with two different views.

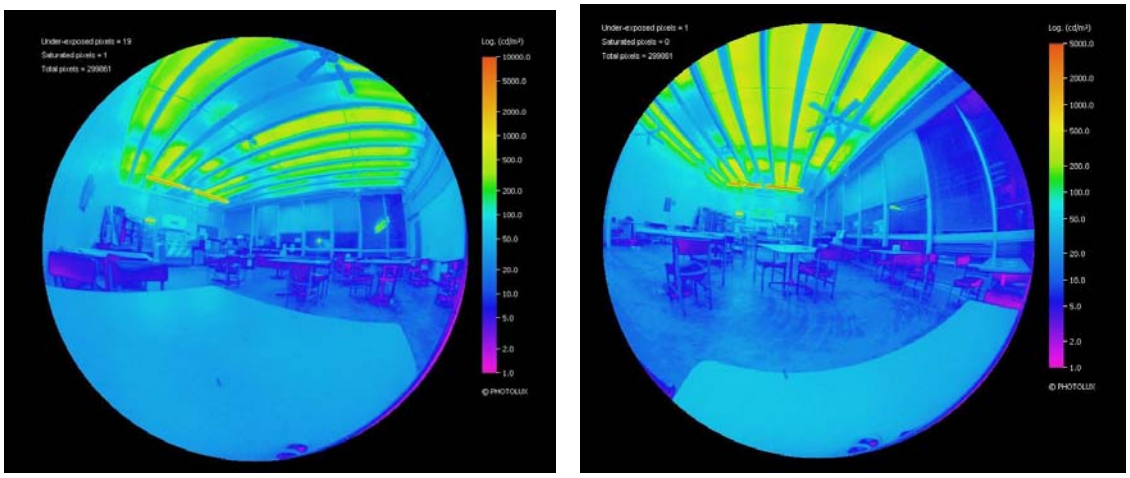

Fig. D-3 .UGR comparison with different view positions using Photolux.

Fig.D-3 shows one of the spaces, Azimuth, photographed at two different positions. Apparently, the UGR value did not change significantly with the position of the camera in electric lighting, and in daylighting (if the external ground horizontal did not change significantly).

APPENDIX E

SELECTION OF DIFFUSER FOR OLP

A box model was created out of foamboard to evaluate 12 diffusers from Optigrafix. A window to allow direct sunlight was kept next to a wall and another opening on the opposite side of the wall was used to mount a camera. It was ensured that there were no light leaks and the only source of light was the sidewindow. The model was moved to allow direct sunlight to create 3 types of patches: on floor only, on floor and wall, and on wall only. Different diffusers were placed infront of the window in the three situations to visually observe the transmission and diffusion characteristics. Finally images for all cases were compared with the basecase and with each other to determine the most appropriate diffuser material.

Fig. E-1. Basecase for the series of observations.

Fig. E-1. Different grades and thicknesses of diffusers tested on the model.

Grade: DFMM , Thickness: 0.004”/100µm
TRANSMISSION=66%, HAZE=89%

Grade: DFMM , Thickness: 0.005”/125µm
TRANSMISSION=66%, HAZE=89%

Grade: DFMM , Thickness: 0.007”/175µm
TRANSMISSION=66%, HAZE=89%

Grade: LBMT , Thickness: 0.003”/75µm
TRANSMISSION=99%, HAZE=45%

Grade: DFPM , Thickness: 0.003”/75µm
TRANSMISSION=87%, HAZE=88%

Grade: DFPM , Thickness: 0.004”/100µm
TRANSMISSION=87%, HAZE=88%

Grade: DFPM , Thickness: 0.005”/125µm
TRANSMISSION=87%. HAZE=88%

Fig. E-1. Continued

.

Fig. E-1. Continued

After careful comparison of all options, DFPM with thickness of 0.007” was selected because of an optimum transmission, best diffusion and the maximum thickness. The area of diffuser used in the present research was 3.39 sq.ft, which for a full scale prototype would equal to 54 sq.ft.. As compared to Martins-Mogo prototype which used 2.68 sq.ft. of diffuser area, the present research used 26% more area.

APPENDIX F

INSTRUMENTS USED FOR DATA COLLECTION

(a) (b)

Fig. F-1. (a) Digisnap2000 used for automated continuous images at a fixed time-lapse, (b) Nikon Coolpix 5400 used for digital images.

(a) (b)

Fig. F-2. (a) LI-210SA used for measuring illuminance, (b) T-10 from Konica Minolta used for measuring illuminance.

(a) (b)

Fig. F-3. (a) LS-100 from Konica Minolta used for measuring luminance, (b) CR23X from Campbell Scientific used for collecting data.

Fig. F-4 Relay Multiplexer AM16/32.

Fig. F-5. Shadow band from Eppley.

APPENDIX G

METHODOLOGY OF SHADING DEVICE DESIGN

SHADE is a solar shading analysis spreadsheet developed by the Building Science Group at UC Berkeley. It uses the balance point temperature to generate the annual shading needs for a rectangular room with windows on south façade. The walls were also assumed to be glazing of similar Uvalues. Uvalues for these glazing were taken from an online reference for suggested windows for South Texas region: http://www.efficientwindows.org/factsheets/texas.pdf

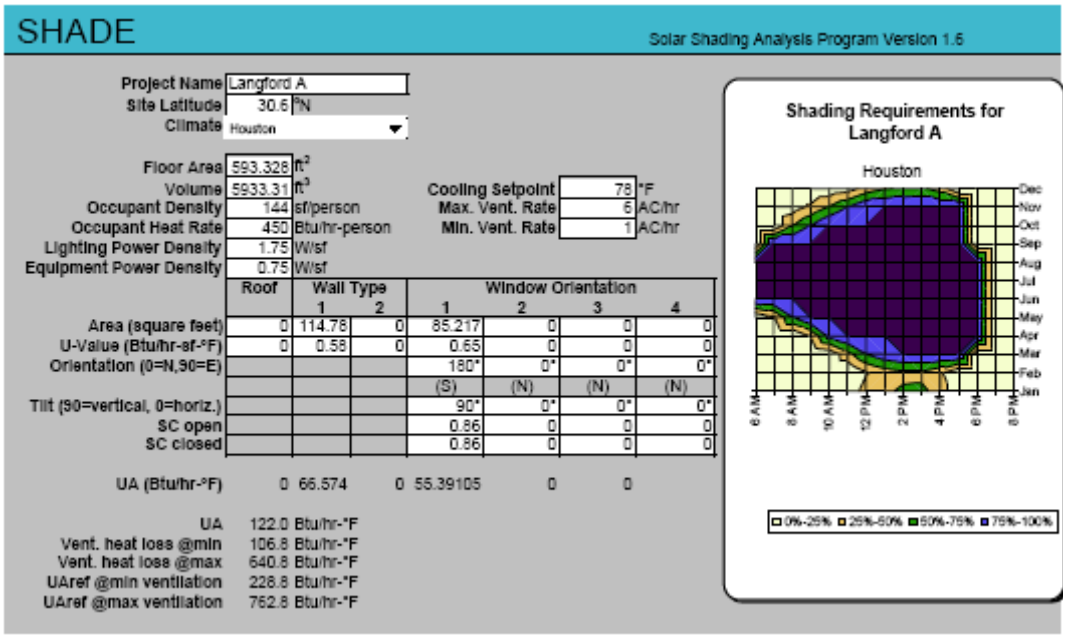

Fig. G-1. Inputs used for generating shading needs in SHADE.

FigG-1 shows the Uvalues used for the present research. Fig.G2 shows the results generated with a timetable showing percentage of shading needs at different times of the year. Out of these, 100% shading needs from July to December were plotted on the sunpath for College Station, TX as shown in Fig.G-3. For the present research, the sunpath is considered symmetrical for one half of the year (effect of analemma is not considered).

Sun or SHADE — Solar Shading Analysis Program Version 1.6

Timetable of Shading Needs
Langford A
Houston
Window Orientation 1 (S)

	Jan	Feb	Mar	Apr	May	Jun	Jul	Aug	Sep	Oct	Nov	Dec
	Jan	Feb	Mar	Apr	May	Jun	Jul	Aug	Sep	Oct	Nov	Dec
6 AM	0%	0%	0%	0%	0%	100%	100%	100%	0%	0%	0%	0%
7 AM	0%	0%	0%	0%	22%	100%	100%	100%	100%	0%	0%	0%
8 AM	1%	0%	0%	0%	74%	100%	100%	100%	100%	48%	12%	0%
9 AM	1%	0%	0%	27%	100%	100%	100%	100%	100%	75%	30%	2%
10 AM	4%	0%	6%	82%	100%	100%	100%	100%	100%	100%	51%	6%
11 AM	11%	0%	41%	100%	100%	100%	100%	100%	100%	100%	74%	13%
12 PM	34%	23%	74%	100%	100%	100%	100%	100%	100%	100%	98%	34%
1 PM	46%	37%	92%	100%	100%	100%	100%	100%	100%	100%	100%	47%
2 PM	53%	44%	100%	100%	100%	100%	100%	100%	100%	100%	100%	54%
3 PM	54%	44%	100%	100%	100%	100%	100%	100%	100%	100%	100%	55%
4 PM	41%	29%	100%	100%	100%	100%	100%	100%	100%	100%	100%	39%
5 PM	0%	0%	100%	100%	100%	100%	100%	100%	100%	100%	100%	0%
6 PM	0%	0%	0%	100%	100%	100%	100%	100%	0%	0%	0%	0%
7 PM	0%	0%	0%	0%	0%	0%	0%	0%	0%	0%	0%	0%
8 PM	0%	0%	0%	0%	0%	0%	0%	0%	0%	0%	0%	0%

Fig. G-2. Timetable of shading needs generated in SHADE .

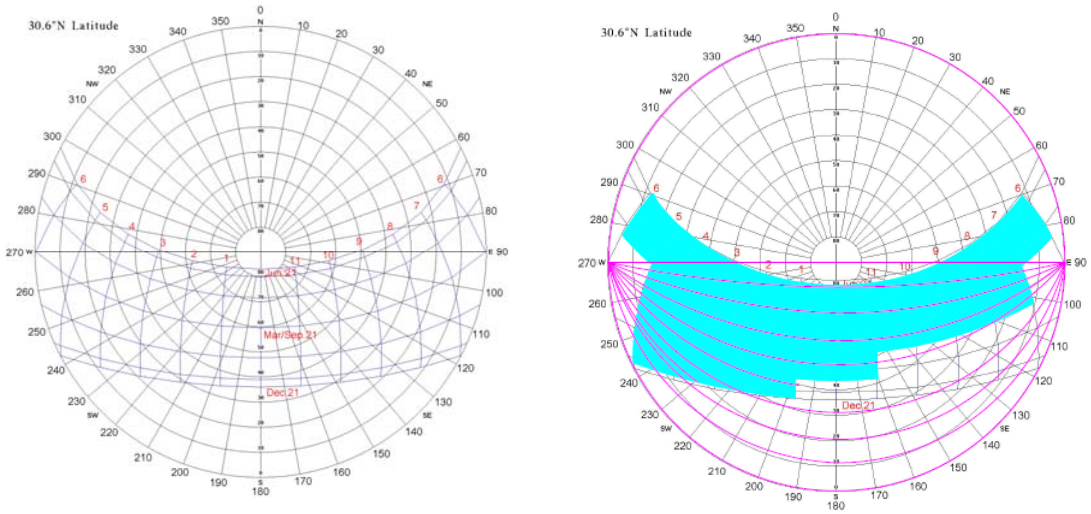

(a) (b)

Fig. G-3. Defining shading needs. (a) Sunpath for College Station, (b) 100% shading needs from SHADE superimposed on the sunpath.

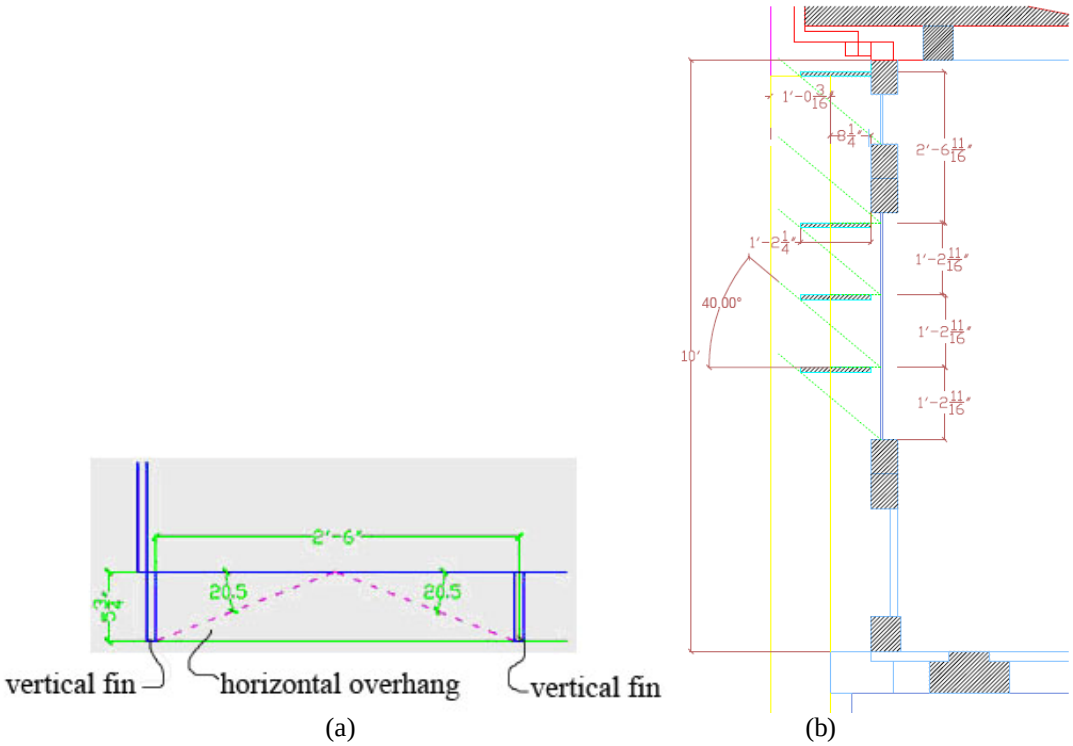

Fig. G-4. Drawings of shading device. (a) Part-plan, (b) section.

Fig.G-4 shows drawings of proposed shading device; the 20.5˚ profile angle was used to define the vertical fin elements and the 40˚ profile angle was used to define the horizontal shading element.

APPENDIX H

REFLECTION CHARACTERISTICS OF MIRO-SILVER

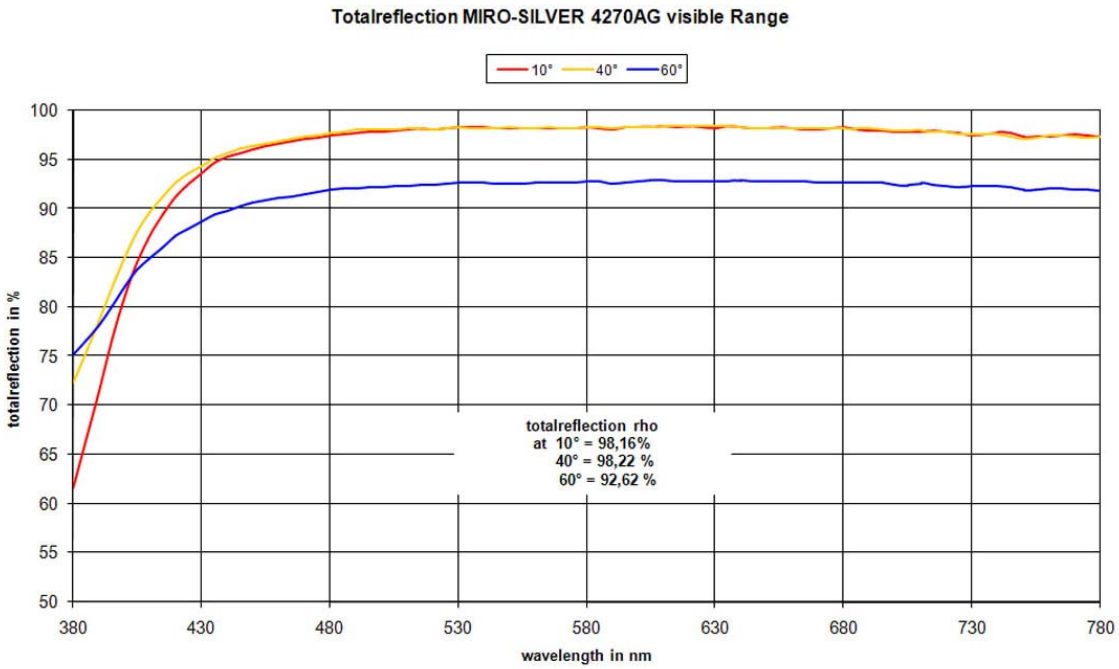

Fig. H-1. Reflection characteristics of Miro-Silver

Fig.H-1 shows reflection characteristics for Miro-Silver. The film is over 98% reflective for incident angles of 40˚ or less, for most of the wavelengths in the visible spectrum (400nm-700nm). This phenomenon may come into play with the sunrays being transported inside OLP. Because a direct sun ray undergoes multiple reflections with varied incident angles before finally reaching the diffuser, it is possible that the reflectance for each reflection is different. However, this may be a desired property for OLP because it might enhance output for low-angle sunrays and diminish it for high-angle sunrays.

APPENDIX I

DAYLIGHT AVAILABILITY IN TEXAS

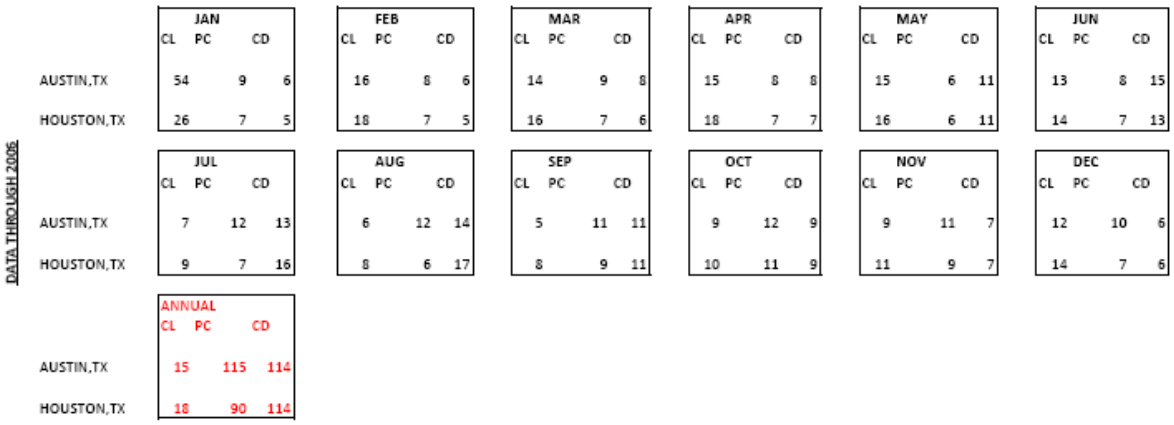

Fig. F-1. Cloudiness - mean number of days for Austin and Houston. *Source: http://lwf.ncdc.noaa.gov/oa/climate/online/ccd/cldy.html*

	CLEAR	PARTLY CLOUDY	CLOUDY	% OF CLEAR AND PARTLY CLOUDY DAYS
ANNUAL DATA THROUGH 2007	209	108	48	86.8%

Fig. F-2. Cloudiness - mean number of days in 2007 calculated for College Station. *Source :http://www.srh.noaa.gov/productview.php?pil=HGXCF6CLL&version=15&max=61*

APPENDIX J

INSTRUCTIONS USED FOR THE DATALOGGER

Instructions for the CR23X datalogger were written and edited using EDLOG. Standard commands were used from CR23X specifications and modified for the present research. The following pages show the instructions which include the following information: interval of data collection, excitation voltage for each terminal, nomenclature of each terminal corresponding to the 32 sensors (KRA1,KRA2, etc.), multipliers for each terminal (obtained from Campbell Sc. after calibration).

EDLOG compiles the instructions created in .CSI file and generates a .dld file which is sent to the datalogger. For any subsequent editing, another .dld file must be created and resent to the datalogger.

```
;{CR23X}
*Table 1 Program
01: 60.0000   Execution Interval (seconds)

1:  Batt Voltage (P10)
1: 1        Loc [ Batt_Volt ]

2:  If time is (P92)
1: 0        Minutes (Seconds --) into a
2: 1440     Interval (same units as above)
3: 30       Then Do

3:  Signature (P19)
1: 2        Loc [ Prog_Sig  ]

4:  End (P95)

5:  Do (P86)
1: 41       Set Port 1 High

6:  Do (P86)
```

1: 72 Pulse Port 2

7: Delay w/Opt Excitation (P22)
1: 1 Ex Channel
2: 0 Delay W/Ex (0.01 sec units)
3: 1 Delay After Ex (0.01 sec units)
4: 0 mV Excitation

8: Volt (Diff) (P2)
1: 1 Reps
2: 22 50 mV, 60 Hz Reject, Slow Range
3: 1 DIFF Channel
4: 41 Loc [KR_A1]
5: 8488.96 Mult
6: 0 Offset

9: Do (P86)
1: 72 Pulse Port 2

10: Delay w/Opt Excitation (P22)
1: 1 Ex Channel
2: 0 Delay W/Ex (0.01 sec units)
3: 1 Delay After Ex (0.01 sec units)
4: 0 mV Excitation

11: Volt (Diff) (P2)
1: 1 Reps
2: 22 50 mV, 60 Hz Reject, Slow Range
3: 1 DIFF Channel
4: 40 Loc [KR_A2]
5: 8271.30 Mult
6: 0 Offset

12: Do (P86)
1: 72 Pulse Port 2

13: Delay w/Opt Excitation (P22)
1: 1 Ex Channel
2: 0 Delay W/Ex (0.01 sec units)
3: 1 Delay After Ex (0.01 sec units)
4: 0 mV Excitation

14: Volt (Diff) (P2)
1: 1 Reps
2: 22 50 mV, 60 Hz Reject, Slow Range
3: 1 DIFF Channel
4: 39 Loc [KR_A3]

5: 8960.57 Mult
6: 0 Offset

15: Do (P86)
1: 72 Pulse Port 2

16: Delay w/Opt Excitation (P22)
1: 1 Ex Channel
2: 0 Delay W/Ex (0.01 sec units)
3: 1 Delay After Ex (0.01 sec units)
4: 0 mV Excitation

17: Volt (Diff) (P2)
1: 1 Reps
2: 22 50 mV, 60 Hz Reject, Slow Range
3: 1 DIFF Channel
4: 38 Loc [KR_A4]
5: 9057.97 Mult
6: 0 Offset

18: Do (P86)
1: 72 Pulse Port 2

19: Delay w/Opt Excitation (P22)
1: 1 Ex Channel
2: 0 Delay W/Ex (0.01 sec units)
3: 1 Delay After Ex (0.01 sec units)
4: 0 mV Excitation

20: Volt (Diff) (P2)
1: 1 Reps
2: 22 50 mV, 60 Hz Reject, Slow Range
3: 1 DIFF Channel
4: 42 Loc [KR_B1]
5: 8431.70 Mult
6: 0 Offset

21: Do (P86)
1: 72 Pulse Port 2

22: Delay w/Opt Excitation (P22)
1: 1 Ex Channel
2: 0 Delay W/Ex (0.01 sec units)
3: 1 Delay After Ex (0.01 sec units)
4: 0 mV Excitation

23: Volt (Diff) (P2)

1: 1 Reps
2: 22 50 mV, 60 Hz Reject, Slow Range
3: 1 DIFF Channel
4: 43 Loc [KR_B2]
5: 5446.15 Mult
6: 0 Offset

24: Do (P86)
1: 72 Pulse Port 2

25: Delay w/Opt Excitation (P22)
1: 1 Ex Channel
2: 0 Delay W/Ex (0.01 sec units)
3: 1 Delay After Ex (0.01 sec units)
4: 0 mV Excitation

26: Volt (Diff) (P2)
1: 1 Reps
2: 22 50 mV, 60 Hz Reject, Slow Range
3: 1 DIFF Channel
4: 44 Loc [KR_B3]
5: 4814.27 Mult
6: 0 Offset

27: Do (P86)
1: 72 Pulse Port 2

28: Delay w/Opt Excitation (P22)
1: 1 Ex Channel
2: 0 Delay W/Ex (0.01 sec units)
3: 1 Delay After Ex (0.01 sec units)
4: 0 mV Excitation

29: Volt (Diff) (P2)
1: 1 Reps
2: 22 50 mV, 60 Hz Reject, Slow Range
3: 1 DIFF Channel
4: 45 Loc [KR_B4]
5: 4650.64 Mult
6: 0 Offset

30: Do (P86)
1: 72 Pulse Port 2

31: Delay w/Opt Excitation (P22)
1: 1 Ex Channel
2: 0 Delay W/Ex (0.01 sec units)

3: 1 Delay After Ex (0.01 sec units)
4: 0 mV Excitation

32: Volt (Diff) (P2)
1: 1 Reps
2: 22 50 mV, 60 Hz Reject, Slow Range
3: 1 DIFF Channel
4: 46 Loc [KR_C1]
5: 9165.9 Mult
6: 0 Offset

33: Do (P86)
1: 72 Pulse Port 2

34: Delay w/Opt Excitation (P22)
1: 1 Ex Channel
2: 0 Delay W/Ex (0.01 sec units)
3: 1 Delay After Ex (0.01 sec units)
4: 0 mV Excitation

35: Volt (Diff) (P2)
1: 1 Reps
2: 22 50 mV, 60 Hz Reject, Slow Range
3: 1 DIFF Channel
4: 47 Loc [KR_C2]
5: 9209.92 Mult
6: 0 Offset

36: Do (P86)
1: 72 Pulse Port 2

37: Delay w/Opt Excitation (P22)
1: 1 Ex Channel
2: 0 Delay W/Ex (0.01 sec units)
3: 1 Delay After Ex (0.01 sec units)
4: 0 mV Excitation

38: Volt (Diff) (P2)
1: 1 Reps
2: 22 50 mV, 60 Hz Reject, Slow Range
3: 1 DIFF Channel
4: 48 Loc [KR_C3]
5: 8826.13 Mult
6: 0 Offset

39: Do (P86)
1: 72 Pulse Port 2

40: Delay w/Opt Excitation (P22)
1: 1 Ex Channel
2: 0 Delay W/Ex (0.01 sec units)
3: 1 Delay After Ex (0.01 sec units)
4: 0 mV Excitation

41: Volt (Diff) (P2)
1: 1 Reps
2: 22 50 mV, 60 Hz Reject, Slow Range
3: 1 DIFF Channel
4: 49 Loc [KR_C4]
5: 5375.42 Mult
6: 0 Offset

42: Do (P86)
1: 72 Pulse Port 2

43: Delay w/Opt Excitation (P22)
1: 1 Ex Channel
2: 0 Delay W/Ex (0.01 sec units)
3: 1 Delay After Ex (0.01 sec units)
4: 0 mV Excitation

44: Volt (Diff) (P2)
1: 1 Reps
2: 22 50 mV, 60 Hz Reject, Slow Range
3: 1 DIFF Channel
4: 50 Loc [KT_A1]
5: 5094.24 Mult
6: 0 Offset

45: Do (P86)
1: 72 Pulse Port 2

46: Delay w/Opt Excitation (P22)
1: 1 Ex Channel
2: 0 Delay W/Ex (0.01 sec units)
3: 1 Delay After Ex (0.01 sec units)
4: 0 mV Excitation

47: Volt (Diff) (P2)
1: 1 Reps
2: 22 50 mV, 60 Hz Reject, Slow Range
3: 1 DIFF Channel
4: 51 Loc [KT_A2]
5: 5148.10 Mult

6: 0 Offset

48: Do (P86)
1: 72 Pulse Port 2

49: Delay w/Opt Excitation (P22)
1: 1 Ex Channel
2: 0 Delay W/Ex (0.01 sec units)
3: 1 Delay After Ex (0.01 sec units)
4: 0 mV Excitation

50: Volt (Diff) (P2)
1: 1 Reps
2: 22 50 mV, 60 Hz Reject, Slow Range
3: 1 DIFF Channel
4: 52 Loc [KT_A3]
5: 4712.86 Mult
6: 0 Offset

51: Do (P86)
1: 72 Pulse Port 2

52: Delay w/Opt Excitation (P22)
1: 1 Ex Channel
2: 0 Delay W/Ex (0.01 sec units)
3: 1 Delay After Ex (0.01 sec units)
4: 0 mV Excitation

53: Volt (Diff) (P2)
1: 1 Reps
2: 21 10 mV, 60 Hz Reject, Slow Range
3: 1 DIFF Channel
4: 53 Loc [KT_A4]
5: 5073.95 Mult
6: 0 Offset

54: Do (P86)
1: 72 Pulse Port 2

55: Delay w/Opt Excitation (P22)
1: 1 Ex Channel
2: 0 Delay W/Ex (0.01 sec units)
3: 1 Delay After Ex (0.01 sec units)
4: 0 mV Excitation

56: Volt (Diff) (P2)
1: 1 Reps

2: 22 50 mV, 60 Hz Reject, Slow Range
3: 1 DIFF Channel
4: 54 Loc [KT_B1]
5: 5375.42 Mult
6: 0 Offset

57: Do (P86)
1: 72 Pulse Port 2

58: Delay w/Opt Excitation (P22)
1: 1 Ex Channel
2: 0 Delay W/Ex (0.01 sec units)
3: 1 Delay After Ex (0.01 sec units)
4: 0 mV Excitation

59: Volt (Diff) (P2)
1: 1 Reps
2: 22 50 mV, 60 Hz Reject, Slow Range
3: 1 DIFF Channel
4: 55 Loc [KT_B2]
5: 4934.81 Mult
6: 0 Offset

60: Do (P86)
1: 72 Pulse Port 2

61: Delay w/Opt Excitation (P22)
1: 1 Ex Channel
2: 0 Delay W/Ex (0.01 sec units)
3: 1 Delay After Ex (0.01 sec units)
4: 0 mV Excitation

62: Volt (Diff) (P2)
1: 1 Reps
2: 22 50 mV, 60 Hz Reject, Slow Range
3: 1 DIFF Channel
4: 56 Loc [KT_B3]
5: 4716.89 Mult
6: 0 Offset

63: Do (P86)
1: 72 Pulse Port 2

64: Delay w/Opt Excitation (P22)
1: 1 Ex Channel
2: 0 Delay W/Ex (0.01 sec units)
3: 1 Delay After Ex (0.01 sec units)

4: 0 mV Excitation

65: Volt (Diff) (P2)
1: 1 Reps
2: 22 50 mV, 60 Hz Reject, Slow Range
3: 1 DIFF Channel
4: 57 Loc [KT_B4]
5: 4640.22 Mult
6: 0 Offset

66: Do (P86)
1: 72 Pulse Port 2

67: Delay w/Opt Excitation (P22)
1: 1 Ex Channel
2: 0 Delay W/Ex (0.01 sec units)
3: 1 Delay After Ex (0.01 sec units)
4: 0 mV Excitation

68: Volt (Diff) (P2)
1: 1 Reps
2: 22 50 mV, 60 Hz Reject, Slow Range
3: 1 DIFF Channel
4: 58 Loc [KT_C1]
5: 4794.76 Mult
6: 0 Offset

69: Do (P86)
1: 72 Pulse Port 2

70: Delay w/Opt Excitation (P22)
1: 1 Ex Channel
2: 0 Delay W/Ex (0.01 sec units)
3: 1 Delay After Ex (0.01 sec units)
4: 0 mV Excitation

71: Volt (Diff) (P2)
1: 1 Reps
2: 22 50 mV, 60 Hz Reject, Slow Range
3: 1 DIFF Channel
4: 59 Loc [KT_C2]
5: 5188.43 Mult
6: 0 Offset

72: Do (P86)
1: 72 Pulse Port 2

73: Delay w/Opt Excitation (P22)
1: 1 Ex Channel
2: 0 Delay W/Ex (0.01 sec units)
3: 1 Delay After Ex (0.01 sec units)
4: 0 mV Excitation

74: Volt (Diff) (P2)
1: 1 Reps
2: 22 50 mV, 60 Hz Reject, Slow Range
3: 1 DIFF Channel
4: 60 Loc [KT_C3]
5: 4952.53 Mult
6: 0 Offset

75: Do (P86)
1: 72 Pulse Port 2

76: Delay w/Opt Excitation (P22)
1: 1 Ex Channel
2: 0 Delay W/Ex (0.01 sec units)
3: 1 Delay After Ex (0.01 sec units)
4: 0 mV Excitation

77: Volt (Diff) (P2)
1: 1 Reps
2: 22 50 mV, 60 Hz Reject, Slow Range
3: 1 DIFF Channel
4: 61 Loc [KT_C4]
5: 4856.64 Mult
6: 0 Offset

78: Do (P86)
1: 72 Pulse Port 2

79: Delay w/Opt Excitation (P22)
1: 1 Ex Channel
2: 0 Delay W/Ex (0.01 sec units)
3: 1 Delay After Ex (0.01 sec units)
4: 0 mV Excitation

80: Volt (Diff) (P2)
1: 1 Reps
2: 22 50 mV, 60 Hz Reject, Slow Range
3: 1 DIFF Channel
4: 27 Loc [Ex_GH_klu]
5: 5.12739 Mult
6: 0 Offset

81: Do (P86)
1: 72 Pulse Port 2

82: Delay w/Opt Excitation (P22)
1: 1 Ex Channel
2: 0 Delay W/Ex (0.01 sec units)
3: 1 Delay After Ex (0.01 sec units)
4: 0 mV Excitation

83: Volt (Diff) (P2)
1: 1 Reps
2: 22 50 mV, 60 Hz Reject, Slow Range
3: 1 DIFF Channel
4: 28 Loc [Ex_GV_klu]
5: 5.12261 Mult
6: 0 Offset

84: Do (P86)
1: 72 Pulse Port 2

85: Delay w/Opt Excitation (P22)
1: 1 Ex Channel
2: 0 Delay W/Ex (0.01 sec units)
3: 1 Delay After Ex (0.01 sec units)
4: 0 mV Excitation

86: Volt (Diff) (P2)
1: 1 Reps
2: 22 50 mV, 60 Hz Reject, Slow Range
3: 1 DIFF Channel
4: 29 Loc [Ex_DH_klu]
5: 5.41763 Mult
6: 0 Offset

87: Do (P86)
1: 72 Pulse Port 2

88: Delay w/Opt Excitation (P22)
1: 1 Ex Channel
2: 0 Delay W/Ex (0.01 sec units)
3: 1 Delay After Ex (0.01 sec units)
4: 0 mV Excitation

89: Volt (Diff) (P2)
1: 1 Reps
2: 22 50 mV, 60 Hz Reject, Slow Range

3: 1 DIFF Channel
4: 30 Loc [Ex_DV_klu]
5: 5.38066 Mult
6: 0 Offset

90: Do (P86)
1: 72 Pulse Port 2

91: Delay w/Opt Excitation (P22)
1: 1 Ex Channel
2: 0 Delay W/Ex (0.01 sec units)
3: 1 Delay After Ex (0.01 sec units)
4: 0 mV Excitation

92: Volt (Diff) (P2)
1: 1 Reps
2: 22 50 mV, 60 Hz Reject, Slow Range
3: 1 DIFF Channel
4: 62 Loc [KC_I1]
5: 5014.02 Mult
6: 0 Offset

93: Do (P86)
1: 72 Pulse Port 2

94: Delay w/Opt Excitation (P22)
1: 1 Ex Channel
2: 0 Delay W/Ex (0.01 sec units)
3: 1 Delay After Ex (0.01 sec units)
4: 0 mV Excitation

95: Volt (Diff) (P2)
1: 1 Reps
2: 22 50 mV, 60 Hz Reject, Slow Range
3: 1 DIFF Channel
4: 63 Loc [KC_I2]
5: 5311.61 Mult
6: 0 Offset

96: Do (P86)
1: 72 Pulse Port 2

97: Delay w/Opt Excitation (P22)
1: 1 Ex Channel
2: 0 Delay W/Ex (0.01 sec units)
3: 1 Delay After Ex (0.01 sec units)
4: 0 mV Excitation

98: Volt (Diff) (P2)
1: 1 Reps
2: 22 50 mV, 60 Hz Reject, Slow Range
3: 1 DIFF Channel
4: 64 Loc [KC_I3]
5: 4989.84 Mult
6: 0 Offset

99: Do (P86)
1: 72 Pulse Port 2

100: Delay w/Opt Excitation (P22)
1: 1 Ex Channel
2: 0 Delay W/Ex (0.01 sec units)
3: 1 Delay After Ex (0.01 sec units)
4: 0 mV Excitation

101: Volt (Diff) (P2)
1: 1 Reps
2: 22 50 mV, 60 Hz Reject, Slow Range
3: 1 DIFF Channel
4: 65 Loc [KC_I4]
5: 4952.53 Mult
6: 0 Offset

102: Do (P86)
1: 51 Set Port 1 Low

103: If time is (P92)
1: 0 Minutes (Seconds --) into a
2: 1 Interval (same units as above)
3: 10 Set Output Flag High (Flag 0)

104: Set Active Storage Area (P80)^27522
1: 1 Final Storage Area 1
2: 101 Array ID

105: Real Time (P77)^795
1: 1220 Year,Day,Hour/Minute (midnight = 2400)

106: Minimum (P74)^29734
1: 1 Reps
2: 0 Value Only
3: 1 Loc [Batt_Volt]

107: Resolution (P78)
1: 1 High Resolution

108: Sample (P70)^20989
1: 1 Reps
2: 2 Loc [Prog_Sig]

109: Sample (P70)^23714
1: 1 Reps
2: 41 Loc [KR_A1]

110: Sample (P70)^20758
1: 1 Reps
2: 40 Loc [KR_A2]

111: Sample (P70)^30636
1: 1 Reps
2: 39 Loc [KR_A3]

112: Sample (P70)^28421
1: 1 Reps
2: 38 Loc [KR_A4]

113: Sample (P70)^7082
1: 1 Reps
2: 42 Loc [KR_B1]

114: Sample (P70)^14838
1: 1 Reps
2: 43 Loc [KR_B2]

115: Sample (P70)^21142
1: 1 Reps
2: 44 Loc [KR_B3]

116: Sample (P70)^20387
1: 1 Reps
2: 45 Loc [KR_B4]

117: Sample (P70)^22504
1: 1 Reps
2: 46 Loc [KR_C1]

118: Sample (P70)^22366
1: 1 Reps
2: 47 Loc [KR_C2]

119: Sample (P70)^4722
1: 1 Reps
2: 48 Loc [KR_C3]

120: Sample (P70)^23129
1: 1 Reps
2: 49 Loc [KR_C4]

121: Sample (P70)^8067
1: 1 Reps
2: 50 Loc [KT_A1]

122: Sample (P70)^5122
1: 1 Reps
2: 51 Loc [KT_A2]

123: Sample (P70)^24721
1: 1 Reps
2: 52 Loc [KT_A3]

124: Sample (P70)^8447
1: 1 Reps
2: 53 Loc [KT_A4]

125: Sample (P70)^31686
1: 1 Reps
2: 54 Loc [KT_B1]

126: Sample (P70)^28374
1: 1 Reps
2: 55 Loc [KT_B2]

127: Sample (P70)^10778
1: 1 Reps
2: 56 Loc [KT_B3]

128: Sample (P70)^24838
1: 1 Reps
2: 57 Loc [KT_B4]

129: Sample (P70)^2693
1: 1 Reps
2: 58 Loc [KT_C1]

130: Sample (P70)^29162
1: 1 Reps
2: 59 Loc [KT_C2]

131: Sample (P70)^18995
1: 1 Reps
2: 60 Loc [KT_C3]

132: Sample (P70)^3682
1: 1 Reps
2: 61 Loc [KT_C4]

133: Sample (P70)^19602
1: 1 Reps
2: 27 Loc [Ex_GH_klu]

134: Sample (P70)^13022
1: 1 Reps
2: 28 Loc [Ex_GV_klu]

135: Sample (P70)^25678
1: 1 Reps
2: 29 Loc [Ex_DH_klu]

136: Sample (P70)^20235
1: 1 Reps
2: 30 Loc [Ex_DV_klu]

137: Sample (P70)^20235
1: 1 Reps
2: 62 Loc [KC_I1]

138: Sample (P70)^20235
1: 1 Reps
2: 63 Loc [KC_I2]

139: Sample (P70)^20235
1: 1 Reps
2: 64 Loc [KC_I3]

140: Sample (P70)^20235
1: 1 Reps
2: 65 Loc [KC_I4]

141: Resolution (P78)
1: 0 Low Resolution

*Table 2 Program
01: 10.0000 Execution Interval (seconds)

1: Serial Out (P96)
1: 71 Destination Output

*Table 3 Subroutines

End Program

Calibration constants (microamps per 100 klux) from Campbell Scientific were used to get the Multiplier for the datalogger:

Multiplier = 10^8/ CC X 604 (Martins-Mogo, 2005)

Calibration constants for all sensors have been listed in the following pages:

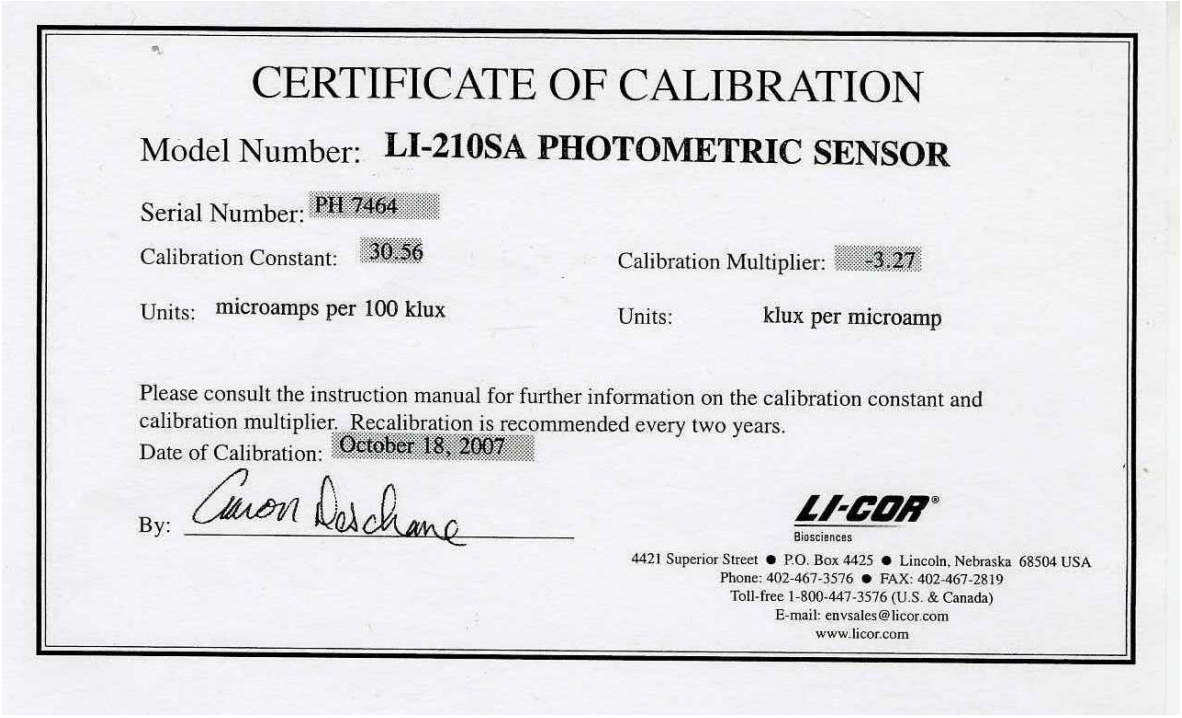

CERTIFICATE OF CALIBRATION

Model Number: **LI-210SA PHOTOMETRIC SENSOR**

Serial Number: PH 7464

Calibration Constant: 30.56 Units: microamps per 100 klux

Calibration Multiplier: -3.27 Units: klux per microamp

Please consult the instruction manual for further information on the calibration constant and calibration multiplier. Recalibration is recommended every two years.

Date of Calibration: October 18, 2007

By: Caron Doschane

LI-COR Biosciences

4421 Superior Street ● P.O. Box 4425 ● Lincoln, Nebraska 68504 USA
Phone: 402-467-3576 ● FAX: 402-467-2819
Toll-free 1-800-447-3576 (U.S. & Canada)
E-mail: envsales@licor.com
www.licor.com

CERTIFICATE OF CALIBRATION

Model Number: **LI-210SA PHOTOMETRIC SENSOR**

Serial Number: PH 7467

Calibration Constant: 33.02 Calibration Multiplier: -3.03

Units: microamps per 100 klux Units: klux per microamp

Please consult the instruction manual for further information on the calibration constant and calibration multiplier. Recalibration is recommended every two years.

Date of Calibration: October 10, 2007

By: Caron Deschane

LI-COR® Biosciences

4421 Superior Street ● P.O. Box 4425 ● Lincoln, Nebraska 68504 USA
Phone: 402-467-3576 ● FAX: 402-467-2819
Toll-free 1-800-447-3576 (U.S. & Canada)
E-mail: envsales@licor.com
www.licor.com

CERTIFICATE OF CALIBRATION

Model Number: **LI-210SA PHOTOMETRIC SENSOR**

Serial Number: PH 7461

Calibration Constant: 32.32 Calibration Multiplier: -3.09

Units: microamps per 100 klux Units: klux per microamp

Please consult the instruction manual for further information on the calibration constant and calibration multiplier. Recalibration is recommended every two years.

Date of Calibration: October 10, 2007

By: Caron Deschane

LI-COR® Biosciences

4421 Superior Street ● P.O. Box 4425 ● Lincoln, Nebraska 68504 USA
Phone: 402-467-3576 ● FAX: 402-467-2819
Toll-free 1-800-447-3576 (U.S. & Canada)
E-mail: envsales@licor.com
www.licor.com

CERTIFICATE OF CALIBRATION

Model Number: **LI-210SA PHOTOMETRIC SENSOR**

Serial Number: PH 7466

Calibration Constant: 30.40 Calibration Multiplier: -3.29

Units: microamps per 100 klux Units: klux per microamp

Please consult the instruction manual for further information on the calibration constant and calibration multiplier. Recalibration is recommended every two years.

Date of Calibration: October 10, 2007

By: Cameron Deschane

LI-COR® Biosciences
4421 Superior Street ● P.O. Box 4425 ● Lincoln, Nebraska 68504 USA
Phone: 402-467-3576 ● FAX: 402-467-2819
Toll-free 1-800-447-3576 (U.S. & Canada)
E-mail: envsales@licor.com
www.licor.com

CERTIFICATE OF CALIBRATION

Model Number: **LI-210SA PHOTOMETRIC SENSOR**

Serial Number: PH 7453

Calibration Constant: 32.63 Calibration Multiplier: -3.06

Units: microamps per 100 klux Units: klux per microamp

Please consult the instruction manual for further information on the calibration constant and calibration multiplier. Recalibration is recommended every two years.

Date of Calibration: October 10, 2007

By: Cameron Deschane

LI-COR® Biosciences
4421 Superior Street ● P.O. Box 4425 ● Lincoln, Nebraska 68504 USA
Phone: 402-467-3576 ● FAX: 402-467-2819
Toll-free 1-800-447-3576 (U.S. & Canada)
E-mail: envsales@licor.com
www.licor.com

CERTIFICATE OF CALIBRATION

Model Number: **LI-210SA PHOTOMETRIC SENSOR**

Serial Number: PH 7465

Calibration Constant: 30.77

Units: microamps per 100 klux

Calibration Multiplier: -3.25

Units: klux per microamp

Please consult the instruction manual for further information on the calibration constant and calibration multiplier. Recalibration is recommended every two years.

Date of Calibration: October 18, 2007

By: Caron Deschane

LI-COR Biosciences
4421 Superior Street ● P.O. Box 4425 ● Lincoln, Nebraska 68504 USA
Phone: 402-467-3576 ● FAX: 402-467-2819
Toll-free 1-800-447-3576 (U.S. & Canada)
E-mail: envsales@licor.com
www.licor.com

CERTIFICATE OF CALIBRATION

Model Number: **LI-210SA PHOTOMETRIC SENSOR**

Serial Number: PH 7457

Calibration Constant: 33.55

Units: microamps per 100 klux

Calibration Multiplier: -2.98

Units: klux per microamp

Please consult the instruction manual for further information on the calibration constant and calibration multiplier. Recalibration is recommended every two years.

Date of Calibration: October 18, 2007

By: Caron Deschane

LI-COR Biosciences
4421 Superior Street ● P.O. Box 4425 ● Lincoln, Nebraska 68504 USA
Phone: 402-467-3576 ● FAX: 402-467-2819
Toll-free 1-800-447-3576 (U.S. & Canada)
E-mail: envsales@licor.com
www.licor.com

CERTIFICATE OF CALIBRATION

Model Number: **LI-210SA PHOTOMETRIC SENSOR**

Serial Number: PH 7462

Calibration Constant: 33.43

Calibration Multiplier: -2.99

Units: microamps per 100 klux

Units: klux per microamp

Please consult the instruction manual for further information on the calibration constant and calibration multiplier. Recalibration is recommended every two years.

Date of Calibration: October 10, 2007

By: Caron Deschane

LI-COR® Biosciences
4421 Superior Street ● P.O. Box 4425 ● Lincoln, Nebraska 68504 USA
Phone: 402-467-3576 ● FAX: 402-467-2819
Toll-free 1-800-447-3576 (U.S. & Canada)
E-mail: envsales@licor.com
www.licor.com

CERTIFICATE OF CALIBRATION

Model Number: **LI-210SA PHOTOMETRIC SENSOR**

Serial Number: PH 7463

Calibration Constant: 31.91

Calibration Multiplier: -3.13

Units: microamps per 100 klux

Units: klux per microamp

Please consult the instruction manual for further information on the calibration constant and calibration multiplier. Recalibration is recommended every two years.

Date of Calibration: October 10, 2007

By: Caron Deschane

LI-COR® Biosciences
4421 Superior Street ● P.O. Box 4425 ● Lincoln, Nebraska 68504 USA
Phone: 402-467-3576 ● FAX: 402-467-2819
Toll-free 1-800-447-3576 (U.S. & Canada)
E-mail: envsales@licor.com
www.licor.com

CERTIFICATE OF CALIBRATION

Model Number: **LI-210SA PHOTOMETRIC SENSOR**

Serial Number: PH 7452

Calibration Constant: 35.13 Calibration Multiplier: -2.85

Units: microamps per 100 klux Units: klux per microamp

Please consult the instruction manual for further information on the calibration constant and calibration multiplier. Recalibration is recommended every two years.

Date of Calibration: October 10, 2007

By: Caron Deschane

LI-COR® Biosciences
4421 Superior Street ● P.O. Box 4425 ● Lincoln, Nebraska 68504 USA
Phone: 402-467-3576 ● FAX: 402-467-2819
Toll-free 1-800-447-3576 (U.S. & Canada)
E-mail: envsales@licor.com
www.licor.com

CERTIFICATE OF CALIBRATION

Model Number: **LI-210SA PHOTOMETRIC SENSOR**

Serial Number: PH 7468

Calibration Constant: 30.80 Calibration Multiplier: -3.25

Units: microamps per 100 klux Units: klux per microamp

Please consult the instruction manual for further information on the calibration constant and calibration multiplier. Recalibration is recommended every two years.

Date of Calibration: October 10, 2007

By: Caron Deschane

LI-COR® Biosciences
4421 Superior Street ● P.O. Box 4425 ● Lincoln, Nebraska 68504 USA
Phone: 402-467-3576 ● FAX: 402-467-2819
Toll-free 1-800-447-3576 (U.S. & Canada)
E-mail: envsales@licor.com
www.licor.com

CERTIFICATE OF CALIBRATION

Model Number: **LI-210SA PHOTOMETRIC SENSOR**

Serial Number: PH 7459

Calibration Constant: 34.53 Calibration Multiplier: -2.90

Units: microamps per 100 klux Units: klux per microamp

Please consult the instruction manual for further information on the calibration constant and calibration multiplier. Recalibration is recommended every two years.

Date of Calibration: October 10, 2007

By: Aaron Deschane

LI-COR® Biosciences
4421 Superior Street ● P.O. Box 4425 ● Lincoln, Nebraska 68504 USA
Phone: 402-467-3576 ● FAX: 402-467-2819
Toll-free 1-800-447-3576 (U.S. & Canada)
E-mail: envsales@licor.com
www.licor.com

CERTIFICATE OF CALIBRATION

Model Number: **LI-210SA PHOTOMETRIC SENSOR**

Serial Number: PH 7454

Calibration Constant: 33.18 Calibration Multiplier: -3.01

Units: microamps per 100 klux Units: klux per microamp

Please consult the instruction manual for further information on the calibration constant and calibration multiplier. Recalibration is recommended every two years.

Date of Calibration: October 10, 2007

By: Aaron Deschane

LI-COR® Biosciences
4421 Superior Street ● P.O. Box 4425 ● Lincoln, Nebraska 68504 USA
Phone: 402-467-3576 ● FAX: 402-467-2819
Toll-free 1-800-447-3576 (U.S. & Canada)
E-mail: envsales@licor.com
www.licor.com

CERTIFICATE OF CALIBRATION

Model Number: **LI-210SA PHOTOMETRIC SENSOR**

Serial Number: PH 7455

Calibration Constant: 33.43 Calibration Multiplier: -2.99

Units: microamps per 100 klux Units: klux per microamp

Please consult the instruction manual for further information on the calibration constant and calibration multiplier. Recalibration is recommended every two years.

Date of Calibration: October 10, 2007

By: Caron Daschane

LI-COR® Biosciences
4421 Superior Street ● P.O. Box 4425 ● Lincoln, Nebraska 68504 USA
Phone: 402-467-3576 ● FAX: 402-467-2819
Toll-free 1-800-447-3576 (U.S. & Canada)
E-mail: envsales@licor.com
www.licor.com

CERTIFICATE OF CALIBRATION

Model Number: **LI-210SA PHOTOMETRIC SENSOR**

Serial Number: PH 7458

Calibration Constant: 30.80 Calibration Multiplier: -3.25

Units: microamps per 100 klux Units: klux per microamp

Please consult the instruction manual for further information on the calibration constant and calibration multiplier. Recalibration is recommended every two years.

Date of Calibration: October 10, 2007

By: Caron Daschane

LI-COR® Biosciences
4421 Superior Street ● P.O. Box 4425 ● Lincoln, Nebraska 68504 USA
Phone: 402-467-3576 ● FAX: 402-467-2819
Toll-free 1-800-447-3576 (U.S. & Canada)
E-mail: envsales@licor.com
www.licor.com

CERTIFICATE OF CALIBRATION

Model Number: **LI-210SA PHOTOMETRIC SENSOR**

Serial Number: PH 7451

Calibration Constant: 34.09 Calibration Multiplier: -2.93

Units: microamps per 100 klux Units: klux per microamp

Please consult the instruction manual for further information on the calibration constant and calibration multiplier. Recalibration is recommended every two years.

Date of Calibration: October 10, 2007

By: Caron Doschane

LI-COR® Biosciences
4421 Superior Street ● P.O. Box 4425 ● Lincoln, Nebraska 68504 USA
Phone: 402-467-3576 ● FAX: 402-467-2819
Toll-free 1-800-447-3576 (U.S. & Canada)
E-mail: envsales@licor.com
www.licor.com

CERTIFICATE OF CALIBRATION

Model Number: **LI-210SA PHOTOMETRIC SENSOR**

Serial Number: PH 7450

Calibration Constant: 32.50 Calibration Multiplier: -3.08

Units: microamps per 100 klux Units: klux per microamp

Please consult the instruction manual for further information on the calibration constant and calibration multiplier. Recalibration is recommended every two years.

Date of Calibration: October 10, 2007

By: Caron Doschane

LI-COR® Biosciences
4421 Superior Street ● P.O. Box 4425 ● Lincoln, Nebraska 68504 USA
Phone: 402-467-3576 ● FAX: 402-467-2819
Toll-free 1-800-447-3576 (U.S. & Canada)
E-mail: envsales@licor.com
www.licor.com

CERTIFICATE OF CALIBRATION

Model Number: **LI-210SA PHOTOMETRIC SENSOR**

Serial Number: PH 8294

Calibration Constant: 35.60 Calibration Multiplier: -2.81

Units: microamps per 100 klux Units: klux per microamp

Please consult the instruction manual for further information on the calibration constant and calibration multiplier. Recalibration is recommended every two years.

Date of Calibration: February 21, 2007

By: Caron Deschane

LI-COR® Biosciences
4421 Superior Street ● P.O. Box 4425 ● Lincoln, Nebraska 68504 USA
Phone: 402-467-3576 ● FAX: 402-467-2819
Toll-free 1-800-447-3576 (U.S. & Canada)
E-mail: envsales@licor.com
www.licor.com

CERTIFICATE OF CALIBRATION

Model Number: **LI-210SA PHOTOMETRIC SENSOR**

Serial Number: PH 8293

Calibration Constant: 35.10 Calibration Multiplier: -2.85

Units: microamps per 100 klux Units: klux per microamp

Please consult the instruction manual for further information on the calibration constant and calibration multiplier. Recalibration is recommended every two years.

Date of Calibration: February 21, 2007

By: Caron Deschane

LI-COR® Biosciences
4421 Superior Street ● P.O. Box 4425 ● Lincoln, Nebraska 68504 USA
Phone: 402-467-3576 ● FAX: 402-467-2819
Toll-free 1-800-447-3576 (U.S. & Canada)
E-mail: envsales@licor.com
www.licor.com

CERTIFICATE OF CALIBRATION

Model Number: **LI-210SA PHOTOMETRIC SENSOR**

Serial Number: PH 8292

Calibration Constant: 34.39 Calibration Multiplier: -2.91

Units: microamps per 100 klux Units: klux per microamp

Please consult the instruction manual for further information on the calibration constant and calibration multiplier. Recalibration is recommended every two years.

Date of Calibration: February 21, 2007

By: Caron Deschane

LI-COR® Biosciences
4421 Superior Street ● P.O. Box 4425 ● Lincoln, Nebraska 68504 USA
Phone: 402-467-3576 ● FAX: 402-467-2819
Toll-free 1-800-447-3576 (U.S. & Canada)
E-mail: envsales@licor.com
www.licor.com

CERTIFICATE OF CALIBRATION

Model Number: **LI-210SA PHOTOMETRIC SENSOR**

Serial Number: PH 8291

Calibration Constant: 35.68 Calibration Multiplier: -2.80

Units: microamps per 100 klux Units: klux per microamp

Please consult the instruction manual for further information on the calibration constant and calibration multiplier. Recalibration is recommended every two years.

Date of Calibration: February 21, 2007

By: Caron Deschane

LI-COR® Biosciences
4421 Superior Street ● P.O. Box 4425 ● Lincoln, Nebraska 68504 USA
Phone: 402-467-3576 ● FAX: 402-467-2819
Toll-free 1-800-447-3576 (U.S. & Canada)
E-mail: envsales@licor.com
www.licor.com

CERTIFICATE OF CALIBRATION

Model Number: **LI-210SA PHOTOMETRIC SENSOR**

Serial Number: PH 7469

Calibration Constant: 31.17 Calibration Multiplier: -3.21

Units: microamps per 100 klux Units: klux per microamp

Please consult the instruction manual for further information on the calibration constant and calibration multiplier. Recalibration is recommended every two years.

Date of Calibration: October 10, 2007

By: Aaron Deschane

LI-COR® Biosciences
4421 Superior Street ● P.O. Box 4425 ● Lincoln, Nebraska 68504 USA
Phone: 402-467-3576 ● FAX: 402-467-2819
Toll-free 1-800-447-3576 (U.S. & Canada)
E-mail: envsales@licor.com
www.licor.com

CERTIFICATE OF CALIBRATION

Model Number: **LI-210SA PHOTOMETRIC SENSOR**

Serial Number: PH 7460

Calibration Constant: 32.16 Calibration Multiplier: -3.11

Units: microamps per 100 klux Units: klux per microamp

Please consult the instruction manual for further information on the calibration constant and calibration multiplier. Recalibration is recommended every two years.

Date of Calibration: October 10, 2007

By: Aaron Deschane

LI-COR® Biosciences
4421 Superior Street ● P.O. Box 4425 ● Lincoln, Nebraska 68504 USA
Phone: 402-467-3576 ● FAX: 402-467-2819
Toll-free 1-800-447-3576 (U.S. & Canada)
E-mail: envsales@licor.com
www.licor.com

CERTIFICATE of CALIBRATION for LI-COR SENSOR

Model Number: LI-210SZ

Serial Number: PH 4164 Calibration Date: October 10, 2007

Output: 10.91 millivolts per 100 klux
604.0 Ω resistor installed in cable.

IMPORTANT: *Read the appropriate instruction manual before using this sensor.*

IMPORTANT: *It is recommended that sensors be recalibrated every two years.*

Calibration Technician: Caron Deschamps

LI-COR Biosciences
LI-COR Biosciences ● Environmental ● 4421 Superior Street ● P.O. Box 4425 ● Lincoln, NE 68504
Phone: 402-467-3576 ● FAX: 402-467-2819 ● Toll-free 1-800-447-3576 (U.S. & Canada)
envsales@licor.com ● envsupport@licor.com ● www.licor.com

CERTIFICATE of CALIBRATION for LI-COR SENSOR

Model Number: LI-210SZ

Serial Number: PH 4157 Calibration Date: October 10, 2007

Output: 12.09 millivolts per 100 klux
604.0 Ω resistor installed in cable.

IMPORTANT: *Read the appropriate instruction manual before using this sensor.*

IMPORTANT: *It is recommended that sensors be recalibrated every two years.*

Calibration Technician: Caron Deschamps

LI-COR Biosciences
LI-COR Biosciences ● Environmental ● 4421 Superior Street ● P.O. Box 4425 ● Lincoln, NE 68504
Phone: 402-467-3576 ● FAX: 402-467-2819 ● Toll-free 1-800-447-3576 (U.S. & Canada)
envsales@licor.com ● envsupport@licor.com ● www.licor.com

CERTIFICATE of CALIBRATION for LI-COR SENSOR

Model Number: LI-210SZ

Serial Number: PH 4162 Calibration Date: October 10, 2007

Output: 11.33 millivolts per 100 klux
604.0 Ω resistor installed in cable.

IMPORTANT: *Read the appropriate instruction manual before using this sensor.*

IMPORTANT: *It is recommended that sensors be recalibrated every two years.*

Calibration Technician: Caron Deschamps

LI-COR Biosciences
LI-COR Biosciences ● Environmental ● 4421 Superior Street ● P.O. Box 4425 ● Lincoln, NE 68504
Phone: 402-467-3576 ● FAX: 402-467-2819 ● Toll-free 1-800-447-3576 (U.S. & Canada)
envsales@licor.com ● envsupport@licor.com ● www.licor.com

CERTIFICATE of CALIBRATION for LI-COR SENSOR

Model Number: LI-210SZ

Serial Number: PH 4160 Calibration Date: October 18, 2007

Output: 11.04 millivolts per 100 klux
604.0 Ω resistor installed in cable.

IMPORTANT: *Read the appropriate instruction manual before using this sensor.*

IMPORTANT: *It is recommended that sensors be recalibrated every two years.*

Calibration Technician: Caron Deschamps

LI-COR Biosciences
LI-COR Biosciences ● Environmental ● 4421 Superior Street ● P.O. Box 4425 ● Lincoln, NE 68504
Phone: 402-467-3576 ● FAX: 402-467-2819 ● Toll-free 1-800-447-3576 (U.S. & Canada)
envsales@licor.com ● envsupport@licor.com ● www.licor.com

CERTIFICATE of CALIBRATION for LI-COR SENSOR

Model Number: LI-210SZ

Serial Number: PH 4158 Calibration Date: October 10, 2007

Output: 11.16 millivolts per 100 klux
604.0 Ω resistor installed in cable.

IMPORTANT: *Read the appropriate instruction manual before using this sensor.*

IMPORTANT: *It is recommended that sensors be recalibrated every two years.*

Calibration Technician: Caron Deschane

LI-COR Biosciences
LI-COR Biosciences ● Environmental ● 4421 Superior Street ● P.O. Box 4425 ● Lincoln, NE 68504
Phone: 402-467-3576 ● FAX: 402-467-2819 ● Toll-free 1-800-447-3576 (U.S. & Canada)
envsales@licor.com ● envsupport@licor.com ● www.licor.com

CERTIFICATE of CALIBRATION for LI-COR SENSOR

Model Number: LI-210SZ

Serial Number: PH 4163 Calibration Date: October 18, 2007

Output: 11.86 millivolts per 100 klux
604.0 Ω resistor installed in cable.

IMPORTANT: *Read the appropriate instruction manual before using this sensor.*

IMPORTANT: *It is recommended that sensors be recalibrated every two years.*

Calibration Technician: Caron Deschane

LI-COR Biosciences
LI-COR Biosciences ● Environmental ● 4421 Superior Street ● P.O. Box 4425 ● Lincoln, NE 68504
Phone: 402-467-3576 ● FAX: 402-467-2819 ● Toll-free 1-800-447-3576 (U.S. & Canada)
envsales@licor.com ● envsupport@licor.com ● www.licor.com

CERTIFICATE of CALIBRATION for LI-COR SENSOR

Model Number: LI-210SZ

Serial Number: PH 4159 Calibration Date: October 10, 2007

Output: 11.78 millivolts per 100 klux
604.0 Ω resistor installed in cable.

IMPORTANT: *Read the appropriate instruction manual before using this sensor.*

IMPORTANT: *It is recommended that sensors be recalibrated every two years.*

Calibration Technician: Caron Deschane

LI-COR Biosciences
LI-COR Biosciences ● Environmental ● 4421 Superior Street ● P.O. Box 4425 ● Lincoln, NE 68504
Phone: 402-467-3576 ● FAX: 402-467-2819 ● Toll-free 1-800-447-3576 (U.S. & Canada)
envsales@licor.com ● envsupport@licor.com ● www.licor.com

CERTIFICATE of CALIBRATION for LI-COR SENSOR

Model Number: LI-210SZ

Serial Number: PH 4161 Calibration Date: October 10, 2007

Output: 11.59 millivolts per 100 klux
604.0 Ω resistor installed in cable.

IMPORTANT: *Read the appropriate instruction manual before using this sensor.*

IMPORTANT: *It is recommended that sensors be recalibrated every two years.*

Calibration Technician: Caron Deschane

LI-COR Biosciences
LI-COR Biosciences ● Environmental ● 4421 Superior Street ● P.O. Box 4425 ● Lincoln, NE 68504
Phone: 402-467-3576 ● FAX: 402-467-2819 ● Toll-free 1-800-447-3576 (U.S. & Canada)
envsales@licor.com ● envsupport@licor.com ● www.licor.com

APPENDIX K

SOLAR SITE ANALYSIS

An analysis of existing site conditions was conducted to asses the shadowing obstructions onsite.

Fig. K-1. South, east and west elevations of the experimental site.

Fig. K-2. The obstructions on east shading the models at 815hrs, 830hrs, 845hrs on Feb. 13, 2008.

Fish-eye images of both the models were taken at sill level and then superimposed with the sunpath diagram for 30˚ 36'N. The images show more solar shading for the basecase model between 800 hours and 830 hours from approximately September 10 to March 21. There is also an year round obstruction of clear sky from the existing building on the east.

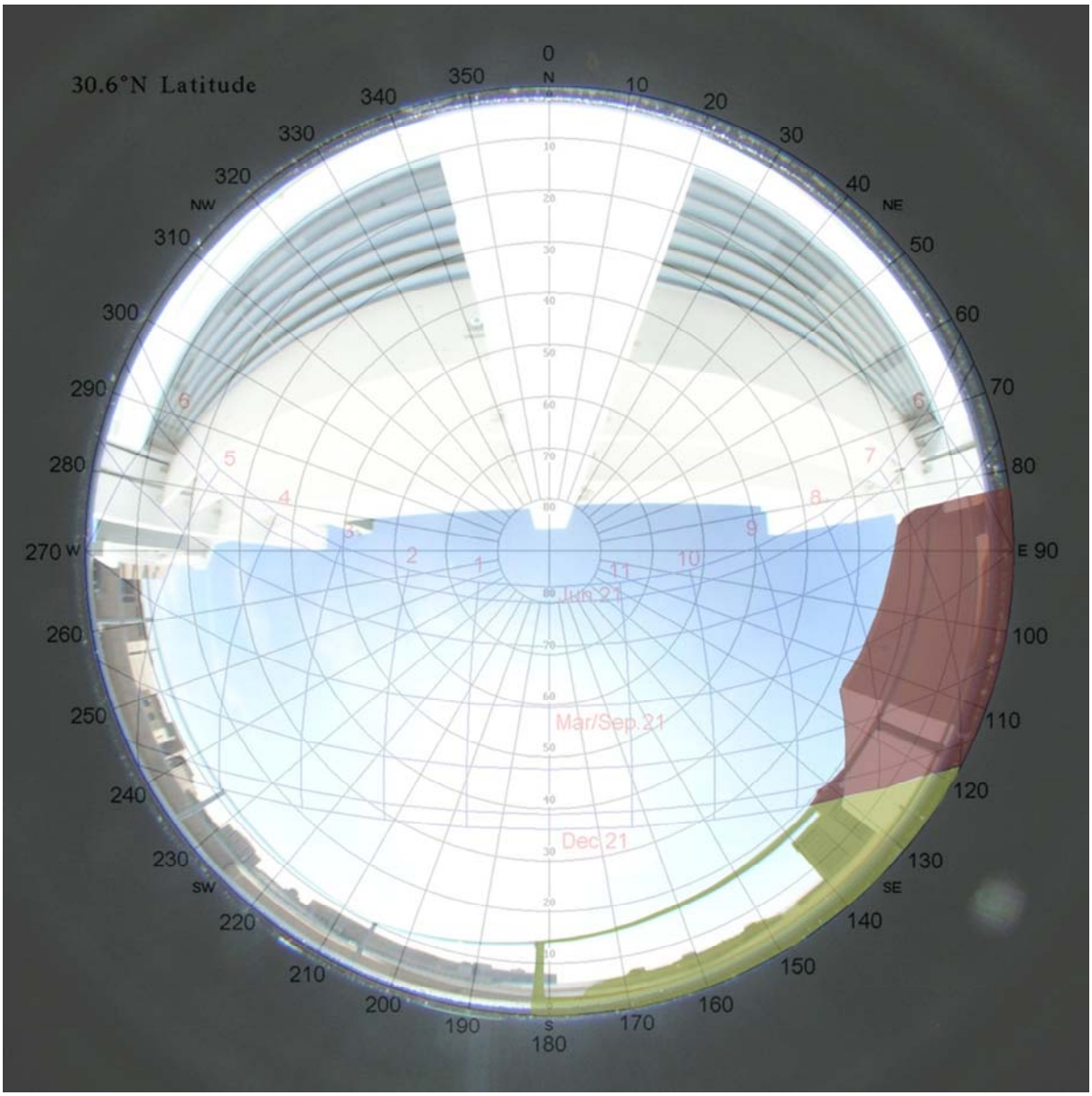

Fig. K-3. Solar site obstruction analysis for basecase model.

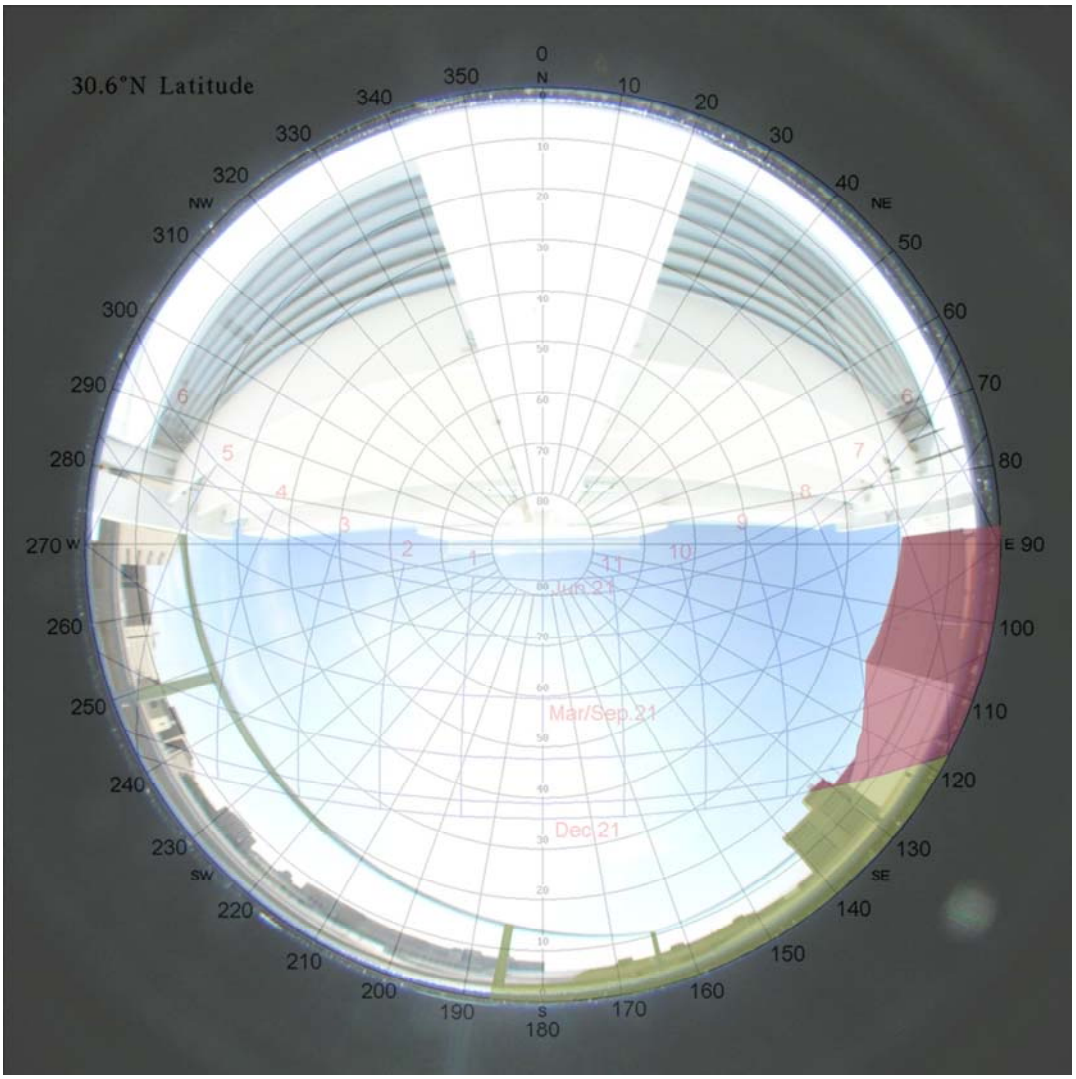

Fig. K-4. Solar site obstruction analysis for test model.

APPENDIX L

MANUAL RAYTRACING FOR SLS

The manual ray-tracing shown here was done while designing the SLS. The outgoing beam was assumed to be follow a symmetrical path about the normal to reflective surface. One of the limitations of this ray-tracing was that the 12°-15° dispersion of outgoing beam was not checked, which actually led to the outgoing beam hitting the walls. Also, as mentioned earlier (Section 2.2) the width of SLS used in the present research is 4' 4-$^{5}/_{8}$" in full scale (1' 1-$^{3}/_{16}$" in 1:4 scale) while the LBNL design (Beltran et al., 1994) was close to 5 feet wide. This may also be a reason for the wider spread of outgoing beam.

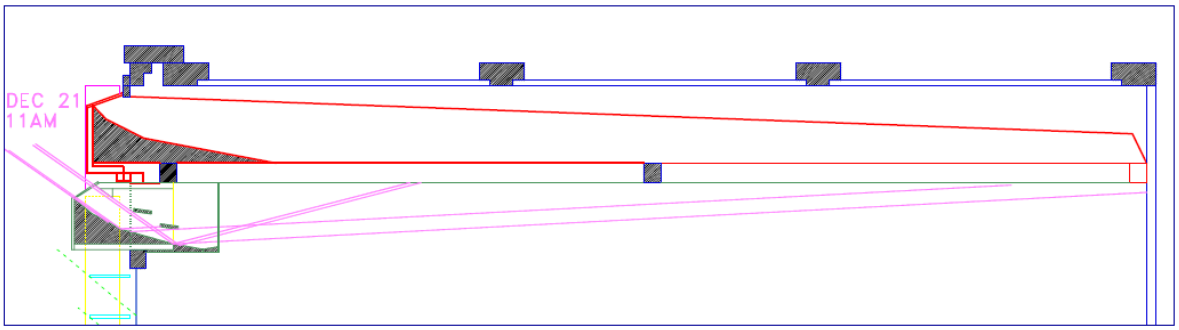

(a)

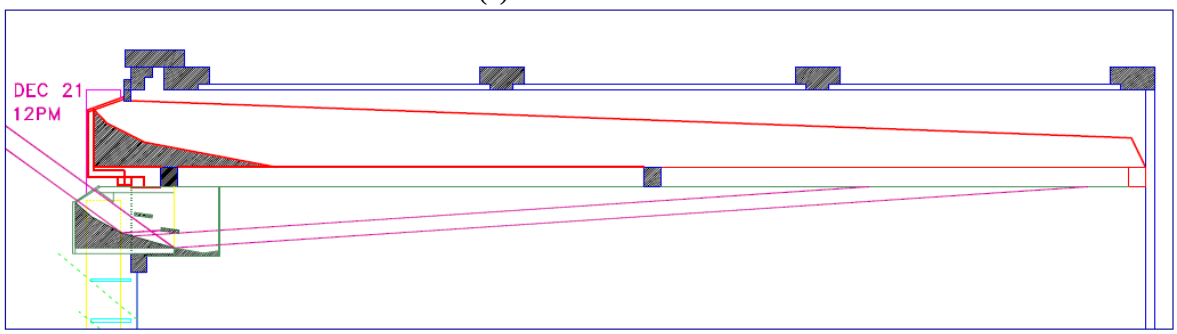

(b)

Fig. L-1. Raytracing for different times of the year for SLS. (a) Dec 21, 11am solar time, (b) Dec 21, 12pm solar time, (c) Mar 21 for all times, (d) June 21, solar time.

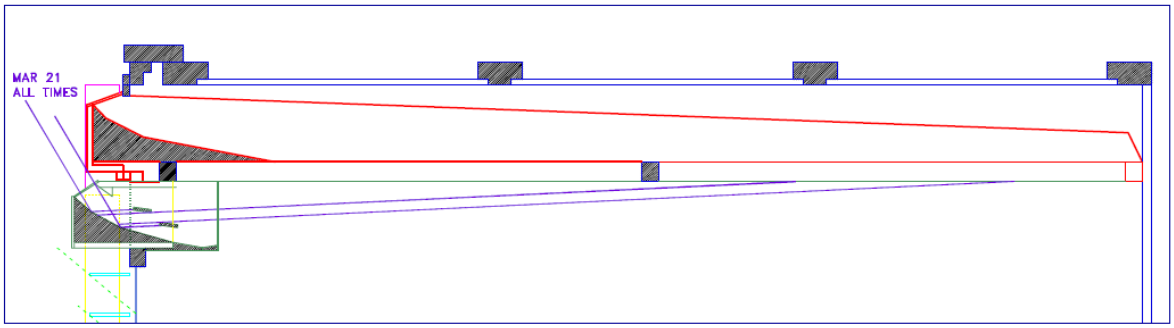

(c)

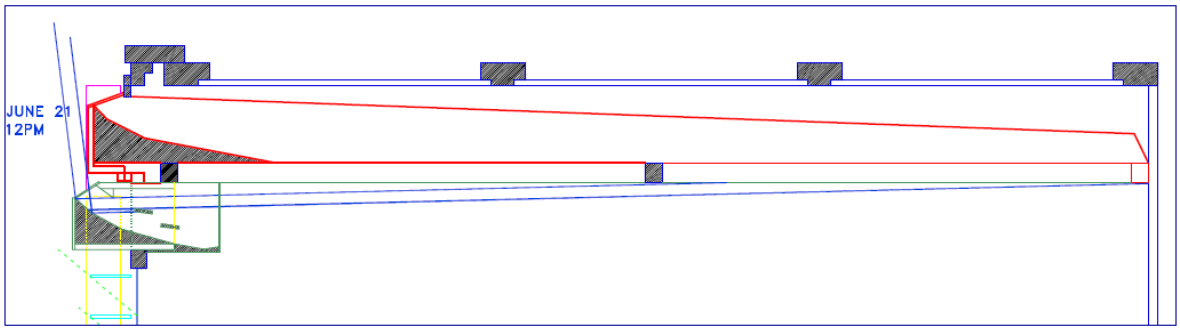

(d)

Fig. L-1. Continued.

APPENDIX M

INNOVATIVE DAYLIGHTING SYSTEMS

Fenestration acts like a daylighting luminaire (Selkowitz et al., 1998) and a number of daylight distribution strategies exist which integrate with it. Some of the systems which may integrate with OLP and may have future implications on it are discussed here. Because OLP transports direct sunlight from the south façade, any strategy which increases daylighting on north facades could be integrated with OLP. Also, efficient windows and blinds systems could combine with OLP to enhance daylighting conditions.

An extensive list of daylighting strategies is provided by Kischkoweit-Lopen (2002) and daylighting systems classified as: shading systems - diffuse skylight systems like prismatic panels and directionally selective glazing and direct sunlight systems like light shelfs and turnable lamellas; optical systems - diffuse light guides like anidolic ceilings, direct light guides like laser cut panels, scattering systems like diffusing glass and light transport systems like light pipes.

A reflective pipe with laser-cut panel as sunlight collector is analyzed by Hansen et al. (2001). The study used a 1:20 scale model with Ken Yeang's bioclimatic skyscraper as the case study. The collector faced North-West and daylight was extracted at multiple points in the interior space. Laser cut panels were also used to extract light at different points. The system achieved between 200-300lux illuminance between 12pm-4pm up to 16 meter.

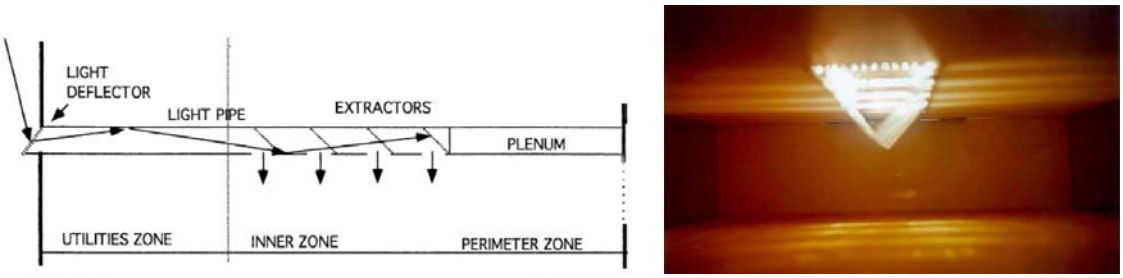

(a) (b)

Fig. 2.7. Light pipe proposed for Waterfront House. (a) Schematic section, (b) laser cut panels were used to extract light at different points. *Source: Hansen et al., (2002).*

One of the horizontal transport systems designed for indirect daylight is using anidolic systems. Scartezzini et al. (2002) have discussed a series of experiments in the development of anidolic reflectors using non-imaging optics to collect diffuse daylight. Fig. 2.8 shows one of the experimental setups using an anidolic ceiling installed in a 6.5 meter deep space that increased average daylight factor in the back of the room by 1.7 in overclouded conditions (Scartezzini et al., 1998).

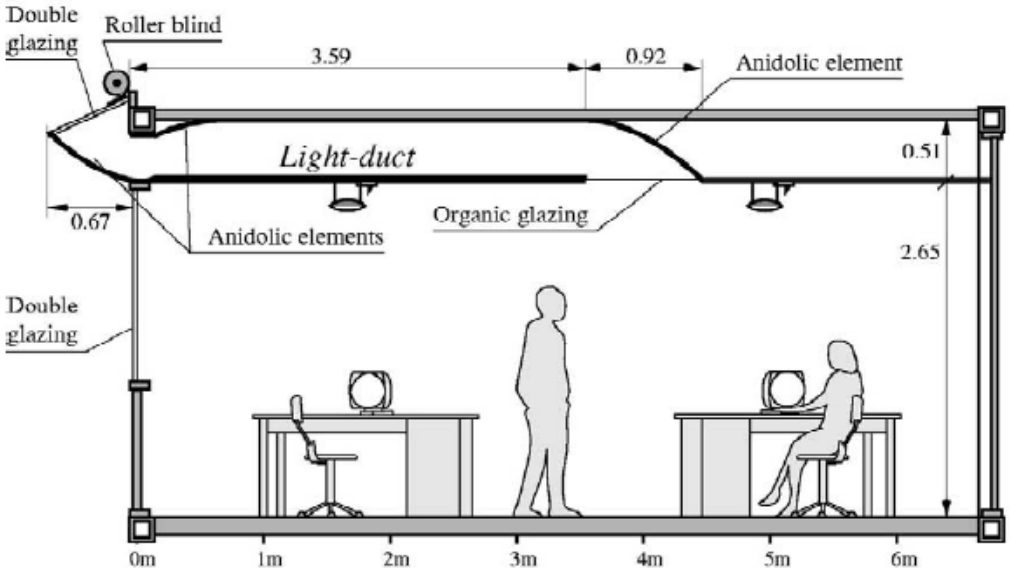

Fig. 2.8. Section of the room with Anidolic Ceiling. *Source: Scartezzini et al. (2002).*

A solar canopy was proposed by Rosemann et al. (2006) which worked with rotating mirrors directing daylight into a hybrid light guide. The light guide, made of prismatic surface, would reflect and diffuse the daylight at the same time. A set of electric lamps were integrated into the light guide. The system was designed for a south facing 3 meter by 8 meter room, and achieved over 500 lux of daylight at 2:15pm on August 3rd.

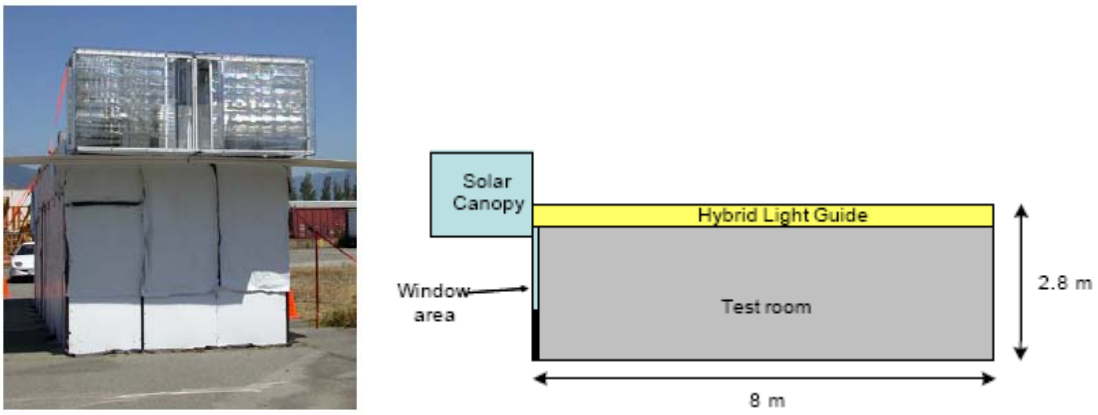

Fig. 2.9. Solar canopy and hybrid light guide. (a) The test cell (b) schematic section. *Source: Rosemann et al. (2006).*

Newer window designs integrate various strategies. One of the more sophisticated examples is the Colt Interactive Window which combines external solar shading, interior light shelf, internal solar blind , exterior noise deflector, mechanically controlled top ventilation window and manual operation for the lower view window.

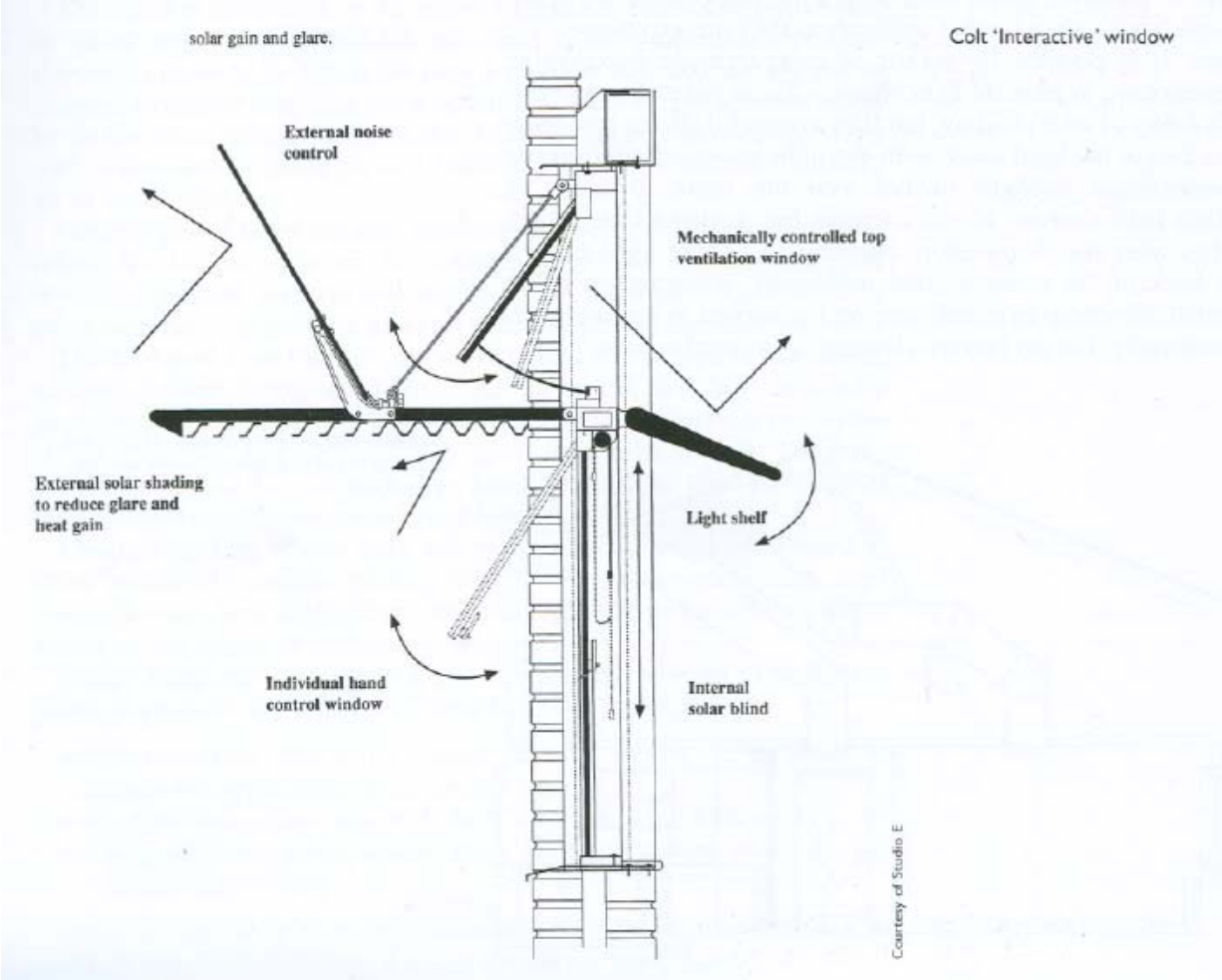

Fig. 2.4. Section of the Colt Interactive Window. *Source: Daylighting: natural light in architecture by Derek, (2004).*

Another interesting shading system is Retrosolar0 by Retrolux Interior which integrates daylight direction through its geometry; it acts as a shading device during summer and reflects direct sunlight to as deep as 6 meter inside a space.

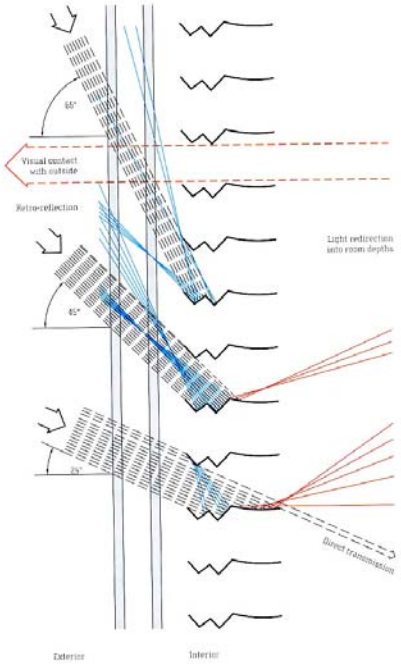

Fig. 2.5. Section through Retrosolar0 showing reflections for high and low sun angles. *Source: Daylighting: natural light in architecture by* Helmut, (2004).

APPENDIX N

NORMALIZED EXTERIOR UGR

The following formula defines the Normalized Exterior UGR, which represents UGR for a particular daylighting condition when the exterior illuminance is 4,000 fc (~40,000 lux).

$$UGR_n = 8\log_{10}[k] + UGR_m$$

$k = 40000/E_{ext,}$ where E_{ext} is the exterior illuminance (Howlett et al., 2006).

No standard exists as of now to compare normalized exterior UGR. It was one of the recommended metrics in Howlett et al. study. It was included in the present research for reference and development in future work. Fig.N1 and Fig.N2 show the variation of UGR_n for the four daylighting systems. One useful result when comparing UGR_n with UGR calculated in Section 4.3.1was that though the curves have a similar pattern, UGR_n curves are flatter and hence more tolerant with lower values of luminance for example in early morning hours. This may indicate of a higher correlation between exterior luminance and UGR_n but would need more data to investigate.

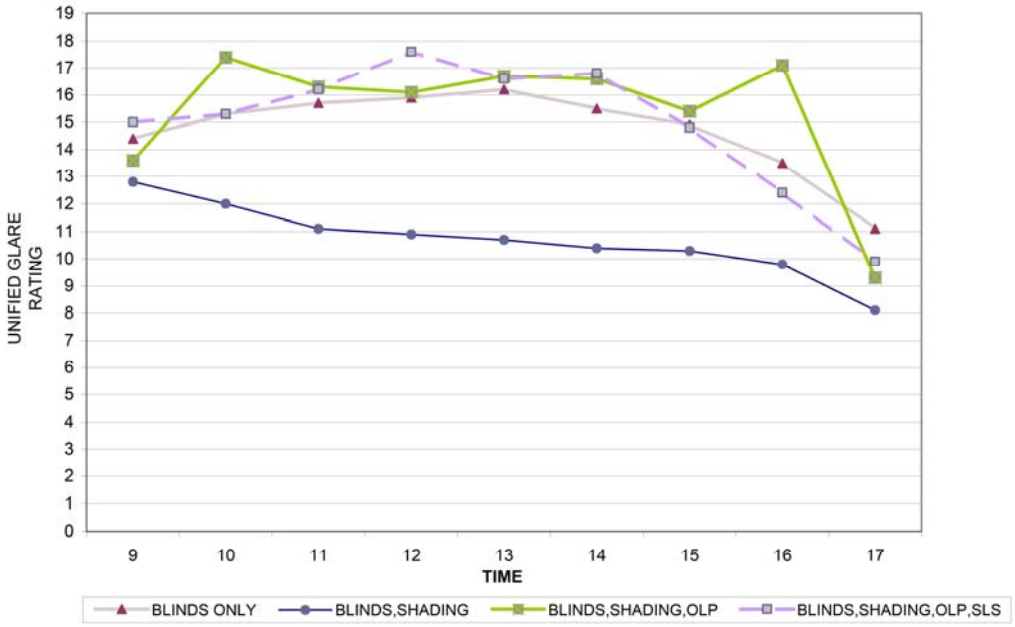

Fig. N.1. Variation of normalized exterior UGR for the four daylighting system: blinds only on Feb 13th; blinds and shading devices on Feb. 6th; blinds, shading devices and OLP on Feb 7th; blinds, shading devices, OLP and SLS on March 5th.

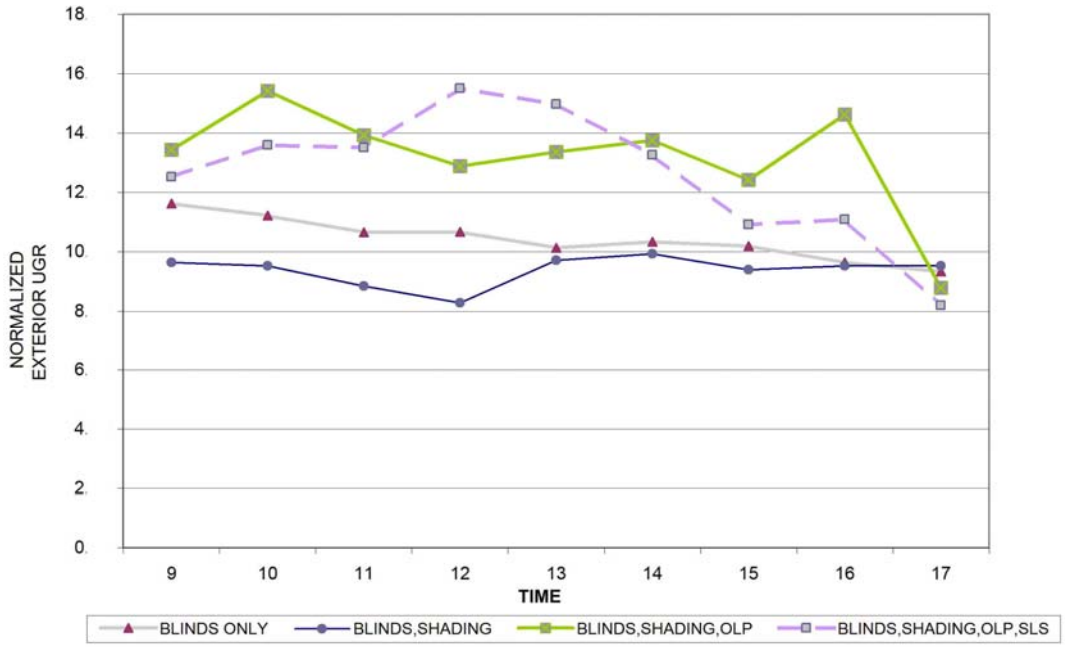

Fig. N.2. Variation of normalized exterior UGR for the four daylighting system: blinds only on Feb 17th; blinds and shading devices on Feb 9th; blinds, shading devices and OLP on Feb 8th; blinds, shading devices, OLP and SLS on March 4th.

VITA

Kapil Upadhyaya received his undergraduate degree in Architecture from IIT Kharagpur. He worked with an architecture firm and then a landscape architecture firm before attending Texas A&M University. His interests lie in sustainable architectural design, building energy simulation and daylighting simulation.

Name: Kapil Upadhyaya

Address: 3137,College of Architecture, TAMU, 77843.

Email Address: k.u.arch@gmail.com

Education: B.Arch (Hons.), Architecture, Indian Institute of Technology, Kharagpur, 2003
M.S., Architecture, Texas A&M University, 2008.